NOTICE

The quality of this microform is heavily dependent upon the quality of the original thesis submitted for microfilming. Every effort has been made to ensure the highest quality of reproduction possible.

If pages are missing, contact the university which granted the degree.

Some pages may have indistinct print especially if the original pages were typed with a poor typewriter ribbon or if the university sent us an inferior photocopy.

Reproduction in full or in part of this microform is governed by the Canadian Copyright Act, R.S.C. 1970, c. C-30, and subsequent amendments.

AVIS

La qualité de cette microforme dépend grandement de la qualité de la thèse soumise au microfilmage. Nous avons tout fait pour assurer une qualité supérieure de reproduction.

S'il manque des pages, veuillez communiquer avec l'université qui a conféré le grade.

La qualité d'impression de certaines pages peut laisser à désirer, surtout si les pages originales ont été dactylographiées à l'aide d'un ruban usé ou si l'université nous a fait parvenir une photocopie de qualité inférieure.

La reproduction, même partielle, de cette microforme est soumise à la Loi canadienne sur le droit d'auteur, SRC 1970, c. C-30, et ses amendements subséquents.

Kinematic Analysis of Workspace and Set-Up of Coordinated Two-Arm Robot Manipulators

Farzam Ranjbaran

A Thesis

in

The Department

of

Mechanical Engineering

Presented in partial fulfillment of the Requirements

for the Degree of Master of Applied Science at

Concordia University

Montreal, Quebec, Canada

March 1991

ISBN 0-315-64655-1

Abstract

Kinematic Analysis of Workspace and Set-Up of

Coordinated Two-Arm Robot Manipulators

Farzam Ranjbaran

In this thesis, primarily, the kinematics of a robotic manipulator with emphasis on the analysis of its workspace is studied. Development of algorithms for detection of two dimensional contours of workspace in both Cartesian and polar coordinates are then given. A graphical three dimensional representation of the manipulator workspace is also developed.

The algorithms for workspace analysis of single robots is extended to systems of coordinated two-arm robots, for which the term **Triplet Workspace** is introduced, since it reflects the fact that the workspace depends on the two collaborating arms and the manipulated object. Based on this approach the effects of the geometry of the robots and the specification of the desired task on the feasibility of the task execution is discussed.

Furthermore, the effects of the relative set-up of the two robots on the triplet workspace and, on a desired operation are studied. Henceforth, an optimization of the relative set-up of a two-arm robotic workcell is formulated. The objective function for this nonlinear programing has been selected as the joint availability of the two robots during the task execution. Theoretical discussions are enhanced by illustrative examples and a case study.

ACKNOWLEDGMENT

I would like to express my sincere appreciation and thanks to Professor A. Hemami and Professor R.M.H Cheng who have provided significant support and technical assistance during my studies, research work and creation of this thesis at Concordia University. It is through their patience, professional guidance, knowledge and experience that I was able to maintain the direction and motivation to accomplish my goals.

I would also like to extend my affection and appreciation to my family who have always been a source of strength to me in all of my endeavors and also to the Barton family who have been very supportive and helpful during my graduate studies at Concordia University.

Table of Contents

NOMENCLATURE

A^{i}_{i-1} : Homogeneous transformation matrix defining frame i with respect to the adjacent frame i-1.

A : Altitude angle of the robots hand, also a dual vector.

$\mathcal{A}$: An aspect defined in the joint space.

$\mathbf{a}$: Approach vector of the robots end effector.

a_x, a_y, a_z : Components of $\mathbf{a}$ along x, y and z directions.

a_i : Link length corresponding to the ith link, according to the Denavit and Hartenberg notations.

$\mathbf{a}_i$: Unit vector along a_i direction.

α : First Euler angle about the z axis.

α_i : Twist angle for link i, according to the Denavit and Hartenberg notations.

β : Second Euler angle about y axis, also rotation angle of the base frame of a manipulator about the world's z axis.

β_j : The opening of the jaw of a pair of pliers.

(C; x,y,z) : Task (workpiece) coordinate frame, assigned to one point of the manipulated object.

C_i, S_i : $Cos(\theta_i)$ and $sin(\theta_i)$ respectively.

Cond(J) : Condition number of the matrix J.

D : The admissible domain in the joint space.

d_i : Offset distance of the link i, according to the Denavit and Hartenberg notations.

$\mathbf{d}_i$: Unit vector along d_i direction.

δ : Step size of the search algorithm.

$\Delta = \{\delta_1, \delta_2, \ldots \delta_n\}$

: The set of minors of J(Q).

(e_{01},e_{02},e_{03}) : Unit vectors for coordinate frame $(O_o;x,y,z)$.

(e_{j1},e_{j2},e_{j3}) : Unit vectors for coordinate frame $(O_j;x,y,z)$.

e_j : Euclidean norm of the error between Q_j and Q^*_j.

E : Global error between Q and Q^* for *m* point of the path.

e_c : Robot's Elbow configuration index.

(F; x,y,z) : Follower manipulator's Tool coordinate frame, assigned to the robots end effector.

f : Unit vector defining the orientation of the hand, also the perspective transformation sub-matrix of the homogeneous transformation matrices.

f(.) : Direct (forward) kinematic transformation from the joint space to the cartesian tool space.

Φ : Objective function in the optimization process.

φ : Role angle of the robots hand about z axis.

$\varphi(.)$: A vector function relating elements of the set-up vector to the joint coordinates.

(f ;x,y,z) : Follower manipulator's base coordinate frame.

F(.) : A vector function representing Inverse kinematics for the main manipulator.

G(.) : A vector function representing Inverse kinematics for the follower manipulator.

g : Unit vector defining the orientation of the hand.

g : Number of working joints in a manipulator.

g_k : Inequality constraint relations in the optimization process.

g_I : Number of joints embedded in the manipulated object.

Γ : Set up vector, defining position and orientation of the base frame of a robot with respect to the world coordinate frame.

Γ_m, Γ_f : Set-up vectors for main and follower manipulators.

γ : Third Euler angle about z axis.

$\mathbf{H}$: The Hessian matrix.

h_j : Equality constraint relations in the optimization process.

I_m : An m dimensional identity matrix.

$J(Q)$: Jacobian matrix of the vector function f(.).

$\mathbf{k}$: A general axis of rotation for a rigid body.

k_x, k_y, k_z : Components of k along x, y and z axes.

λ_q : A scalar used for construction of conjugate directions.

m_o : Mobility of a two-arm robot (where grasp has D.O.F.).

m : Mobility of a general coordinated two-arm robot.

(M; x,y,z) : Main manipulator's Tool coordinate frame, assigned to the robots end effector.

(m ;x,y,z) : Main manipulator's base coordinate frame.

$\mathbf{n}$: Normal Vector of the end effector.

n_x, n_y, n_z : x,y and z components of n.

n : Number of links for a general manipulator.

n_I : Number of internal links comprising the manipulated object.

O : Orientation angle for the robots hand.

$(O_i;x,y,z)$: Coordinate frame attached to the link i of the manipulator.

$(O_j;x,y,z)$: Any given body attached coordinate frame.

$(O_o;x,y,z)$: General manipulator's base coordinate frame.

$(O_W;x,y,z)$: World (inertial) coordinate frame.

$\mathbf{p}$: A general position vector defining a point in cartesian coordinates, also position vector of the robot's end effector defined in the base frame.

$p(x)$: Penalty function in the optimization process.

$\hat{\mathbf{p}}$: P expressed in the homogeneous coordinates.

p_0^a : General form for a Position vector, defining point *a* in coordinate frame 0.

p_x, p_y, p_z : Components of p along x, y and z axes.

p_o : Position vector defining a point in $(0_o;x,y,z)$ coordinate frame.

p_{ox}, p_{oy}, p_{oz} : Components of p_o along x, y and z axes.

p_j : Position vector defining a point in $(0_j;e_1,e_2,e_3)$ coordinate frame.

p_{jk} : A position vector from 0_j to 0_k.

p_{j1}, p_{j2}, p_{j3} : Components of p_j along 1, 2 and 3 directions.

Π : A cutting plane for representation of the 2-D workspaces.

Πm , Πf : Cutting planes for main and the follower's hands.

Q_j : Vector of joint variables for point *j* of the trajectory.

Q^* : A vector representing midpoint values of admissible range of joints variations.

q : Vector of joint variables (general).

$\dot{q}$: Joint Velocity vector.

q_i : Joint variable (general) of the *i*th joint.

q_i^u, q_i^l : Upper and lower limits of the joint q_i.

q_i^* : Midpoint of the admissible range of variations of joint *i*.

$\dot{q}_i$: Velocity of joint *i* of the manipulator.

R : A general Rotation matrix, also a position vector from the origin of the robot to its hand.

R : Magnitude of the position vector from the origin to the hand of the manipulator.

R_{max} , R_{min} : Actual Maximum Minimum reach of the robot.

R'_{min} :TheoreticalMinimumreachthehand(withlimitlessjoints).

Rot(k, ϕ) : A homogeneous transformation matrix performing pure rotation

of ϕ about the axis k.

R_o^j : Rotation matrix defining the orientation of frame $(O_j;x,y,z)$ with respect to the coordinate frame $(O_o;x,y,z)$.

r^w : Position vector from the robot's base origin to the wrist point.

r_p, r'_p : Penalty multipliers for the exterior and interior penalty function methods respectively.

r , r' : Position vectors for two general points of rigid body.

r_o : Normal distance of the cutting plane to the origin.

ρ : A dummy parameter used in inverse kinematic solutions, also the radial component in the polar coordinate system.

ρ_{max}, ρ_{min} : Projection of the R_{max} and R_{min} to the cutting plane.

S^{q-1}, S^q : Conjugate search directions for the minimization process.

s : Slide vector of the end effector.

s_x,s_y,s_z : x,y and z components of s.

s_c : Robot's Shoulder configuration index.

ψ : Yaw angle of the robots hand about x axis.

σ_1 σ_2 ... σ_m : Singular values of J(Q).

σ_{min}, σ_{max} : Smallest and largest singular values of J(Q).

T_b^a or T_b^a : Homogeneous transformation matrix defining coordinate frame a with respect to frame b.

T : Tool angel of the robots hand.

Trans(Δx,Δy,Δz)

: A homogeneous transformation matrix performing pure translation of Δx, Δy and Δz along the x, y and z directions.

θ_i : Joint variable (for revolute Joints) of the ith joint.

θ_i^u , θ_i^l : Upper and Lower limits of for joint i.

$\dot{\theta}_i$: Joint velocity (for revolute joints)for the ith joint.

θ : Pitch angle of the robots hand about y axis.

Θ : Vector of Joint variables (for revolute Joints).

Θ_m , Θ_f : Vector of joint variables for main and follower manipulators.

Θ_m^* , Θ_f^* : Vector of joint mid-point values for main and follower.

V : Joint availability function.

v_h : Translational velocity of the hand.

$W_\pi(p)$: Workspace associated with the point p, mapped to the plane π.

$W(C)$: Workpiece workspace.

w_h : Rotational velocity of the hand.

w_i : A weighting factors corresponding to joint i.

w : Scale factor in Homogeneous transformation matrices.

w : Yoshikawa's manipulability index.

w_m : Modified manipulability index.

x : Vector of design variables in the optimization process.

X : An m (m <= 6) dimensional vector, the components of which represent position and orientation of the hand.

X_o : The normal distance from the cutting (parallel to the YZ plane) to the origin.

ξ : A dummy variable used in the inverse kinematic solutions.

Y_o : The normal distance from the cutting plane (parallel to the ZX plane) to the origin.

Z_o : The normal distance from the cutting plane (parallel to the XY plane) to the origin.

LIST OF FIGURES

CHAPTER 1
INTRODUCTION

In the past two decades, tele-operations and robotic manipulations have merged into the main stream of the human's perpetual desire for a more automated and a more extended exploitation of its environment. In this respect, research and development, equipped with powerful computers and sophisticated electronic sensors have been in a constant struggle to duplicate the humankind's perception and manipulation of its surroundings. The outcome of this ongoing struggle, have led to the utilization of the robot arms and manipulators, on the ground, under the ground, under the water and in space. More specifically at the present time, manipulators are being extensively employed in the factories, and to lesser extend in hazardous/contaminated or harsh environments, deep-sea operations, prosthetic limbs and biomedical and yet many other potential applications are forthcoming in the future.

Throughout the years of research and development in automation and flexible manufacturing systems, it has been observed that in numerous applications, a single robot arm with six degrees of freedom or even more is merely not capable of performing some of the assigned tasks. This is mainly due to the limited load capacity of a single arm, geometrical characteristics of the tasks and required dexterity for complex operations. Hence in recent years, multi-arm robotic systems in general and two-arm robotic systems in particular have been put atop in the agenda of many researchers all around the globe.

The main purpose of this thesis is to investigate a two-arm robotic system with emphasis on those aspects which although bear essential roles in the real world applications, have been ignored so far. Namely the focus of this work will be on:

a) Workspace Analysis and feasibility of tasks.

b) Synthesis of the Relative set-up of the workcell.

These two major aspects of the multi-arm robotic systems are crucial in the set-up and operations of both single arm and multi arm robots in a wide variety of operations, for example in material handling and in complex assembly operations. Different methodologies and formulations developed in this thesis can be applied to a general robot manipulator, however to show the validity of the different aspects of this work, the specifications of a PUMA-560 industrial robot arm will be used.

1.1- OBJECTIVES

The objectives of this thesis can be outlined as follows,

1- To review the previous work and reported results relevant to multi-arm or two-arm robotic systems. This is necessary in order to observe the track which has been followed in this area by the researchers throughout the years, and to point out those aspects of the field which have not been promoted sufficiently.

2- To define and analyze the workspaces of a robot arm and investigate the measures of manipulability for manipulators, and to device an AutoCad based approach to represent the three dimensional image of the workspace.

3- To define coordinated multi-manipulator systems and their components, with emphasis on two-arm robotic workcell. This implies the investigation of the kinematics and geometrical interactions between the members of the workcell, and representation of a systematic and general approach to categorize the possible required tasks in the practical applications.

4- To device a means of analyzing the workspaces associated with the coordinated two-arm robots. Thus the concept of triplet workspaces for this purpose is proposed. Moreover, the effects of the relative set-up of the workcell (*i.e.* position and orientation of the robots base frame and the task with respect to the world coordinate) on the triplet workspace are discussed.

5- To investigate the feasibility of the operation in terms of the accessibility of the robots and finally to propose a methodology to synthesize the set-up of the workcell in order to achieve an optimum set-up while satisfying certain performance criterion.

6- To discuss the further needs for research and development regarding different aspects of coordinated multi-arm robotic systems.

In order to emerge into a more detailed discussion of the workspace and multi-arm systems, definition of some of the pertinent features of the robot manipulators is in order. Thus some of the fundamental aspects to which frequent references will be made are explained.

1.2- GENERAL DESCRIPTION OF ROBOT MANIPULATORS

Kinematically, a robotic manipulator can be considered to be an open-loop articulative chain of links connected in series by either revolute (rotary) or prismatic (sliding) joints. Generally, one end is relatively free and commonly attached to a specialized tool such as a multi-fingered hand or a gripper (these are called the end effector). The other end of the chain is attached to a supporting base that is generally stationary. The location and orientation of the robots hand is a result of the collective effect of translation and rotation of each joint of the robotic manipulator. A central issue in industrial robotic manipulator is the ability to position the robotic hand at a specified location with a specified orientation at a given time. This issue lies at the heart of flexible and automated manufacturing (Shahinpoor 1988).

Each pair of one link and one joint will constitute one degree of freedom for the manipulator, hence for an n-degree-of-freedom manipulator, n joint-link pairs should comprise the structure of the manipulator. Since the links can rotate and/or translate with respect to the reference coordinate frame, a body-attached coordinate frame is assigned to each joint for each link. The position and orientation of the robotic end effector (its attitude) can be described in terms of the position and orientation of a coordinate frame attached to the hand with respect to a world coordinate frame (which is inertial to the robotic system). Therefore to this end, in order to analyze the kinematics of a robotic manipulator one would need a mathematical tool for transformations between the position and orientation of the end effector and the corresponding vector of joint coordinates and vice versa, as well as

for transformation between the generalized velocities of the end effector to the robots generalized joint velocities and vice versa. Different mathematical approaches have been established throughout the years for the development of the foregoing transformations, such as the use of screw coordinates, dual number quaternions , homogeneous transformation matrices and tensors. In what follows we will review two of the more popular methods which have been the concerns of the researchers in this area, and have shown to be the most efficient and convenient ones.

1.3- KINEMATICS OF ROBOT MANIPULATORS

Kinematics of robotic manipulators is the science of motion of the objects regardless of the forces that generate the motion, applied to the robotic manipulators and the objects to be manipulated (Shahinpoor 1988). Kinematics is one of the most important facet of robotics since without motion a robot will be just a name to a rigid structure.

Robot kinematics can be described completely by the translation and rotation of the coordinate frames attached to the robot links, hand, tools, parts and objects. Hence the first step in development of the robot kinematics is to assign a coordinate frame to each and every component which is of interest and will actually be involved in the motion or will affect the motion of other elements of the system (this is sometimes called a body attached coordinate frame). Moreover the main reference frame is called the world coordinate frame and is attached to a point on the ground.

Position and orientation (or attitude) of the robot hand is usually

related to the joints coordinates of the manipulators through a set of highly nonlinear equations. These equations are sometimes called closure equations for the robot. Depending on different mathematical approaches one can formulate the closure equations in different ways. The general attempt in recent years however, has been directed towards reducing the computational requirements of kinematic equations. This is mainly due to the fact that in the real time control of the mechanical manipulators, computational efficiency of the algorithms plays a significant role.

The relationships between different coordinate frames of the robotic workcell are usually expressed in terms of 4x4 homogeneous transformation matrices or for short HTM. These 4x4 matrices map a position vector expressed in homogeneous coordinates from one coordinate system to another coordinate system.

The advantage of using 4x4 homogeneous transformation matrix is its algorithmic universality in deriving the kinematic equation of a robot arm. This is evident since the closure equation of an n-degree of freedom robot can be obtained by multiplying n 4x4 transformation matrices corresponding to each joint. However the disadvantage of this representation is the redundancy intrinsic to the number of elements of these matrices. Sixteen elements comprise a transformation matrix, of which 3 are always zero and one is always one. Furthermore the elements of the 3x3 rotation matrix are not independent due to the orthonormal nature of these matrices. The redundant elements of 4x4 transformations will increase the computational burden which is not desirable in real-time control of manipulators. Several authors have used different means of extracting the independent closure equations produced

by homogeneous transformation matrices. In this thesis computational efficiency is not the major issue since calculations will be performed off-line. Furthermore with rapid advancements in the field of transputer technology and parallel processing a great deal of computational power can be attained which will accommodate the necessary on-line kinematics and/or dynamic calculations of a robot.

1.4- WORKSPACE OF ROBOT MANIPULATORS

In this section we introduce some basic concepts and definitions regarding the workspaces of the manipulators. These definitions will be used in the development of the formulations and algorithms which constitute the contents of the subsequent parts of these thesis.

Two important measures of evaluating the performance of robot manipulators in practical applications are the size and the shape of its **reachable space**, where by **reachable space** it is meant the set of all points, in cartesian space, at which a reference point located at the hand, can arrive. Moreover considerations regarding the size and the shape of the reachable space, although necessary, are not sufficient for performance evaluation of the robot manipulators. This is due to the fact that, inside the reachable space adroitness of the hand is not always uniform and in fact it decreases when the extreme reaches are approached. The term "**workspace**" has been unanimously used by the researchers in robotics and automation to designate the reachable space of a manipulator.

It is well accepted that analytical representation of the the workspace

of a general robot manipulator with limited joint motions, is an extremely complex task if not impossible. However in the recent years the pioneers of this field have attempted to examine other approaches to the problem, such as iterative or recursive methods. Albeit many of these attempts disregard the physical limits of the robots joints.

Furthermore due to the highly nonlinear nature of the kinematic models of robot manipulators, a given manipulator usually can attain a reachable point in more than one posture or configuration. This in fact will signify the complexity of the analysis for a given manipulator. In chapter five of the thesis we will propose two different iterative methods of analysis of the workspace. It will be discussed that these two method take into account the physical limits of the manipulator as well as the robots posture or configuration of the arm in the process of evaluation of the workspaces. The number of iterations for the said methods assume significant reductions, thus make possible, to generate large number of points for the analysis in a short time (almost ten times faster than the existing algorithms).

1.5- COORDINATED MULTI-MANIPULATOR SYSTEMS

In the most general sense the problem of multi-arm robotic systems can be investigated under five categories which are outlined as follows:

a) Dynamic modeling and control.

b) Kinematics, motion programing and collision avoidance.

c) Feasibility of the tasks and workspace studies.

d) Relative set-up of the workcell.

e) sensing.

Dynamics and control, which are two of the most important features of the multi-arm robots have attracted the attention of many researchers in the recent years, and currently extensive investigations of the dynamics and control of the multi-manipulator systems are being carried out. On the other hand a few attempts have been reported regarding other important issues involved in the real world applications of such systems. For example very few researchers have investigated the feasibility of the tasks, workspace interactions and the relative set-up of the multi-arm robotic systems.

The history of cooperative or collaborating multi-manipulators goes back to 1974, when (Gavrilovic 1974) and (Selic 1974) first introduced the problem of using two robot arm in assembly and material handling operations. However some rudimentary work on cooperative **Master-Slave** manipulators have been reported in 1966 (Guertz et al., 1966). **Master-Slave** terminology for cooperative two-arm robots has been used by some researchers ever since, while some others have chosen the name **Leader-Follower**, or a simple numbering of the robots for designation.

Most of the research work in coordinated multi-manipulators have been concerned with the development of two coordinated robot arms only, and some of the pioneers in this area have referred to them as **cooperative two-arm robots**. At the present time however, the general terminology of **cooperative robots** is replaced by the more restricted terminology of **coordinated robots**. Furthermore, some aspects of the research have been extended to multi robot

arm working together instead of only two robots. It is worth mentioning that even today the problem of **coordinated two-arm robots** have not been fully developed and experiments in this area have been limited to the laboratory tests only.

Some researchers have classified the cooperative multi-arm robotic tasks under the two major categories of **synchronized and coordinated** tasks, (Hemami et. al., 1990). Synchronized tasks refer to cases where at each instant of time only one arm is working on the workpiece or in other words the arms follow independent, but possibly synchronized motions, for instance in an assembly operations. Coordinated tasks on the other hand call for involvement of more than one robot arm at each instant with the workpiece, like materials handling. In this manner the trajectories of the end effectors involved are dependent through the manipulated object, (coordination is necessary between the positions, velocities and forces of every end effector involved in the motion).

Furthermore some other researchers have referred to any cooperative operation of multi-arm robots as a **coordinated multi-manipulators (CMM)** operation, and their subsequent classifications of the operation has been made, based upon the degree of coordination between the manipulators involved. Degree of coordination of the manipulators in turn has been defined in terms of the geometry of the overlapping between workspaces of the coordinated manipulators (Fortune et. al., 1986) and (Shirkhodaie et. al., 1987).

A more detailed definition of the coordination of the multi-manipulator systems will be given in chapter 6. However the main emphasis of this thesis will be focused on two-arm robots in particular.

1.6- MULTI-ARM SET-UP ARRANGEMENT

A major emphasis of this thesis is on the, synthesis and optimization of the relative set-up of the multi-arm robotic systems. In this regard some preliminary definitions are given here and more elaboration will be made in chapter 7, where a two-arm robotic system is chosen for the development of the formulations and algorithms. As the first step towards devising an efficient and dexterous multi-arm robotic system, it is of great importance to take into considerations the general features and characteristics of the desired task(s) assigned to the robotic workcell.

Task Definition

The word "task" will be used throughout this thesis and it refers to an assignment which has been defined by the application for the robotic workcell. It includes the entire execution of the assignment while the corresponding requirements are kept satisfied. A robotic task in general can range from material handling in a flexible manufacturing system to the deep sea explorations.

In the practical applications of the robotic systems a task or a family of tasks are defined, bearing certain kinematic and dynamic characteristics. In most cases however, these tasks will be performed in batch operations

where during the course of operation the required characteristics will not go through drastic variations. For example in assembly operations and pick-and-place in factories, different batches of jobs will be required with consistent demands on each batch. Next it is essential to obtain all of the information available regarding the defined tasks; some of the necessary information required prior to the installation and set-up of the system are outlined as follows:

- Requirements And Constraints Of The Trajectory.

In this category one should define all of the positional and orientational requirements and constraints of the task to be performed (object to be handled), as well as the bounds on velocities and accelerations involved in the motion. For example in the case of material handling one should specify the initial and final position/orientation of the object if required and allowable tolerances on them. Moreover if any particular path is of interest of the user, it should be defined with the associated tolerances allowed.

Any obstacles and accessories which would be present in the workcell should be defined in terms of their geometry and their respective position and orientation to the workcell's world coordinate frame. The former will particularly be important while dealing with collision avoidance of the robot with other elements of the workcell.

- Grasp Requirements And Constraints.

In addition to the trajectory definition, one should be able to gather

the necessary information concerning the grasp of the object or the workpiece by the grippers. For example if there are particular points of the object which the grippers must hold, or with a certain orientation of the hands by which the grasping is required, they must be specified with the corresponding tolerances. The foregoing considerations may be originated due to the geometry of the object, or compliance and load distribution during the task performance.

- Compliance Requirements And Constraints.

It is always necessary to know the magnitudes and directions of the various forces and moments that are at work during the operation of a robotic task. First these forces and moments should satisfy either static or dynamic equilibria in the various stages of a task. Also the collective effect of all forces and moments must not cause any structural failures in the robots hands or the objects to be manipulated. Finally the analysis of the forces and moments in robotic manipulators are absolutely essential in the understanding and control of compliance, that is, the ability of a robot to sense and react to external contact forces by modifying its trajectory (Shahinpoor 1988). Thus compliance effects may pose constraints on the defined trajectories which must be well understood prior to the set-up of the workcell. Furthermore gripper stiffness, workpiece stiffness, stopping forces and exerting forces on the object should be defined and analyzed in advance.

In the process of the set-up of a multi-arm robotic system the criteria mentioned above can be collectively used to choose the suitable robots which comply with the required characteristics. In this respect load capacity and workspace geometry of the robots are the most essential matters to be

considered.

Once the robots are chosen, the next major issue is to design the best layout or what we call, the synthesis of the relative set-up of the workcell. This issue is one of the major concern of this thesis, since we assume that the dynamic requirements and compliance of the robots have already been chosen and are available. In this regard we will define certain performance criteria upon which the optimum relative set-up of the workcell will be developed.

1.7- STRUCTURE OF THE THESIS

In Chapter Two a survey of the published research papers relevant to the objectives of this thesis is given. Section 2.1 is devoted to survey of general kinematics definition and analysis of the robot manipulators. Extensive investigations of the kinematics of the manipulators have been fully developed by numerous researchers in this field, however, the references will be made only to the major contributions upon which the subsequent chapters are related. Section 2.2 will present a complete and comprehensive survey of the research work in the area of workspace studies of the robot manipulators. The major contributions to the area of coordinated two/multi robot systems are addressed in section 2.3, while those research works which directly or indirectly relate to the optimum set-up of two-arm robotics system will be listed in section 2.4.

Chapter Three provides the general kinematics definitions and formulations for robot manipulators which be required in subsequent

chapters. Section 3.2 gives the review of the frame assignment techniques and the Denavit and Hartenberg representation of the manipulators. In section 3.3 homogeneous transformation matrices will be defined and their elements will be investigated. Moreover the applications of these matrices in the kinematic equations of the robot manipulators will be discussed.

In Chapter Four, kinematic parameters and formulations for a PUMA-560 will be represented. Section 4.2 deals with frame assignment strategies, in section 4.3, and 4.4 forward and inverse kinematics solutions for displacements of the manipulator will be derived.

Chapter Five is devoted to the development of the methodology for the analysis and evaluation of the workspaces associated with the robot manipulators. Extreme reaches, measures of manipulability, reachable, dextrous and total workspaces will be defined in section 5.2. In section 5.3 different methods of contour mapping for the workspace onto a cutting plane will be discussed and the results of the proposed algorithms in cartesian and polar coordinates will be given. Next a novel adaptive search technique for the contour detection of the boundaries of the workspaces will also be presented. Section 5.4 is devoted to discussing an AutoCad-based methodology for the three dimensional reconstruction of the working envelope of the robots. This will be done by creating a data base and interchanging its format according to the AutoCad file interchanging formats.

In Chapter Six the problem of two-arm robotic systems in particular and multi-arm units in general will be discussed. Section 6.2 defines in general terms the Cooperative Multi-Manipulator workcell, and Concepts of

Synchronized Multi-Manipulators (SMM) and Coordinated Multi-Manipulators (CMM). In section 6.3, coordinated two-arm robot organizations in particular will be discussed, and the frame assignments and transformations between elements of the workcell will be given. Section 6.4 is devoted to discuss different methods of defining a two-arm robotic trajectory and grasp. In section 6.5 basic kinematic relations and constraints between the two manipulators and the workpiece will be investigated.

Chapter Seven is the major contribution of this thesis in which an important facet of the practical development of a two-arm robotics system will be expanded, which has not received much attention in the past. Namely, analysis of the workspace associated with coordinated two-arm robotic systems. Section 7.2 describes in general the workspace of a coordinated two-arm robot as a closed kinematic chain. In section 7.3 the concept of **workpiece workspace** for coordinated operation will be proposed and the idea of two-dimensional contour detection will be extended for the evaluation of the triplet workspace and an algorithm for the determination of this workspace will be developed. Based on this algorithm, section 7.4 will illustrate some numerical examples of the triplet workspace.

In Chapter Eight we introduce the problem of synthesis of the set-up for a coordinated two-arm robotic workcell. Section 8.2 defines a nonlinear optimization problem in order to obtain a workcell set-up which satisfies certain performance criteria for the coordinated two-arm robots operation. A performance criterion in this regard is chosen to be the joint availability of both manipulators involved in the operation. In section 8.3 an overview of the **Sequential Unconstrained Minimization Technique or SUMT** for solving

nonlinear problems will be given, and two particular methods of Interior and Exterior penalty functions for the conversion of our constrained problem to an unconstrained one, will be discussed. At the end of this section the Conjugate Gradient Method for solving the modified unconstrained problem will be investigated and the formulation of the optimization problem will be presented.

Chapter Nine is devoted to illustrating examples of the optimum set-up of a coordinated two-arm robot workcell based on the formulations of Chapter Eight. Two numerical examples will be given in section 9.2. In the first example it is required to set-up a coordinated two-arm robot in order to perform a material handling task with maximum joint availability or minimum risk of joint limit violations throughout the operation. In this example the trajectory is a straight line connecting an initial to a final pose of the workpiece. The orientation of the workpiece is required to remain unchanged during the task execution. In the second example the trajectory is an arc of a circle with a given radius from the initial to the final pose, where orientation of the workpiece uniformly changes from the initial to the final values. In section 9.3 a case study in a particular material handling operation will be presented. In this study it is required to set-up the workcell for loading/unloading of long beams with varying lengths from a conveyor. Optimization is avoided in this problem because only one design parameter is chosen for the investigation which is the distance between the origins of the two robots, instead, the workspace knowledge of the manipulators will be employed for this analysis.

Finally in Chapter Ten we will discuss the contribution of this work and

conclude the thesis. Also the needs for further study and development in the related area will be discussed in this chapter.

CHAPTER 2
LITERATURE SURVEY

In this Chapter the attempt is to follow the track of the previous research work which have contributed to the research work, concerned by this thesis. The collected references will be referred to under four major categories in the subsequent sections. Moreover these references will be explained in a chronological order under each category including books or research/technical papers.

2.1- KINEMATICS OF MANIPULATORS

Kinematics of spatial mechanisms, and robot manipulators in particular, constitute a wide spectrum of work which has been developed and presented throughout the years. Due to the generality of this spectrum in the literature, only the major contributions to the area will be presented and referred to here in this section.

In kinematics, four different representations have been used to specify the position of a rigid body in space (Khatib et al., 1989).

1- Point coordinate transformations in three dimensions, consisting of a rotation followed by a translation, (Hunt 1978), (Bottema and Roth 1979), (Chen 1987).

2- Homogeneous point coordinate transformations in four dimensions,

known as 4X4 homogeneous transformations, (Denavit and Hartenberg 1955), (Hartenberg and Denavit 1964), (Paul 1981b), (Craig 1986)

3- Line coordinate transformations which may be written as 6x6 matrices operating on six dimensional vectors, called screws, or equivalently as the dual orthogonal matrix transformation of three dimensional vectors of dual numbers, (Veldkamp 1976), (Hunt 1978), (Roth 1984), (Sugimoto and Matsumoto 1984), (Pennock and Yang 1985), (McCarthy 1986), (Gu and Luh 1987), (Sugimoto 1987).

4- Line transformation algebra called Dual Quaternions, (Yang and Freudenstein 1964), (Bottema and Roth 1979).

Although the four approaches to the kinematics of manipulators and spatial mechanisms mentioned above have been proposed and developed to a great extent, it seems that a majority of the robotic engineers and researchers have resorted to the homogeneous transformations proposed by Denavit and Hartenberg.

In 1955 Denavit and Hartenberg proposed a manipulative symbolic notation which not only completely describes a mechanism, but could also be used directly in a matrix method of analysis. Their symbolism (referred to as the Denavit and Hartenberg notation or DH notation for short) coupled with the availability of high speed computers has proved to be a very useful tool for a variety of computer assisted studies of mechanisms and manipulators over the past years.

Some of the numerous published works regarding the kinematics of manipulators based on the Denavit and Hartenberg symbolisms are given by (Duffy 1980), (Paul 1981a), (Featherstone 1983), (Goldenberg et al., 1985), (Angeles 1985), (Paul and Rosa 1986), (Shahinpoor 1988), (Wolovich 1987), (Fu et al., 1988).

In this thesis the basic approache for the analysis of the manipulator kinematics and workspace will be based on the homogeneous point coordinate transformation and the Denavit and Hartenberg symbolic notations. Since the specification of a wrist partitioned robot, namely a PUMA-560, is used in the development of the numerical examples in this thesis, reference to the following research works have been made, mainly in the development of the forward and inverse kinematics formulations: (Lee 1982), (Algazar 1985), (Hemami 1988a).

2.2- WORKSPACE STUDIES

In this section we will overview the not so long history of the studies concerned with the admissible or reachable spaces associated with a robot manipulator. The number of published research work, concerning the workspace of manipulators is by far smaller than the number of the reports that have appeared in the literature concerning other aspects of robotics. Furthermore, since the workspace of the manipulators is one of the major concerns of this thesis, therefore the attempt is to cover almost all of those works which have contributed to the development of the current stage of the workspace studies and have been published in the literature.

The origin of the studies of the workspaces associated with robot manipulators goes back to the studies of simpler spatial kinematic chains. Fichter and Hunt (1975) investigated the toroidal surfaces (torus), swept by a point attached to a body that is joined back to the reference frame through a dyad of two series-connected turning-pairs (hinges). Subsequently Roth (1976) for the first time defined the terminology of **Working Spaces** as the spaces, associated with possible positions and orientations of the last link of the manipulator. He asked two major question dealing with the working spaces which constituted a basis for the subsequent workspace studies, these questions were:

1- Which points can be reached by the end point of the manipulators?

2- At each point which can be reached, what orientations can be obtained?

Moreover he used an analytic approach to identify the toroidal surfaces generated by two and three link manipulators.

Derby (1981) investigated the maximum reach of revolute jointed manipulators, by applying the screw axis and discussed the working volume of the robots through the maximum distances of reach.

Kumar and Waldron (1981a,b) for the first time presented the terminologies of Reachable and Dexterous workspaces and subsequently they developed an iterative algorithm for tracing the bounding surfaces of mechanical manipulator workspaces. However they assumed that all joint

actuators are ideal and they are capable of a complete rotation.

Sugimoto and Duffy (1981a,b) presented and proved two useful theorems about determination of the extreme reaches of a general robot manipulator, and for robots with special configurations. Based on these theorems, they developed algorithms for searching for the extreme distances that a robot hand can reach.

Tsai and Soni (1981) investigated the analysis of the region for two and three link robotic arms. Moreover, they proposed a methodology to synthesize two or three link robot arms, to calculate the dimensions and the location of the robot arm which will enclose within its accessible region the prescribed design points.

Gupta and Roth (1982) in their illuminating paper presented some new definitions to the workspace studies of the robot arms. They posed two major questions of: 1- Given the structure of the manipulator, what is the workspace associated with it? and 2- Given a designed workspace, what should be the manipulator's structure? Moreover, they proposed the terminologies of the **Primary** and the **Secondary** workspaces, and also they synthesized manipulators with three orthogonal mutually intersecting axes for their corresponding workspaces.

Tsai and Soni (1983) developed an algorithm to determine the workspace of an arbitrary plane for an n-R robot. Their algorithm is based on a linear optimization technique and on small incremental displacements applied to coordinate transformation equations relating the kinematic parameters of the

n-R robots. Both primary and secondary workspaces can be distinguished using this algorithm, since the user has the flexibility of treating the robot hand as a point (Reachable workspace), and a line or a rigid-body (Dexterous workspace). Furthermore in this proposed approach the revolute joints of the manipulators can assume both full and partial rotatability. The disadvantage of this method is the need for employment of two optimization routines first to move the robot hand to the cutting plane and with the desired orientation and next to move the hand along the boundary of the workspace. Also, no information regarding the configuration of the manipulator throughout the envelop detection routine will be gained.

Yang and Lee (1983) and Lee and Yang (1983) presented an analytic investigation of the workspace and developed a recursive formula for determining the work envelope of a manipulator on a plane parallel to XZ, YZ or XY planes. Also they presented a theorem regarding manipulator workspace based upon which a performance index is found which relates the volume of the workspace to the link length of the manipulator. They found that for a given manipulator structure the ratio of the volume of the workspace to the cube of its total link length is a constant.

A study of numerical workspace delineation for industrial roboots was described by Jou and Waldron (1983). They proposed new techniques based on the convergence theorem to compute the volumes of the segments in the workspace. Moreover intersections between the manipulator workspace and those of other devices in the workcell such as a conveyor were explored.

Hansen et al., (1983) developed a noniterative generation algorithm for

determining the workspace of n-R manipulators. Revolute joints in the proposed technique can be ideal (full rotatable) or limited . By using polar coordinates instead of cartesian coordinates and by employing some special reduction technique, they were able to decrease the computational load of the workspace determination towards a more feasible strategy.

Huang (1984) presented a general expression for describing the workspace of an n-R robot on a cutting plane parallel to the XZ plane, with emphasis on the influences of geometric parameters of robot linkages on shapes of the tori which generate the working volume. Also he made some comments on the existence of **Voids, Holes** and **Bubbles** in the workspace.

Korein (1984) presented an extensive geometric investigation of the manipulator's reach. He emphasized on man-modeling applications of the robotic manipulators. He also addressed the workspace of linkages with redundant degrees of freedom and revolute and spherical joints with irregular joint limits. He developed a polyhedra sweep for generation of the workspace.

The problem of optimum design of an RRRS manipulator workspace was discussed by Yang and Lee (1984). With an attractive methodology they incorporated heuristic combinatorial optimization to optimize a criteria called normalized volume index (NVI) of the manipulator. This index resembles a normalized ratio of the total volume of the workspace to the total link length. They also made a comparison between the optimality of the workspaces of some of the commercially available robot arms, finally they made an interesting comparison between the proportion of a human arm and an optimum RRRS manipulator.

Cwaiakala and Lee (1985) presented an algorithm to detect the boundary profile of a general n-Link manipulator as well as to perform quantitative evaluation of the workspace volume. This algorithm is not limited to the robots with revolute joints. The algorithm is based on an optimum path search technique to facilitate a partial grid scanning of the workspace projected onto a cutting plane.

Yang and Lai (1985) made an extensive investigation of the dexterity of 6R manipulators in their corresponding reachable working space. The concept of service angle of a robot to a given point was expanded and also the concepts of service points, service regions and free service regions in the workspace were introduced.

Kohli and Spanos (1985) and Spanos and Kohli (1985) proposed a new technique for analytical investigation of the workspace of manipulators with spherical wrists (those whose last three revolute joint axes intersect orthogonally at a point). This technique is based on polynomial displacement equations and their discriminants. Also the dexterity of the manipulators in terms of number of ways to reach a specified position in their workspace was investigated and subsequently they proposed a method to obtain the boundaries separating regions of different order of accessibility. Finally degeneracy conditions for several types of manipulators were derived.

The concepts of **aspects** and **aspect decomposition** of the workspace of n-Link manipulators were proposed by Liegeois et al., (1985). They presented an algorithm for automatic determination of the volumetric model of the

workspace of arbitrary robots in cartesian space. They examined the rank of minors of the Jacobian matrices in order to detect the various aspects or postures in the joint space which are the subsets of the workspace, and are bounded by the mechanical limits of the joint variables and by families of special singular configurations of the manipulators.

The reachable workspace and effects of the link lengths on its shape for a simple closed loop manipulator (planar, revolute jointed, five-bar chains) was investigated by Bajbai and Roth (1986).

Kumar and Patel (1986) developed an iterative computer graphics system to map the workspace of a generalized manipulator with constrained revolute or prismatic joints. They also discussed the workspace characteristics such as size, shape and presence of Holes and Voids.

Borrel and Liegois (1986) expanded on the concepts of aspects and aspect decomposition which was presented by their earlier paper and based on the aspects of a workspace they discussed the predetermined trajectories which avoid mechanical limits of the manipulator actuators. Moreover a CAD system was used to develop three dimensional image of a 5-R robot manipulator.

Manipulator design problem with considerations on the workspace optimization was discussed by Shaik and Dutseris (1986). A method was presented for the calculation of workspace volume of generalized manipulators which include both revolute and prismatic joints.

Nelson et al. (1987) reported the development of a graphical package

which can automatically locate a part assembly task in a robot's workspace in order to optimize the manipulability of the robot for that task. Manipulability was defined in terms of the eigenvalue and eigenvector of the Jacobian matrix.

Davidson and Hunt (1987) and Davidson and Pingali (1987) presented a thorough investigation of the attitudinal dexterity of the end effectors workspace (possibilities and limitations of orientation of the hand in reaching a point inside the workspace). The concept of plane workspace of end effector was also defined as the set of all directed planes attached to the end effector with respect to the fixed frame of the manipulator. Moreover an algorithm for the generation of the envelop of the plane-workspace of generally proportioned manipulators was proposed. Finally they discussed design conditions which ensure that a manipulator will posses certain dexterity properties in its workspace.

Oblak and Kohli (1988) defined the bounding surfaces of a regional structure manipulator workspace in the form of Jacobian surfaces (where the Jacobian is singular) and D-surfaces (where one or more of the joints achieve a limit position). Moreover a methodology was proposed for identification of these surfaces ,and examples of RPP and 3R regional structures were presented for illustration of the proposed method.

Tsai and Chiou (1990) presented an attractive and thoughtful investigation of the manipulability of robot manipulators. Different manipulability criteria were discussed and joint availability index was proposed to be incorporated in the control algorithm to make full use of the

joint availability. They also maintained that by testing the closeness of a manipulator to singularity, a robot can change aspect before one of its joints limits is reached. Screw system and its properties were used as the basic kinematic tool to formulate the singularities and degenerate cases of the manipulators.

2.3- MULTI-MANIPULATOR SYSTEMS

In this section we will present a survey of the published research work pertinent to the problem of multi-arm or two-arm robotic systems and closed kinematic chains. Since among these works not many of them dealt with the kinematics and geometrical considerations and the only major contributions have been focused on the dynamical behavior and control schemes for such systems, thus we will review major contributions which in part are concerned with the kinematics and geometrical considerations such as workspaces and the layout of the multi or two arm robots and in part concerned with dynamic and control.

The first paper published to present the concept of Master-Slave in remote manipulation can be considered as the origin of the multi-manipulator systems. It was published by Guertz et al., (1966). In this scheme an operator had to specify internal coordinates of the executive manipulator (Master) with the neuromuscular complex of his hand.

In 1974 two papers were published separately dealing with the use of two manipulators (bilateral manipulator system) in coordination. Gavrilovic and

Selic (1974) discussed synergistic control of pair of manipulator systems versus the Master-Slave concept. Coordination between two manipulators, constraints, singularities and computation of synergistic control of bilateral manipulator systems were considered. It was argued that in a Master-Slave model presented by Guertz et al., (1966) the operator specifies internal coordinates of the executive manipulator with the neuromuscular complex of his hand, whereas with the synergistic control concept, the operator specifies the parameters of motion for the object which is being manipulated.

The second paper was done by Eiji et al., (1974) which presented the studies on a pair of anthropomorphous manipulators called "MELARM" to achieve manipulation of objects, without human interaction, by the effective use of two mechanical arms. Coordination between all the actuators as well as effective cooperation of the arms to do work were discussed. Melarm was a human-like manipulator with seven joints on each arm and a force sensor on each joint. The pair of manipulators were symmetrical and they were controlled by a minicomputer as well as manually by a master manipulator and Joysticks.

Ishida (1977) discussed in more detail about the two-arm robots. He considered two fundamental tasks, 1- The parallel transfer task and 2- The rotational transfer task. He maintained that the more complex tasks can be viewed as combinations of the aforementioned basic tasks. He proposed to use force control schemes by mounting force sensors on the wrist of the robots to control the motor's torque instead of joint position control.

Konstantinov and Markov (1980) presented a method of analysis of complex assembly operations which require more than six degrees of freedom. They discussed a kinematic inversion of the frame towards one of the middle links which in turn would lead to the concept of two-hands robots. They discussed the organization of any fitting motions with a closed kinematic chain using the relative space between the two end effectors. Mobility of a two-hand robot was considered by them.

Orin and Oh (1981) investigated the control of the force distribution in locomotion and manipulation systems containing closed kinematic chains. They solved the input joint torques for a particular system trajectory. They used linear programing to obtain a solution which optimizes a weighted combination of energy consumption and load balancing. Inequality constraints on the maximum actuator torques and reaction forces at the tip of each chain of the system were imposed, in addition to equality constraints which specify movement in a desired system trajectory.

Konstantinov et al., (1983) discussed a particular assembly operation namely fitting a prismatic body in a prismatic opening by using a two-hand robotics unit. This was an extension to the earlier work; Konstantinov and Markov (1980).

Nonlinear control of multi-robot system was first presented by Freund (1984). He considered the dynamics of all the robots involved in developing a design strategy for the nonlinear control system.

Coordinated control of two robot arms was also discussed by Alford and

Belyeu (1984). They used a Master-Slave strategy for the control of a pick and place operation with some imposed constraints on the orientation of the workpiece throughout the path. This work has been referenced by the majority of the subsequent research works in the related research area.

Acker et al., (1985) presented the design and development of a multi-arm assembly robots called **TROIKOBOT**. They used three puma-560 robot in coordination for a complex three dimensional assembly operation which required variety of parts mating and insertion procedures.

Luh and Zheng (1985) first elaborated on the computation of input generalized forces for robots with closed kinematic chain mechanisms. Industrial robots with three-dimensional closed linkages were considered. The basic idea was to virtually cut open then analyze the kinematics of the virtual open-chain and next apply the holonomic constraints. This would lead to a tree-structured open-chain mechanism with kinematic constraints.

Zheng and Luh (1985a) and (1985b) primarily analyzed the coordinated relations between two robot arms by deriving the imposed sets of holonomic constraints on the relative positions and orientations of the two end-effectors. Three different cases were investigated for, two arms handling a rigid body object, handling a pair of pliers and handling an object with a spherical joint. It was also discussed that one of the arms (called the main arm) is assigned to carry the major part of the task and its motion is planned accordingly. The motion of the second arm (called the follower arm) is to follow that of the first robot as specified by the constraint relations between their joint velocities so that the motion error between them is

eliminated. In the second paper they extended their analysis to the constraint relations between joint accelerations of the two robots for the three aforementioned cases. Using the Jacobian they expressed generalized joint forces in terms of forces/torques exerted on the end effectors and finally they developed a control scheme based on the generalized joint forces.

In the work by Zheng and Sias (1986) the collision effects on the robot motion were studied for coordinated two-arm robots. It was suggested that by measuring the magnitude and direction of impulsive forces produced by the direct or indirect collision between the two hands one can compute the position and the orientation of the end effectors.

Hemami (1986b) discussed the kinematic relationship between a two-arm robotic system. The elements of the homogeneous matrices for the follower arm were obtained in terms of those of the main (master) arm for two different set-up of the dual arm configurations. And in (Hemami 1996a) the problem of collision and obstacle avoidance schemes were investigated.

Tarn et al., (1986) presented a new control method for the coordinated control of two robot arms based on exact system linearization by appropriate nonlinear feedback. The proposed method uses a dynamic coordinator acting on relative position and velocity errors and/or on relative force-torque errors between the two arms.

A mathematical model for several constrained robot system configuration was proposed by McClamroch (1986). This model was expressed as singular

system of differential equations. One potential application to this model can be two robot arms with end effectors grasping an inertial load (a common work piece).

Hayati (1986) expanded on the hybrid position/force control of multi-arm cooperating robots.

Roach and Boaz (1987) investigated the problem of path-planning for concurrent actions of two manipulators operating within a shared environment. A time/space planning system to coordinate the actions of two robots for transfer movements was reported.

Mechanics of coordinated multi-manipulation was discussed by Nakamura et al., (1987). They investigated the internal forces between the robot hands and the resultant forces on the manipulated object. Also the optimal internal force was defined as the internal force that yield the minimal norm force, satisfying static frictional constraints.

Tarn et al., (1987) used closed chain formulation to treat a coordinated two-arm robot and the manipulated object as a whole and thus discussed the design of dynamic control of the closed chain.

Lim and Chyung (1987) used a resolved position control strategy to execute a coordinated material handling task by a two-arm robot. The path of the object was first determined in the cartesian coordinate system, and the corresponding joint variable trajectory was evaluated for each robot, and then each robot was position controlled.

Optimal load distribution for two industrial robots, handling a single object was discussed by Zheng and Luh (1988). Two performance criteria were examined for the optimization of the load distribution between the robots, namely the least energy consumption which lead to computationally inefficient scheme for real time, and the minimum exerted forces on the object which found to be more efficient.

A nonlinear optimization technique was used by Lim and Chyung (1988) to find an admissible trajectory for two cooperating robot arms with limited joints acting on a common object.

Swern and Tricamo (1988) used the force/torque sensors data of a two-arm robot handling a common object to reduce the constraint forces (internal forces) acting on the object during the task execution. This was done by supplying a position correction scheme to each arm to decrease the internal forces.

Kazerooni (1988) investigated the compliance control and stability analysis of cooperating robot manipulators.

An extensive discussion on real-time path finding and coordinated nonlinear control of multi robot systems was made by Freund and Hoyer (1988). They proposed a hierarchical coordinator for real-time collision avoidance. An analytically described avoidance trajectory was developed which served both as collision detection and avoidance.

Koivo and Bekey (1988) produced a summary of a workshop on coordinated multiple-manipulators (CMM). The major topics of the survey were discussed under three research subjects of;

1- Motion planning, obstacle avoidance and sensing of the CMM.

2- Dynamical modeling and control systems of the CMM.

3- Software and artificial intelligence in the CMM.

Crignan and Akin (1989) presented a parameter optimization technique for deciding the force distribution on the payload being transported along a predetermined trajectory using two planar robot arms. And collision-free trajectory planning for two planar robot arms was discussed by Shin and Bien (1989).

Nahon and Angeles (1989) investigated force optimization in redundantly actuated closed kinematic chains in multiple manipulators, walking machines and mechanical hands. They discussed the origin of redundant actuation in closed kinematic chains, their relationship with time-varying topologies and their desirability in practical applications.

Dynamic and kinematic behavior of the coordinating robots in assembly was mathematically modeled by Zheng (1989). He decomposed a typical assembly task into three phases as, independent motion phase, contact phase and constraint motion phase. He then derived the mathematical model for each phase.

Tao and Luh (1989) described coordination of two redundant robots in a coordinated operation. They developed the optimal force distribution strategy

under the known posture. Manipulability was defined in terms of the Jacobian matrix, and was set to be the optimization criterion. Singularity, manipulability and force ellipsoids were also discussed.

In Gardner et al., (1989) the instantaneous kinematics of a parallel manipulator with redundantly actuated closed chains were discussed. It was shown that, in force control or hybrid control schemes for such systems, the redundancy in actuation allows the specification of force set-points that would ensure an optimal load distribution. Moreover, the singularities in the inverse kinematics and static equations for such systems were analyzed.

O'Donnell and Lozano-perez (1989) investigated the path planning strategies for coordinated two-arm robot systems. Their main emphasis have been on the collision avoidance between the two robots as well as on deadlock avoidance (situations where each manipulator is waiting for the other to proceed). Degree of coordination in this scheme was assumed to be low, that is two robots share a common workspace but they are not dynamically coupled through the manipulated object.

The distribution of the internal forces applied to a commonly held object by multi manipulators was investigated by Walker I.D. et al. ,(1989). And Walker W.M. et al., (1989) expanded on the adaptive coordination control of two-arm robots.

Adaptive control of multiple coordinated robot arms was also investigated by Hu and Goldenberg (1989). They generated three subsystem error equation in the adaptive control scheme, namely a position error

subsystem, a contact force error subsystem and an internal force error subsystem.

A hybrid position/force control strategy for multiple manipulators handling a common object on a constrained environment was proposed by Yoshikawa and Zheng (1990). They considered simultaneous control of the object motion and of the internal forces exerted by the arms on the object, as well as the control of constrained forces due to the contact between the object and the environment.

The simulation of cooperating two-arm robots on a mobile platform was presented by Murphy et al., (1990). They developed the dynamic equations of motion for two manipulators holding a common object on a freely moving mobile platform, and the dynamic interactions from arms-to-platform and arm-tip to arm-tip were included in the simulations.

Kinematic constraint relations in differential form among internal velocities and accelerations of manipulators involved in cooperative manipulation was discussed by Djurovic and Vukobratovic (1990). They investigated the dynamic model of cooperative manipulation of a rigid object in the absence of external constraints on the motion.

Koivo and Unseren (1990) developed a Dynamic model for the closed chain motion of two N-joint manipulators holding a rigid object. They derived the holonomic constraints and combined them with the equations of the motion of the manipulators and of the object to obtain the dynamical model of the entire system. Subsequently the behavior of the generalized contact forces

and their impacts on the coupling among the individual components of the system in the model were investigated.

Hemami et al., (1990a) presented an investigation of feasibility of coordinated two-arm robotic operations in material handling. This investigation primarily deals with the reachability of a desired task, and necessary adjustments which one can made on an un-acessible path in order to verify the reachability along the path.

2.4- OPTIMIZATION OF THE SET-UP OF TWO-ARM ROBOTICS SYSTEMS

Among the published research papers dealing with two-arm robots, there has not been any report investigating exclusively the relative set-up (or layout) of the work cell, that is the best position/orientation of each robot's base coordinate frame relative to the desired trajectory. However the aforementioned problem has been touched indirectly by some authors while discussing optimum path planning, optimal dynamic analysis and optimization of the workspaces.

For example in Tsai and Soni (1981) one section has been devoted to the synthesis of robots which can reach some specified planar working positions. They assigned some arbitrary values to the coordinates of the origin of the planar robots expressed with respect to the world coordinate frame (X_o,Y_o). Next they optimized the reachable working area of the robot which encompasses the pre defined trajectory. Design variables in this scheme were chosen to be the X_o, Y_o coordinates as well as the link length ratio and the joint limits

of the robot, θ_{max} and θ_{min}.

Schmitt et al., (1985) discussed the optimal motion programming of a single robot arm. They defined several performance indices to be incorporated in the optimization procedures to determine the optimal path which satisfies the initial and final position/orientation of the defined task. For example joint reaction torque values, output power and execution time were proposed as some suitable performance criteria.

Longman et al., (1987) presented the kinematics and dynamics of satellite-mounted robot manipulators. They discussed that, since the base frame of the satellite-mounted robots is fixed in the space shuttle which is not inertially fixed, therefore the commanded motion of the robot arm produces reaction forces and reaction moments on the shuttle. The effects of these forces and moments were then investigated on the kinematics of the manipulator. However since reachability, manipulability and relative position/orientation of the robot and the task have not been taken into consideration in this work, thus the aforementioned robotics systems are primary candidates for the optimization of the relative set-up introduced in this thesis.

On the other hand in Nelson et al., (1987) the reachability and manipulability of a robotic task execution was improved by assuming that the robot is already fixed with respect to an inertial coordinate frame but one has the flexibility to locate the desired trajectory inside the workspace of the robot.

Murphy et al., (1990) described the simulation of the dynamics of cooperating two-arm robots which are mounted on a freely moving platform. However they did not consider the relative position and orientation of the robot bases with respect to the desired task. This matter will be discussed in chapter seven of this thesis.

Hemami et al., (1990), discussed synthesis of the set-up for a case study, in material handling, by two collaborating robot arms. The feasibility of the task was investigated in terms of the robot workspaces and the relative position of the two robots.

Ranjbaran et al., (1990), presented synthesis of the set-up of coordinated two-arm robots by formulating a non linear programming inorder to optimize the joint availabnility of the collaborating robots. In the synthesis of the set-up both position and orientation of the bases of the manipulators were considered.

CHAPTER 3
KINEMATICS OF ROBOT MANIPULATORS

3.1- INTRODUCTION

This chapter is devoted to the construction of the basic kinematics formulations of a general robot arm These formulations will constitute a basis for construction of the forthcoming methodologies and algorithms in the subsequent chapters. Numerous books and research papers have been published, dealing with the kinematics of spatial kinematic chains and robot manipulators. These extensive investigations cover a wide spectrum of the kinematic analysis and synthesis of the manipulators and spatial multi-body systems (for the references see section 2.1). Different approaches proposed by the kinematicians have been directed towards a common objective of developing transformations or mappings between the manipulators joint coordinate space and its hands cartesian space (and vice versa). However different mathematical tools and strategies have been employed in the process of these developments.

The intention in this chapter is not to contribute any novelties to the aforementioned subject, but merely to represent a review of the kinematic method of analysis based on homogeneous point coordinate transformation which have been very popular and commonly used amongst the researcher in the field of robot kinematics and dynamics, and will be used in this thesis as well.

Section 3.2 is devoted to review a systematic methodology of frame

assignments to a given manipulator. In section three homogeneous point coordinate transformations and the corresponding Denavit and Hartenberg symbolic notations will be discussed and based on this formalism the kinematic formulations of a robot manipulator will be developed. Section four is devoted to give insight into the application of line coordinate transformations and screw coordinates in the kinematics of manipulators.

3.2- FRAME ASSIGNMENTS DENAVIT AND HARTENBERG NOTATIONS

In this section the Denavit and Hartenberg (DH) notations and parameters as well as the coordinate frames assigned to each link of a robot manipulator will be discussed. The approach taken in this thesis for definition of the parameters is based on Denavit and Hartenberg discussed in Lee (1982). The first link of the manipulator namely O_0 frame which is not considered part of the robot is attached to a supporting base which normally is considered inertial. However as we will discuss in the following chapters sometimes the base of the robot is attached to a moving frame relative to the inertial frame (*e.g.* space shuttle mounted manipulators). In this case a world coordinate frame O_w will be assigned to designate the inertial coordinate frame.

The joints and links are numbered outward from the base, thus joint 1 is the connection between link *1* and the supporting base link *0*. Each link is connected to two other links at most, so no closed loop will be formed. A joint axes is established at the connection of two links (Figure 3.1). An orthonormal Cartesian coordinate system $(O_i;x_i,y_i,z_i)$ can be assigned to each

link at its joint axis, i = 1,2,3,...n, where n is the degree of freedom of the manipulator. Each $(O_i;x_i,y_i,z_i)$ coordinate frame of a robot arm correspond to joint $(i+1)$ and is fixed in link i. When the joint actuator activates the joint i, link i will move with respect to link $(i-1)$. Since the ith coordinate system is fixed in link i, it moves together with link i. Thus the nth coordinate frame moves with the hand (link n).

The base coordinates are defined as the *0th* coordinate frame $(O_0;x_0,y_0,z_0)$, which is usually the same as the inertial frame. In order to assign coordinate frames to each link we follow the same steps as suggested by Lee (1982), namely;

a) The z_{i-1} axes lies along the axis of motion of the ith joint.

b) The axis x_i is normal to the z_{i-1} axis pointing away from it.

c) The y_i axis completes the right hand coordinate system.

Hence the location of the base frame O_0 can be chosen anywhere in the supporting base, as long as the z_0 axis lies along the axis of motion of the first joint. The last coordinate frame (nth frame) can be chosen anywhere in the hand as long as the x_n axis is normal to the z_{n-1} axis.

Four geometric parameters can be defined for a manipulator which can completely describe any revolute or prismatic joint and its displacements relative to the neighboring joints. These four parameters are called the Denavit and Hartenberg or DH parameters and are defined as follows.

θ_i : The joint angle from the x_{i-1} axis to x_i axis about z_{i-1}axis (using

right hand rule).

d_i : The distance from origin of the $(i-1)th$ coordinate frame to the intersection of the z_{i-1} with the x_i axis along the z_{i-1} axis.

a_i : The distance from the intersection of the z_{i-1} axis with the x_i axis to the origin of the ith frame along the x_i axis (or shortest distance between $z_{i-1}$and z_i).

α_i : The offset angle from the z_{i-1} axis to the z_i axis about the x_i axis, (using the right hand rule).

For a rotary joint, d_i, a_i and α_i are the joint parameters and remain constants for a robot, while θ_i is the joint variable that changes when link link i moves (rotates) with respect to link i_{i-1}. For a prismatic joint, θ_i, a_i and α_i are joint parameters and remain constant but d_i is the joint variable and changes when link i translates along z_i relative to z_{i-1}. a_i and α_i are usually called the length and twist angles of the link i, respectively, and d_i is called the joint offset.

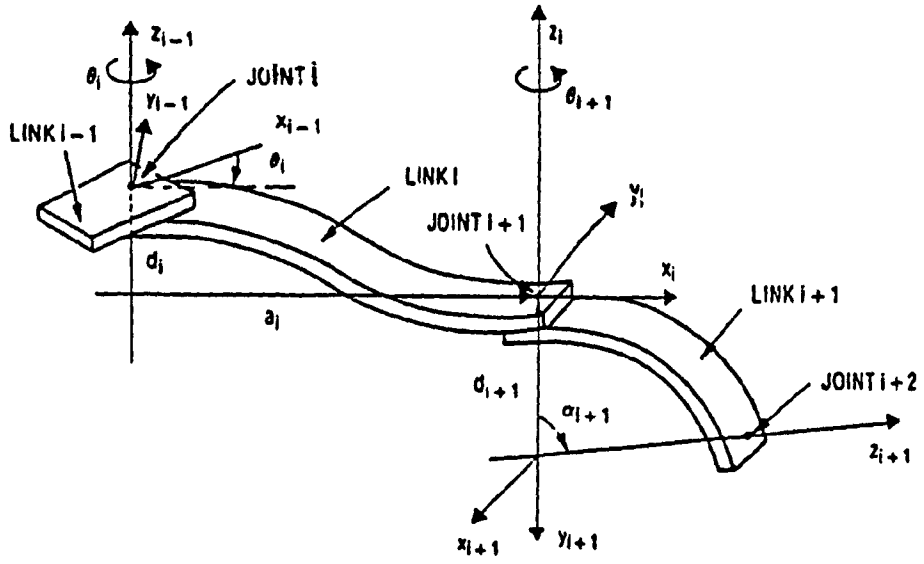

Figure 3.1 - Representation of the DH parameters (C.S.G. LEE 82)

3.3- HOMOGENEOUS TRANSFORMATIONS WITH 4X4 MATRICES

Although by and large homogeneous transformations are the most popular tools for handling the kinematics problem of the robotic systems, other approaches have been introduced by the researchers as well, some of these techniques are, **Screw Calculus, Tensor Analysis, Vector Analysis with Dual Number Quaternion Algebra** (references are given in chapter 2).

The homogeneous transformations are used to solve two major problem of Direct (or Forward) and Inverse kinematics of the robot manipulators:

- The direct kinematics or the forward kinematics problem is to find the kinematic attitude of the end point (End Effector) of the robot, given the vector of the joint displacements;

$$\theta = [\theta_1 \ \theta_2 \ \theta_3 \ \theta_4 \ \cdots \theta_n]^T \quad \text{for a n-axis robotic manipulator.}$$

- The inverse kinematics problem involves in finding the vector of the joint displacements θ_i, $i = 1,2,\cdots n$ for n-axis manipulator, given the kinematic attitude of the gripper or the end effector with respect to the base coordinate frame. The inverse kinematic problem is the most desirable problem to solve, since it is the basic tool in flexible automated manufacturing and assembly operations.

Point coordinate transformation by using 4x4 homogeneous transformations matrices were introduced in chapter one. In this section the characteristics of the elements of these mathematical tools for the kinematic studies of mechanical manipulators will be discussed.

The general structure of these matrices is shown as follows:

$$T=\left[\begin{array}{c|c} R_{3x3} & p_{3x1} \\ \hline f_{1x3} & 1 \end{array}\right]=\left[\begin{array}{c|c} \begin{matrix}\text{rotation}\\ \text{matrix}\end{matrix} & \begin{matrix}\text{position}\\ \text{vector}\end{matrix} \\ \hline \begin{matrix}\text{perspective}\\ \text{transformation}\end{matrix} & \begin{matrix}\text{scaling}\\ \text{factor}\end{matrix} \end{array}\right] \tag{3.1}$$

R_{3x3} is an orthogonal rotation matrix which defines the orientation of on coordinate frame with respect to another. This sub matrix together with perspective sub matrix and the scale factor will be further discussed in the following section. p_{3x1} is the position vector defining a point in the cartesian coordinate system.

3.3.1- ROTATION MATRIX

A 3x3 rotation matrix can be used to describe the rotational operations of the body attached frames with respect to the world reference frame. In other words a 3x3 rotation matrix is a transformation matrix that operates on a position vector in a 3 dimensional Euclidean space and maps its coordinates expressed in a rotated coordinate system to a reference coordinate system (Lee 1982). In order to obtain a geometrical image of the rotational transformation we consider a cartesian 3-dimensional Euclidean reference frame $(O_o;x,y,z)$ which is fixed in 3-D. space. Moreover consider a rigid body which is rotating with respect to this reference frame. We attach temporarily and conveniently a local reference frame to the body say $(O_j;x_j,y_j,z_j)$ this is called a body-attached coordinate frame. Let (e_{01},e_{02},e_{03}) and (e_{j1},e_{j2},e_{j3}) be the unit vectors along the coordinate axes of $(O_0;x_0,y_0,z_0)$

and $(O_j;x_j,y_j,z_j)$ respectively. A point p in space can be represented by its coordinate with respect to both coordinate systems. If p is fixed with respect to $(O_j;x_j,y_j,z_j)$ then it can be represented by its coordinates in both system as follows

$$p_0 = (p_{0x},p_{0y},p_{0z})^T \quad \text{and} \quad p_j = (p_{jx},p_{jy},p_{jz})^T \quad \text{respectively.}$$

The foregoing vectors represent the same point in space with respect to two different coordinate systems. If we are given the coordinates of p in O_j system (rotated frame) and we want to obtain its coordinate in the reference inertial frame O_0 frame, then we look for an operator for mapping defined with matrix R which maps the O_j coordinate to the corresponding O_0 coordinates or

$$p_0 = R_0^j p_j \tag{3.2}$$

Moreover if we show the vector p_j in terms of its components along the axes

$$p_j = p_{j1}e_{j1} + p_{j2}e_{j2} + p_{j3}e_{j3} \tag{3.3}$$

Components of p in the O_0 system are basically the projection of p onto the respective axes, thus using the inner or scalar product definition we can get

$$\begin{aligned} p_{0x} &= e_{01}\cdot p_j = e_{01}\cdot e_{j1}p_{j1} + e_{01}\cdot e_{j2}p_{j2} + e_{01}\cdot e_{j3}p_{j2} \\ p_{0y} &= e_{02}\cdot p_j = e_{02}\cdot e_{j1}p_{j1} + e_{02}\cdot e_{j2}p_{j2} + e_{02}\cdot e_{j3}p_{j2} \\ p_{0z} &= e_{03}\cdot p_j = e_{03}\cdot e_{j1}p_{j1} + e_{03}\cdot e_{j2}p_{j2} + e_{03}\cdot e_{j3}p_{j2} \end{aligned} \tag{3.4}$$

Or expressed in matrix form, equation (3.2) will get the following form

$$\begin{bmatrix} p_{0x} \\ p_{0y} \\ p_{0z} \end{bmatrix} = \begin{bmatrix} e_{01}\cdot e_{j1} & e_{01}\cdot e_{j2} & e_{01}\cdot e_{j3} \\ e_{02}\cdot e_{j1} & e_{02}\cdot e_{j2} & e_{02}\cdot e_{j3} \\ e_{03}\cdot e_{j1} & e_{03}\cdot e_{j2} & e_{03}\cdot e_{j3} \end{bmatrix} \begin{bmatrix} p_{0x} \\ p_{0y} \\ p_{0z} \end{bmatrix} \tag{3.5}$$

Where

$$R_0^J = \begin{bmatrix} e_{01}\cdot e_{j1} & e_{01}\cdot e_{j2} & e_{01}\cdot e_{j3} \\ e_{02}\cdot e_{j1} & e_{02}\cdot e_{j2} & e_{02}\cdot e_{j3} \\ e_{03}\cdot e_{j1} & e_{03}\cdot e_{j2} & e_{03}\cdot e_{j3} \end{bmatrix} \tag{3.6}$$

Similarly, we can obtain the inverse transform, or the transformation matrix which maps the coordinates in O_0 system to O_j. In other words if A_j^0 is a transformation matrix which operates on p_0 and gives the coordinates of p_j then

$$\begin{bmatrix} p_{jx} \\ p_{jy} \\ p_{jz} \end{bmatrix} = \begin{bmatrix} e_{j1}\cdot e_{01} & e_{j1}\cdot e_{02} & e_{j1}\cdot e_{03} \\ e_{j2}\cdot e_{01} & e_{j2}\cdot e_{02} & e_{j2}\cdot e_{03} \\ e_{j3}\cdot e_{01} & e_{j3}\cdot e_{02} & e_{j3}\cdot e_{03} \end{bmatrix} \begin{bmatrix} p_{0x} \\ p_{0y} \\ p_{0z} \end{bmatrix} \tag{3.7}$$

Where

$$R_j^0 = \begin{bmatrix} e_{j1}\cdot e_{01} & e_{j1}\cdot e_{02} & e_{j1}\cdot e_{03} \\ e_{j2}\cdot e_{01} & e_{j2}\cdot e_{02} & e_{j2}\cdot e_{03} \\ e_{j3}\cdot e_{01} & e_{j3}\cdot e_{02} & e_{j3}\cdot e_{03} \end{bmatrix} \tag{3.8}$$

By comparing 3.8 and 3.6 and noting that dot product is commutative,we can realize the following relationship

$$R_j^0 = (R_0^j)^{-1} = (R_0^j)^T \tag{3.9}$$

or,

$$R_0^j R_j^0 = R_0^j (R_0^j)^{-1} = I_3$$

This shows that the rotation matrix is orthogonal and since the elements of **R** are all unit vectors thus **R** is orthonormal as well. If we agree that all of the rotations considered are made with respect to the base coordinate frame O_0 then it is possible to omit the subscript indicating the reference frame from **R**. However we introduce new subscript to **R** in order to designate the axis and the angle of rotation respectively for example, If coordinate frame O_j is rotated about the x axis of the reference frame O_0 then the position vector of a point in O_j coordinate system can be transformed into the O_0 system from the following relationship,

$$p_0 = R(x,\alpha)p_j = \begin{bmatrix} 1 & 0 & 0 \\ 0 & \cos\alpha & -\sin\alpha \\ 0 & \sin\alpha & \cos\alpha \end{bmatrix} \tag{3.10}$$

or

$$R(x,\alpha) = \begin{bmatrix} 1 & 0 & 0 \\ 0 & \cos\alpha & -\sin\alpha \\ 0 & \sin\alpha & \cos\alpha \end{bmatrix} \tag{3.11}$$

By the same token one can obtain two more rotation matrices defining rotations of φ about y and θ about z axis respectively as,

$$R(y,\varphi) = \begin{bmatrix} \cos\varphi & 0 & \sin\varphi \\ 0 & 1 & 0 \\ -\sin\varphi & 0 & \cos\varphi \end{bmatrix} \tag{3.12}$$

$$R(z,\theta) = \begin{bmatrix} \cos\theta & -\sin\theta & 0 \\ \sin\theta & \cos\theta & 0 \\ 0 & 0 & 1 \end{bmatrix} \tag{3.13}$$

$\mathbf{R}(x,\alpha)$, $\mathbf{R}(y,\varphi)$ and $\mathbf{R}(z,\theta)$ are called the basic rotation matrices. Some authors have referred to them as the canonical form of the rotation matrices or proper orthogonal matrices (Angeles 1982). It is possible to obtain a rotation matrix about an arbitrary direction $\mathbf{k}$ by an angle θ. Let express $\mathbf{k}$ by its components k_x, k_y, k_z in the O_0 reference frame as

$$\mathbf{k} = k_x \mathbf{e}_{01}, k_y \mathbf{e}_{02}, k_z \mathbf{e}_{03} \tag{3.14}$$

Then it can be shown that the rotation matrix $\mathbf{R}(\mathbf{k},\theta)$ has the following form (Lee 1981).

$$\mathbf{R}(\mathbf{k},\theta) = \begin{bmatrix} k_x k_x vers\theta + cos\theta & k_y k_x vers\theta - k_z sin\theta & k_z k_x vers\theta + k_y sin\theta \\ k_x k_y vers\theta + k_z cos\theta & k_y k_y vers\theta + cos\theta & k_z k_y vers\theta - k_x sin\theta \\ k_x k_z vers\theta - k_y cos\theta & k_y k_z vers\theta + k_x sin\theta & k_z k_x vers\theta + cos\theta \end{bmatrix} \tag{3.15}$$

Some of the useful properties of the rotation matrices are as follows (Angeles 1982).

a) Knowing rotation $\mathbf{R}$ The angle of rotation about an axis $\mathbf{k}$ can be obtained from

$$\theta = cos^{-1}\{\frac{1}{2}(\mathrm{Tr}(\mathbf{R}))\} \tag{3.16}$$

however the sign of the angle θ can not be inferred from the above equation since $cos(-\theta) = cos(\theta)$, and instead the following identity can be used to detect the sense of rotation;

$$sgn(\theta) = sgn(\mathbf{r}\times\mathbf{r}'\cdot\mathbf{k})$$

Were $\mathbf{r}$ and $\mathbf{r}'$ are initial and final position vectors of a point not lying on the axis of rotation and measured in O_0 coordinate system.

b) Rotation matrices are proper orthogonal matrices, this implies that their determinant is always +1 irrespective of the choice of coordinate frame, moreover, they posses only one real eigenvalue which is unity.

c) The direction vector of a rotation expressed by a rotation matrix is the eigenvector of the rotation matrix associated with its +1 eigenvalue.

d) Any rotation matrix **R** can be expressed as

$$\mathbf{R} = e^{\mathbf{A}\theta} \tag{3.17}$$

where θ is the angle of rotation and **A** is a nilpotent matrix with its real eigenvector being the axis of rotation

$$\mathbf{A} = \begin{bmatrix} 0 & -k_z & k_y \\ k_z & 0 & -k_x \\ -k_y & k_x & 0 \end{bmatrix} \tag{3.18}$$

3.3.2- HOMOGENEOUS COORDINATES AND TRANSFORMATION MATRICES:

When a rotation matrix operates on a position vector no information regarding the translation or scaling will be obtained. However by adding a fourth coordinate d to the 3 dimensional position vector $\mathbf{p} = [p_x, p_y, p_z]^T$ one can write $\hat{\mathbf{p}} = [p_x, p_y, p_z, w]^T$ (see Lee 1988). We say that $\hat{\mathbf{p}}$ is expressed in

the homogeneous coordinate. In general the representation of an n-component position vector by an (n+1)-component is called homogeneous coordinate representation. In order to avoid complexities in our notations from now on the hat representing homogeneous coordinates will be omitted thus **p** alone will represent position vector in 3-D space expressed with homogeneous coordinates. In a homogeneous coordinates representation, the transformation of an n-dimensional vector is performed in an n+1 dimensional space, and the physical n-dimensional vector is obtained by dividing the homogeneous coordinates by the forth coordinate *w*. In fact the forth coordinate *w* can be viewed as a scale factor therefore if this factor is unity (w=1), then the transformed homogeneous coordinates of a position vector are the same as the physical coordinates of the vector. In robotic the scale factor always equals 1, however in computer graphics it can take on any nonzero value for scaling. Homogeneous coordinate representation of points in a 3-D Euclidean space is useful in developing matrix transformation that include rotation, translation, scaling, and perspective transformation. The general structure of these matrices is given in equation 3.1, and so far the upper left 3x3 submatrix (the rotation matrix) has been defined. Next the perspective submatrix of 3.1 will be discussed.

The perspective transformation is a 1x3 sub-matrix which is useful for computer vision and the calibration of the camera model. For a null perspective the elements of this sub-matrix take on zero values.

If a position vector **p** is expressed in homogeneous coordinates ($p=(p_x,p_y,p_z,1)^T$) then the 3x3 rotation matrix can be extended to a 4x4 homogeneous transformation matrix for pure rotation operations. Thus the

basic rotation matrices defined in equations 3.11-13 can be expressed in a homogeneous form as follows:

$$Rot(x,\alpha) = \begin{bmatrix} 1 & 0 & 0 & 0 \\ 0 & \cos\alpha & -\sin\alpha & 0 \\ 0 & \sin\alpha & \cos\alpha & 0 \\ 0 & 0 & 0 & 1 \end{bmatrix} \tag{3.19}$$

$$Rot(y,\varphi) = \begin{bmatrix} \cos\varphi & 0 & \sin\varphi & 0 \\ 0 & 1 & 0 & 0 \\ -\sin\varphi & 0 & \cos\varphi & 0 \\ 0 & 0 & 0 & 1 \end{bmatrix} \tag{3.20}$$

$$Rot(z,\theta) = \begin{bmatrix} \cos\theta & -\sin\theta & 0 & 0 \\ \sin\theta & \cos\theta & 0 & 0 \\ 0 & 0 & 1 & 0 \\ 0 & 0 & 0 & 1 \end{bmatrix} \tag{3.21}$$

These matrices are called *basic homogeneous rotation matrices*. Similarly one can define *basic homogeneous translation matrix*. Since the upper right 3x1 sub-matrix of the homogeneous transformation matrix has the effect of translating the $(O_j;x_j,y_j,z_j)$ coordinate system, which has parallel axes as the reference frame $(O_0;x_0,y_0,z_0)$ but whose origin is at $(\Delta x,\Delta y,\Delta z)$ of the reference coordinate system or,

$$Trans = \begin{bmatrix} 1 & 0 & 0 & \Delta x \\ 0 & 1 & 0 & \Delta y \\ 0 & 0 & 1 & \Delta z \\ 0 & 0 & 0 & 1 \end{bmatrix} \tag{3.22}$$

In summary a 4x4 homogeneous transformation matrix maps a vector expressed in homogeneous coordinates with respect to the $(O_j;x_j,y_j,z_j)$

coordinate system to the reference coordinate system $(O_0;x_0,y_0,z_0)$. That is

$$p_0 = T_0^J p_J \tag{3.23}$$

The homogeneous transformation matrices defining the position and orientation of one coordinate frame with respect to another reference frame are sometimes called the attitude matrices and usually the following notations to represent their elements are used.

$$T = \begin{bmatrix} n_x & s_x & a_x & p_x \\ n_y & s_y & a_y & p_y \\ n_z & s_z & a_z & p_z \\ 0 & 0 & 0 & 1 \end{bmatrix} = \begin{bmatrix} \mathbf{n} & \mathbf{s} & \mathbf{a} & \mathbf{p} \\ 0 & 0 & 0 & 1 \end{bmatrix} \tag{3.24}$$

n, **s**, and **a** are respectively called the normal, slide and approach vectors defining the orientation of the frame $(O_J;x_J,y_J,z_J)$ with respect to the reference frame.

Due to the orthogonality of the rotation matrix, which implies that its inverse is equal to its transpose, the following equation is a characteristic of the homogeneous transformation matrices,

$$T^{-1} = \begin{bmatrix} n_x & n_y & n_z & -\mathbf{n}\cdot\mathbf{p} \\ s_x & s_y & s_z & -\mathbf{a}\cdot\mathbf{p} \\ a_x & a_y & a_z & -\mathbf{s}\cdot\mathbf{p} \\ 0 & 0 & 0 & 1 \end{bmatrix} = \begin{bmatrix} & R_{3x3}^T & & -\mathbf{n}\cdot\mathbf{p} \\ & & & -\mathbf{a}\cdot\mathbf{p} \\ & & & -\mathbf{s}\cdot\mathbf{p} \\ 0 & 0 & 0 & 1 \end{bmatrix} \tag{3.25}$$

3.3.3- KINEMATIC EQUATIONS FOR MANIPULATORS

Having defined the D-H parameters for a robot manipulator as well as the homogeneous transformation matrices in the foregoing sections, we are able to define the homogeneous transformation matrices for a robot manipulator which relate the position and orientation of the ith link to that of the $(i-1)$th link. This transformation can be performed via two translations and two rotations as follows (Lee 1982):

a) Rotate about the z_{i-1} axis by an angle θ_i to align the x_{i-1} axis with the x_i axis . b) Translate along the z_{i-1} a distance d_i to bring the x_{i-1} and x_i axes into coincidence. c) Translate along the x_i axis a distance a_i to bring the two origins together and d) Rotate about the x_i axis an angle α_i to bring the two coordinate systems into complete coincidence.

These four operations can be performed by a basic homogeneous transformation as discussed before. The product of these four basic transformations yields a composite homogeneous transformation matrix A^i_{i-1}, known as the D-H transformation matrix for two adjacent coordinate frames of a manipulator thus:

$$A^i_{i-1} = Trans(z,d_i).Rot(z,\theta_i).Trans(x,a_i).Rot(x,\alpha_i)$$

$$= \begin{bmatrix} C\theta_i & -C\alpha_i S\theta_i & S\alpha_i S\theta_i & a_i C\theta_i \\ S\theta_i & C\alpha_i C\theta_i & -S\alpha_i C\theta_i & a_i S\theta_i \\ 0 & S\alpha_i & C\alpha_i & d_i \\ 0 & 0 & 0 & 1 \end{bmatrix} \qquad (3.26)$$

where $C(.) \equiv cos(.)$, $S(.) \equiv sin(.)$, and α_i, a_i, d_i are constants while θ_i is the joint variable for a revolute joint. In the case of prismatic joint, the joint variable is d_i and α_i, a_i θ_i are constant parameters thus A^i_{i-1} becomes

$$A^i_{i-1} = \begin{bmatrix} C\theta_i & -C\alpha_i S\theta_i & S\alpha_i S\theta_i & 0 \\ S\theta_i & C\alpha_i C\theta_i & -S\alpha_i C\theta_i & 0 \\ 0 & S\alpha_i & C\alpha_i & d_i \\ 0 & 0 & 0 & 1 \end{bmatrix} \tag{3.27}$$

The foregoing matrices in fact relate the homogeneous coordinates of a point p_i which is at rest relative to the link i to its homogeneous coordinates in coordinate system $i-1$ at link $i-1$ or

$$p_{i-1} = A^i_{i-1} p_{i-1} \tag{3.28}$$

- Representation of the hand orientation

The orientation of the robots hand in the tool space as well as the orientation of the object to be manipulated in the task space are usually defined with ,**Euler angles, Role, Pitch, Yaw angles (RPY)** and **Orientation, Attitude, Tool angles (OAT).** In what follows a brief description of these approaches is given.

Euler Angles: Orientation of a body attached coordinate frame (Robots hand or manipulated object) can be specified by a sequence of three rotations, namely a rotation of α about the z axis followed by a rotation of

β about the new y axis and finally a rotation of γ about the new z axis or

$$\mathbf{Euler}(\alpha,\beta,\gamma) = \mathbf{Rot}(z,\alpha)\ \mathbf{Rot}(y,\beta)\ \mathbf{Rot}(z,\gamma)$$

multiplying the three foregoing rotation matrices one can obtain the following rotation matrix (Paul 1981), where the familiar abbreviations for the trigonometric function will be used as, S(.) = *sin*(.), C(.) = *cos*(.).

$$\mathbf{Euler}(\alpha,\beta,\gamma) = \begin{bmatrix} C\alpha C\beta\ C\gamma & -S\alpha S\gamma - C\alpha C\beta\ S\gamma & -S\alpha C\gamma - C\alpha\ S\beta & 0 \\ S\alpha C\beta\ C\gamma & +C\alpha S\gamma - S\alpha C\beta\ S\gamma & +C\alpha C\gamma - S\alpha\ S\beta & 0 \\ -S\beta\ C\gamma & S\beta\ S\gamma & C\beta & 0 \\ 0 & 0 & 0 & 1 \end{bmatrix} \tag{3.29}$$

Figure 3.2 shows the three Euler angles (Paul 1981).

Role, Pitch and Yaw: These three rotations also are used to specify the orientation of the hand of a manipulator. These rotations are made about z, y and x axis respectively and figure 3.3 depicts the definition of each rotation. The final RPY rotation matrix will be in as shown below (Paul 1981).

$$\mathbf{RPY}(\varphi,\theta,\psi) = \begin{bmatrix} C\varphi\ C\theta & C\varphi\ S\theta\ S\psi - S\varphi\ C\psi & C\varphi\ S\theta\ C\psi + S\varphi\ S\psi & 0 \\ S\varphi\ C\theta & S\varphi\ S\theta\ S\psi + C\varphi\ C\psi & S\varphi\ S\theta\ C\psi - C\varphi\ S\psi & 0 \\ -S\theta & C\theta\ S\psi & C\theta\ C\psi & 0 \\ 0 & 0 & 0 & 1 \end{bmatrix} \tag{3.30}$$

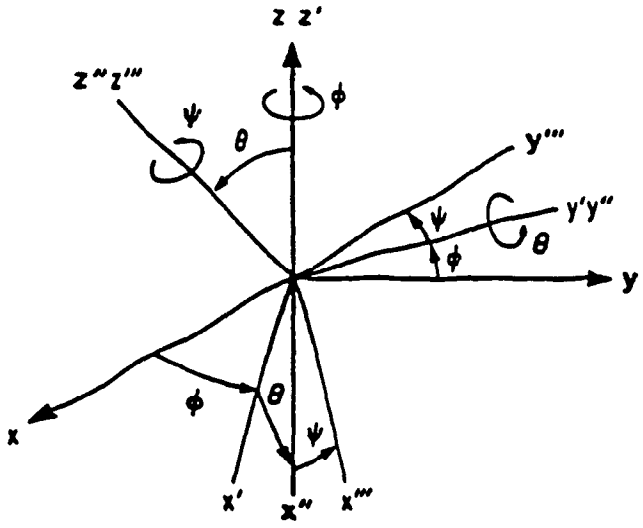

Figure 3.2 - Euler angles

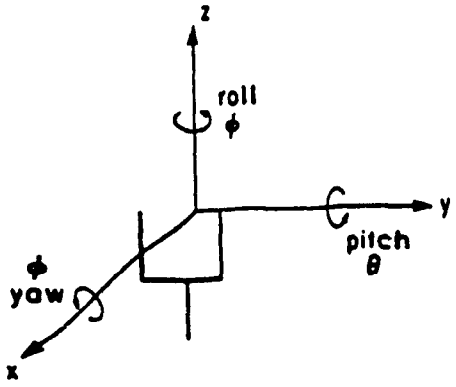

Figure 3.3 - Roll Pitch and Yaw angles

OAT angles: Some of the commercially available manipulators have used the following rotations to specify the orientation of hand or end effector(Hemami 1989). Since there is a close relationship between the zyz Euler angles and the OAT angles thus in figure (3.4) both Euler and OAT rotations are shown to indicate their relationships. Here $(O_h;x_h,y_h,z_h)$ is the tool coordinate and $(0_w;x_w,y_w,z_w)$ is the world (reference) coordinate frame.

Orientation angle: The angle between the y-axis of the world coordinate (base frame) y_w and the projection of the z-axis of the hand frame z_h onto the worlds xy plane. This is an angle in the $x_w y_w$-plane and therefore can be considered as a rotation about z_0. By comparing the Euler angle α and the O angle shown the figure it can be concluded that

$$O = 90^\circ + \alpha \tag{3.31}$$

Altitude angle: The angle between the hands z-axis z_h and a plane parallel to the world xy-plane. This is in fact the angle between z_h and x_1, where x_1 is the projection of the z_h on world xy-plane. By comparing the Euler angle β and the A angle (fig. 3.4) one can conclude that

$$A = 90^\circ - \beta \tag{3.32}$$

Tool angle: The angle between the hand y-axis (y_h) and the intersection of the world xy-plane and a plane normal to the hand z-axis (z_h). In other words this is the angle between y_h and the intersection of the hand xy-plane and the world xy-plane, from figure 3.4 it is evident that

$$T = \gamma \tag{3.33}$$

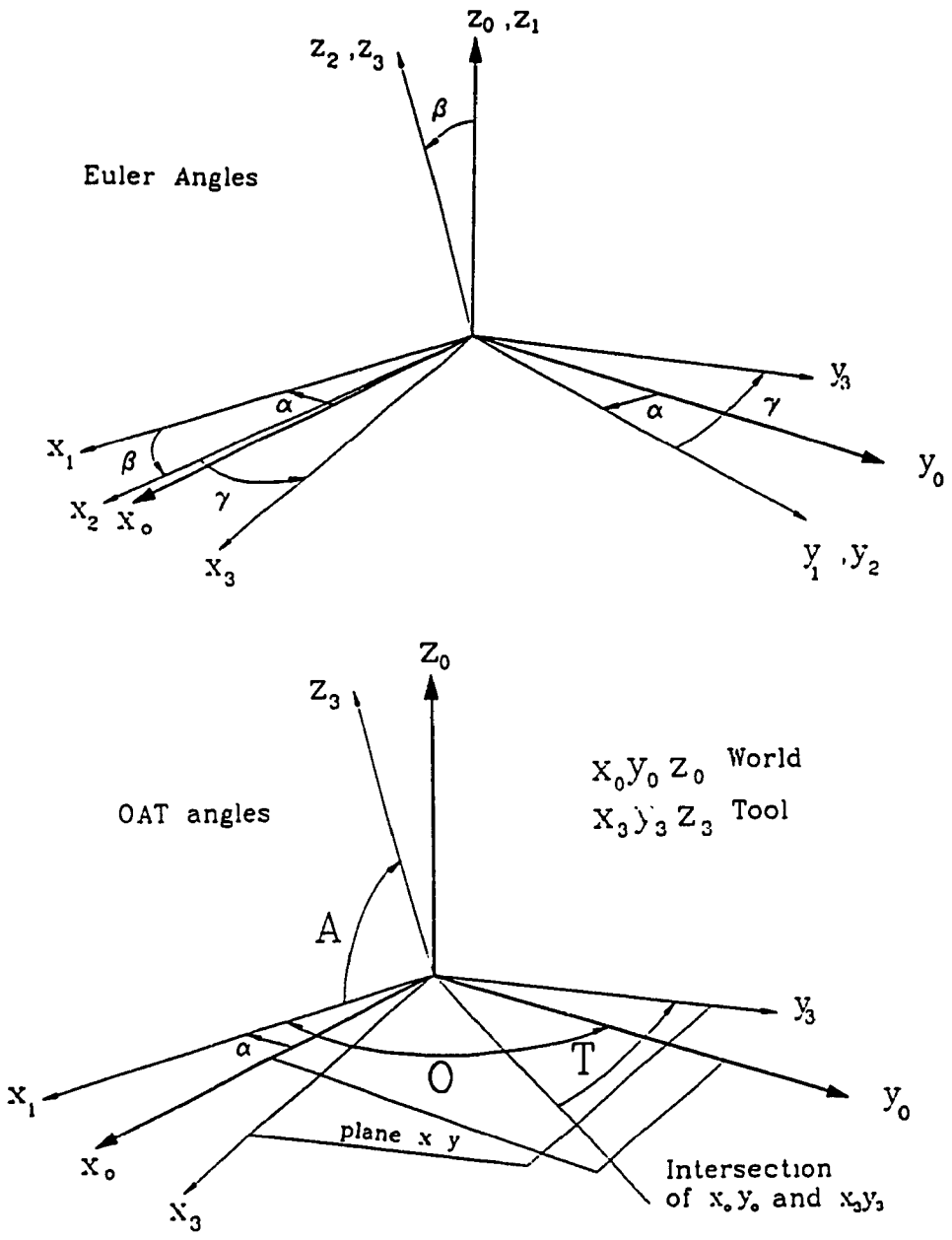

Figure 3.4 - Comparison of the Euler and OAT angles

From the foregoing definitions of the OAT angles and their relationships with the Euler angles, the attitude matrix of the hand expressed in terms of the Euler angles can be modified as follows

$$\mathbf{OAT}(O,A,T) = \begin{bmatrix} \mathbf{SO\ SA\ CT + CO\ ST} & \mathbf{-SO\ SA\ ST + CO\ CT} & \mathbf{SO\ CA} & 0 \\ \mathbf{-CO\ SA\ CT + SO\ ST} & \mathbf{CO\ SA\ ST + SO\ CT} & \mathbf{-CO\ CA} & 0 \\ \mathbf{-CA\ CT} & \mathbf{CA\ ST} & \mathbf{SA} & 0 \\ 0 & 0 & 0 & 1 \end{bmatrix} \quad (3.34)$$

- Direct (Forward) Kinematics:

In the direct kinematics problem the objective is to determine the position and orientation of the robots hand (the attitude matrix of the end effector), given a vector of joint variables $q = (q_1, q_2, \ldots q_n)$ for a general robot or joint angles $\Theta = (\theta_1, \theta_2, \ldots, \theta_n)$ for robots with revolute joints.

The homogeneous matrix T_0^i which specifies the position and orientation of the end point of link i with respect to the base coordinate system, is the chain product of successive coordinate transformation matrices of A_{i-1}^i, expressed as

$$T_0^i = A_0^1 A_1^2 \ldots\ldots A_{i-1}^i = \prod_{j=i}^{1} A_{j-1}^j; \quad i=1,2,\ldots n \quad (3.35)$$

hence if for a robot with 6 degree of freedom (6 joints), the position and orientation of the hand is wanted, then one can use equation (2.35) with i taken as 6 or $T_0^H = A_0^6$. This matrix is used very frequently in robotics kinematics and control. Some authors have referred to this matrix as the

attitude matrix of the hand or arm matrix (Lee 1982). Consider the arm matrix as

$$T_0^h = \begin{bmatrix} \mathbf{n} & \mathbf{s} & \mathbf{a} & \mathbf{p} \\ 0 & 0 & 0 & 1 \end{bmatrix} = \begin{bmatrix} n_x & s_x & a_x & p_x \\ n_y & s_y & a_y & p_y \\ n_z & s_z & a_z & p_z \\ 0 & 0 & 0 & 1 \end{bmatrix} \tag{3.36}$$

Definition of the normal, slide, approach and position vectors which comprise the rotation sub-matrix of the attitude of the hand are given as follows (in figure 3.2 these vectors are drawn for a PUMA robot arm):

The normal vector n: If the hand of the robot has parallel jaw, it is orthogonal to the fingers of the robot arm.

The slide vector s: This vector points in the direction of the finger motion as the grippers opens and closes.

The approach vector a: This vectors points in the direction normal to the palm of the hand

The position vector p: The position vector of the hand is a vector which points from the base-frame origin of the manipulator to the origin of its end effector or hand, which is usually located at the center point of the fully closed fingers.

Equation (3.36) gives 12 values for the elements of the position and orientation of the hand, however due to the orthogonality of the rotation matrix all 9 elements of the rotation matrix are not independent and the following relationships hold for n,s and a.

$$\mathbf{n}.\mathbf{n} = \mathbf{s}.\mathbf{s} = \mathbf{a}.\mathbf{a} = 1 \tag{3.37}$$

and $$\mathbf{n} \times \mathbf{s} = \mathbf{a}.$$

Thus, one is dealing with only six independent parameters in the T matrix, this is evident since any 3-D motion of a rigid body can be uniquely specified by six parameters.

In the real-time control of the manipulators usually the OAT angles are being used as the representative of the hands orientation. Therefore in the forward kinematics formulations it is useful to calculate these three angles in terms of the elements of the attitude matrix of the hand T_0^h (3.36), one can easily obtain the following relationships

$$\begin{aligned} O &= \text{ATAN2}(-a_x, a_y) \\ T &= \text{ATAN2}(-s_z, n_z) \\ A &= \text{ATAN2}([tanT(n_x - cosO\ sinT)],\ s_z sinO) \end{aligned} \tag{3.38}$$

The last equation for A can be expressed explicitly in terms of the elements of the attitude matrix, however in order to do that one needs to calculate $sinT$, $cosO$ and $sinO$ which in turn will require the term $\sqrt{1 + tan^2(.)}$.

In what follows the final explicit form of the A angle is given.

$$A = \text{ATAN2}\{[a_y s_z - n_x(1 - a_z^2)],\ [n_z a_x \sqrt{1 - a_z^2}\,]\} \tag{3.39}$$

When using the explicit formula mentioned above, care should be taken to

avoid a solution of **A** in an unwanted quadrant. More elaboration on the direct kinematics formulations will be made for a PUMA-560 robot arm in section 3.5.

•Inverse Kinematics: In computer-based control of robot manipulators it is necessary to supply the joint actuators with the required joint motion in order to have the tip of the end effector to follow the prescribed motion. Therefore, forward kinematics fail to assist the system. On the other hand inverse kinematics formulations will find significant importance in order to perform a task defined with respect to the world coordinate frame. In other words given the position and orientation of the end effector (the attitude matrix) what would be the corresponding joint-variable vector **q** for a general robot or joint-angles for a revolute manipulator. However, some researchers have proposed a more general definition for this problem specially when the robot has more than six degree of freedom, for instance in (Angeles 1985) the following definition is stated.

Given a simple *n*-link, lower-pair-coupled, open kinematic chain, the motion of its terminal link being perfectly known, determine the motion of the remaining links.

Inverse kinematics formulations are highly nonlinear and configuration dependent (Goldenberg et al., 1985), and therefore closed form solutions for any general robot manipulator can not be found. One should resort to the numerical and/or iterative method of analysis (Angeles 1985) and (Goldenberg et al., 1985). However, in this thesis we mainly deal with available robots in the industry for many of which the closed form solution can be obtained. On the other hand different geometrical and/or algebraic methods have been

proposed for the evaluations of the closed form solutions for a class of industrial robots (see chapter 1 for references).

A solution to the inverse kinematics problem for a PUMA-560 robot arm will be presented in chapter 4. This solution is based on the approach developed by (Lee 1982) with some modification.

CHAPTER 4

KINEMATIC FORMULATIONS FOR PUMA-560 MANIPULATORS

4.1- INTRODUCTION

In this chapter firstly coordinate frames will be established to each joint of a PUMA-560 robot arm and consequently the forward and inverse kinematics for theses manipulators will be developed. In many research papers these formulations can be found however in the majority of the previous work one of the link offset distance namely a_3 has been disregarded due to its rather small magnitude. In this thesis however all of the physical and measurable link length and offset will be included in the formulations.

The focus of the kinematics formulations presented in this chapter are mainly on the displacements of the robot and velocity analysis is not considered, this is due to the fact that in the following chapters only displacement formulations will be used.

4.2- FRAME ASSIGNMENTS

The basic approach followed in this section is a modified version of what was presented by (Lee 1982). Using the procedure discussed in section 3.2 link coordinate frames have been assigned to a PUMA-560 manipulator which is shown in figure 4.1.

Moreover, the link parameters as well as the physical limits of the rotation on different joints are given in Table 4.1.

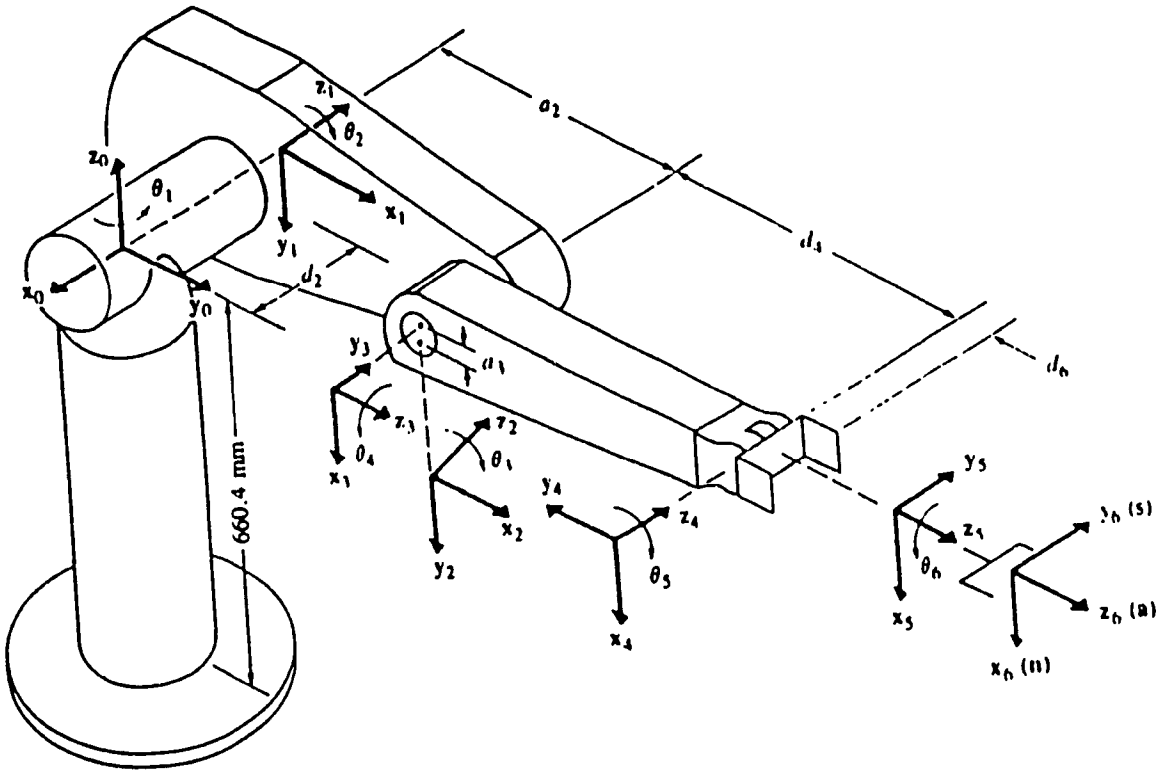

Figure 4.1 - Structure of a PUMA-560 manipulator

Table 4.1. PUMA-560 robot arm link parameters

JOINT i	θ_i (Deg.)	${}_i\alpha$(Deg.)	a_i (mm)	d_i (mm)	RANGE
1	90	-90	0	0	-160 to +160
2	0	0	431.8	149.1	-185 to +45
3	90	90	-20.3	0	-45 to +225
4	0	0	0	433.1	-110 to +170
5	0	0	0	0	-100 to +100
6	0	0	0	56.3	-266 to +266

4.3- FORWARD KINEMATICS

According to equation 3.25, one can easily obtain the **A** matrices corresponding to the six links of a PUMA-560 robot arm with the parameters in Table 4.1. These matrices are as follows

$$A_0^1 = \begin{bmatrix} C_1 & 0 & -S_1 & 0 \\ S_1 & 0 & C_1 & 0 \\ 0 & -1 & 0 & 0 \\ 0 & 0 & 0 & 1 \end{bmatrix} \qquad A_1^2 = \begin{bmatrix} C_2 & -S_2 & 0 & a_2C_2 \\ S_2 & C_2 & 0 & a_2S_2 \\ 0 & 0 & 1 & d_2 \\ 0 & 0 & 0 & 1 \end{bmatrix} \qquad (4.1)$$

$$A_2^3 = \begin{bmatrix} C_3 & 0 & S_3 & a_3C_3 \\ S_3 & 0 & -C_3 & a_3S_3 \\ 0 & 1 & 0 & 0 \\ 0 & 0 & 0 & 1 \end{bmatrix} \qquad A_3^4 = \begin{bmatrix} C_4 & 0 & -S_4 & 0 \\ S_4 & 0 & C_4 & 0 \\ 0 & -1 & 0 & d_4 \\ 0 & 0 & 0 & 1 \end{bmatrix}$$

$$A_4^5 = \begin{bmatrix} C_5 & 0 & S_5 & 0 \\ S_5 & 0 & -C_5 & 0 \\ 0 & 1 & 0 & 0 \\ 0 & 0 & 0 & 1 \end{bmatrix} \qquad A_5^6 = \begin{bmatrix} C_6 & -S_6 & 0 & 0 \\ S_6 & C_6 & 0 & 0 \\ 0 & 0 & 1 & d_6 \\ 0 & 0 & 0 & 1 \end{bmatrix}$$

The arm matrix (attitude matrix of the end effector) thus can be obtained by

$$T_0^h = A_0^1 A_1^2 A_2^3 A_3^4 A_4^5 A_5^6 = \begin{bmatrix} n & s & a & p \\ 0 & 0 & 0 & 1 \end{bmatrix} \tag{4.2}$$

One straightforward but not very efficient algorithms for the direct kinematics is to calculate these matrices and sequentially multiply by them one by one. However as was mentioned before in this chapter, owing to the redundant number of information, we will actually perform extra number of mathematical operations which are not useful to begin with. An alternative method is to perform the chain multiplications and equating the elements of the vectors **n**, **s**, and **a** to the corresponding elements of the T_0^h matrix. One can obtain the following closed form solution for the elements of the attitude matrix of the hand, in terms of the elements of the vector of joint angles θ, and thus only the elements required will be calculated.The number of operations are drastically reduced.

$$\begin{aligned} n_x &= C_1C_{23}C_4C_5C_6 - S_1S_4C_5C_6 - C_1S_{23}S_5C_6 - C_1C_{23}S_4S_6 - S_1C_4S_6 \\ n_y &= S_1C_{23}C_4C_5C_6 + C_1S_4C_5C_6 - C_1S_4S_5C_6 - S_1C_{23}S_4S_6 + C_1C_4S_6 \\ n_z &= -S_{23}C_4C_5C_6 - C_{23}S_5C_6 + S_{23}S_4S_6 \end{aligned} \tag{4.3}$$

$$\begin{aligned} s_x &= -C_1C_{23}C_4C_5S_6 + S_1S_4C_5S_6 + C_1S_{23}S_5S_6 - C_1C_{23}S_4C_6 - S_1C_4C_6 \\ s_y &= -S_1C_{23}C_4C_5S_6 - C_1S_4C_5S_6 + C_1S_4S_5S_6 - S_1C_{23}S_4C_6 + C_1C_4C_6 \\ s_z &= S_{23}C_4C_5S_6 - C_{23}S_5S_6 + S_{23}S_4C_6 \end{aligned} \tag{4.4}$$

$$a_x = C_1C_{23}C_4S_5 - S_1S_4S_5 + C_1S_{23}C_5 \quad (4.5)$$
$$a_y = S_1C_{23}C_4S_5 + C_1S_4S_5 + C_1S_{23}C_5$$
$$a_z = -S_{23}C_4S_5 + C_{23}C_5$$

$$p_x = (C_1C_{23}C_4S_5 - S_1S_4S_5 - C_1S_{23}C_5)d_6 + C_1S_{23}d_4 + C_1C_{23}a_3 + C_1C_2a_2 - d_2S_1 \quad (4.6)$$
$$p_y = (S_1C_{23}C_4S_5 + C_1S_4S_5 + S_1C_{23}C_5)d_6 + S_1S_{23}d_4 + S_1C_{23}a_3 + S_1C_2a_2 + d_2C_1$$
$$p_z = (-S_{23}C_4S_5 + C_{23}C_5)d_6 + C_{23}d_4 - a_3S_{23} - S_2a_2$$

4.4- INVERSE KINEMATICS

In this section the inverse kinematics solution for a PUMA-560 robot manipulator will be derived. Our approach is based on the algebraic methodology presented by Lee (1982). In a general class of robot manipulators the last three joint axes are collinear (intersecting one another at one point which is called the wrist point). This class is called robots with spherical wrist or wrist partitioned robots. PUMA-560 being a spherical wrist robot, allows us to exploit a characteristics of this class of robots. Of manipulators with this kind of joint arrangement have the property that the position of the wrist point can be calculated directly from the position and orientation of the end effector, without the knowledge of any of the joint variables (Featherstone 1983). Thus the solution of the inverse kinematics can be calculated in two stages. First a position vector pointing from origin of the base frame to the wrist point is derived. It is then used to derive the solution of the first three joints. The last three joints are solved using the calculated values from the first three joints and the orientation submatrix of the T^1_{i-1} $i = 4,5,6$ (Lee 1982).

Let p_0^h and p_0^w denote the position vectors of the end effector (hand) and the wrist point (origin of joint 4) of the robot. Then one can easily see from Figure 4.1 that

$$p_0^w = p_0^h - d_6 a_0 \tag{4.7}$$

or

$$\begin{bmatrix} p_x^w \\ p_y^w \\ p_z^w \end{bmatrix} = \begin{bmatrix} p_x^h \\ p_y^h \\ p^h \end{bmatrix} - d_6 \begin{bmatrix} a_x \\ a_y \\ a_z \end{bmatrix} \tag{4.8}$$

The wrist point is the origin of the frame 4 attached to joint 4. This implies that the position vector p_0^w is actually the position vector embedded in the homogeneous transformation matrix of the joint 4 with respect to the robot origin, or T_0^4, therefore

$$T_0^w = T_0^4 = A_0^1 A_1^2 A_2^3 A_3^4 \tag{4.9}$$

or

$$T_0^w = T_0^4 = \left[\begin{array}{c|c} R_o^w & p_0^w \\ \hline 0\ 0\ 0 & 1 \end{array}\right] = \tag{4.10}$$

$$\begin{bmatrix} C_1C_{23}C_4 - S_1S_4 & -C_1S_{23} & -C_1C_{23}S_4 - S_1C_4 & C_1S_{23}d_4 + a_3C_1C_{23} + a_2C_1C_2 - d_2S_1 \\ S_1C_{23}C_4 + C_1S_4 & -S_1S_{23} & -S_1C_{23}S_4 + C_1C_4 & S_1S_{23}d_4 + S_1C_{23}a_3 + S_1C_2a_2 + C_1d_2 \\ -S_{23}C_4 & -C_{23} & S_{23}S_4 & C_{23}d_4 - S_{23}a_3 - S_2a_2 \\ 0 & 0 & 0 & 1 \end{bmatrix}$$

or

$$\begin{bmatrix} p_x^w \\ p_y^w \\ p_z^w \end{bmatrix} = \begin{bmatrix} C_1 S_{23} d_4 + a_3 C_1 C_{23} + a_2 C_1 C_2 - d_2 S_1 \\ S_1 S_{23} d_4 + S_1 C_{23} a_3 + S_1 C_2 a_2 + C_1 d_2 \\ C_{23} d_4 - S_{23} a_3 - S_2 a_2 \end{bmatrix} \tag{4.11}$$

By solving the three trigonometric equations obtained from equation 4.11, one can obtain the expressions for joint one, two and three in terms of the wrist point coordinates. Since these trigonometric equations have, in general, more than one unique solution one should distinguish between different solutions by resorting to the topology or configuration of the manipulator. For example the shoulder of the robot can be lefty or righty while reaching to a point. At the same time the elbow of the arm is either up or down. Hence in general four configurations are possible with which the wrist point can be positioned. These are Left-Shoulder/Elbow-Up (LU), Left-Shoulder/Elbow-Down (LD), Right-Shoulder/Elbow-Up (RU) and Right-Shoulder/Elbow-Down (RD).

Two indices for determining the shoulder and elbow configurations are introduced in the formulations in what follows, they are

$$\text{s\_c (shoulder configuration index)} = \begin{cases} +1 & \text{Left shoulder} \\ -1 & \text{Right shoulder} \end{cases} \tag{4.12}$$

and

$$\text{e\_c (elbow configuration index)} = \begin{cases} +1 & \text{Elbow down} \\ -1 & \text{Elbow up} \end{cases} \tag{4.13}$$

Denoting by r^w, the magnitude of the position vector from the origin of

the robot to the wrist point, then

$$r^w = \sqrt{(p_x^w)^2 + (p_y^w)^2 + (p_z^w)^2} \tag{4.14}$$

also let

$$\rho = \sqrt{(p_x^w)^2 + (p_y^w)^2 - (d_2)^2} \tag{4.15}$$

then

$$\theta_1 = \text{ATAN2}\left[(s\_c\ p_y^w\ \rho - d_2 p_x^w),\ (\ s\_c\ p_x^w\ \rho + d_2 p_y^w)\right] \tag{4.16}$$

$$\theta_3 = \text{ATAN2}(d_4, a_3) + \text{ATAN2}\left[-s\_c.e\_c.\sqrt{a_3^2 + d_4^2 - \xi^2}\ \right] \tag{4.17}$$

$$\text{Where}\quad \xi = \left((r^w)^2 - a_2^2 - a_3^2 - d_2^2 - d_4^2\ \right) / (2a_2) \tag{4.18}$$

Next θ_2 can be obtained as follows,

$$\theta_2 = \text{ATAN2}\left[s\_c.\ \sqrt{d_4^2 + a_3^2 + a_2^2 + 2a_2 d_4 sin\theta_3 + 2a_2 a_3 cos\theta_3 - (p_z^w)^2}\ ,\ p_z^w\right] -$$

$$\text{ATAN2}\left[(d_4 cos\theta_3 - a_3 sin\theta_3),\ (d_4 cos\theta_3 + a_3 sin\theta_3 + a_2)\right] \tag{4.19}$$

Once the first three joints are obtained, one can use equations (4.3), (4.4) and (4.5 to derive relationships for the last three joints in terms of the orientation elements and joint variables one, two and three obtained above. The final results of the last three joints are given in what follows

$$\theta_4 = \text{ATAN2}\left[(C_1 a_y^w - S_1 a_x^w\ ),\ (C_1 C_{23} a_x + S_1 C_{23} a_y - S_{23} a_z)\right] \tag{4.21}$$

$$\theta_5 = \text{ATAN2}\left[\left((C_1 C_{23} C_4 - S_1 S_4) a_x^w + (S_1 C_{23} C_4 + C_1 S_4) a_y^w - C_4 S_{23} a_z^w\right),\right.$$

$$\left(C_1 S_{23} a_x + S_1 S_{23} a_y + C_{23} a_z\right)\Big] \tag{4.22}$$

$$\theta_6 = \text{ATAN2}\Big[\Big((-S_1 C_4 - C_1 C_{23} S_4) n_x + (C_1 C_4 - S_1 C_{23} S_4) n_y + (S_4 S_{23}) n_z\Big),$$

$$\Big((-S_1 C_4 - C_1 C_{23} S_4) s_x + (C_1 C_4 - S_1 C_{23} S_4) s_y + (S_4 S_{23}) s_z\Big) \tag{4.23}$$

The foregoing equations for the last three joints may produce two sets of solutions for each arm configuration mentioned before. In other words depending on the configuration of the end effector while reaching a point one can have a *flipped or a no-flipped* hand. If $\Theta = (\theta_1, \theta_2, \theta_3, \theta_4, \theta_5, \theta_6)$ is the vector of joint variables for a no-flip configuration then it is evident that in order to flip the end effector the following joint variables may be used instead,

$$\Theta = \Big(\theta_1, \theta_2, \theta_3, (\theta_4 + \pi), -\theta_5, (\theta_6 + \pi)\Big) \tag{4.24}$$

Therefore, for a general point reachable to the robot arm there may exist up to eight number of solutions for the robots configurations and thus for its joint variables.

CHAPTER 5

WORKSPACE ANALYSIS FOR ROBOT MANIPULATORS

5.1- INTRODUCTION

This chapter discusses the general approaches of workspace analysis for robotic manipulators proposed by researchers in the past decade, as well as to present the contributions of this thesis to the manipulators workspace studies. In section 5.2 basic definitions and concepts of workspaces associated with robot manipulators are given. In section 5.3 algorithms for mapping the two dimensional envelope of the workspaces are proposed, also the techniques for the evaluation of the workspaces are presented. A comparison among the different approaches will be made. Section 5.4 introduces an AutoCad-based approach for the three dimensional reconstruction of the graphical image of the complex surfaces which define the workspace of the manipulators.

5.2- PRELIMINARIES

Generally there are two main issues involved in analyzing robot workspaces (Shahinpoor 1988),

1- Given the robotic structure, what is the geometric shape of the workspace?

2- Given a desired geometrical description of a workspace for robotic applications, what is the necessary robotic structure ?

In this chapter we will elaborate only on the first issue where two algorithms for the evaluation of the work envelope will be developed. The

second aspect of the workspace analysis mentioned above is a basic concern in the design of robot manipulators for specific operations and will be outside the scope of this thesis. Primarily, in what follows, the extreme reaches of general robot manipulators which usually comprise some portions of the bounding surfaces of the workspace will be defined, and for a PUMA-560 these parameters will be identified. Subsequently the reachable and dextrous workspaces will be defined. Finally the measures of manipulability for a robot arm will be discussed.

5.2.1- EXTREME REACH OF A ROBOT MANIPULATOR

A study of the determination of extreme distances of the joints and hand of a robot arm is important since it provides a foundation for an understanding of how the types and numbers of joints of kinematic chain together with the linkage dimensions are related to workspaces. In addition, such a study will provide useful information for the design of robot arms.

For geometrically simple manipulators (*i.e.* those with intersecting axes, which represent simple DH parameters etc.), the maximum and minimum reaches can be derived easily. But, for arms of arbitrariy architecture no satisfactory results have been given (Derby 1981), (Sugimoto and Duffy 1981). Intensive discussions for the analysis of the extreme reaches of general robots with arbitrary number of joints are given in the aforementioned references. However, in these studies due to the complexities involved in the kinematic analysis of general robots, the development of a general expression for the extreme reaches, has not been feasible, and iterative techniques have been used instead. Moreover, in these studies joint actuators are assumed to

be ideal with full rotateabilities. On the contrary almost all of the commercially available robots have limitations on their joint motions. These considerations imply that for the purpose of this thesis it is not feasible nor desirable to follow the same general investigations of the extreme reaches. It will be shown in this section that the minimum and maximum reaches of a PUMA-560 can be derived by using a straightforward geometrical approach. In fact, all of the available robots can be investigated with the same idea. However, for the sake of completeness, two important theorems which have been proved by Sugimoto and Duffy (1981) will be presented as follows.

THEOREM 1: *All intermediate joint axes of a robot arm with an arbitrary number of joints intersect an extreme distance line between an arbitrary base point and the center point of the hand (extreme reach).*

THEOREM 2: *All intermediate joint axes of a robot arm with an arbitrary number of joints intersect an extreme perpendicular distance line from the center point of the hand to any arbitrary line in space.*

Let the position vector from origin of the robot to point p located in the hand be denoted by **P**, thus in the base coordinate system of the arm one can write

$$\mathbf{P} = [x_p,\ y_p,\ z_p]^T \tag{5.1}$$

the magnitude of this vector is

$$R = \|P\| = \mathbf{P}^T \cdot \mathbf{P} \tag{5.2}$$

$$R = (x^2 + y^2 + z^2)^{1/2}. \tag{5.3}$$

where, $x = X(\Theta),\ y = Y(\Theta),\ z = Z(\Theta)$

and x, y and z are the cartesian coordinates of the hand of the robot with respect to its base coordinate frame. On the other hand one can write the vector equation for the position vector of a general *n*-DOF robot hand with respect to the robots base in terms of the Denavit and Hartenberg notations as

$$\mathbf{R} = \sum_{j=1}^{n} (a_j \mathbf{a}_j + d_j \mathbf{d}_j) \tag{5.4}$$

where definitions of the unit vectors $\mathbf{a}_j$ and $\mathbf{d}_j$ are given in chapter 3. In order to determine the extreme values of R one need to maximize or minimize R with respect to the elements of the vector of joint displacements Θ. But this involves lengthy and complex process for a six degree of freedom robot and yet there will be no contributions from the physical limits to the obtained extremes. However, as it was mentioned earlier considering usual structures of industrial robots, this task will be very straightforward. Let R_{max} R_{min} be, respectively, the maximum and minimum reaches of the manipulator. By inspecting figure 5.1 , where the link *j* of the robot is shown with its corresponding link length a_j and its offset distance d_j, one can rewrite equation 5.4 for the PUMA-560 as

$$\mathbf{R} = d_2\mathbf{d}_2 + a_2\mathbf{a}_2 + a_3\mathbf{a}_3 + d_4\mathbf{d}_4 + d_6\mathbf{d}_6. \tag{5.5}$$

where the numerical values of a_j and d_j are given in Table 4.1. Next we

examine theorem 1 stated above for the stretched robot shown in figure 5.1. It is obvious that at this configuration all joint axes of the arm intersect the distance line from origin of the first joint to point P of the hand.

Since the posture of figure 5.1 is consistent with the extreme reach of the robot (*i.e.* all joint axes intersect the distance line to the point P) the magnitude of the maximum reach can be derived from equation 5.5 as

$$R_{max} = \sqrt{d_2^2 + \left(a_2 + \sqrt{a_3 + (d_4 + d_6)}\right)^2} \tag{5.6}$$

Substituting the numerical values of the link lengths and offsets in equation 5.5 the maximum reach for the PUMA-560 robot arms is

$$R_{max} = 935.3 \text{ mm} \tag{5.7}$$

It is observed that the joint limits do not play any limiting role on the magnitude of R_{max}. However, in what follows it will be shown that for R_{min} the minimum reach of the PUMA arm, joint limits will come into the picture and actually affect the magnitude of R_{min}. If joint three is able to rotate without any limits, then for a fully folded configuration of the forearm, one could construct the posture shown in figure 5.2. by applying theorem 1

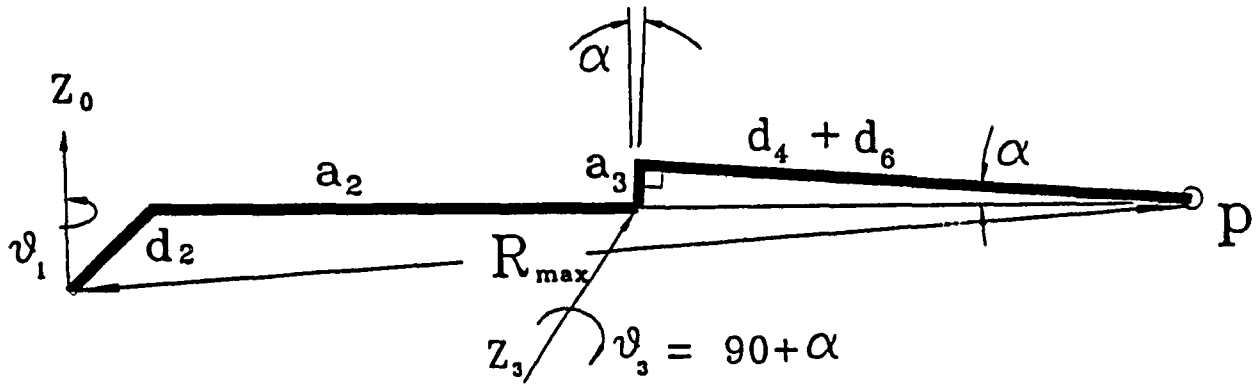

Figure 5.1 - A typical manipulator in fully stretched configuration

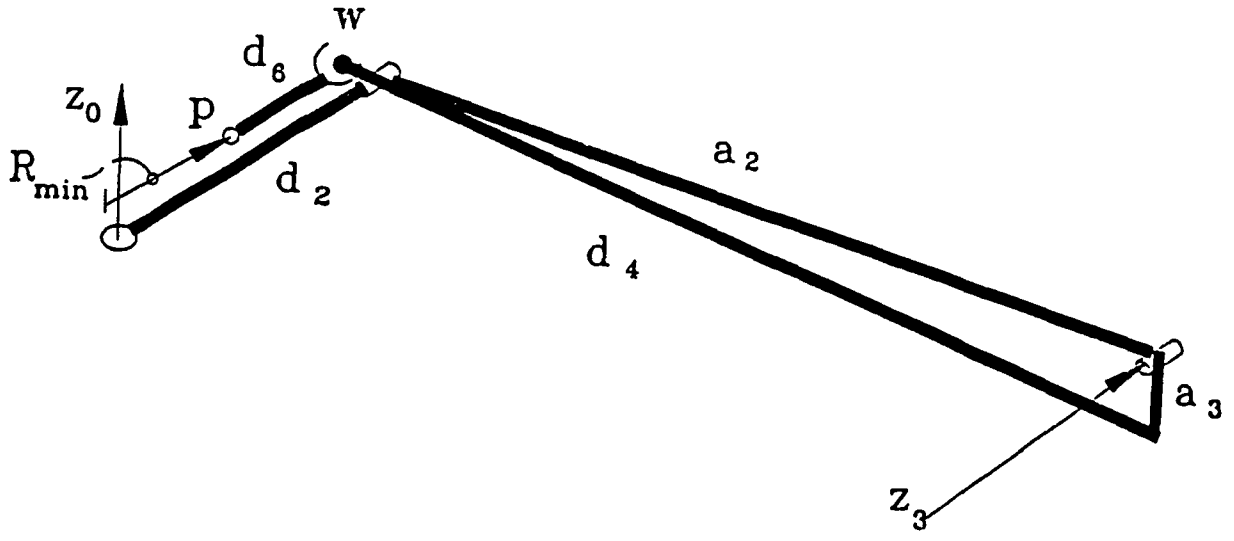

Figure 5.2 - A typical manipulator in a folded configuration

By inspecting figure 5.2 the following relationship can be written for the *theoretical minimum reach* R'_{min},where the joints are not limited.

$$(R'_{min} + d_6) = \sqrt{d_2^2 + \left(\sqrt{d_4^2 + a_3^2} - a_2\right)^2} \tag{5.8}$$

$$\text{or} \qquad R'_{min} = 93 \text{ mm} \tag{5.9}$$

However, due to the physical limits imposed on joint three, the forearm can not fold back completely, and the posture of the robot in its closest position to the origin will become as shown in figure 5.3,

Thus the *actual minimum reach* R_{min} for the PUMA arm is as follows

$$(R_{min} + d_6) = \sqrt{d_2^2 + \left(d_4^2 + l^2 - 2ld_4\cos(\theta_3^l)\right)} \tag{5.10}$$

$$\text{or} \qquad R_{min} = \sqrt{d_2^2 + \left(d_4^2 + l^2 - 2ld_4\cos(\theta_3^l)\right)} - d_6 \tag{5.11}$$

where

$$l = \sqrt{a_3^2 + d_4^2} \tag{5.12}$$

and θ_3^l is the lower limit of the joint 3.

Using the numerical values we get actual minimum reach of PUMA-560 as

$$R_{min} = 306 \text{ mm.} \tag{5.13}$$

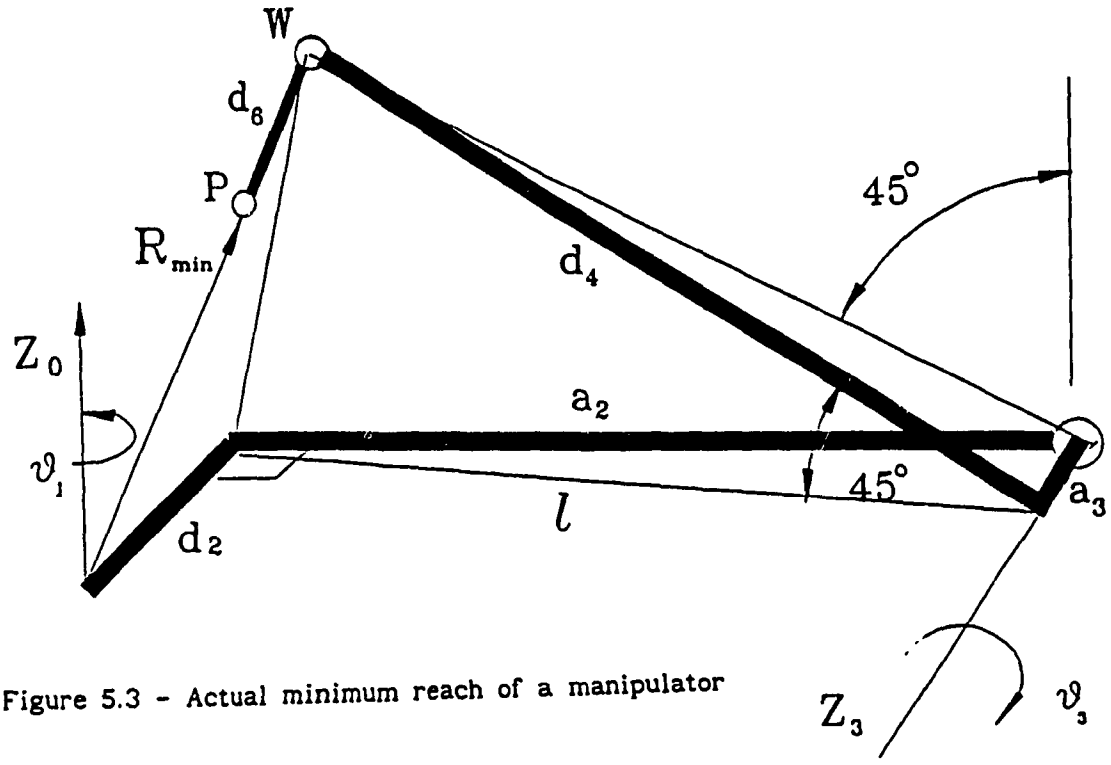

Figure 5.3 - Actual minimum reach of a manipulator

5.2.2- REACHABLE WORKSPACE OF MANIPULATORS

The totality of the set of all points aggregated in the workspace of a robot manipulator is composed of two parts which have been defined under different names in the literature. The main and the largest workspace of a robot manipulator has been named by **Reachable workspace** or sometimes by **Primary workspace.** A subsection of the reachable workspace of manipulators which bears important features regarding the maneuvreability of the manipulators has been named by **Dextrous** or **Secondary workspace.**

The reachable workspace by definition is the set of all three dimensional points that can be reached by a reference point, located at either the center of the wrist, the center of the hand or the tip of a finger (Shahinpoor 1988), (Gupta and Roth 1982). Kumar and Waldron (1981a,b) referred to the total workspace as the **"Reachable Workspace"** whereas Gupta and Roth (1982) used the name **"Primary Workspace"**. In this thesis the reachable or the primary workspace of a point p attached to the hand or wrist of a robot will be designated by $W^P(p)$ hereafter.

In the previous section we discussed the extreme reaches of manipulators, and mentioned that when the robot assumes one of its theoretical extreme reaches, it will loose at least one of its degrees of freedom. In these positions the Jacobian matrix of the robot becomes singular. It has been shown also that, if one uses polynomial representation of the closure equation for the manipulators, the discriminant of the polynomial vanishes in the aforementioned surfaces. These surfaces are called *Jacobian surfaces* and comprise portions of the reachable workspace. (Oblak

and Kohli 1988). On the other hand there are the so-called *non-jacobian* surfaces which are also limiting boundaries of the reachable workspace. These non-jacobian surfaces in fact exist solely because of the joint motion limits. In the subsequent sections where the algorithms for the generation of the reachable workspace are discussed, both *jacobian* and *non-jacobian* bounding surfaces will be considered.

5.2.3- DEXTROUS WORKSPACE OF MANIPULATORS

A subsection of the **Reachable Workspace** is called the **Dextrous Workspace** (Kumar and Waldron 1981b) or **Secondary Workspace** (Gupta and Roth 1982), and it is denoted by $W^s(p)$. By definition this is the volume within which every point can be reached by a reference point on the manipulator hand, with the hand in any desired orientation (Kumar and Waldron 1981a). In other words while the reference point of the hand being kept at a point p under consideration, the hand can be completely rotated about any axis through that point. This concept in comparison with the reachable space is in many ways, a more useful guide to the manipulative capabilities of the robot hand. Sometimes the reference point may lie within the reachable workspace, but the manipulator exhibits severely limited operational capacity (adroitness). The hand at these situations can be posed with a very restricted range of orientation. Within the dextrous workspace, on the other hand complete manipulative capability is possible since the hand can be placed in any desired orientation.

Kumar and waldron (1981b) have shown that there is no guarantee that a manipulator of arbitrary geometry will posses a dextrous workspace. In fact

the existence of a dextrous workspace is strongly dependent on the link dimensions. They have argued that the smaller the hand size of the manipulator is, the higher the chance of having the dextrous workspace. (The hand size is defined as the magnitude of the offset distance between the reference point p and the wrist of the robot). In the aforementioned reference it has been concluded that for a class 6 or 7 revolute robot which satisfies the following three geometrical requirements, the dextrous workspace exists, and it exactly coincides with the reachable workspace. These requirements are,

(*i*) If the last three joint axes of the robot are concurrent.

(*ii*) All of the last three joint axes are at right angles to one another.

(*iii*) If the reference point is taken at the point of concurrence.

It is obvious that these requirements are exactly those which define a wrist partitioned robot such as PUMA, where the point of concurrence mentioned above is in fact the wrist point of the manipulator. Thus if one takes the point of reference p of the manipulator and place it at the wrist point w instead of the hand, then the dextrous workspace can be generated if one generates the reachable workspace of the arm.

5.2.4.- TOTAL WORKSPACE

Although the previous discussions made by the pioneers of the workspace studies are illuminating and systematic, non-jacobian surfaces due to the joint limits may bound the dextrous workspace as well. Nevertheless, these considerations were not included in the aforementioned discussions. Moreover, these discussions do not take into account the posture or configurations of the robot while reaching a point in its workspace. This is an important consideration in practical applications. Any point inside the workspace of the robot may be reachable through more than one configuration of the manipulator. If the workspace of a robot has been generated without having a knowledge about the robots configuration, there is no guarantee that two reachable points inside the workspace can be accessed with the same configuration. For example one point may be reachable with a Left Shoulder Elbow Up posture while the other with a Right Shoulder Elbow Up. This is strongly prohibited in any practical robotic operation.

In this thesis, we propose to use the terminology **Total Workspace** for the reachable space of the robot. And in order to signify the maneuvering capabilities or adroitness of the hand inside this reachable space we will resort to the measures of manipulability which have been discussed in recent years. This is, in fact, some sort of unification between the terminologies given in the past as reachable and dextrous workspaces. The distinction between the two will be thoroughly investigated by employing different measures of manipulability. We will also propose a methodology for the evaluation of the total workspace by which we can have control over the posture or the configuration of the robot.

Our proposed method, in essence is similar to the one presented by Borrel and Liegeois (1986), where they defined the concepts of *aspects* and *aspect decompositions*. However, our algorithms will be developed in a different fashion, in the former, they considered only the position of the robot's end effector and no information regarding its orientation was given while in our algorithms we will take into account the hand's orientation. The objective is to combine the jacobian surfaces and the limiting surfaces due to the joint limits, and obtain the total workspace, while the robot does not go through any configuration or posture changes. We will first represent the definition of an aspect from Borrel and Liegeois (1986).

Definitions:

For an n-link robot manipulator,

Let $Q = [q_1, q_2 \ldots q_n]^T$ be the vector of n joint variables.

Let q_i^u and q_i^l be respectively the upper and lower limits of joint i, i=1,2,...*n*

X be the *m* dimensional column-vector, the components of which represent the position and orientation of the robot's terminal device.

Let f be the direct coordinate transformation from joint space to the cartesian space or

$$X = f(Q) \tag{5.14}$$

and locally the following linear model is valid

$$dX = J(Q)\, dQ \tag{5.15}$$

Where J is the (*mxn*) Jacobian matrix of the vector function f.

Let D be the admissible domain in the joint space:

$D \in R^n$

$$D = \{Q \mid q_i^l < q_i < q_i^u \ , \ i=1,2,...n\} \tag{5.16}$$

$$\text{and} \quad \Delta = \{\delta_1, \delta_2, \ldots \delta_\rho\}, \ \rho = C_m^n \tag{5.17}$$

the set of m-order minors of J(Q)

Then, an aspect *A* is a connected set of points in R, such that

$A \subset D$

$$\forall \ Q \in A, \ \delta_i(Q) \neq 0, \ i \leq \rho \tag{5.18}$$

By the definition of an aspect thus given, it is obvious that any solution to the equation **5.14** will be unique when, $(n-m)$ are kept fixed and the rest obtained. In other words the robot will not change posture in an aspect.

5.2.5- MEASURES OF MANIPULABILITY

In the previous section it was discussed that the dextrous and reachable workspaces will be considered simultaneously in our algorithms, and the distinction between the two will be made by introducing manipulability indices. In this section some of these indices which have been proposed in the literature will be represented, and also a performance index which will relate to the joint limits of the manipulator, will be introduced. This is called the joint availability index. This index will play a significant role in the contents of the chapter 7, where it will basically form the performance index for a coordinated two-arm robotic system.

It was observed in the previous section that at the Jacobian surfaces which partly define the boundary of the workspace, the Jacobian matrix of the manipulator is singular or in general rank deficient; in other words J degenerates and is not invertible. A manipulator is said to be locally maneuverable if the rank of the Jacobian equals 6 (for a six degrees of freedom manipulator). However when the Jacobian matrix is ill-conditioned the robot arm is near the singular configuration and the maneuverability of the robot is very poor, in fact the robot's hand is reaching the Jacobian bounding surfaces of its workspace. Therefore, a quantitative measure of how close the robot is to a singular state will be useful. This measure is usually called the *manipulability* (Tsai and Chiou 1990).

Yoshikawa (1984) proposed the manipulability of a manipulator as

$$w \equiv \sqrt{\{\det\ (J\ J^T)\}} = \sigma_1\sigma_2\ldots\sigma_m \tag{5.19}$$

where $\sigma_1\sigma_2\ldots\sigma_m$ are the singular values of the jacobian matrix, and in order to evaluate them, one can resort to a singular value decomposition technique. w is a quantitative measure of maneuverability of the robot arm, which is proportional to the volume of an m dimensional ellipsoid with major axes along the eigenvectors of JJ^T and with the length of the major axes corresponding to $\sigma_1,\sigma_2,\ldots\sigma_m$. The volume of the ellipsoid is sensitive to the scale of singular values. Since the manipulability is a measure of the "nearness" of the Jacobian to degeneracy one can measure the shape of the ellipsoid by detecting the magnitude of $\sigma_{min} / \sigma_{max}$ or the ratio of the smallest to the largest singular values of J or in other words the ratio of the smallest length to the largest length of the major axes of the ellipsoid. Moreover, this ratio is in fact the reciprocal of the condition number of the Jacobian matrix or *cond*(J). Hence a normalized version of the

manipulability index can be defined to be

$$w \equiv \frac{1}{cond(J)} = \frac{\sigma_{min}}{\sigma_{max}} \tag{5.20}$$

Nelson et al., (1987) used the manipulability index defined in 5.19 and determined the principal axes of the manipulability ellipsoids. The volume of the ellipsoid is proportional to the manipulability measure, so the farther the manipulator is from a singularity position, the larger the volume of these ellipsoid will be. Figure 5.4 shows the ellipsoid for a PUMA-560 manipulator near its workspace boundary.

The foregoing discussion on the manipulability index was limited to the evaluation of the nearness to the Jacobian surfaces, and the bounding surfaces due to the joint limits were not considered. In what follows these limiting surfaces will be taken into account by introducing the joint availability function V, which accounts for the nearness to the joint limits.By multiplying a properly chosen V (as a penalty function) by the Yoshikawa's index (Eq. 5.19) one can force the overall manipulability index to decrease rapidly as a joint limit is approached. Tsai and Chiou (1990) proposed the following modified manipulability index as

$$w_m = V\sqrt{\{\det\ (J\ J^T)\}} \tag{5.21}$$

$$\text{where} \quad V = 1 - \exp\left\{-k \prod_{i=1}^{n} (\theta_i - \theta_i^l)(\theta_i^u - \theta_i) \,/\, (\theta_i^u - \theta_i^l)^2\right\} \tag{5.22}$$

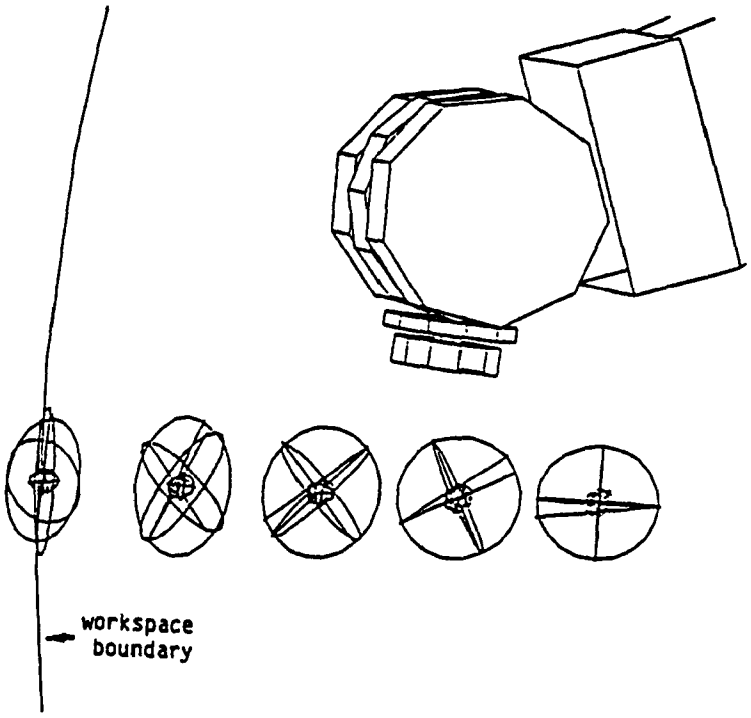

Figure 5.4 - Manipulability ellipsoid for PUMA-560 (Nelson 87)

is the proposed availability function and k is a scale factor to adjust for a desired shape of the availability function. On the other hand in terms of the reciprocal of the condition number one can modify equation 5.20 to obtain w_m,

$$w_m = Vw = V \frac{\sigma_{min}}{\sigma_{max}} \tag{5.23}$$

5.3- TWO-DIMENSIONAL MAPPING OF THE WORKSPACES

The total workspace of a manipulator in conjunction with the manipulability indices will provide sufficient information regarding the dexterity or manipulability of the arm. In this section the proposed algorithms for the evaluation of the boundary of the workspaces will be provided.

The boundary of a robotic workspace is called the robotic work envelope which is usually a complex surface, very difficult to represent explicitly by geometrical equations. In order to represent the geometrical shape of the work envelope it is usual to cut the total workspace with a given plane and obtain the cross section of the workspace on that plane. The projected workspace onto the cutting plane is referred to as the **"Two-Dimensional Workspace"**.

Previous work on the workspace determination can be classified into three categories (Borrel and Liegeois 1986).

(*i*) Scanning algorithms along defined lines of the Cartesian space, and

application of the inverse kinematics until a joint limit or a Jacobian surface is attained (Tsai and Soni 1982).

(*ii*) Extremalization algorithms which compute the joint variables values corresponding to points on the envelope (extreme reach) of the workspace (Kumar and Waldron 1981).

(*iii*) Recursive algorithms which compute the envelope by allowing the joint variables to move one after another within their entire range of motion (Gupta and Roth 1982).

The proposed method of determining the envelope of the workspace in this thesis is based on a modified version of method (*i*) stated above. It will be shown that this method is very efficient with respect to the methods (*ii*) and (*iii*) which are based on numerical optimization and recursive algorithms. In what follows the requirements of this approach will be discussed.

REQUIREMENTS:

1- First we require that the inverse kinematics solutions for the manipulator exist. This condition is met for all of the available robots at the present day.

2- In the inverse kinematics solutions, one can control the posture of the robot, this requirement is also accessible for most of the present robots. It is usual to define configuration coefficients in the form of ±1 to dictate the posture of the arm while reaching for a pose.

Borrel and Liegeois (1986) argued that the approaches based on method (i) can fail in most cases where the number of solutions to the inverse kinematics are more than one. However as will be shown in the next section, by introducing the configuration coefficient, not only the algorithm does not fail, but also we are able to have control over the posture or the configuration of the robots. In other words in the process of the tracking the contour of the robot we will not allow any aspect changes, or configuration changes.

5.3.1- DIRECT SEARCH METHOD

The first proposed approach, for the contour detection algorithm of the workspace of a manipulator is based on a simple search technique. This approach was implemented in both Cartesian and polar coordinates. First step in both Cartesian and polar coordinates is to choose the cutting plane π on which the contour of the workspace is to be mapped. In the developed algorithms, although one can choose any given plane, but the most natural case would be a plane parallel to one of xy, xz or yz planes of the robot's reference frame. Next the maximum and minimum reaches of the robot (R_{max} and R_{min}) are calculated by using the formulae of section 5.2. Then a sweeping area will be constructed on plane π which is bounded by two concentric circles of radii R_{max} and R_{min} respectively. Next the sweeping area will be divided into meshes of appropriate shape and size and the reachability of each and every of these meshes will be examined. A *Reachability Index* (RI) of unity will be assigned to a mesh which is reachable by the end effector and an index of zero otherwise.

Next step is to record the x, y and z coordinates of all of the meshes whose RI is unity, with at least one of their neighboring meshes possessing a zero RI, in other words the coordinates of a contour point on the working envelope will be recorded. The reachability of a mesh is checked by solving the inverse kinematics of the robot with a desired posture or configuration given the cartesian coordinates of the center of the mesh and a given orientation of the end effector. If the point is not on a Jacobian surface (it does not lie near a singularity) or the corresponding joint variables consistently do not violate their physical limits then the the point under consideration will be assigned the RI of unity. It should be mentioned that in this algorithm we have the flexibility of either considering the orientation of the hand which will result in a more limited working area for the manipulator, or ignoring the orientation which will in turn result in the reachable workspace for the arm. In either case the workspace boundaries are realistic, since the arm need not change its configuration within the reachable area.

In what follows, the first method, which is based on the cartesian coordinates of the points, on the cutting plane will be presented. The basic idea of this method is not new, and it has been discussed by Tsai and Soni (1982). However the new features added to this conventional method by this thesis will enable one to first investigate the effects of the hand's orientation on the shape of the workspace.

Search in Cartesian coordinate:

Figure 5.5 shows the general structure of the contour detection algorithm when the cutting plane is a vertical plane parallel to the yz plane of the robot's base frame. In our first approach, discussed here the sweeping area is subdivided into meshes in cartesian coordinates. Next maximum and minimum reach must be mapped to the cutting plane in order to determine the corresponding maximum and minimum reaches on the plane. This can be easily done by writng

$$\rho_{max} = \sqrt{R_{max}^2 - r_o^2} \qquad \text{for} \quad r_o < R_{max} \tag{5.24}$$

$$\rho_{min} = \sqrt{R_{min}^2 - r_o^2} \qquad \text{for } R_{min} < r_o < R_{max} \tag{5.25}$$

where ρ_{max} and ρ_{min} are the new maximum and minimum reach on the cutting plane and r_o is the normal distance from the cutting plane to the origin of the robot's base frame.

After defining the cutting plane and the new maximum and minimum reaches on the piane, the user should specify if the hand orientation is to be considered in the workspace determination or not. If the hand orientation is immaterial then the program will assign arbitrary orientation to the hand and only the reachability of the wrist point will be examined. Then the obtained workspace area will be added upon by the constant distance of the hand size (or d_6 for PUMA Robots) of the robot to produce the reachable workspace of the end effector. However, if the effects of the hand's orientation is to be observed on the shape of the workspace then the desired hand's orientation will be fed in to the program.

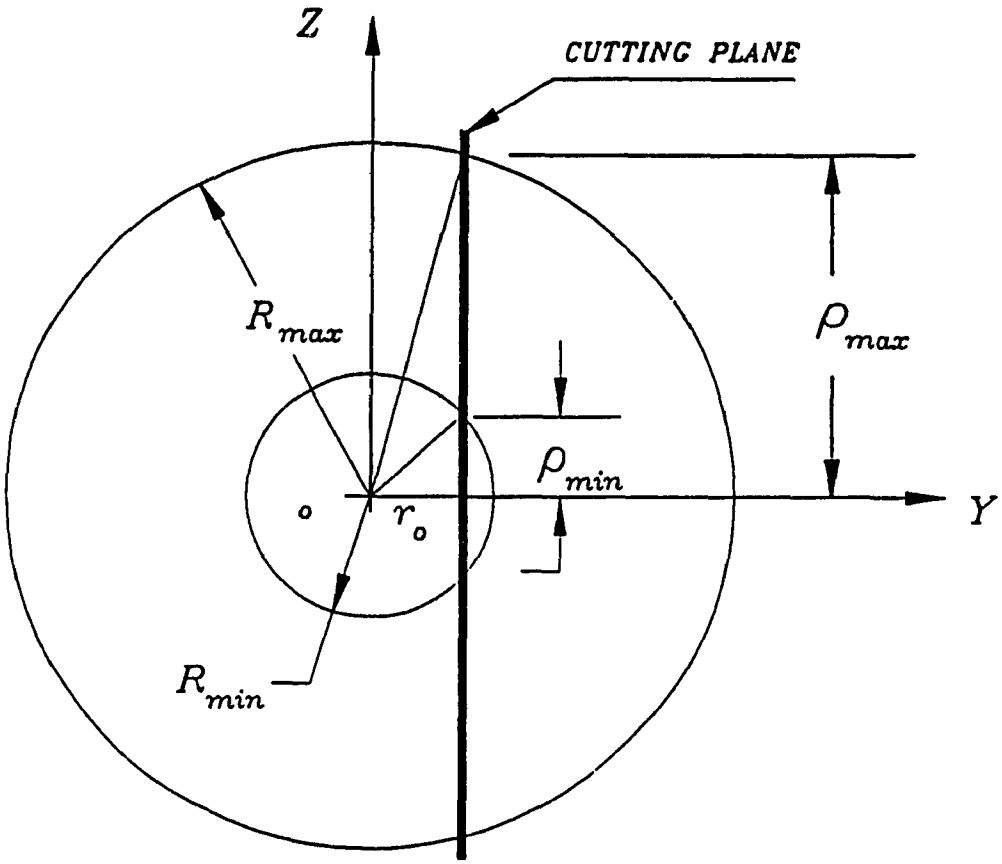

Figure 5.5 - Construction of the search area

Next step is to enter the desired resolution or step size for sweeping process. One can choose three different values for the step size along x, y or z axes of the base frame or Δ_x, Δ_y and Δ_z respectively. Next the search algorithm starts sweeping in one direction from two mesh size outside the maximum reach area, the two extra mesh will account for the resolution and possible errors due to round-offs in the numerical calculations. Obviously the RI for the first mesh should be assigned zero by the initialization part of the algorithm. At this stage either the hand or the wrist of the robot (depending on the importance of the orientation) will be moved to the second mesh and the RI corresponding to that mesh will be examined by first solving the inverse kinematics corresponding to that pose and then checking for the reachability of the point (both for the Jacobian and the joint limits). Then the coordinates of those meshes with an RI of unity whose at least one of neighboring RI is zero, will be recorded in a data file. Increments will be added to the coordinates of the hand (or wrist point) along the search direction until two meshes beyond the negative of the maximum reach is checked. At this point the search direction itself will be incremented and thus the whole searching area will be swept and consequently the coordinates of the point of the workspace located at the bounding surfaces will be obtained. The aforementioned steps in the presented algorithm are outlined in the flow chart of the program given in the appendix C.

A computer program called **CONTOUR1.C** was developed in C language to implement the aforementioned algorithm. This program has to be linked with the Inverse and the Forward kinematic subroutines in the corresponding module called **PUMA_KIN.C**. Another subroutine which will be called by the program is the **CHECK_LIMIT.C** program which tests the reachability of the point in

question in terms of the joint limits, this function also is available in PUMA_KIN.C. It has to be mentioned here that in the inverse kinematic module if the point in question is a singular point and the Jacobian degenerates then solving the inverse kinematic formulation will be formidable, in these cases deliberately the returned parameters of the subroutine will be given such values which will violate the joint limit requirements in the CHECK_LIMIT subprogram.

RESULTS:

Figures 5.6 to 5.8 are some illustrative examples obtained by this first algorithm, in the cartesian space. In these plots it is intended to show the effects of the hands orientation on the shape of the workspace. Figure 5.6 compares the working envelopes mapped to the ZX plane in the cartesian space (with $Y_o = 0.0$), for the wrist point (boundary of the dexterous workspace) with the workspace generated for the hand, with the orientation given by equation 5.26.

Figure 5.7 shows the boundary of the aforementioned working envelope mapped to the YZ plane (with $X_o = 0.0$). And finally in figure 5.8, these two workspaces are shown in the XZ plane (with $Y_o = 0.0$). Orientation of the hand for the foregoing cases is given as follows,

$$R_o^h = \begin{bmatrix} 0 & 1 & 0 \\ 0.7071 & 0 & -0.7071 \\ -0.7071 & 0 & -0.7071 \end{bmatrix} \tag{5.26}$$

It can be seen by comparing figures 5.7 and 5.8, that, how a given desired and fixed orientation for the hand can limit and deform the boundary of the work envelop.

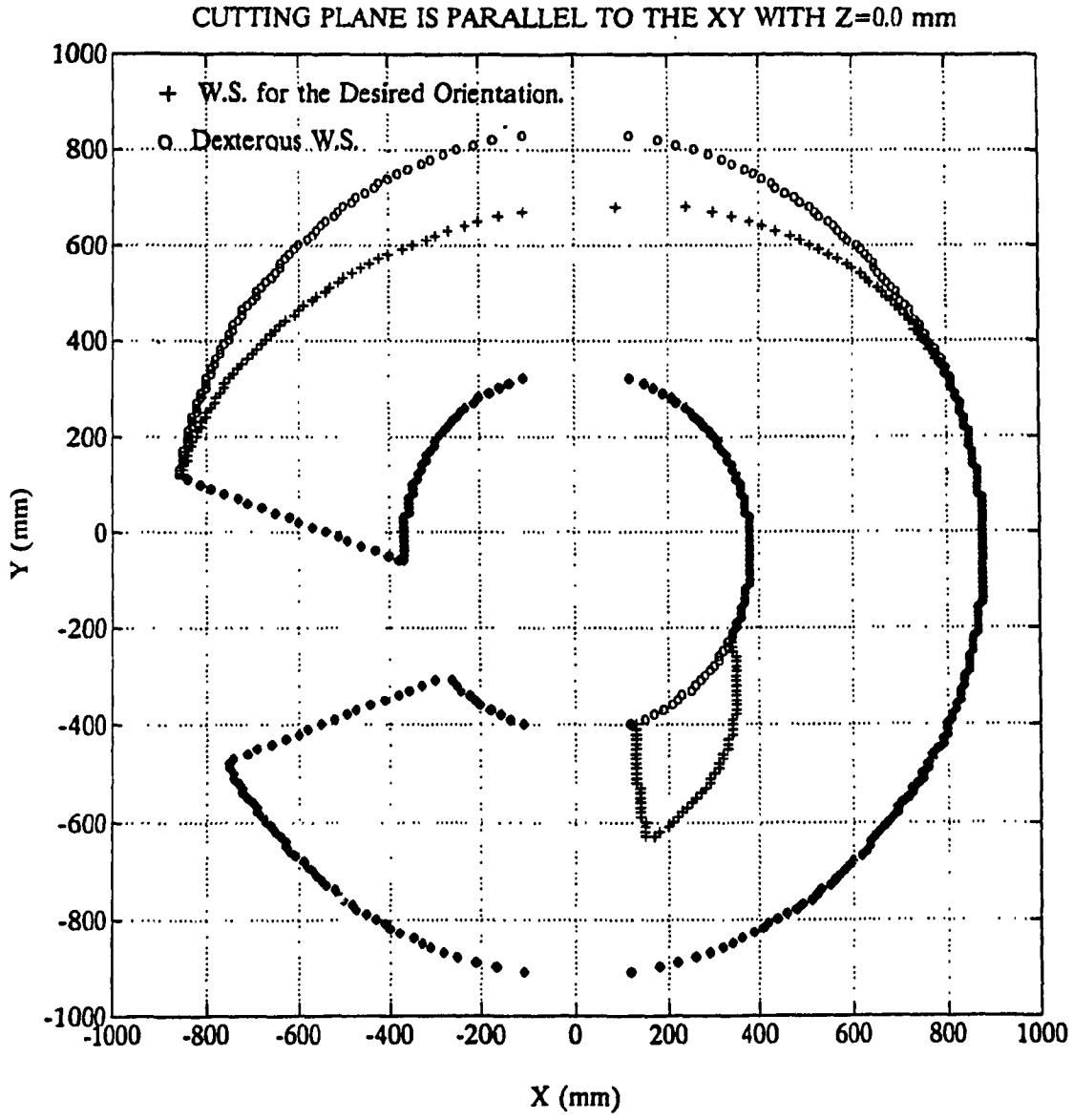

Figure 5.6 - Two dimensional workspace on XY plane (direct search)

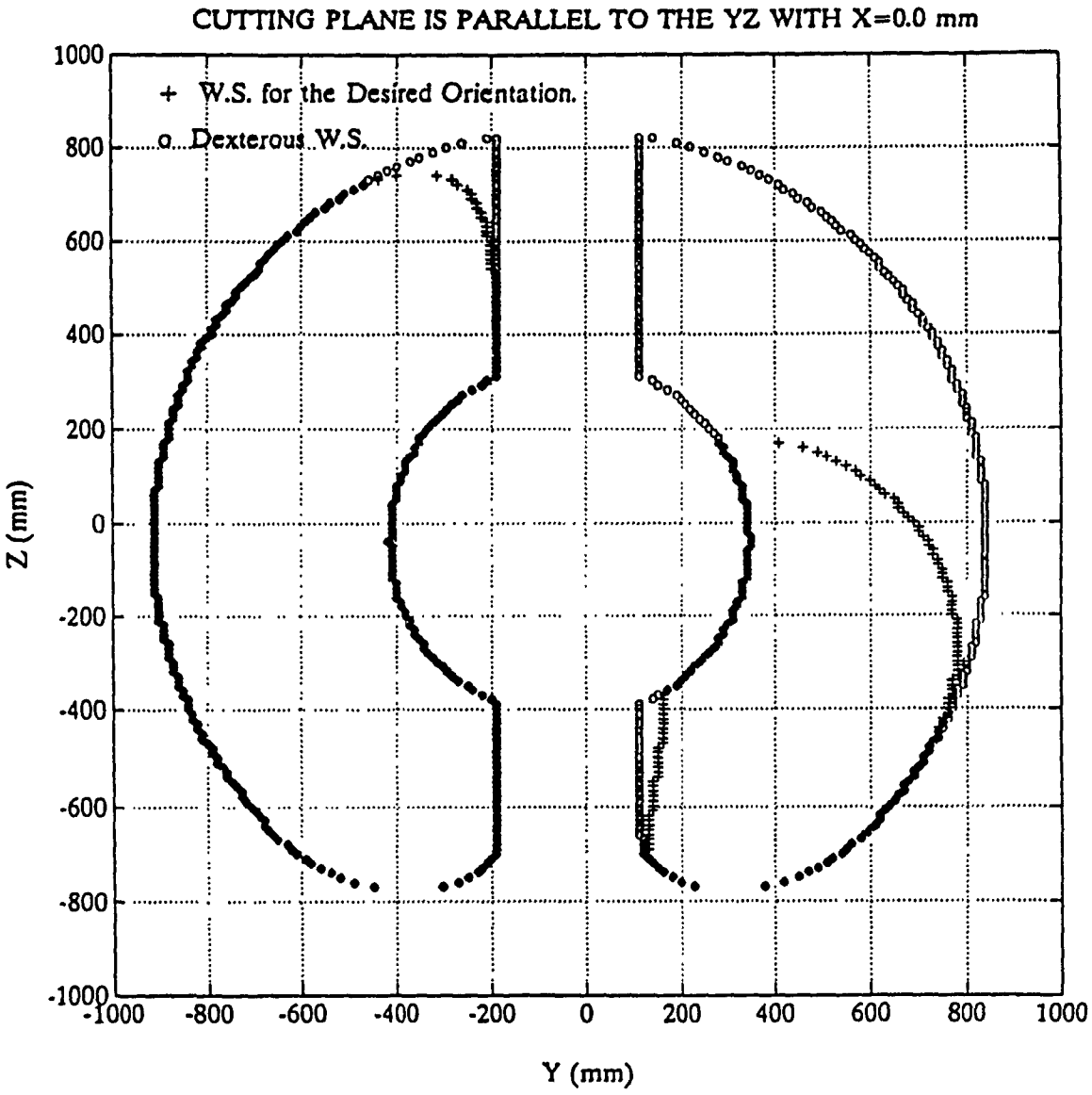

Figure 5.7 - Two dimensional workspace on YZ plane (direct search)

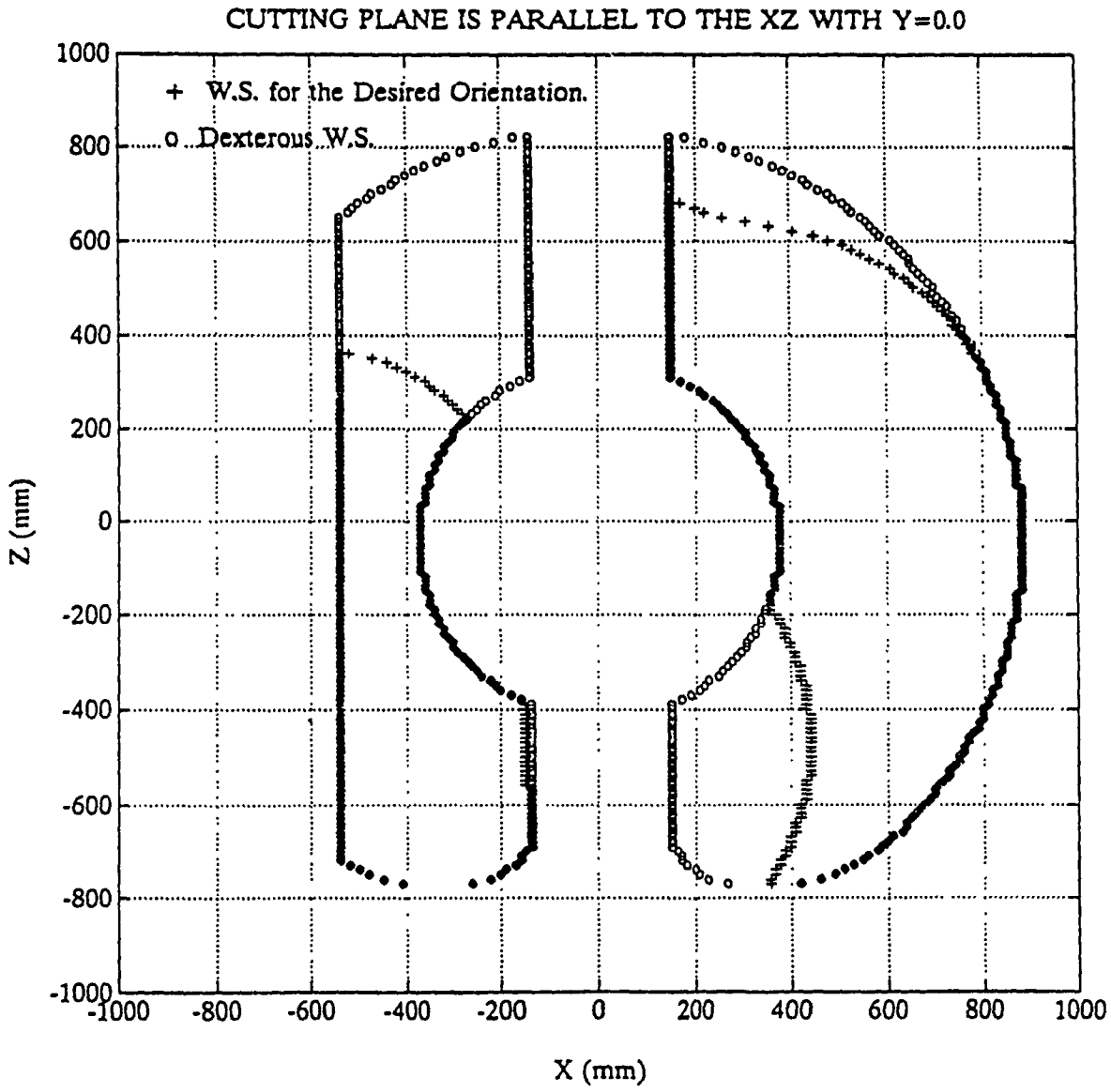

Figure 5.8 - Two dimensional workspace on XZ plane (direct search)

Search in Polar coordinate:

By referring to figures 5.7 to 5.8, it can be seen that sometimes if the boundary of the envelope is partially lined up along the search direction (Fig. 5.6) then the resolution of the detected points will be diminished, or in other words the number of detected boundary points will locally decrease.Therefore a novel approach is proposed which is essentially based on the same idea as the previous case, with the difference that the searching area will be divided into meshes in the polar coordinates. Hence the search directions will become ρ and θ and thus the increments will be denoted by $\Delta\rho$ and $\Delta\theta$ along the radial and tangential directions respectively. After defining the cutting plane and determination of the extreme reaches of the robot, first, the searching area will be constructed on the cutting plane. Next for one value of θ, the meshes lined up on the ρ direction will be checked, and after covering all of the meshes radially then θ will be incremented and the similar sweep will be performed along the new ρ. This will be repeated for $2\pi/\Delta\theta$ times, until the whole area is covered. The basic structure of the polar search method is shown in figure 5.9. The computer program responsible for the implementation of the polar search algorithm is called **CONTPOLAR1.C.**

It has to be mentioned that in order to solve the inverse kinematics one needs to use the Cartesian coordinates of the end effector, therefore, although the sweeping operation is performed in the polar coordinates, but the following well known transformations are used to obtain the cartesian coordinates for the inverse kinematics module. If the cutting plane is parallel to the XY plane with $Z_o = r_o$.

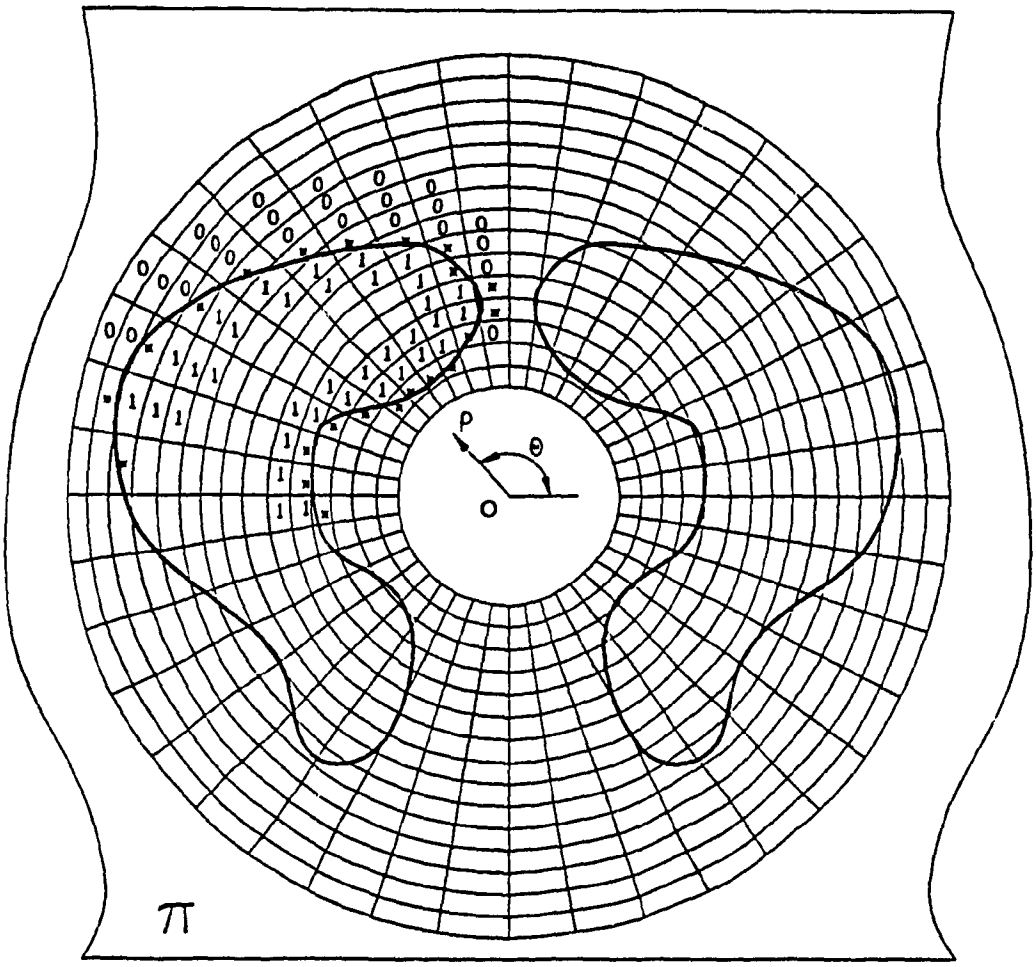

Figure 5.9 - Construction of the polar coordinate searching area

$$x = \rho\cos\theta, \quad y = \rho\sin\theta \quad \text{and} \quad z = r_o \tag{5.28}$$

If the cutting plane is parallel to the XZ plane with $Y_o = r_o$.

$$x = \rho\cos\theta, \quad z = \rho\sin\theta \quad \text{and} \quad y = r_o \tag{5.29}$$

If the cutting plane is parallel to the ZY plane with $X_o = r_o$.

$$y = \rho\cos\theta, \quad z = \rho\sin\theta \quad \text{and} \quad x = r_o \tag{5.27}$$

Results:

The results of the polar search algorithm are given in figure 5.10 to 5.12. These plots similar to the cartesian space signify the effects of the hand's orientation on the shape of the dexterous workspaces mapped to the planes parallel to the XY, YZ and ZX respectively. The normal distance of these cutting planes to the origin are arbitrarily chosen to be 100 mm, (*i.e.* $X_o = Y_o = Z_o = 100$ mm.).

Comparison between the Cartesian and Polar search algorithms:

By comparing figures 5.6 and 5.10, one can observe the difference between the resolutions obtained in cartesian coordinates and the corresponding polar coordinates. In fact in figure 5.6 the search direction is horizontal whereas in figure 5.9, it is radial, and thus local reductions in the resolution occur at different locations of the boundaries.

Another major criterion for the evaluation of the two methods, is the computational cost. It was observed that the polar search method is more efficient and thus faster, the benchmark given in what follows, will establish this difference.

Benchmark obtained on VAX-8550:

Method	Number of points	Execution Time (sec)	cost sec/point
Cartesian	448	28.6	0.0638
Polar	338	9.5	0.0281

To this end having compared the resolution and computational cost of the two search algorithms, it can be concluded that by using polar search technique discussed before, the overall resolution of the mapped working envelop is enhanced, while the computational cost is decreased. Hence between the two methods of cartesian and polar search methods the latter is recommended.

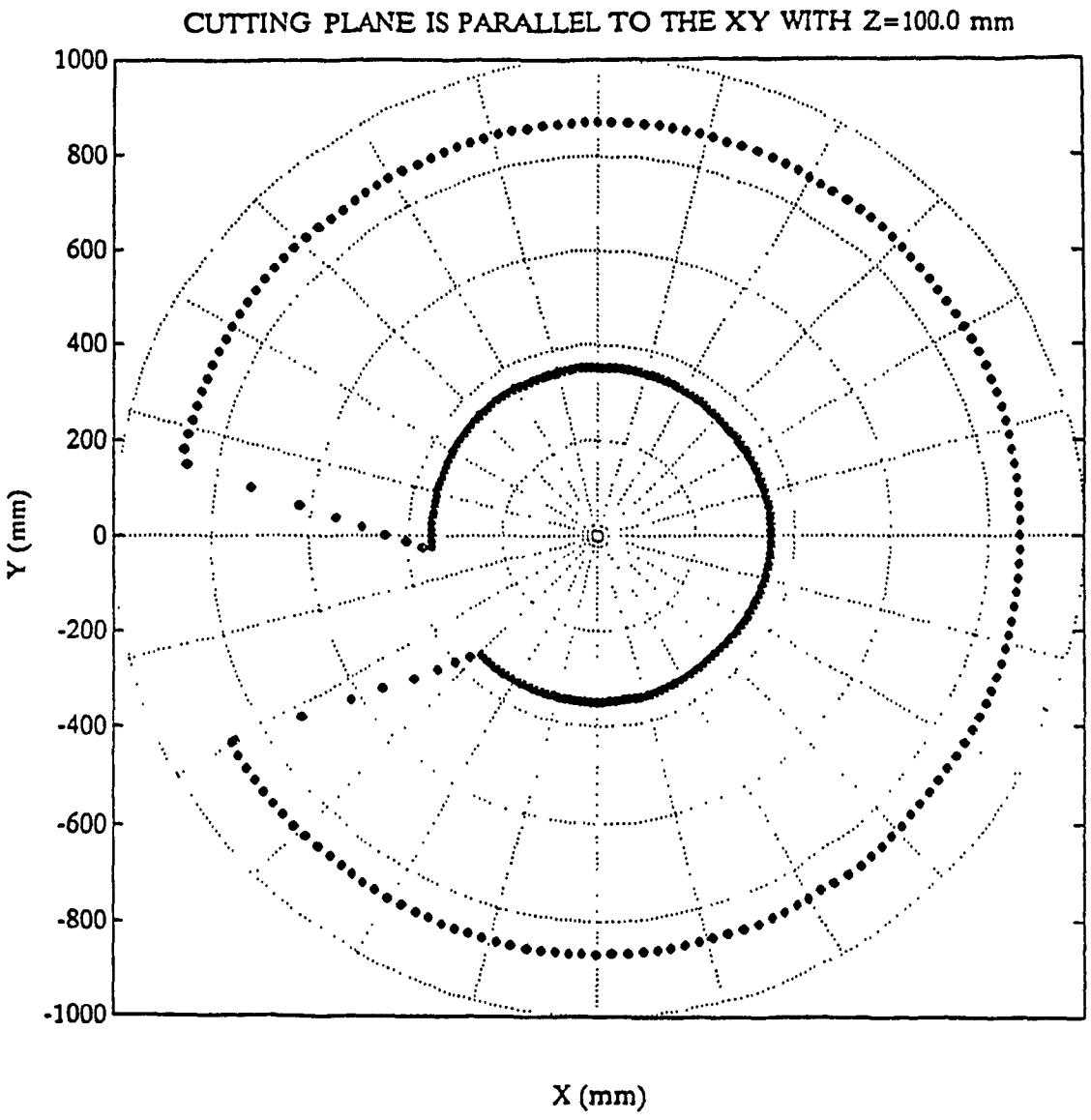

Figure 5.10 - Workspace on XY plane in the polar coordinates

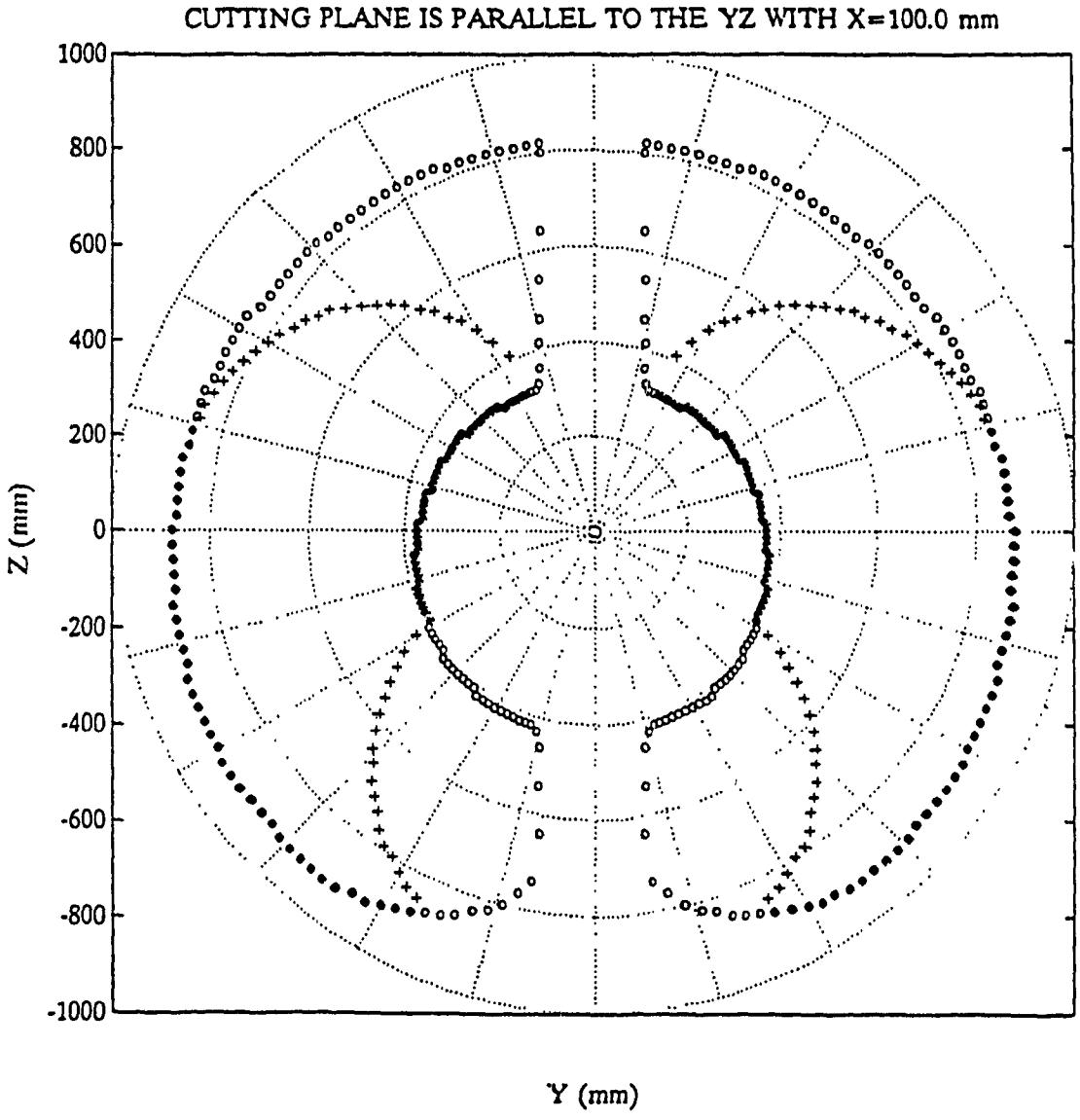

Figure 5.11 - Workspace on YZ plane in the polar coordinates

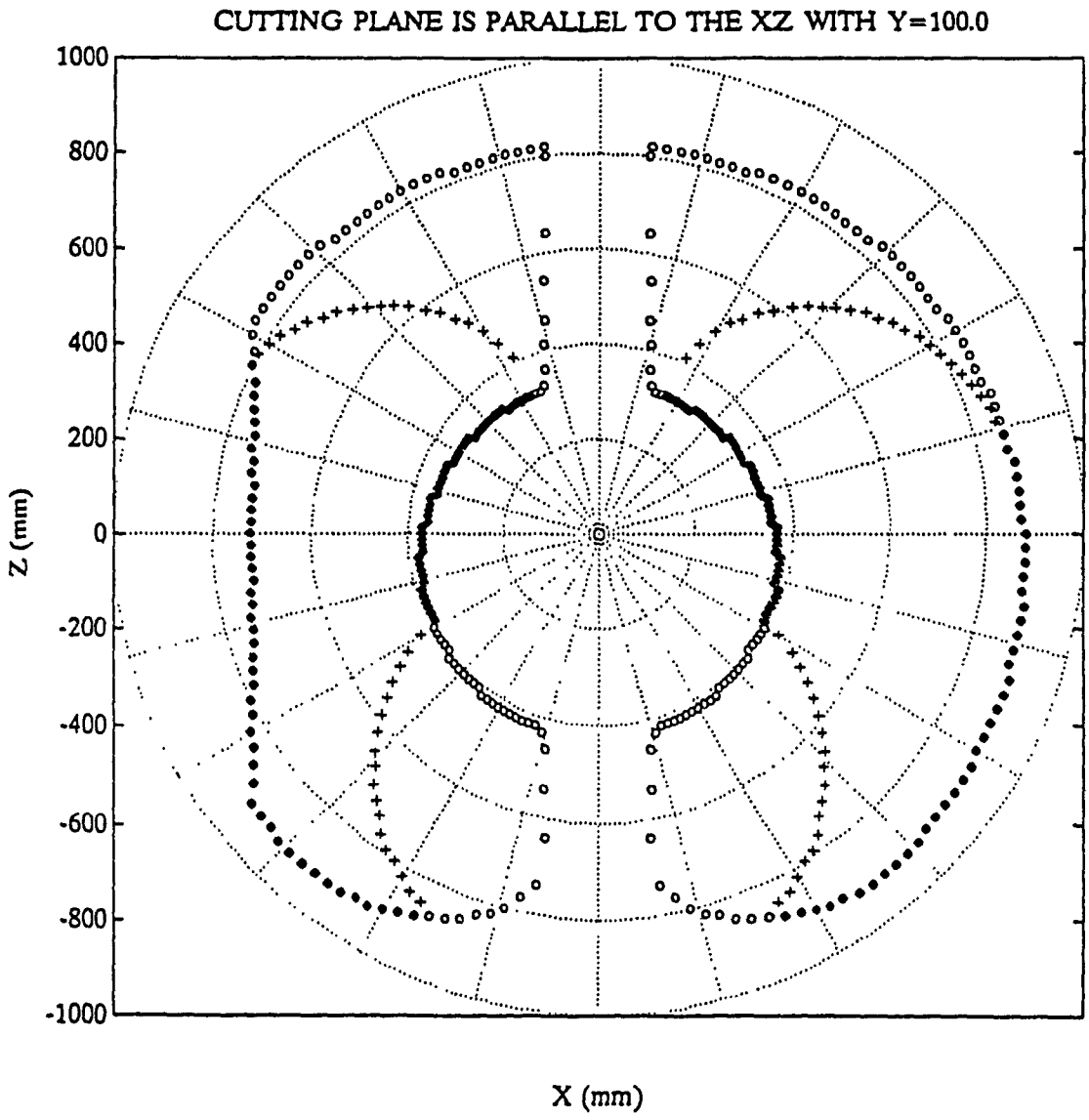

Figure 5.12 - Workspace on XZ plane in the polar coordinates

5.3.2- ADAPTIVE SEARCH METHOD

In the previous section, direct search methods in cartesian and polar coordinates were introduced and the characteristics of the two, with some examples were discussed. The direct search methods in general, are very robust, and able to detect the contour of the working volume with any shape, in other words, depending on the resolution of the search, all of the boundary points can be detected. Despite the power of the direct search methods in the contour detection algorithms, they are not the most recommended ones, when one has to obtain several contours in relatively short time. This is due to the fact that all of the points fallen within the constructed search area will be indiscriminately examined. But if, one is able to make use of the previously detected points, in order to limit the search to a specific direction, then the computational burden of the algorithm will reduce to a great extend.

Since in the following section, when we introduce the three-dimensional reconstruction of the workspace, it will be necessary to obtain several two-dimensional images of the workspace, thus it is required to device a more intelligent search method to detect the mapped coordinates of the workspace onto the cutting planes in the shortest time possible. This urge gave rise to a third algorithm which was named as **"Adaptive Search Method"** or **ASM** in contour detection, for short. The step by step procedure to follow in order to find the contour points via **ASM** algorithm, will be explained next.

- First similar to the direct search methods discussed before, the cutting plane is specified. For the sake of discussion assume this is plane

parallel to the YZ plane with $X_o = r_o$

- Next the maximum reaches R_{max} of the robot will be mapped into the cutting plane to give ρ_{max}, and thus the search area will be constructed by a circle with its origin at the origin of the robot and a radius equal to $\rho_{max} + 2\delta$ where δ is the step size, and twice of it is added to the search radius to ensure that the search starts outside the reachable area ,this is shown in figure 5.13

- At this point, it is required to detect one point of the workspace, and one point of any hole or void inside it. In order to do that, a one time direct search can be used (similar to the direct search methods) for example for figure 5.13, at a starting value of x_1 a column will be searched along the z axis from $z = (\rho_{max} + 2\delta)$ to $z = -(\rho_{max} + 2\delta)$.

- Having found a starting point on the contour of the working envelope, which will be addressed as the current point hereafter, next only the neighboring points to the current point will be checked. In order to decide in what direction the neighboring points will be examined, we have made use of the slope of the line connecting previous two boundary points. Since at starting points, there is not available a history of any previous points, thus an arbitrary slope (zero degrees) is assigned for the history corresponding to the starting points. The new reachable point being sought for the current point will be among eight neighboring points to the current point. Figure 5.14 is an illustration of the current point versus the previous reachable and its neighboring points. For example in this figure the slope of the search corresponding to point C will be 45°.

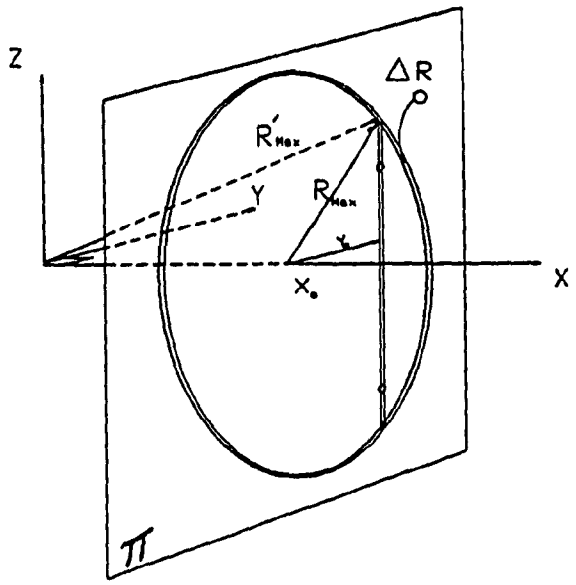

Figure 5.13 - Cutting plane

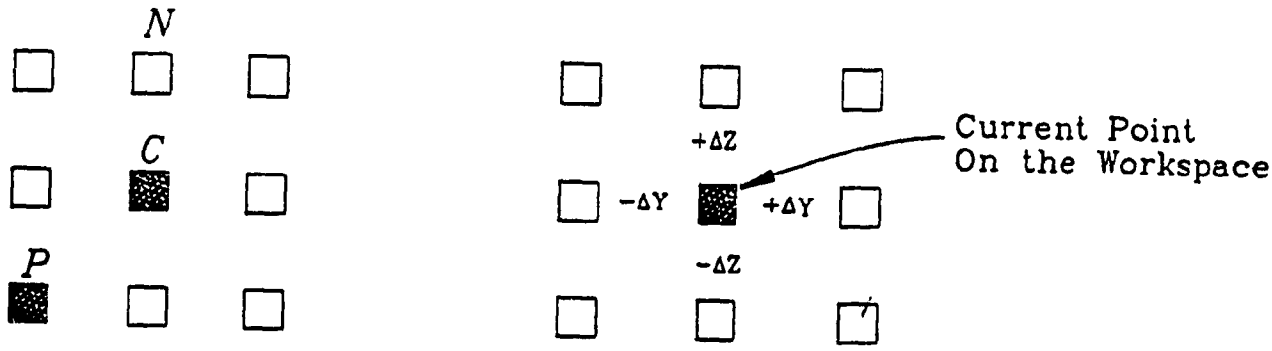

Figure 5.14 - Search pattern

- Based on the slope of the search obtained in the previous step, four different directions will have to be examined. These patterns are shown in figure 5.15. Moreover for each slope determined three different search pattern can be laid down. For example when the slope is between -45° and 45° these pattern are given in figure 5.16.

- After checking for the reachability of the neighboring points the one which is reachable and also has at least one not-reachable neighbor will be recorded as the current point and its coordinates will be saved. The computer program responsible for the implementation of this algorithm is called "CONTOUR3.C".

RESULTS:

Figure 5.17 and 5.18 are some illustrative sample results, obtained from "CONTOUR3.C". Figure 5.17 shows two boundary of the workspaces cut by a vertical plane parallel to the XZ plane with Y_o = 350 mm. One of these boundaries corresponds to the Dextrous workspace and the other shows the deformed boundary of the workspace, while a given orientation of the hand is fixed. This desired orientation is given in equation 5.26. The execution time for this plot was recorded as 3.0 seconds for 444 points. Figure 5.18 depicts the boundary of the aforementioned workspaces on a plane with Y_o = -400 mm, while the desired orientation is chosen to be a rotation by 60° about the Z axis. The rotation matrix corresponding to this configuration is given as,

$$R_o^h = \begin{bmatrix} 0.5 & 0.0 & 0.86602 \\ 0.0 & 1.0 & 0.0 \\ -0.86602 & 0.0 & 0.5 \end{bmatrix} \qquad (5.27)$$

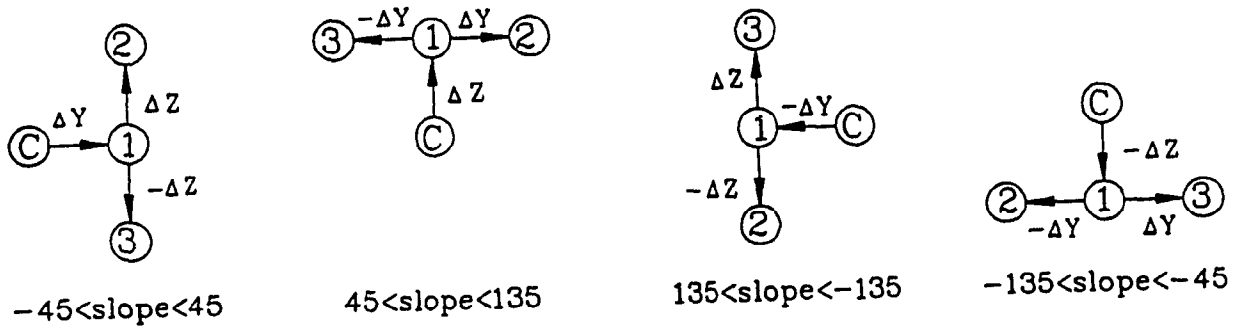

Figure 5.15 - Search direction on the cutting plane

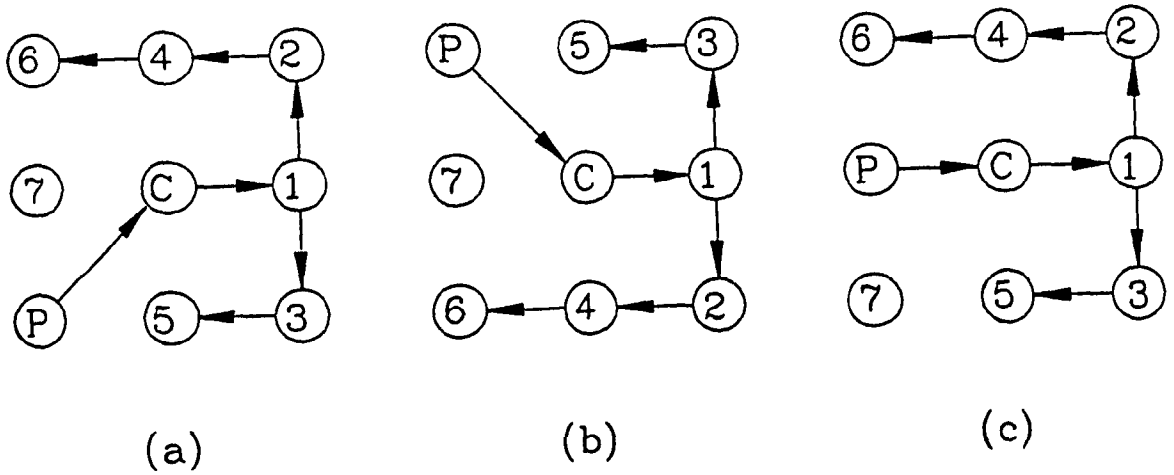

Figure 5.16 - Search direction based on the previous slope

The execution time for the aforementioned plot was recorded to be about 4.5 seconds, for generation of about 441 points.

Advantages: The advantages of using SME are outlined in what follows,

1- As a major advantage, since in the ASM algorithm we do not search all over the searching area, but rather concentrate on the close proximities of a boundary point, thus the execution time for the generation of a large number of contour points is reduced significantly as compare to the DSM algorithm. In fact the benchmark obtained showed that the computational cost of the ASM is less than ten times that of the DSM. For example for the plot given in figure 5.17, 444 number of points were obtained in 3.0 seconds. This will imply a computational cost of 0.0067 second per contour point detected. By comparing this figure with the benchmark given in table 5.1, one can see that, it is more than nine times smaller than the cost obtained for the DMS in cartesian coordinates and more than four times smaller, relative to the DMS in polar coordinates. Hence the main objective of the time effectiveness for the algorithm is fulfilled.

2- Second desirable characteristic of the ASM as opposed to the DSM, is the smoothness of the detected boundaries. This can be seen by comparing the results of figures 5.17 to 23 obtained by ASM to the results of DSM shown in figure 5.6, to 5.9. The main reason for this is the fact that ASM benefits from the slope of the boundary and will search in the direction locally tangent to the contour, thus with the same step size of 10 mm, as was used for the DMS, we were able to obtain smoother boundaries.

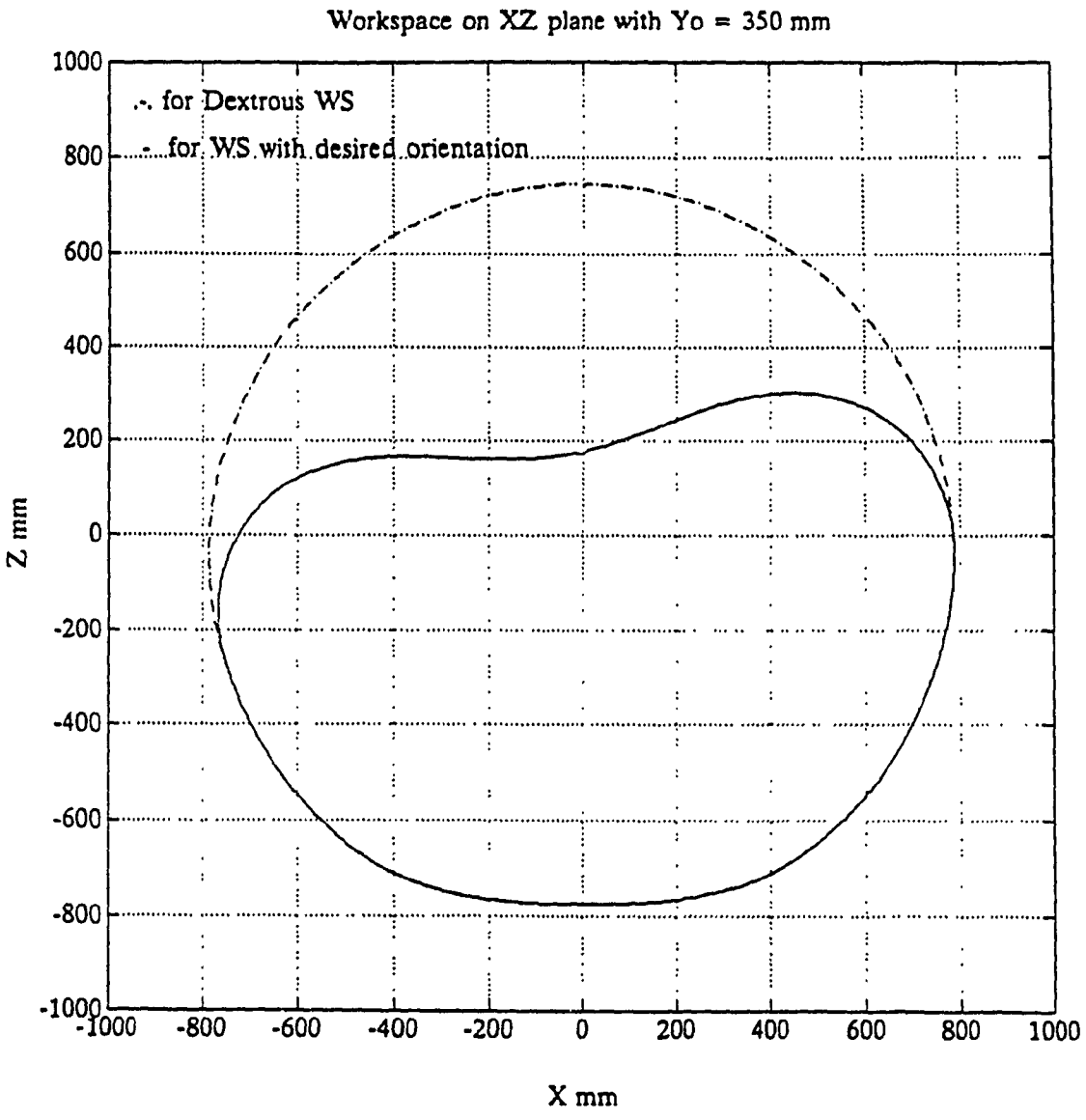

Figure 5.17 - Workspace on XZ plane by adaptive search method

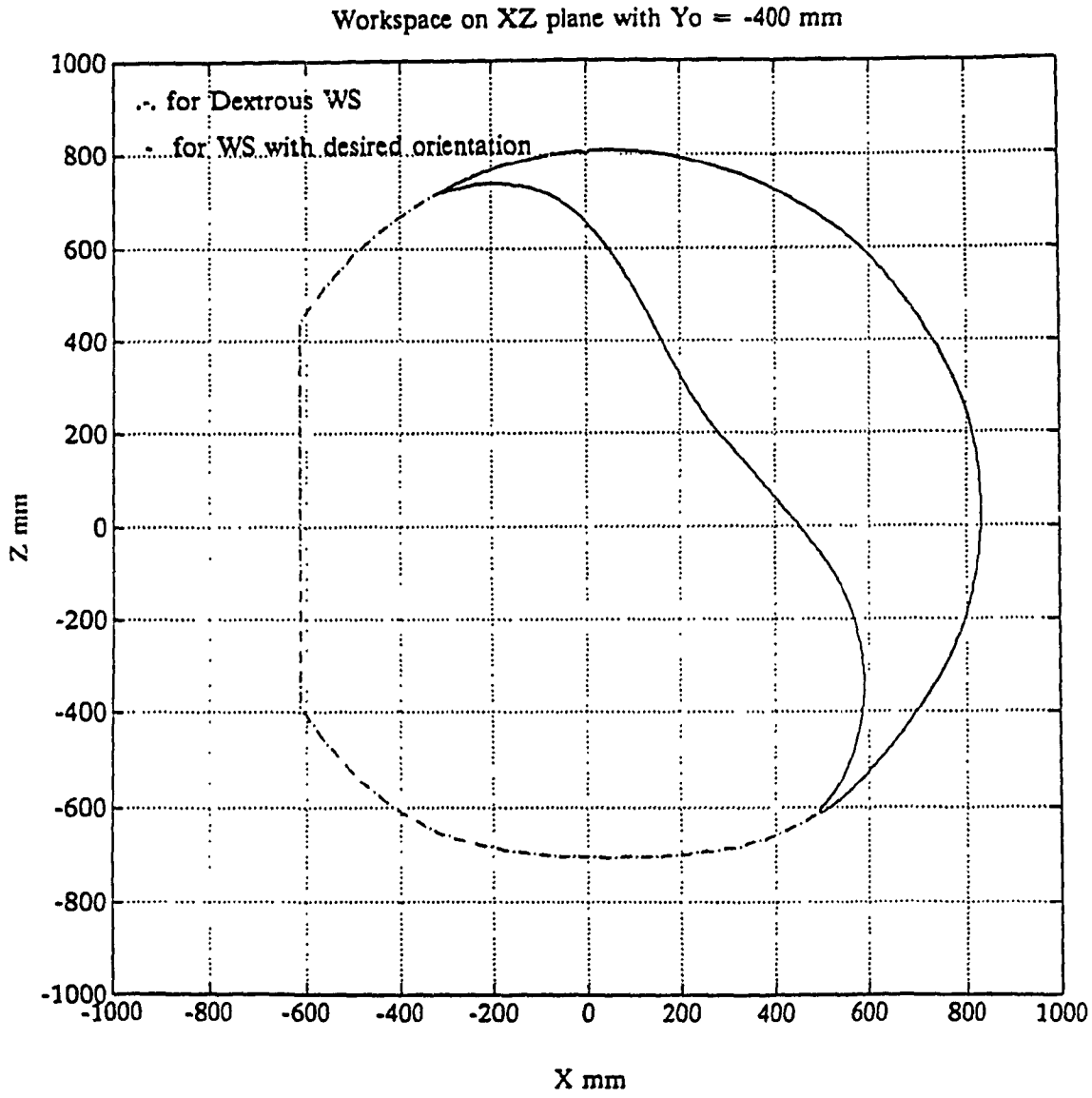

Figure 5.18 - Workspace on XZ plane by adaptive search method

Disadvantage: The only disadvantage intrinsic in the ASM algorithm, is the fact that, there exist cases where the adaptive search can fail to detect the next point of the contour. This can mainly occur where there is a *cusp* with sharp corner along the contour, in other words if the slope of the contour is not continuous the algorithm can get lost or perhaps return back along the previously detected contour.

5.3.3- EFFECTS OF THE MANIPULATOR POSTURES ON THE SHAPE OF THE WORKSPACES

In this section the effects of the manipulator posture or the corresponding aspect of the joint space, on the shape of the workspace associated with the arm will be discussed. As was mentioned in the previous sections, in the process of contour generation, the configuration or posture of the arm was required to remain the same, in other words no aspect or configuration changes in a workspace was admissible.

In order to observe how the arm's posture affects the boundary of the workspace for a given orientation of the hand we will resort to an example. Assume that the given orientation of the hand is defined by equation **5.27**, next we will generate the workspaces of the manipulator for both the wrist point (Dextrous) and for the end effctor on XZ plane with Y_o = -400 mm. The results of these trials by using DSM in polar coordinates, are given in figures 5.19 , 5.20, and 5.21. Figure 5.19 shows the Dextrous workspace of the manipulator for four possible arm's postures namely, 1- Left Shoulder Elbow Up (LS/EU), 2- Left Shoulder Elbow Down (LS/ED) 3- Right Shoulder Elbow Up (RS/EU) and 4- Right Shoulder Elbow Down (RS/ED).

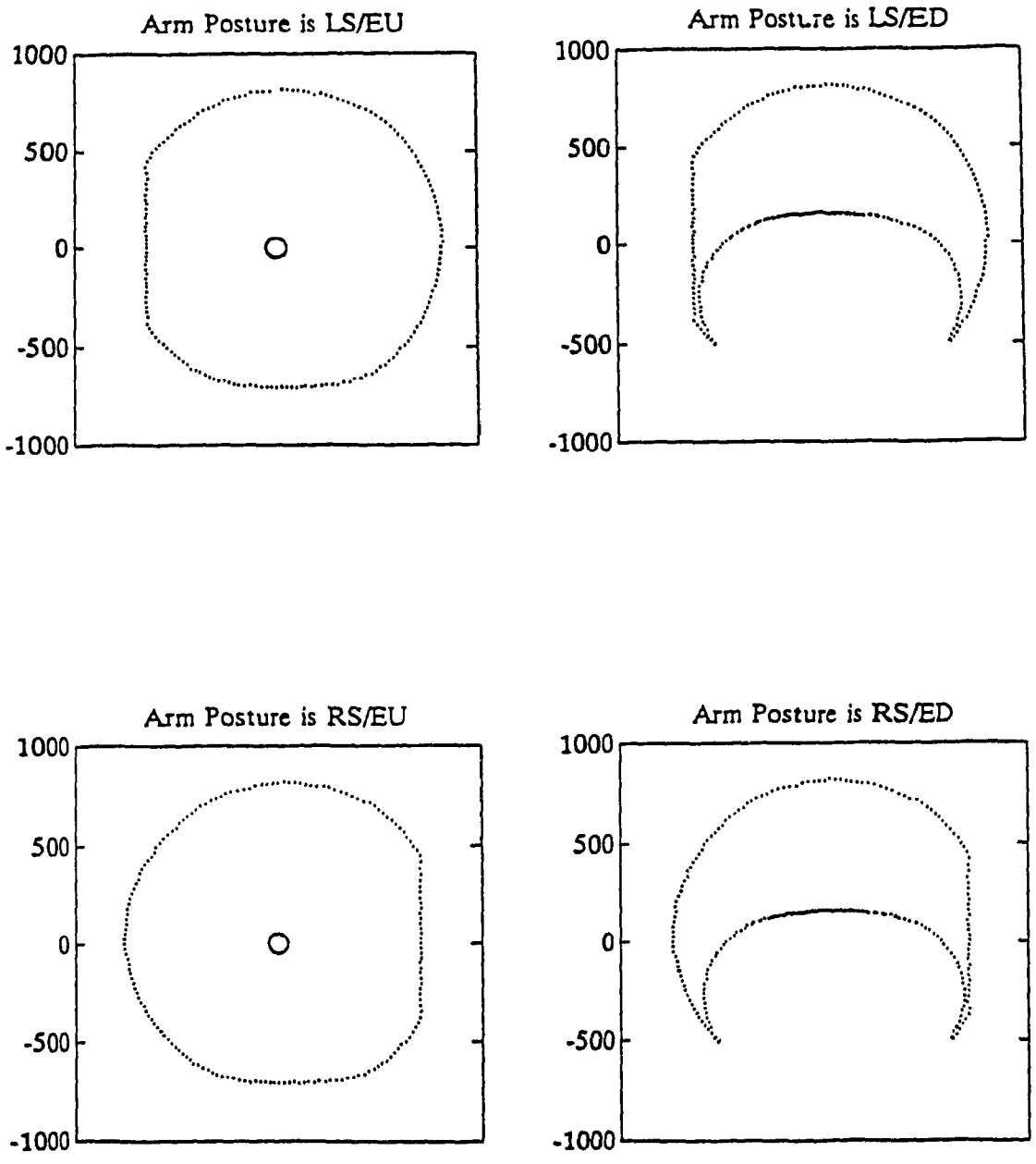

Figure 5.19 - Effects of the robot's posture on its workspace

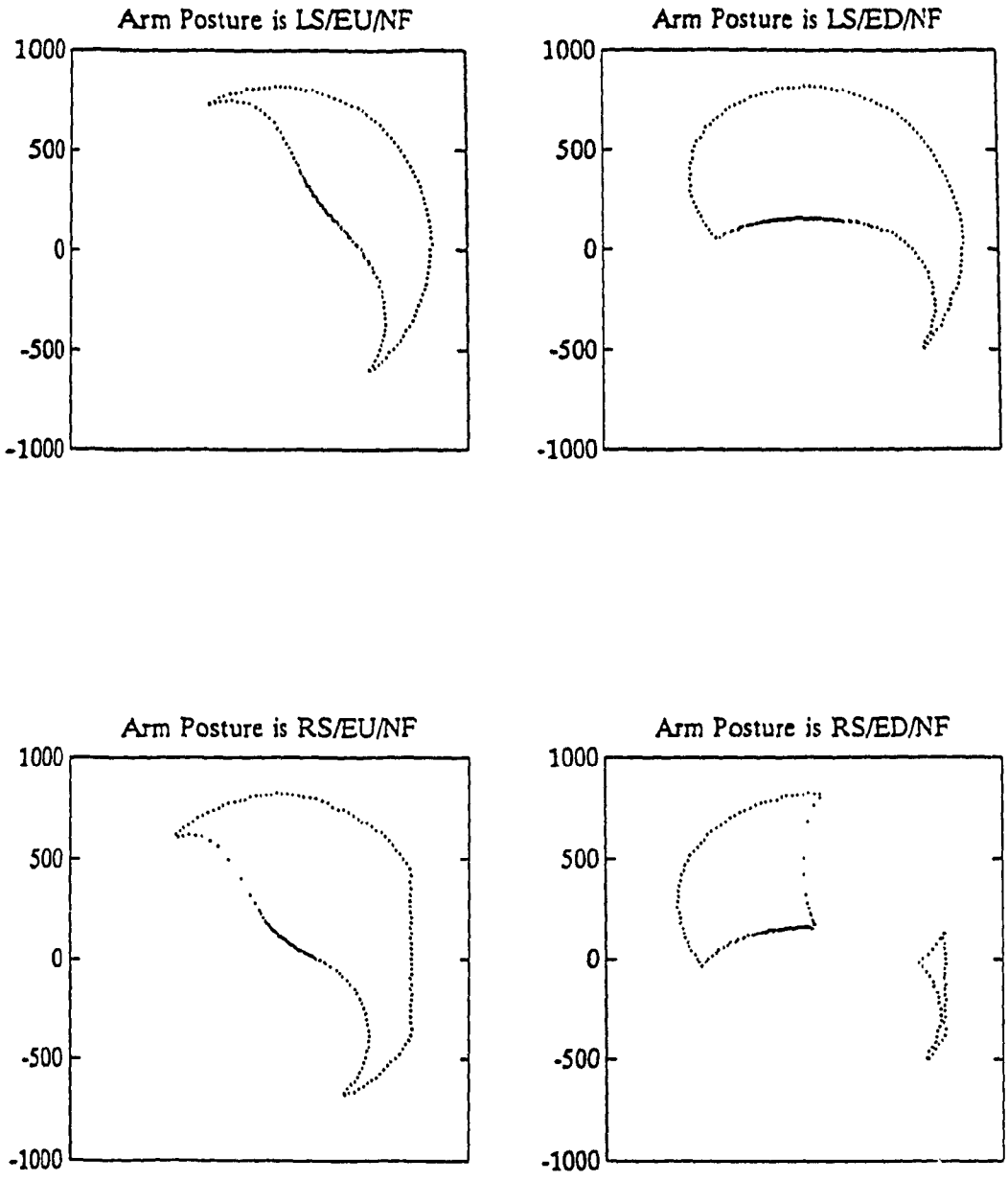

Figure 5.20 - Effects of the robots posture on its workspace

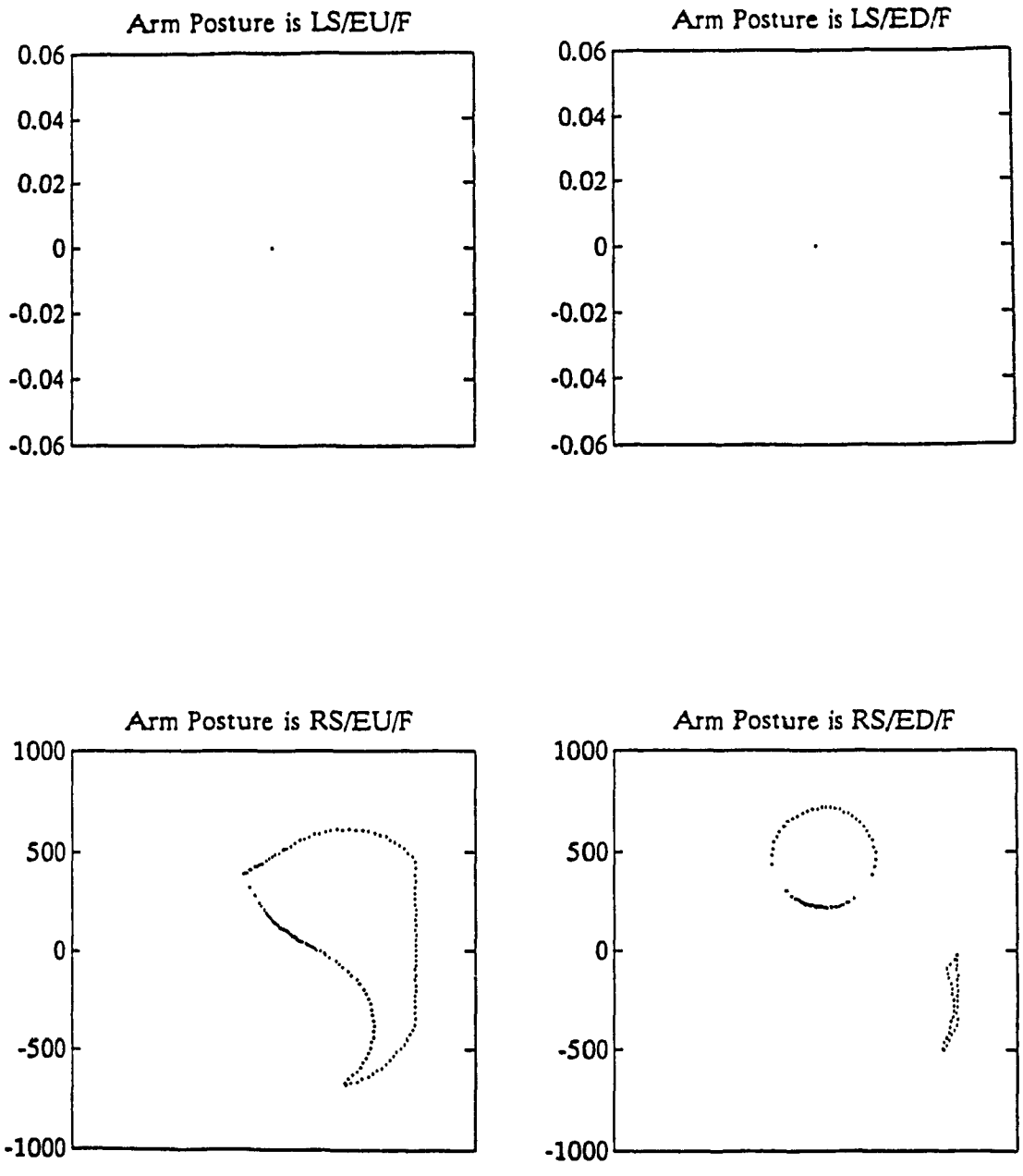

Figure 5.21 - Effects of the robots posture on its workspace

Figuures 5.20 and 5.21 show the workspaces of the end effector with the desired orientation. For any desired pose of the end effector there exists up to eight different aspects (postures), they are the aforementioned four postures of the arm with each being able to have the robot's hand in a flip (../F) or no flip (../NF) configurations.

5.4- AUTOCAD-BASED THREE-DIMENSIONAL RECONSTRUCTION OF THE WORKSPACES

Two dimensional contours of the workspace are useful to give an understanding of the general structure of the workspaces, and have been investigated before. However, there has not been any attempt to present a three dimensional image of the robot's workspaces. One of the major contributions of this thesis to the workspace studies, is fulfilling this need. A three dimensional image of a robot's workspace can give a great deal of knowledge about the geometrical shape of the working envelop and thus can have significant importance in the process of the set-up of a robotic workcell.

In the previous sections we discussed three different algorithms for detecting the boundary of the workspaces associated with a robot arm, moreover presented some illustrative examples for PUMA-560. In the following sections, the attempt is to reconstruct a graphical three-dimensional image of the workspace, by using several two-dimensional contours. The graphical tools which will be employed for this purpose is AutoCad-10.

As the first step for the 3-D reconstruction of the workspace, it is necessary to store the cartesian coordinates of the contour points mapped to

several parallel planes cutting the entire workspace. By resorting to one of the previous algorithms, one can create a data-base which include several cutting planes, on each, two coordinates of the boundary points are given. As an example, in this thesis, vertical planes parallel to the ZY plane cut the workspace of a PUMA-560, and the yz coordinates of the mapped points onto these planes were saved, as well as the X_o coordinate of the plane itself. Over the entire workspace more than fifty of such planes with successive normal distances of 50 mm. were used, and an ASCII file containing X, Y and Z coordinates of the contour points, was created on VAX-8550.

Next step is to customize this data-base in the form of a file readable by AutoCad. One possible form of these files is the so called DXF files in AutoCad. DXF files in AutoCad has been defined as "Drawing Interchange" file format which can assist interfacing AutoCad with files created external to the package (AutoCad reference manual 1989). All implementations of AutoCad accept this format, and are able to convert it to and from their internal drawing file representation.

5.4.1- INTERCHANGING THE DATA-BASE WITH AUTOCAD

In order to import cartesian coordinates of the contour points into the AutoCad environments the Drawing Interchange File capabilities of the AutoCad were used. A Drawing Interchange File is simply an ASCII text file with a file type of ".dxf" and specially-formatted text. The overall organization of a DXF file is as follows:

1-HEADER section

2-TABLES section

3-BLOCKS section

4-ENTITIES section

5-END OF FILE

By setting up the AutoCad in the HEADER and TABLES sections the instructions were given to treat the subsequent three coordinates of every two points as coordinates of the end points of a three-D polly line. After assembling the data file into the DXF file, they become extremely long files, therefore it is not possible to represent them in this thesis. After feeding the assembled DXF file into the AutoCad, the image shown in figure 5.22 was obtained. This is in fact a top view of the cutting planes over the workspace.

5.4.2- THREE-DIMENSIONAL RECONSTRUCTION OF THE WORKSPACE

Once having all of the contour points, as the vertices of the polly lines in AutoCad, one is able to manipulate these polly lines as desired. However one still needs to connect the cutting plane together in order to create a wire frame image of the workspace. A wire frame image is necessary for the removal of the hidden lines in a realistic 3-D view. One of AutoCad's feature called "**RULESURF**" was used for this purpose. This is a function which will generate a wire frame mesh connecting two closed curve together to create a three dimensional entity which will be able to hide other entities located behind. Having done this and some small housekeeping jobs the three dimensional images were constructed, yet the hidden lines are present. Next

step is to rotate the wire framed 3-D object to a desired orientation and setting up a proper view point and finally asking AutoCad to remove all the hidden lines. The latter process is extremely slow given the large quantity of points that we were dealing with.

RESULTS:

Figure 5.23 depicts the dexterous workspace of a PUMA-560 where the two halves of the workspace along the positive X and negative X axis are deliberately pulled apart for better visualization. Moreover in figure 5.24 the assembled real workspace is shown from a viewpoint on the positive a axis, and finally in figure 5.25, the dexterous workspace in its entirety is viewed from the negative X axis.

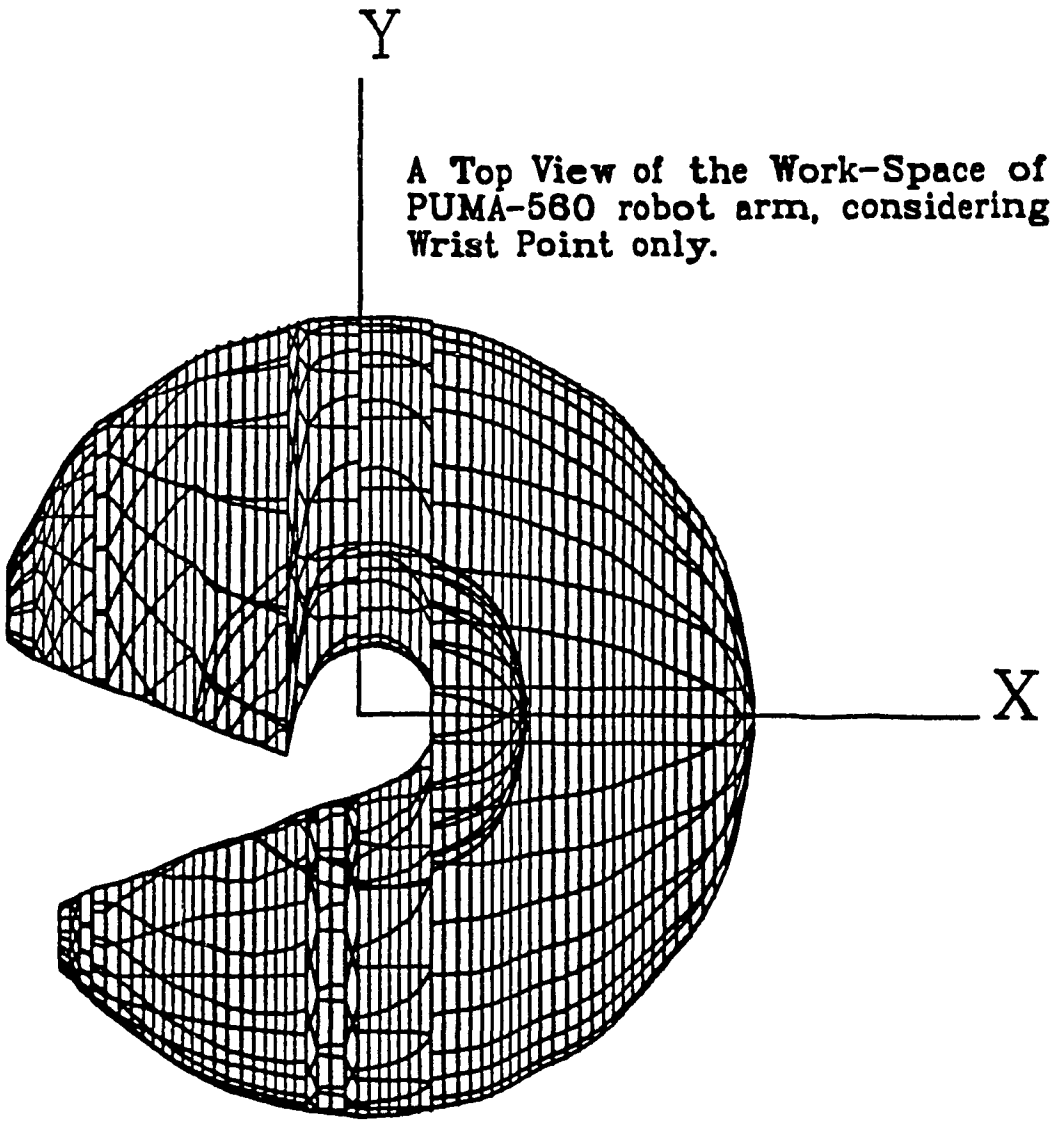

Figure 5.22 - Three dimensional workspace from a top view

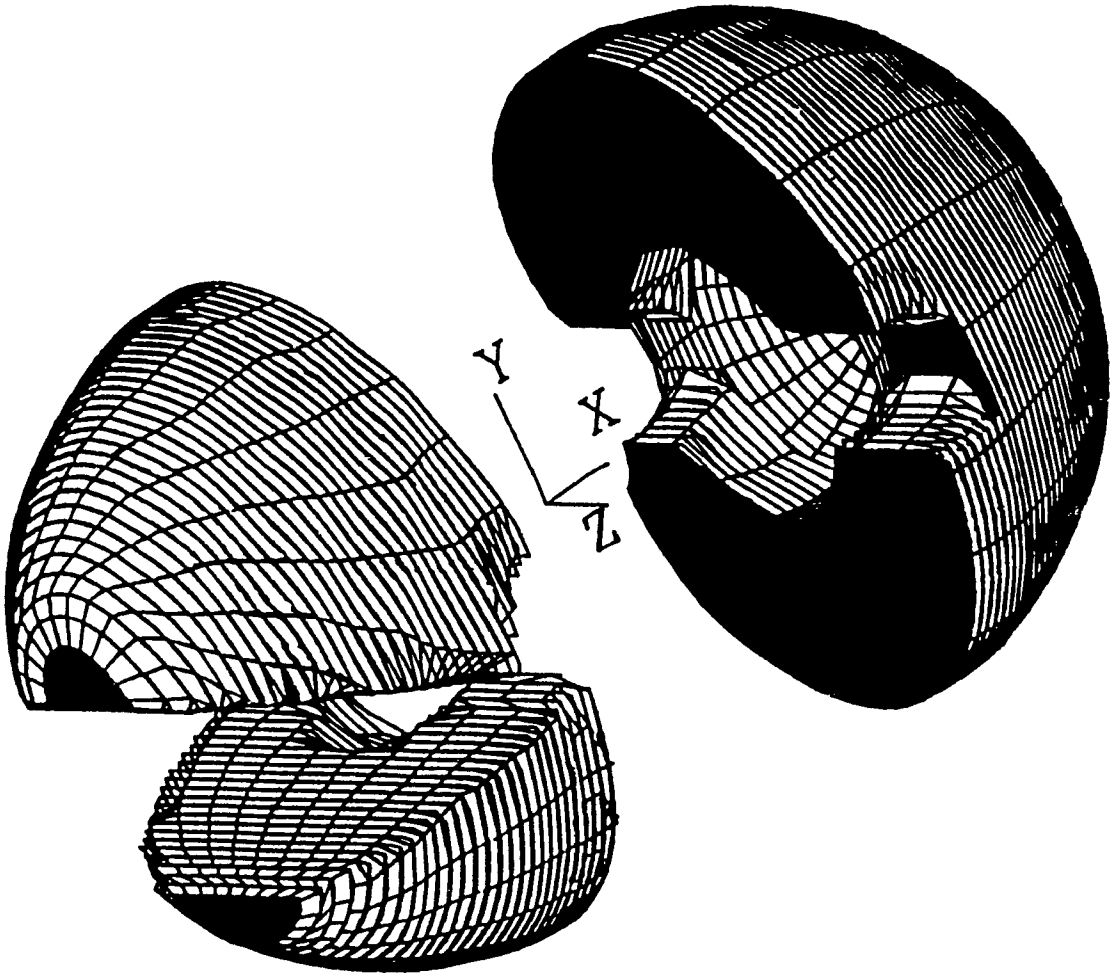

Figure 5.23 - Three dimensional workspace separated in two halves

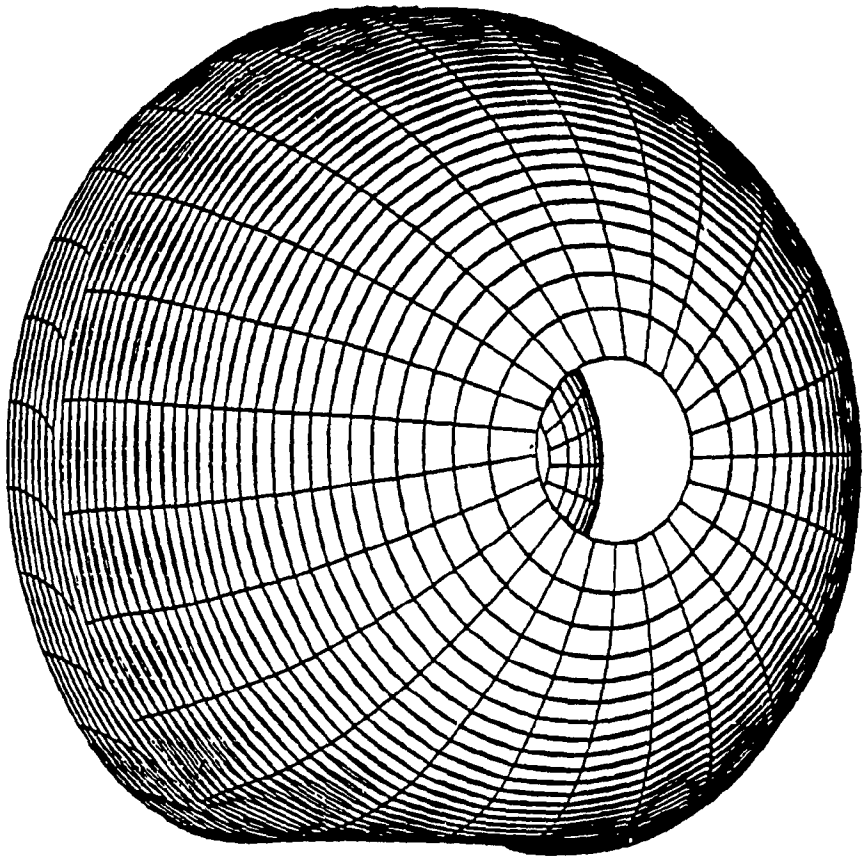

Figure 5.24 - Three dimensional workspace from positive X direction

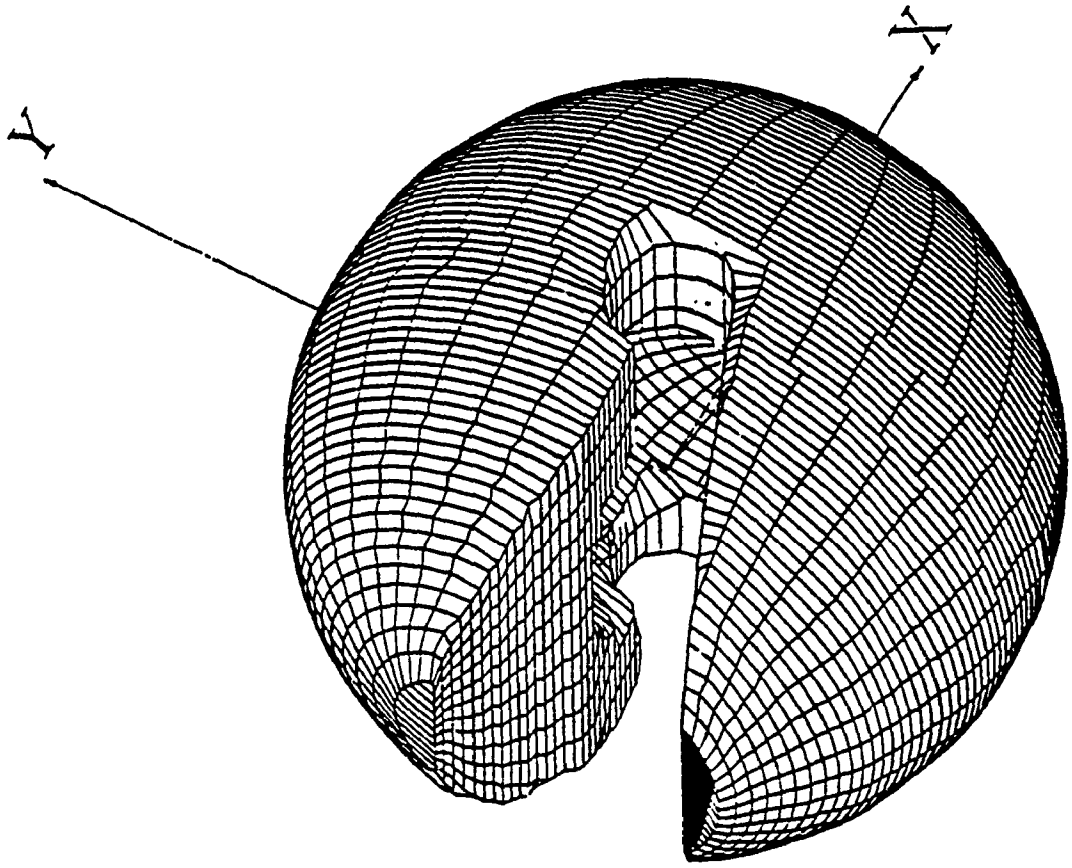

Figure 5.25 - Three dimensional workspace from negative X direction

CHAPTER 6

COORDINATED TWO-ARM ROBOTIC SYSTEMS

6.1 INTRODUCTION

There are many applications in materials handling and assembly operations in which one single robot arm fails to fulfill the kinematics and/or dynamics requirements of the task. In material handling, for instance, if the object to be manipulated is relatively large in comparison to a robot's structure, or the payload is beyond the robot's capacity, one may employ two or more robots in a cooperative manner to perform the task. The need for more than one robot in assembly operations, is more obvious since the flexibility, introduced by the additional robots to the workcell, will make possible the assembly of more complex parts in less time. Manipulation of tools in particular applications such as welding, over complex surfaces, may call for more than one robot. One example which can potentially exploit the advantages of two coordinated robots is the process of production of composite materials, where the filament (fibers) should regularly be wrapped around a matrix with a pre-defined orientation and tension. If the geometry of the matrix is not a simple cylindrical surface, then two robots with bilateral accommodation with each other will exhibit significant versatility for these complex processes.

In chapter 2 we presented a survey on various aspects of research which have merged in the past ten years in the field of cooperative robotic

operations. Currently every aspect of cooperative multi-manipulator systems described in section 2.3 can form a research area by itself, as the needs for more versatile and powerful robotics workcell grow.

In this chapter we elaborate on the geometrical and kinematic considerations of two-arm robots and their operations. In section 6.2 general multi-manipulator systems are defined and their operations are discussed in terms of the nature of the cooperation needed in such tasks. Section 6.3 is concerned with the definition of two-arm robots operations. In section 6.4 a classification of the tasks defined in terms of the path and grasp configurations will be made, and mobility of the closed kinematic chains formed by the two manipulators and the manipulated object under different grasp configurations will be discussed. Section 6.5 is concerned with the constraint relations and kinematic formulations for two-arm robotics systems.

6.2 COOPERATIVE MULTI-MANIPULATOR WORKCELL

We refer to any robotic workcell composed of more than one robot arm whose motions are somehow related, in a cooperative manner as a "multi-manipulator" workcell. This is the most general case in the sense that there exists two or more robot manipulators in a common workcell, and the motion of each manipulator can be performed upon taking into consideration the structure and the motion of other manipulators in the workcell .

In a more technical sense we define a cooperative multi-manipulator system as a robotic workcell with more than one robot involved, while

satisfying one of the following conditions:

a) At least two of the robot arms involved in the workcell, have partially overlapping workspaces.

b) If the workspace of the robots do not intersect, at least two of the end effector's motions are dynamically coupled through the workpiece and/or tools.

As an example for case (a) one can think of an assembly operation where although the end effectors do not hold a common object but their motions are synchronized according to a pre-defined schedule, or an intelligent on-line decision making scheme. Handling a common object with more than one robot at the same time is an example for case (b) above.

Having defined the main category of the cooperative multi-manipulator systems, we further propose two sub-categories for these systems, namely

1)Synchronized Multi-Manipulator system (SMM).

2)Coordinated Multi-Manipulator system(CMM).

Although the concern of this thesis is focused mainly on the latter, both categories will be defined in what follows.

6.2.1 SYNCHRONIZED MULTI-MANIPULATOR SYSTEMS (SMM)

In synchronized multi-manipulators the robots usually have overlapping workspaces. The motion of each arm although synchronized with respect to the others, is dynamically unrelated or uncoupled to the other robots motions. An

example for this type of operation in flexible manufacturing is when two (or more) robots pick up objects from the same bin, or two robots assembling different components into the same workpiece. Some authors have referred to these types of operations as *loosely coupled,* that is, the arms may share partially overlapping workspaces and may actually transfer parts or tools between them (O'Donnell and Lozano-Perez 1989).

The major concern in these types of operations is a collision-free trajectory planner which guarantees the execution of the tasks assigned to each arm satisfactorily according to the required schedule. Other factors to be taken into consideration for these systems are the speed capabilities and the range of motion for each manipulator, or minimization of the cycle time or spent energy, to name a few. At the present time, synchronized operations of multi-manipulators are practicable (Acker et. al., 1985, Roach and Boaz 1987 and Fortune et. al., 1986)

6.2.2 COORDINATED MULTI-MANIPULATOR SYSTEMS (CMM)

We denote a cooperative multi-manipulator system as a *coordinated multi-manipulator system* (CMM) when at least two of the robots motions are dynamically coupled through a common workpiece. In other words, if a closed kinematic chain is formed by two of the robots and the manipulated object, we consider the system as a coordinated multi-manipulator.

The foregoing definition is valid for multi-fingered dexterous hands and multi-legged vehicles as well. For instance in dexterous hands there are

multiple closed kinematics chains formed by the fingers and the manipulated object. This is similar to the closed chains formed by robot manipulators and the load in the CMM systems. Multi-legged vehicles have multiple closed kinematic chains formed by the legs and the main body (figure 6.1)

Focusing on coordinated multi-manipulators we further define two types of coordinations between the manipulators and the object, as follows;

(A) Tightly Coordinated Multi-Manipulator systems (TCMM)

In this family of operations, coordination between the positions, velocities and forces among the collaborating end effectors and the held object are rigidly defined, and need to be satisfied at each instant throughout the time for execution of a task. It is assumed that the grasp configuration (*i.e.* position and orientation of the end effectors with respect to the object) for every manipulator is pre-defined and remains fixed during the execution of the task (no relative motion will occur between the hands and the object). In terms of *mobility* or *degrees of freedom* of the grasp, one may state that, there is zero mobility or degree of freedom between the hands and the manipulated object. In practical applications tight coordination requires a precise position and/or force control strategy in order to avoid damages to the manipulated object. Manipulation of a common load by two or more robot arms can be considered as an example for TCMM operations (figure 6.2).

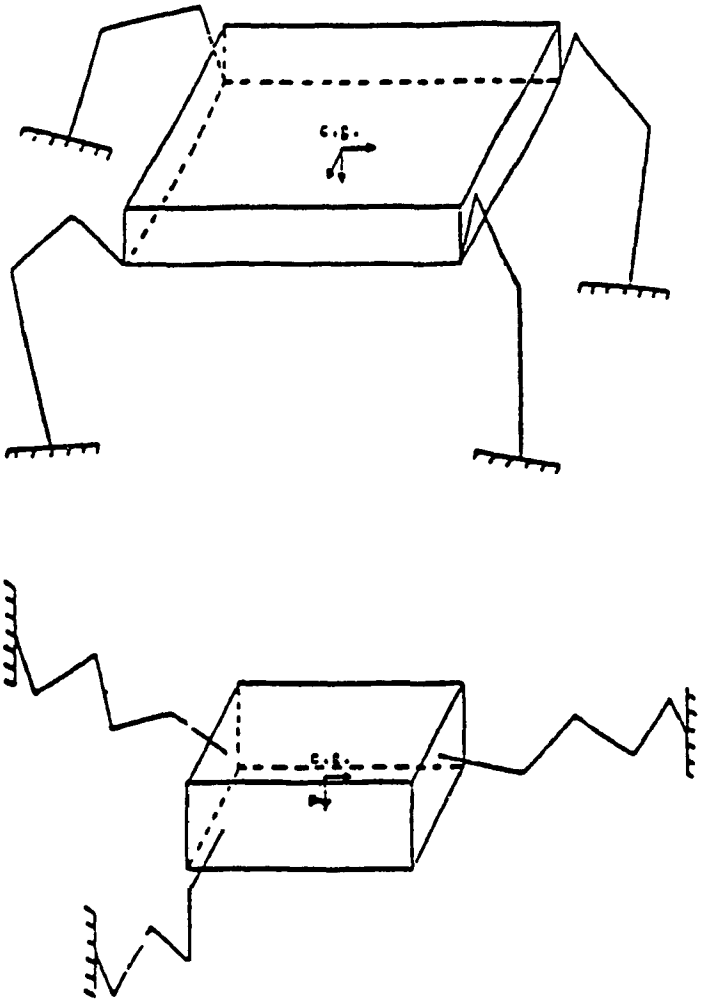

Figure 6.1 - Multi-Legged and Multi-Arm Manipulators

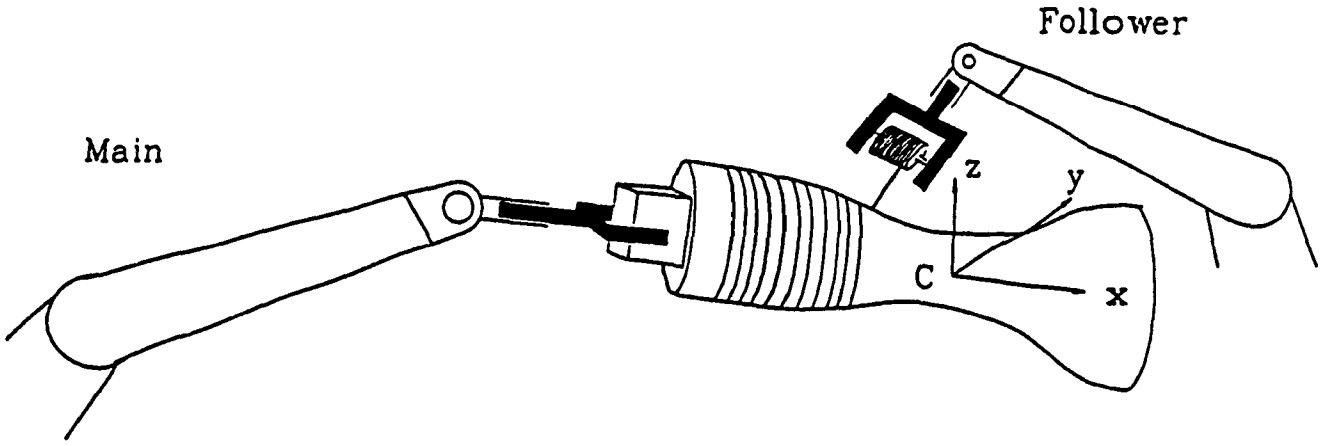

Figure 6.2 - Two-Arm robots used for winding

(B) Loosely Coordinated Multi-Manipulator systems (LCMM)

Loosely coordination of multi-manipulators, in contrast to **TCMM**, introduces some flexibilities (freedom) in the grasp configurations or relative positions/orientations of the end effectors and the common workpiece. In other words the degree of freedom of the hands with respect to the manipulated object or the workpiece is not zero, and depending on the application should be defined by the characteristics of the operation.

As an example for this case, one can consider manipulation of an object by two manipulators, where the end effectors are hinged to the workpiece, thus leaving one degree of freedom for each grasp . Figure 6.2 shows another example for the **LCMM** operations, which can be thought of in the process of filament winding of composite materials. It can be seen that the position and orientation of the *winder hand* has some freedom relative to the object. This is due to the fact that, in order to satisfy the required orientation and tension of the fibers, all six degrees of freedom of the winder hand are not required.

In the following sections we will discuss in more detail the grasp configurations and the overall degree of freedom of **CMMs** based on the grasp geometry. Our discussions and development of the algorithms in this thesis are limited to *Tightly Coordinated Two-Arm Robotic Workcells.* And as practical case we consider two **PUMA-560** arms working together in a materials handling environment. An example of such a system is shown in figure 6.3.

6.3 COORDINATED TWO-ARM ROBOT ORGANIZATION

In this section we investigate the general structure and definitions of components of a tightly coordinated two-arm robots in handling a common object. The **Grübler-Kutzbach** criteria will be used to develop a general formula for the evaluation of the degree of freedom of a coordinated two-arm robots with tight grasps. A classification scheme for the definition of the tasks will be proposed which can cover most possible real-world applications; and also the constrained relations as well as the inverse kinematics solutions of the coordinated manipulators will be discussed.

6.3.1 DEFINITIONS

The basic terminologies of the coordinated two-arm robots that we use in this thesis are based on those proposed by Luh and Zheng (1987). In a two-arm robot workcell (Fig. 6.3), primarily we assign a world coordinate which is an inertial reference frame for the workcell. It is convenient to have the world coordinate frame coincided with the base frame of one of the robots. The two robots are given the names, **main** (or **Leader**) and **follower** respectively. Luh and Zheng (1987) have discussed an approach that the motion of the main arm is controlled based on its hand trajectory which is in turn dictated by the desired trajectory of the workpiece. The follower will be responsible to accommodate the main arm in a sense that the coordination error (position or velocity) become minimum, or in the task level the constraint relations remain satisfied. This method of coordinated motion control will enhance more flexibility in the system if the desired motion of the object has to be

modified or redefined. Because whenever the trajectory is modified, the operator need to modify the trajectory of the main arm only, whereas that of the follower would be modified implicitly through the constraints.

6.3.2 FRAME ASSIGNMENTS AND TRANSFORMATIONS MATRICES

Figure 6.3 depicts the general organization of a two-arm robot. The frame assignments to the joints of every robot is according to the strategy explained in chapter 3, and individual frames to the intermediate joints of the robots are not shown. The world reference, and the body-attached coordinate frames are assigned as follows:

$(W;x_w,y_w,z_w)$, is the world coordinate frame (usually is coincided with the main manipulator's base frame)

$(m;x_m,y_m,z_m)$, is the base coordinate of the main manipulator.

$(f;x_f,y_f,z_f)$, is the base coordinate of the follower manipulator.

$(M;x_F,y_F,z_F)$, is the tool coordinate of the main manipulator attached to its end effector.

$(F;x_F,y_F,z_F)$, is the tool coordinate of the follower manipulator attached to its end effector.

$(C;x_C,y_C,z_C)$, is the coordinate frame attached to one point of interest of the manipulated object (center of gravity, geometrical center, etc.).

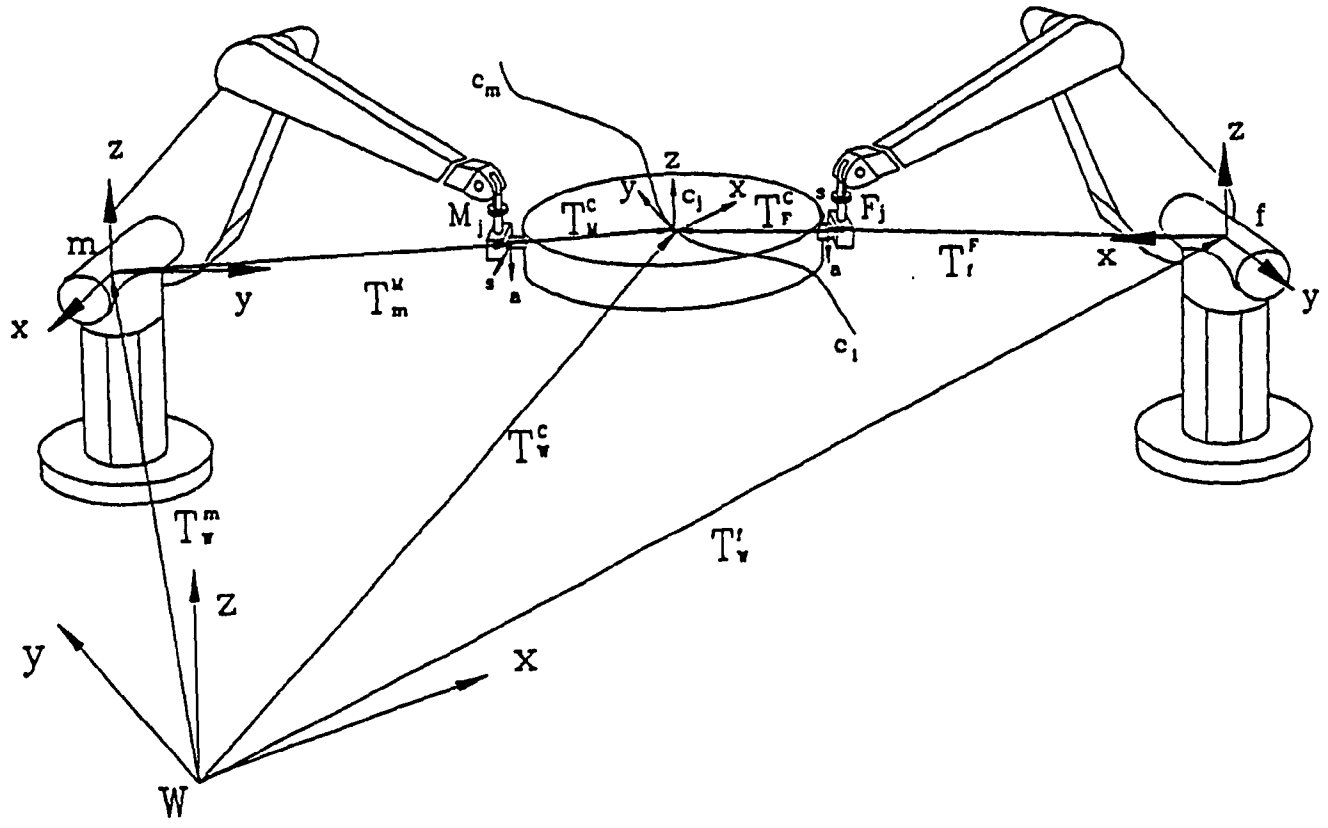

Figure 6.3 - Coordinated two-arm robots

The motion of the manipulated object will be resolved into m number of finitely separated poses along the desired trajectory. Position and orientation defining these poses are expressed with homogeneous transformation matrices with respect to the world coordinate frame, for the jth pose of the trajectory we have

$$(T_w^C)_j = \left[\begin{array}{c|c} (R_w^C)_j & (p_w^C)_j \\ \hline 0\ \ 0\ \ 0 & 1 \end{array}\right] \qquad j = 1,2,\ldots m. \tag{6.1}$$

Grasp configurations for both main and follower arms can also be defined with two homogeneous transformation matrices. These two matrices will define the grasping points as well as the grasping orientations with which the object is to be manipulated, they are defined in the task space and are

Main arm grasp configuration
$$T_C^L = \left[\begin{array}{c|c} (R_C^L) & (p_C^L) \\ \hline 0\ \ 0\ \ 0 & 1 \end{array}\right] \tag{6.2}$$

Follower arm grasp configuration
$$T_C^F = \left[\begin{array}{c|c} (R_C^F) & (p_C^F) \\ \hline 0\ \ 0\ \ 0 & 1 \end{array}\right] \tag{6.3}$$

The subscript j has been dropped in the foregoing transformation matrices because of the assumption that the grasp is rigid and does not allow for any relative movement between the end effectors and the object. In other words, T_C^L and T_C^F will remain constant during the execution of a task. More elaborations on the task definition strategies will be made in the following section.

6.4 TASK DEFINITION FOR TIGHTLY COORDINATED TWO-ARM ROBOTS

To this end we have defined the transformation matrices expressing the required task with respect to the world coordinate frame, as well as the degrees of freedom of general coordinated two-arm robots in material handling. In this section a classification scheme which can fully cover possible ways, with which the user may define a task, will be proposed. An important application of this approach in task definition scheme can be found in the potential knowledge-based and intelligent two-arm robotic workcells of the future.

The **Grübler-Kutzbach** criteria will be used to determine the overall degree of freedom of a closed kinematic chain formed by the tightly coordinated two robot arms and the manipulated object. The general form of this criteria is expressed with the following equation (Hunt 1978)

$$m = 6(n - g - 1) + \sum_{i=1}^{g} f_i \qquad (6.4)$$

In equation 6.4,

m is the mobility of the system (with zero internal and grasp mobilities)

n is the number of bodies in the system (links, manipulated object)

g is the number of working joints connecting the bodies. For single loop mechanisms g is equal to n the number bodies.

f_i is the number of degree of freedom of the *ith* joint.

Figure 6.4 shows the two end effectors in handling a rigid body with tight grasps, for this case each robot has 6 links and thus the total number of links in the system will be,

n = 2x6 - 1 = 11 (the base link is the common ground for both robot)

+ 1 (object) = 12

and

f_i = 1 for all i.

g = 2x6 (six joint for each robot) = 12

Thus the relative degree of freedom of the two-arm robot with the grasp of zero mobility can be computed as

$$m = 6(12 - 12 - 1) + 12 = 6 \tag{6.5}$$

This means that if the grasp does not allow any relative slippage between the end effectors and the object and also the object is rigid, one would need six independent parameter to uniquely define the motion of the manipulated object. Although we are concerned with tightly coordinated systems for which the general mobility criteria was discussed, but for the sake of completeness a more general formula, for mobility analysis of the coordinated two-arm robots in the presence of redundancy will be derived in the appendix B. By redundancy in the coordination, it is meant, manipulation of objects with non-zero internal mobilities (*e.g.* a pair of pliers) and also with the grasps of non-zero mobilities.

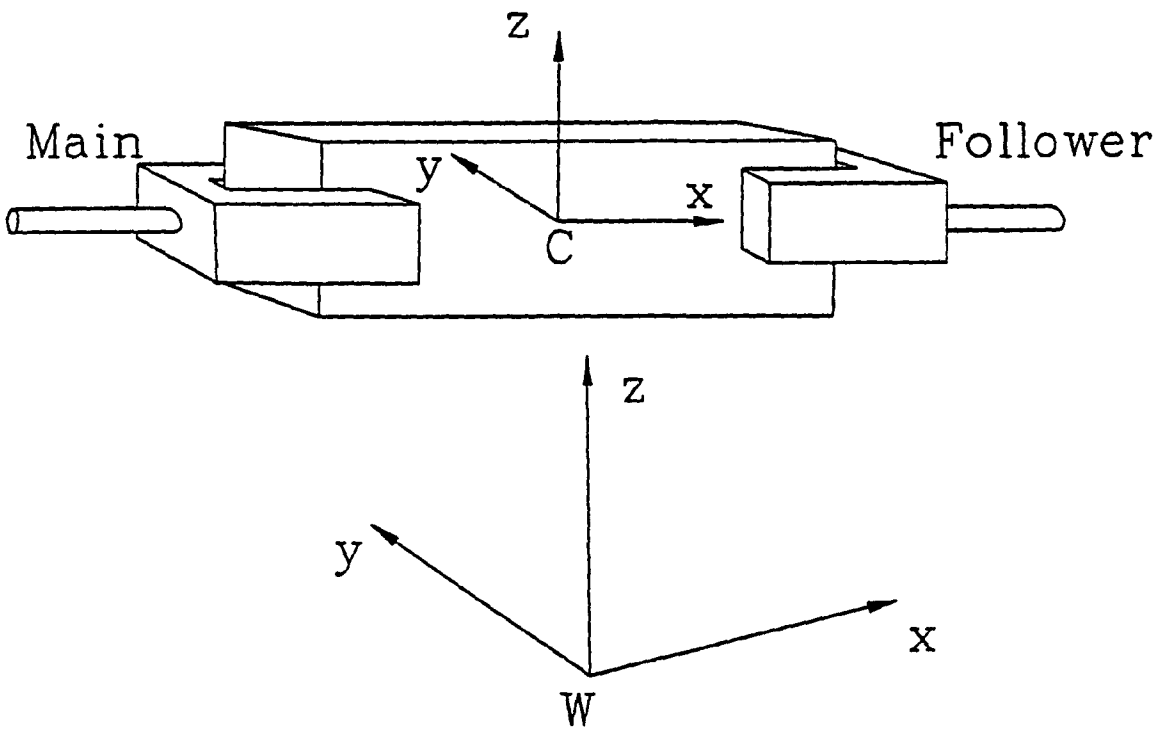

Figure 6.4 - Tight grasp in coordinate two-arm robots

Having defined the required degree of freedom of the coordinated two-arm robots with tight coordination, it was observed that six parameters are needed to uniquely define the motion of the object. In fact these six parameters consist of three cartesian coordinates of the object and three rotation angles for its orientation. These information as well as the grasp configurations can be defined in different ways depending on the application. Thus we will next discuss the proposed task definition scheme based on two different and independent elements which will comprise the characteristics of the tasks to be performed. These elements are namely **grasp classification** and **trajectory classification** respectively.

6.4.1 GRASP CLASSIFICATION

The grasping configuration of a rigid body object by the end effectors is usually dictated by its geometry, dimension, physical characteristics and the load balance requirements during the task execution. By resorting to either a precise position control of both end effectors, or by employing the coordination error minimization strategy (Luh and Zheng 1989) we can assume that relative movements between the hands and the object are small enough to be ignored. Therefore, one can define a required grasping configuration via one of the following four categories

G1) This is the most restricted category of the grasp identification. The user will define both grasping points and grasping orientation of the main and the follower hands with respect to the workpiece. In other words T_c^M and T_c^F are given.

G2) In This case the user allows flexibilities regarding the grasping orientation and will rigidly define the grasping points for both end effectors. This case arises when end effectors have to grab the object at specific points while their orientation are immaterial, thus only P_C^M and P_C^F are given.

G3) In contrast to case **G2** above, this category will introduce flexibilities on the grasping points and will define tightly the orientations of the hands with which the object should be grabbed, (*i.e.* R_C^M and R_C^F are given).

G4) This is the case when neither the position nor the orientation of the end effectors with respect to the object frame are defined by the user. In other words, we have the flexibility to locate the grasp positions and orientations.

6.4.2 TRAJECTORY CLASSIFICATION

Four different cases may arise which can fully cover any possible application. These four groups of path definitions are

P1) In this case for every point of the trajectory both position and orientation of the manipulated object is defined. As an example one can think of handling a liquid container in a workcell with obstacles present. Thus $(T_w^C)_j$, $j=1,2,...m$ are given.

P2) In this case, the trajectory (positions of the origin of the task frame C_j, for *j=2,3,...m-1*) is given but there is no restrictions on the orientation of the object during motion. The given data for this case are, $(T_w^C)_1$ and $(T_w^C)_m$ and $(P_w^C)_j$ for *j=2,3...m-1* .

P3) This is the complement of case **P2** in that, in addition to the initial and final poses of the trajectory, the orientation of the object is restricted whereas the path is not defined. An example for this sort can be thought of as handling a liquid container (with a specified orientation of the container) in an obstacle-free workspace, thus $(T_w^C)_1$, $(T_w^C)_m$ and $(R_w^C)_j$ for *j=2,3,...m-1* are given.

P4) In this case neither the position nor the orientation of the object for the intermediate points along the path are specified and there is room for choosing or adjusting both, for a particular task. However similar to the other cases discussed above initial and destination poses must be defined by the application. In this category of motion one will have the maximum flexibility for satisfaction of path planning requirements such as cycle time, consumed energy, load distribution and reachability. As an example consider transfer of a rigid object from the initial pose to the final pose regardless of the intermediate points of the path. The given information are $(T_w^C)_1$ and $(T_w^C)_m$.

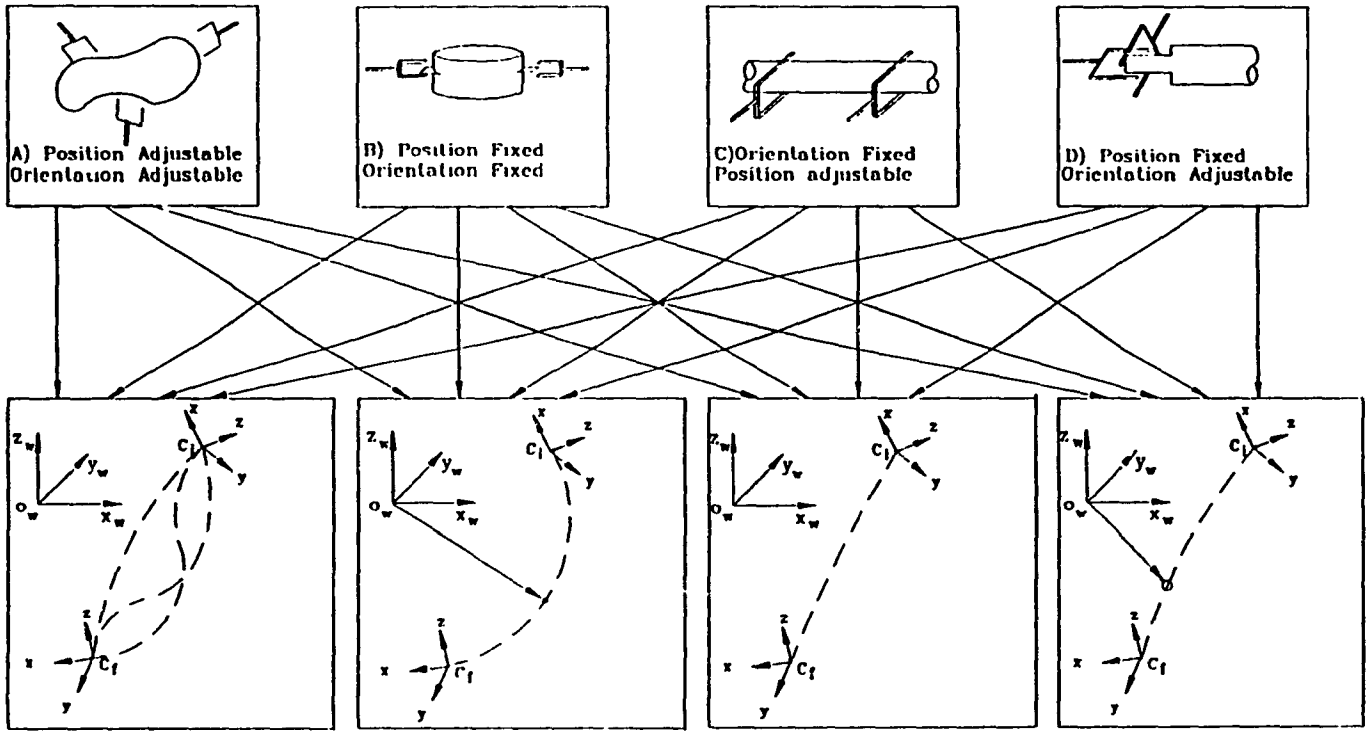

Figure 6.5 - Task definition flow diagram

6.4.3 INTERACTION BETWEEN THE GRASP AND TRAJECTORY CLASSIFICATIONS

Any combination of the foregoing categories for the grasp and the path configurations can be chosen to define completely a material handling task. Figure 6.5 shows a tree-like inter-connection between the grasp and path configuration schemes. This will introduce 16 different cases under which a task can be defined. For example one can define a task by using G2P1 route. This will define a task for which the grasping points are given as well as the position/orientation of the object throughout the trajectory.

Although figure 6.5 suggests 16 different cases, by which a task may be defined, but it can be shown that if other performance criteria of the operation, such as reachability, load balancing requirements and so on. are considered, one will be able to reduce the trajectory classifications of the cases **P2, P3 and P4**, to the case of **P1**; this is discussed in what follows.

In case **P2**, where $(T_w^C)_1$, $(T_w^C)_m$ for the initial and final poses are given as well as the position of the intermediate points $(P_w^C)_j$ for $j=2,3...m-1$, then one can use the orientation sub-matrices embedded in $(T_w^C)_1$ and $(T_w^C)_m$ of the terminal points, that is $(R_w^C)_1$ and $(R_w^C)_m$, in order to obtain a guideline for the variations of the orientation of the object from the initial to the final pose. For example the change in orientation from the initial to final poses can be uniformly distributed over the m points of the path. Once an orientation $(R_w^C)_j$ is assigned to each point j of the path, for $j=2,3,..m$, then one can combine $(R_w^C)_j$ and $(P_w^C)_j$ to obtain $(T_w^C)_j$ $j=2,3...m-1$. Then together with $(T_w^C)_1$ and $(T_w^C)_m$ which were given as part of the data, the

values for all $(T_w^C)_j$ $j=1,2,3...m$, are known. Therefore as far as task definition is concerned, case **P2** is converted to the case **P1**.

In the same manner one can convert case **P3** to **P1**. In case **P3** orientation of the frame C for the intermediate points of the path are given and the position of the point C along the path are to be adjusted. Similar to the previous argument, one can uniformly distribute the variations of the positions, from the initial to the final pose, over the m points of the trajectory, and consequently determine $(T_w^C)_j$ $j=1,2,3...m$. Alternatively one can set an arbitrary trajectory for the object.

In case **P4**, where neither position nor orientation of the intermediate points are prescribed, one primarily has the freedom to arbitrarily assign a path with appropriate variation of orientation from the initial point to the final one. The problem thus is converted to case **P1**.

From the foregoing discussion it can be concluded that if the task is defined according to one of the last three cases mentioned above, where either position or orientation or both along the trajectory can be assigned arbitrarily, then one may introduce a performance index for the operation. In fact it is possible to exploit the available flexibility of the position/orientation of the workpiece along the path in order to maintain an optimum performance based on a defined performance criteria. For instance if the task encounter non admissible points along the trajectory the position and/or orientation can be altered accordingly. On the other hand load balance requirement and other dynamics characteristics can be chosen instead as the

desired performance criteria.

6.5 KINEMATIC FORMULATIONS FOR COORDINATED TWO-ARM ROBOTS

When the robots and the manipulated object form a closed kinematic chain, the displacements, velocities, accelerations and forces of the two end effectors are not independent and their behavior are coordinated through some holonomic constraints (Luh and Zheng 1985). In this thesis since our concern is mainly about the displacements and the availability of workspace of the coordinated robots we will not discuss the dynamic coordination of the closed chain.

In this section the kinematic relationship for only case P1 of the previous section is determined. For this case, since for each pre-specified pose of the workpiece on its desired trajectory the position/orientation of each arm end-effector is uniquely determined, therefore the kinematic relations of the two robots are in fact decoupled. We will make use of this feature in chapter 8, where the problem of the set-up of the workcell is investigated.

6.5.1 CONSTRAINED KINEMATIC EQUATIONS

Let the position and orientation of the base frames of the main and the follower are defined with respect to the world coordinate frame respectively by, T_w^m and T_w^f, and at each instant of time designated by the index j along the trajectory the end effectors are defined with respect to their own base

frame respectively by $(T_m^M)_j$ and $(T_f^F)_j$. Then from figure 6.3 it can be seen that at each instant the following matrix relationship holds,

$$T_w^m \, (T_m^M)_j \, T_M^C = T_w^f \, (T_f^F)_j \, T_F^C \tag{6.6}$$

or,

$$(T_w^M)_j \, T_M^C = (T_w^F)_j \, T_F^C \tag{6.7}$$

Multiplying both sides of equation 6.7, by $(T_F^C)^{-1}$ or T_C^F we obtain,

$$(T_w^M)_j \, T_M^C \, T_C^F = (T_w^F)_j [T_F^C \, (T_F^C)^{-1}] = (T_w^F)_j \tag{6.8}$$

or

$$(T_w^M)_j \, [T_M^C \, T_C^F] - (T_w^F)_j = 0 \tag{6.9}$$

Equation 6.9 is the general holonomic constraint expressed in a matrix form. Both position and orientation constraints can be extracted from this relationship. It has to be mentioned that this matrix equation introduces three independent relationships for the position coordinates and nine dependent relations for the orientations because any orientation can be uniquely specified by three rotations (Euler angles etc.).

In the case of handling a rigid body with the tightly coordinated robots the transformation matrices T_C^M and T_C^F are given and remain constant throughout the entire execution period. Thus the bracket in equation 6.9 can be rewritten as

$$[T_M^C \, T_C^F] = (T_C^M)^{-1} \, T_C^F = T_M^F = const. \tag{6.10}$$

where T_M^F is the transformation matrix defining position and orientation of the main end effector with respect to the follower end effector, and remains constant. Hence 6.9 can be written as

$$(T_w^M)_j \; T_M^F - (T_w^F)_j = 0 \tag{6.11}$$

Then three holonomic constraints that was introduced by Luh and Zheng (1987) can be extracted from equation 6.11 as follows

$$(R_w^M)_j \; P_M^F + (P_w^M)_j - (P_w^F)_j = 0 \tag{6.12}$$

Equation 6.12 introduces three independent equations which relate the positions of the main and the follower at each pose j of the workpiece. Moreover, three holonomic constraints can be obtained from the following nine dependent relationship extracted from the orientation part of equation 6.11 as follows

$$(R_w^M)_j \; R_M^F = (R_w^F)_j$$

or

$$(R_w^M)_j \; (R_w^F)_j^{-1} = (R_M^F)^{-1}$$

thus

$$(R_w^M)_j \; (R_w^F)_j^T = R_F^M = const. \tag{6.13}$$

6.5.2 INVERSE KINEMATICS FORMULATIONS

To this end we assume that the task has been completely defined by the applications and/or other criteria which have to be satisfied during the task execution. In other words the position and orientation of the object frame is known for every point j of the trajectory. Therefore one can easily obtain the position and orientation of the main end effector with respect to the world coordinate frame for every point j of the path, that is

$$(T_w^M)_j = (T_w^C)_j \, T_C^M \tag{6.14}$$

On the other hand it was mentioned that the base frame of the main manipulator is defined by the transformation matrix T_w^m, therefore the attitude matrix of the leader arm with respect to its own base frame or T_m^M can be obtained by the following equation

$$(T_m^M)_j = (T_w^m)^{-1} \, (T_w^M)_j \tag{6.15}$$

Once the attitude matrix of the main is determined we solve the inverse kinematics formulations to determine the vector of joint angle Θ_j^M for the main manipulator at point j of the trajectory. But first we can express the attitude matrix in terms of six independent parameters three position coordinates denoted by vector Λ and three rotations denoted by Γ (for example the Euler angles), or

$$(\Lambda^M)_j = [X_m^M \; Y_m^M \; Z_m^M]_j^T \quad \text{and} \quad (\Gamma^M)_j = [\alpha_m^M \; \beta_m^M \; \gamma_m^M]_j^T$$

then

$$\Theta_j^M = F((\Lambda^M)^T\ (\Gamma^M)^T) \tag{6.16}$$

where $F(.)$ is a vector function of the inverse kinematics. Depending on the nature of the grasp configuration the attitude matrix of the follower can be determined as shown in what follows

$$(T_w^F)_j = (T_w^M)_j\ [T_M^C\ T_C^F] \tag{6.17}$$

If the base frame of the follower is defined with respect to the world coordinate frame by T_w^f then

$$(T_f^F)_j = (T_w^f)^{-1}\ (T_w^F)_j \tag{6.18}$$

And similarly the vector of joint displacements Θ_j^F for the follower arm can be determined for every point j when its attitude matrix is defined in terms of the six parameters of

$$(\Lambda^F)_j = [X_f^F\ Y_f^F\ Z_f^F]_j^T \quad \text{and} \quad (\Gamma^F)_j = [\alpha_f^F\ \beta_f^F\ \gamma_f^F]_j^T\ ,$$

that is

$$\Theta_j^F = G((\Lambda^F)^T\ (\Gamma^F)^T). \tag{6.19}$$

CHAPTER 7

WORKSPACE ANALYSIS FOR COORDINATED TWO-ARM ROBOT OPERATIONS

7.1 INTRODUCTION

The workspace analysis of two-arm robots have been discussed very briefly in the literature. In previous chapters, kinematics and workspace analysis of a single manipulator, as well as the basic kinematics and constrained relations for the coordinated two robot arms were discussed, and two different algorithms for determination of the workspace of a single arm were developed. In this chapter the workspace associated with tightly coordinated two-arm robots in material handling, will be discussed.

In section two workspace of a coordinated two-arm robot will be discussed in a general sense. The concept of **Triplet Workspace** of a particular case in coordinated two-arm robotic operations, namely when the object is rigid and the grasps are tight will be proposed and, consequently an algorithm for the evaluation of the two-dimensional contours of this workspace will be devised in section 7.3. In section 7.4 illustrative examples are given, in order to primarily observe the two dimensional contours of the triplet workspace. Moreover, In this section the effect of the relative position of the origins of the base frames of the two robots, as well as the effects of different grasp configurations on the triplet workspace will be illustrated.

7.2 WORKSPACE ANALYSIS FOR TWO-ARM ROBOTS

In this section the problem of workspace associated with a general cooperative two-arm robotic workcell will be discussed. To this end we have investigated the workspace of a single robot arm (chapter five) and illustrated graphical methods of representation of the boundaries of these complex surfaces. Now we extend the problem to the cooperative two-arm robotic systems.

In synchronized two-arm robotic operations where the motions of the arms are synchronized (chapter six), and there is no coupling between them through a common workpiece, each manipulator will posses its own workspace in the same sense as defined for single arm robots. For these kinds of cooperative operations the robots will be placed at different position and orientation with respect to the other. Depending on this relative set-up of the system, the individual workspace of one arm may or may not intersect the workspace of the other manipulator. However since the end effectors move independent from each other, the individual workspace will not be affected by the existence of the other robot. Thus the same methods of workspace analysis as discussed for single manipulators can be applied to the synchronized two-arm robots from the workspace point of view. The only difference is that now one should put a great deal of emphasis on the obstacle avoidance and path planning strategies to avoid collisions between the two robots.

In coordinated two arm robots, on the other hand, coupling between the motion of the end effectors through the common object will restrict the reachable space of each robot, and thus the shape of individual workspace may change significantly. Bearing in mind that for the coordinated operations the workspace of two robots are not independent and the two manipulators and the common object form a triplet, we propose to investigate the overall workspace associated with the workcell as a whole, and thus propose the concept of **Triplet Workspace.**

We define the Triplet workspace as the workspace associated with a reference point located at one point of interest (C) on the manipulated object. In general this workspace consist of all those points of the three dimensional space which can be attained by point C, no matter what the orientation of the object may be. This general definition of the triplet workspace in fact, represents the dextrous workspace of the point C. In other words this amounts to the analysis of the dextrous workspace of one link of a closed kinematic chain, this link being the manipulated object.

A general geometrical or analytical definition of the dexterous and reachable workspaces associated with a single robot manipulator is a complex process, (chapter 5). By introducing more than one robot into the workcell, while handling a common workpiece and producing the triplet, the difficulties of the analysis of the workspace will be magnified significantly. The increased difficulties in this respect, will not be limited to the need for representing each additional robot's workspace, added to the system, but to the complex analysis of the workspace of a closed kinematic chain formed by

the triplet. Therefore in order to illustrate the shape of the triplet workspace we will resort to the two dimensional contours as explained in chapter five. However because of the aforementioned complexities involved, the search algorithms used for single robots will not work for the dextrous triplet workspace. For a single robot the developed algorithms perform a two-dimensional search in either cartesian or polar coordinates on a given cutting plane, whereas for the dextrous triplet workspace one should search among five independent parameters. Namely two cartesian coordinates of the boundary point on the plane and three parameters which define the orientation of the workpiece (Euler angles for instance). One way of locating the boundary points of the contour on the cutting plane may be resorting to a constrained optimization procedure. However by making the assumption that orientation of the object is given when point C is on the cutting plane, one can use this orientation and perform a two dimensional search over the cutting plane in order to locate the boundary points associated with the triplet workspace with constant orientation. This simplified approach will be discussed in more detail in the next section.

7.3 TRIPLET WORKSPACE WITH CONSTANT ORIENTATION- W(C)

In this section we elaborate on the concept of triplet workspace with constant orientation for tightly coordinated two-arm robotic operations. Primarily we discuss the basic features of the defined workspace on a given cutting plane, and then present an algorithm for the generation of the two dimensional contours of the triplet workspace. In the remaining chapter we will use the name *triplet workspace* instead of *triplet workspace*

with constant orientation.

7.3.1 TWO-DIMENSIONAL CONTOUR DETECTION FOR TRIPLET WORKSPACE

Figure 7.1 shows the general organization for the evaluation of the boundaries of the triplet workspace W(C). In this figure the two coordinated robots are shown as well as the manipulated workpiece in an initial pose defined in the world coordinate frame, with the following information

T_C^M, T_C^F: The grasp transformation matrices for the main and the follower end effectors, respectively.

T_W^m, T_W^f: The transformation matrices defining the position and orientation of the base frame of the main and the follower arms with respect to the world coordinate frame.

T_W^C : The transformation matrix defining the pose (position and orientation) of the workpiece with respect to the world coordinate frame.

The cutting plane on which a two-dimensional contour of the workspace is sought will be defined in a similar fashion as was discussed for the single manipulator workspace. As an example the cutting plane denoted by $\prod$ in figure 7.1, is chosen to be the world's XZ plane.

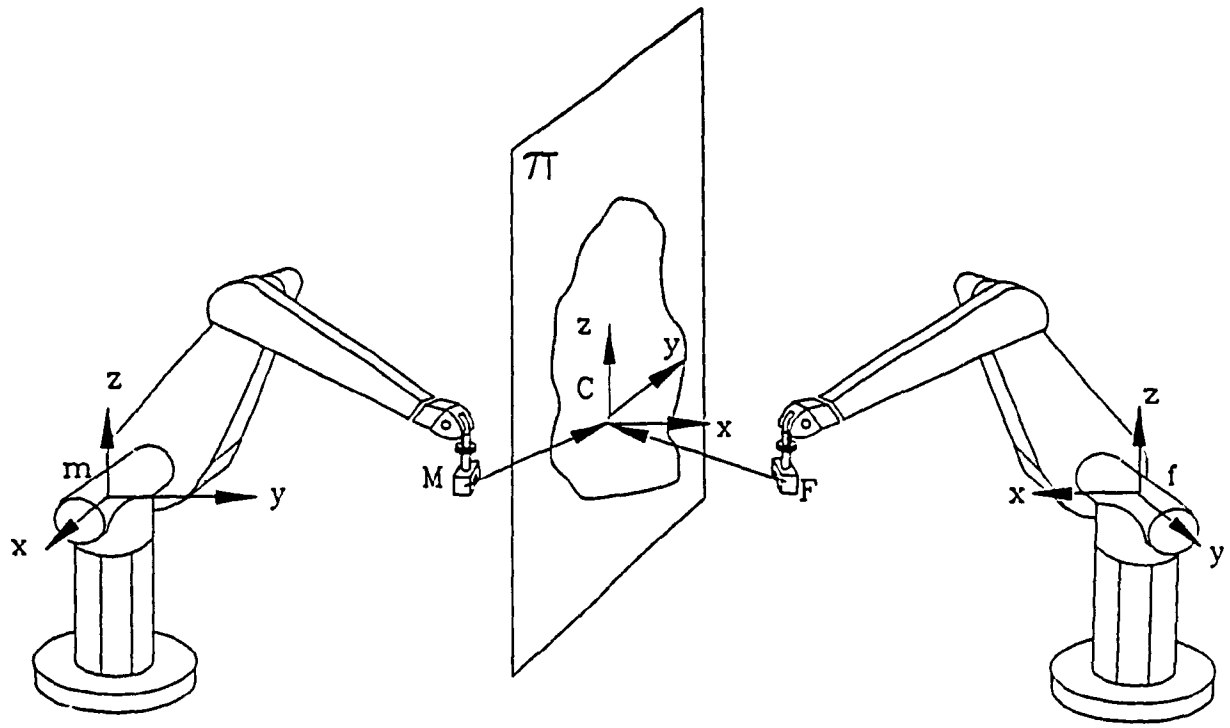

Figure 7.1 - Cutting plane through the triplet workspace

To every plane Π, cutting the triplet workspace, there corresponds a parallel plane which passes through the main end effector and cuts its workspace and another parallel plane which cuts the follower workspace and passes through its end effector. These planes are denoted by Π_m and Π_f receptively. The mapping between any points, on plane Π defined in the world coordinate frame, and its corresponding points on plane Π_m and Π_f of the main and the follower arms in their respective base coordinate frames (m; x, y, z) and (f; x, y, z), can be performed by using the following matrix relations,

$$T_m^M = (T_W^m)^{-1}\ T_W^C\ T_C^M \tag{7.1}$$

$$T_f^F = (T_W^f)^{-1}\ T_W^C\ T_C^F. \tag{7.2}$$

With the same token the mapping of the points on the hands cutting planes Π_m and Π_f , to the plane Π will be readily obtained from the following equations,

$$T_M^C = (T_m^M)^{-1}\ (T_W^m)^{-1}\ T_W^C \tag{7.3}$$

$$T_F^C = (T_f^F)^{-1}\ (T_W^f)^{-1}\ T_W^C. \tag{7.4}$$

Having defined the cutting planes and the mappings among them, boundaries of the corresponding workspaces associated with each end effector on its cutting plane will be mapped to the plane Π passing through the point C of the workpiece by employing equations **7.3** and **7.4**. Therefore, two sets of mapped contours of the hand's workspaces will be obtained on plane Π, one for the main and the other for the follower manipulators. If we denote these two sets of contours by, $W_\pi(M)$ and $W_\pi(F)$ respectively, then the triplet workspace for point C on plane Π or $W_\pi(C)$ will be the intersection of them on plane Π,

or,

$$W_{\pi}(c) = W_{\pi}(M) \cap W_{\pi}(F) \tag{7.5}$$

Equation 7.5 is a mathematical representation of the triplet workpiece, however in the search algorithm which will be developed next a different route will be followed.

7.3.2 TRIPLET WORKSPACE ALGORITHM

A step by step representation of the algorithm for evaluation of the triplet workspace with constant orientation is given in what follows,

1) Define the relative position and orientation of the two robot's base frames in the world coordinate frame (w; X, Y, Z), namely T_w^m and T_w^f.
2) Define the grasping configurations for both end effectors in the workpiece coordinate frame (C; x, y, z), namely T_C^M and T_C^F.
3) Define the cutting plane (Π), on which the working envelope of the point C of the object is being sought.
4) Define the orientation of the workpiece (R_w^C).
5) Use the grasping configurations and the object orientation to construct the two cutting planes in each robots workspace parallel to the plane Π, namely Π_m and Π_f.
6) Determine R_{max}^m and ,R_{max}^f, the maximum reaches of the main and the follower robots on their corresponding planes Π_m and Π_f.

7) Use the position part of transformations given in 7.3 and 7.4, to obtain the corresponding maximum and minimum reaches on plane Π, and take the larger of the two as the maximum reach for constructing the searching area on plane Π.

8) Start the search by changing the coordinates of point C on plane Π, and use transformations of 7.1 and 7.2 to obtain the coordinates of the main and the follower hands in their respective base frames, corresponding to the current coordinates of point C.

9) Check the reachability for both end effectors on Π_m and Π_f. If both are boundary points on their corresponding hand workspaces in plane Π_m and Π_f assign a status of unity to the current coordinates of point C and save its coordinates, Otherwise go to the next step.

10) Perform step 8, until the search area is completely covered.

The flow chart representing the aforementioned procedure is given in the appendix C.

7.4 ILLUSTRATIVE EXAMPLES FOR TRIPLET WORKSPACE

In order to show the results of the algorithm for evaluation of the triplet workspace, specification of two PUMA robot arms were used. For the purpose of discussion, three examples are given in what follows.

Example 1:

In this example the general set-up of a workcell, that is the position and orientation of the base frames of the main and the follower with respect to the world coordinate frame are given by the following matrices

$$T_w^m = \begin{bmatrix} 1 & 0 & 0 & 0 \\ 0 & 1 & 0 & 0 \\ 0 & 0 & 1 & 0 \\ 0 & 0 & 0 & 1 \end{bmatrix} \qquad T_w^f = \begin{bmatrix} -1 & 0 & 0 & 1000 \\ 0 & -1 & 0 & 0 \\ 0 & 0 & 1 & 0 \\ 0 & 0 & 0 & 1 \end{bmatrix} \tag{7.6}$$

and the grasp configurations are defined as follows,

$$T_C^M = \begin{bmatrix} -1 & 0 & 0 & 0 \\ 0 & -1 & 0 & 0 \\ 0 & 0 & 1 & 0 \\ 0 & 0 & 0 & 1 \end{bmatrix} \qquad T_C^F = \begin{bmatrix} 1 & 0 & 0 & 0 \\ 0 & 1 & 0 & 0 \\ 0 & 0 & 1 & 0 \\ 0 & 0 & 0 & 1 \end{bmatrix} \tag{7.7}$$

Finally the desired orientation of the workpiece is given with the rotation matrix.

$$R_w^C = \begin{bmatrix} 0 & -1 & 0 \\ -1 & 0 & 0 \\ 0 & 0 & -1 \end{bmatrix} \tag{7.8}$$

In this example in order to minimize the coupling effects between the end effectors it is assumed that the grasping points are coincided with the point C (position vectors of the main and the follower hands are zero with respect to the frame C). Obviously this is not a realistic configuration and in the real applications both end effectors can not grab the same point of the object, however since it will produce the maximum workspace for the aforementioned workpiece and grasp orientations, and also for the sake of

comparison we use the said configuration. Figures 7.2.a ,b ,and c are the results of the sought triplet workspace. In these figures respectively the cutting planes are taken as xz, yz and xy of the object reference frame (C; x,y,z).

As it can be seen from the contours shown in figures 7.2, the triplet workspace in a coordinated two-arm robot is significantly smaller in size as opposed to the workspace of single robots. This reduction is mainly due to the coupling effects between the two end effectors while carrying a common workpiece.

Example 2:

This example is provided here, in order to show the changes made to the shape and the size of the workspace associated with the triplet with constant orientation, by changing the position vector defining the grasping points of the main and the follower hands. The general set-up of the workcell is the same as example 1, and also the same grasping orientations for both end effectors are used. The new grasps for the main and the follower hands are given as,

$$T_C^M = \begin{bmatrix} -1 & 0 & 0 & 150 \\ 0 & -1 & 0 & 200 \\ 0 & 0 & 1 & 200 \\ 0 & 0 & 0 & 1 \end{bmatrix} \quad T_C^F = \begin{bmatrix} 1 & 0 & 0 & -150 \\ 0 & 1 & 0 & -200 \\ 0 & 0 & 1 & 200 \\ 0 & 0 & 0 & 1 \end{bmatrix} \tag{7.9}$$

The workspaces associated with point C, on the same cutting planes as in example 1 are shown in figures 7.3.a, 7.3.b and 7.3.c respectively for xz, yz and xy planes.

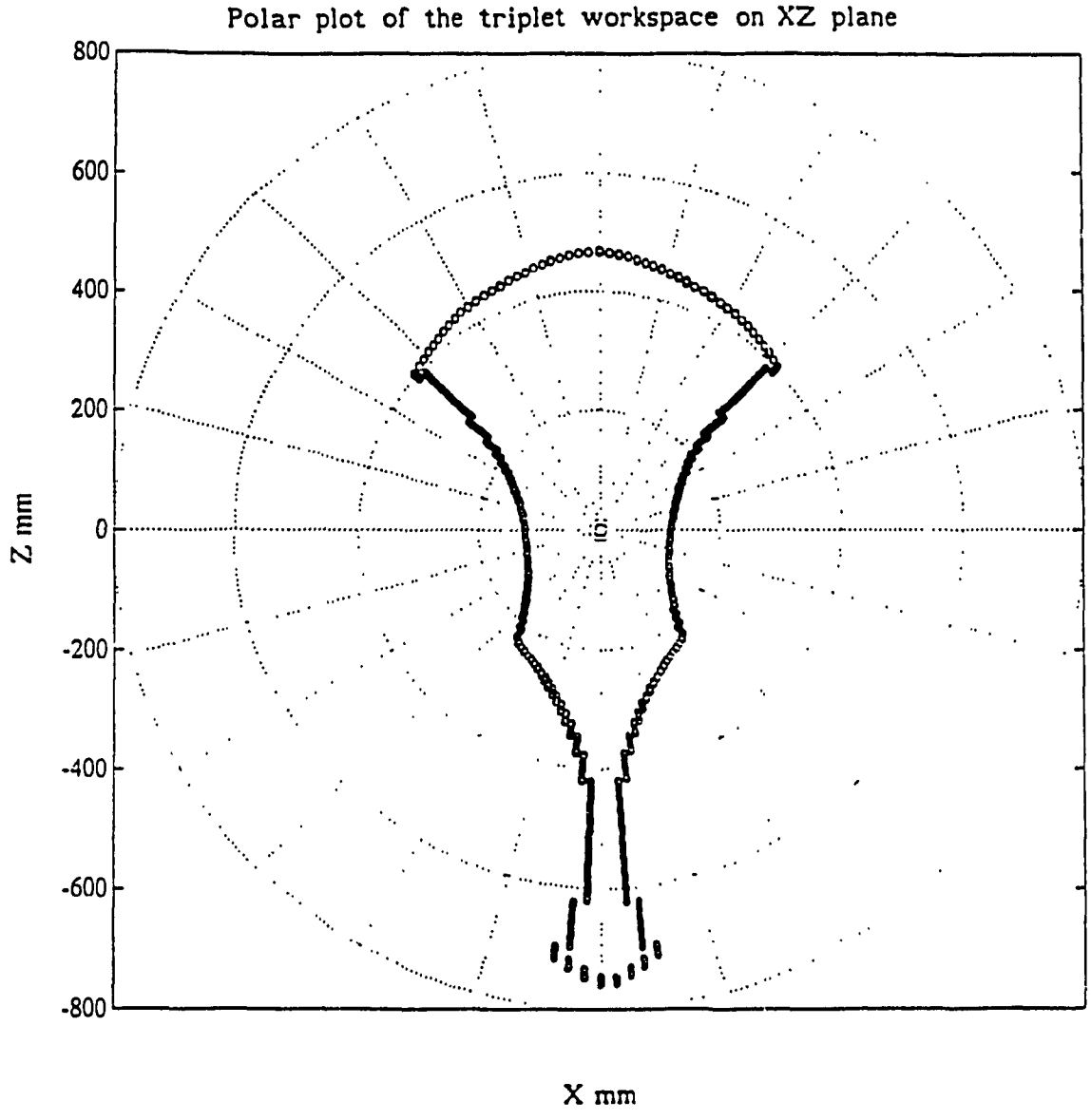

Figure 7.2.a - Polar plot of the triplet workspace on XZ plane

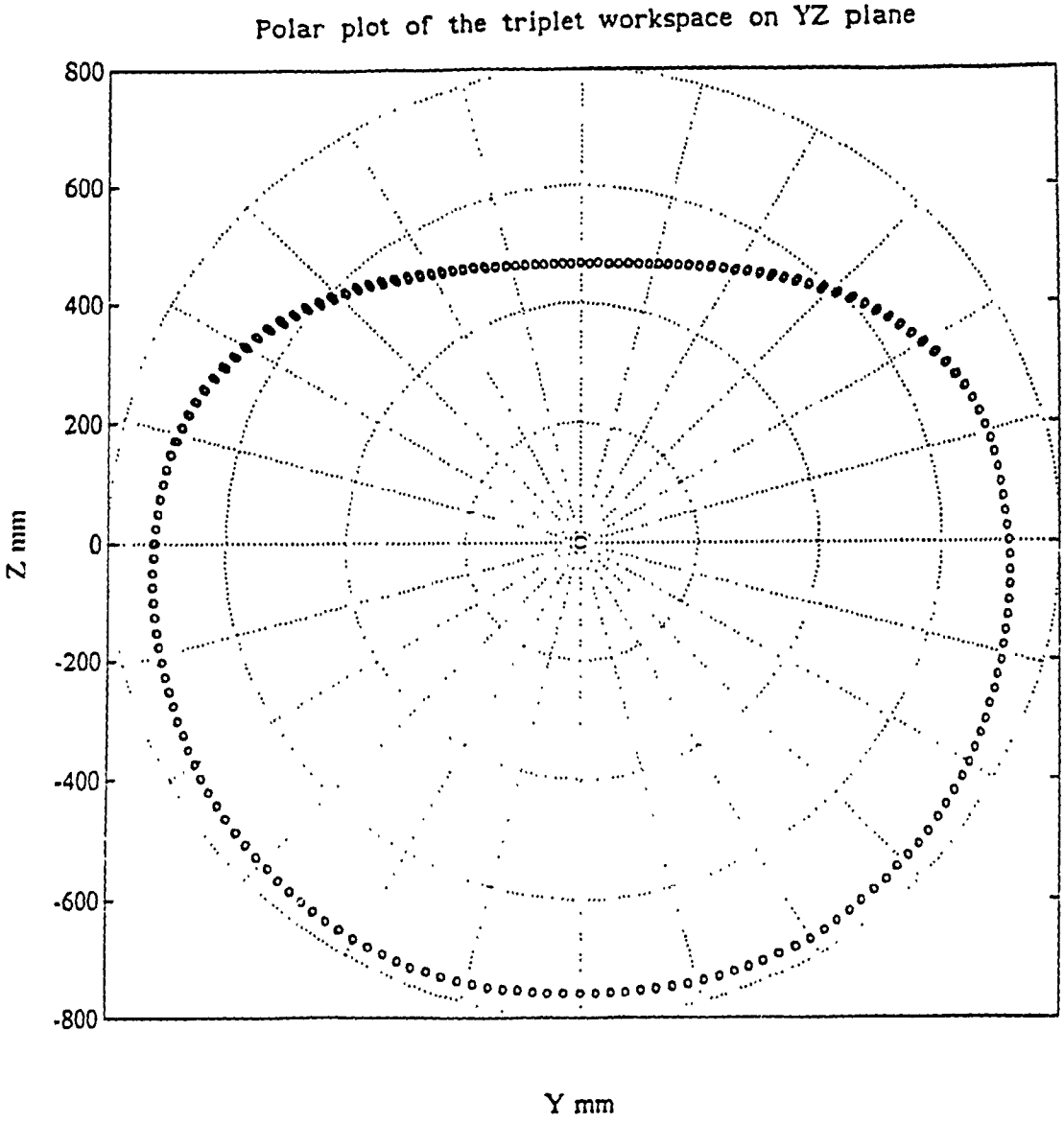

Figure 7.2.b - Polar plot of the triplet workspace on YZ plane

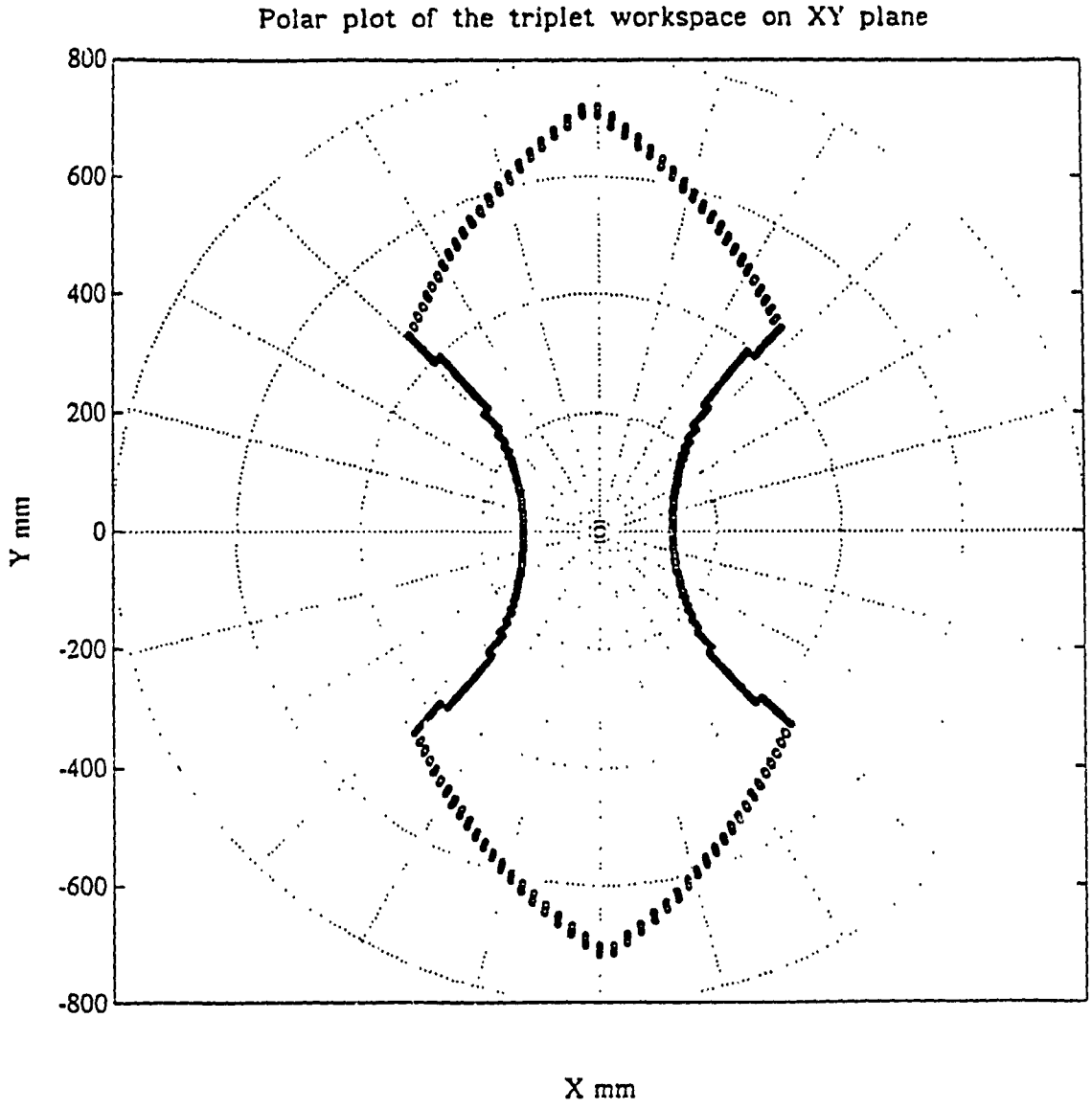

Figure 7.2.c - Polar plot of the triplet workspace on XY plane

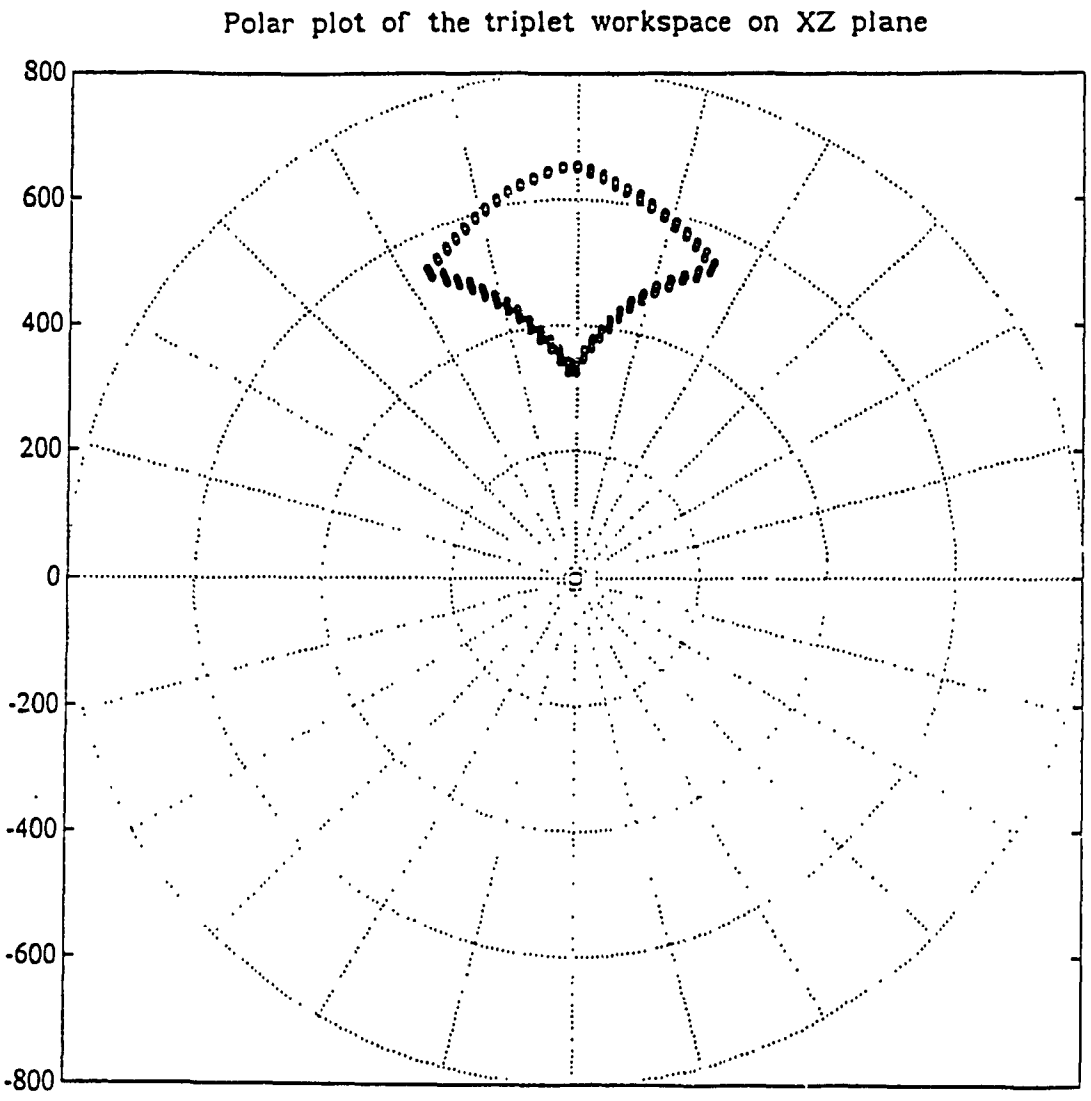

Figure 7.3.a - Polar plot of the triplet workspace on XZ plane

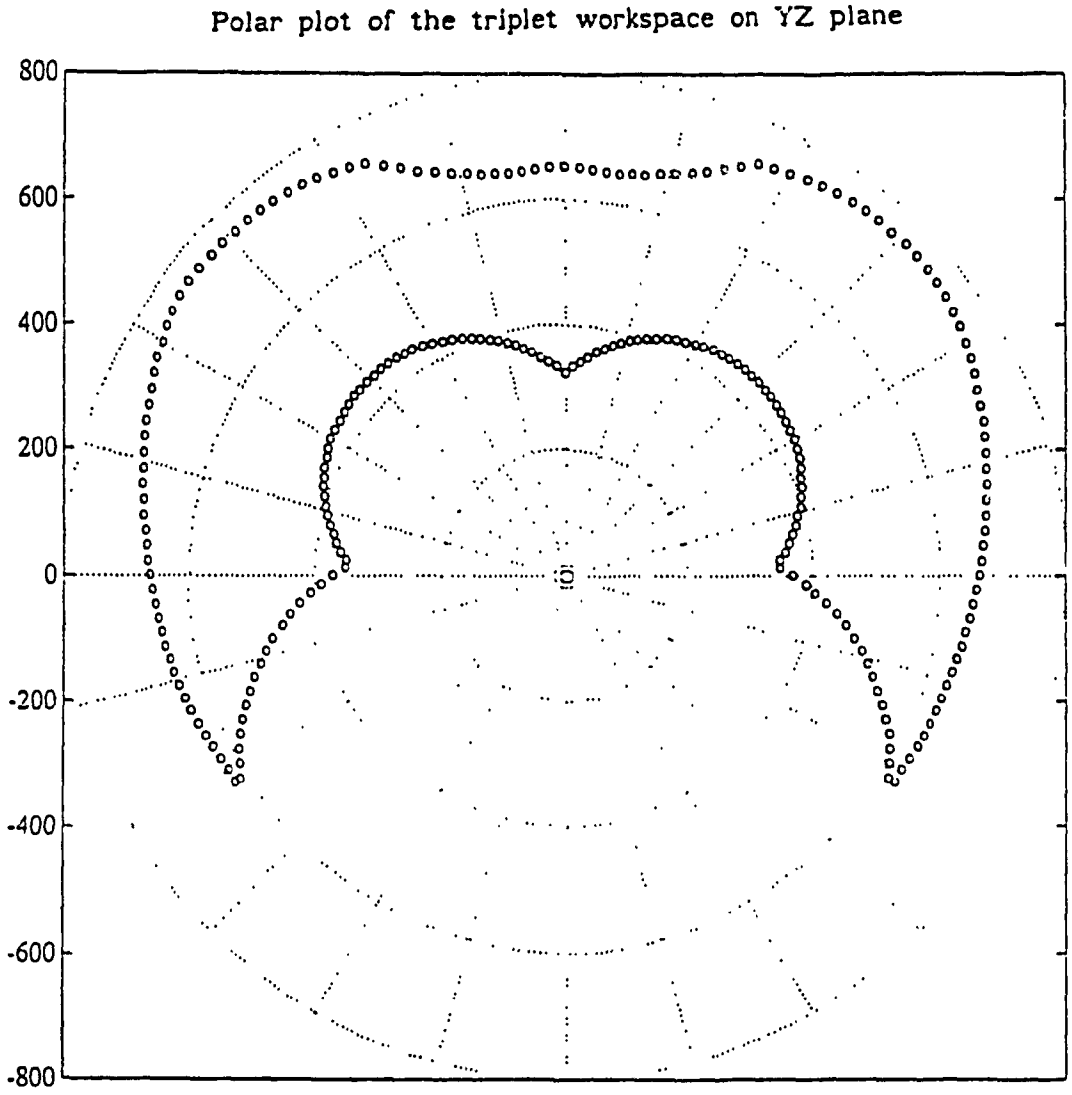

Figure 7.3.b - Polar plot of the triplet workspace on YZ plane

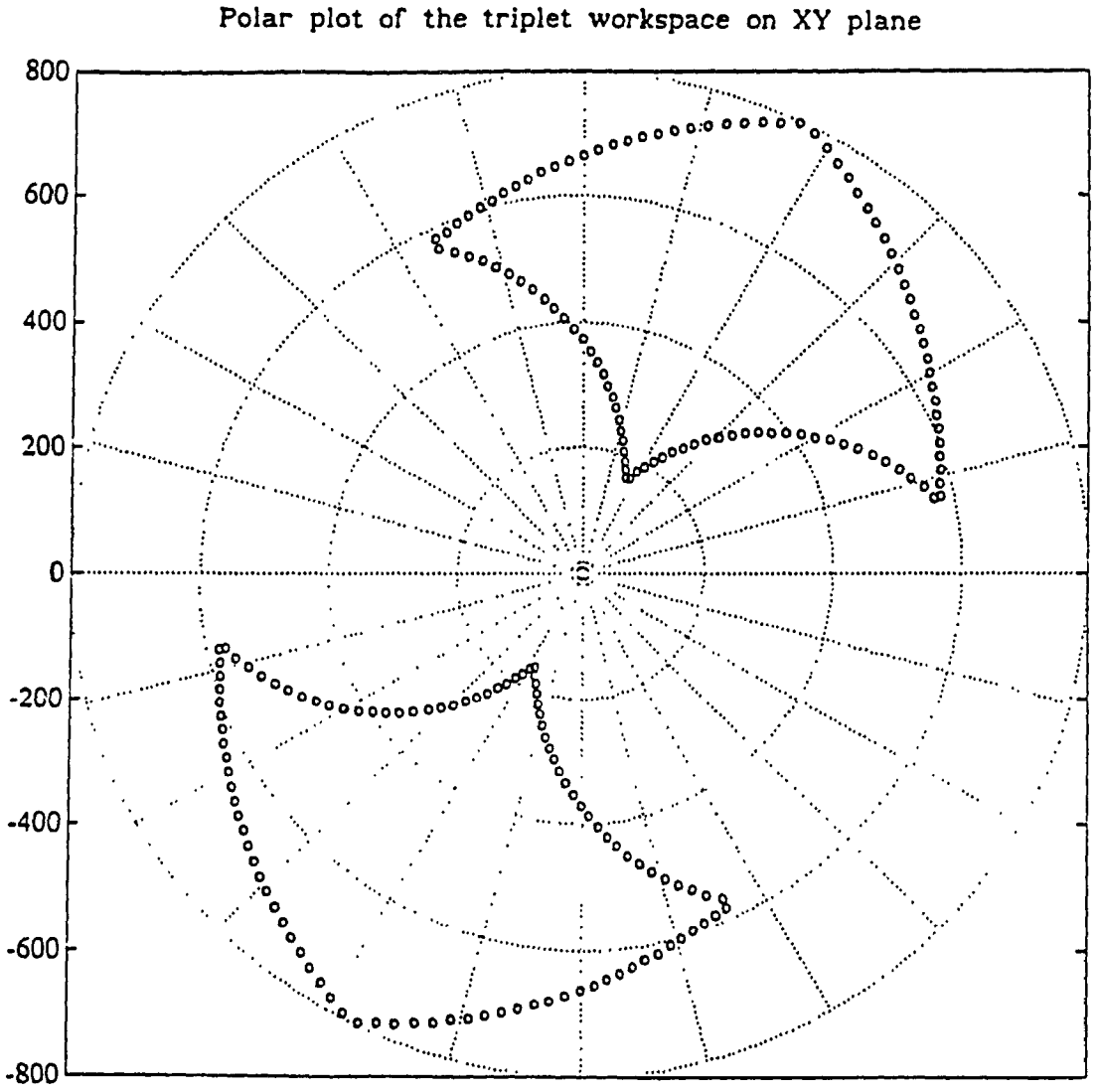

Figure 7.3.c - Polar plot of the triplet workspace on XY plane

It can be observed from the figures shown above, that by moving the end effectors away from each other (changing the grasp positions), the workspace of the point C on the same cutting planes has drastically deformed and decreased in size.

Example 3:

The purpose of this example is to show how the shape of the triplet workspace will change, if the relative position of the base frames of the two manipulators are modified. If we denote by h, the distance between origins of the main and the follower manipulators, one can use this parameter as an adjusting tool in order to establish a set-up which produce larger triplet workspace for given grasp configurations. For instance if the set-up of the workcell and the grasp configurations are defined with the following matrices,

$$T_w^m = \begin{bmatrix} 1 & 0 & 0 & 0 \\ 0 & 1 & 0 & 0 \\ 0 & 0 & 1 & 0 \\ 0 & 0 & 0 & 1 \end{bmatrix} \qquad T_w^f = \begin{bmatrix} -1 & 0 & 0 & h \\ 0 & -1 & 0 & 0 \\ 0 & 0 & 1 & 0 \\ 0 & 0 & 0 & 1 \end{bmatrix} \tag{7.10}$$

$$T_c^M = \begin{bmatrix} -1 & 0 & 0 & 100 \\ 0 & -0.707 & -0.707 & 150 \\ 0 & -0.707 & 0.707 & 200 \\ 0 & 0 & 0 & 1 \end{bmatrix} \quad T_c^F = \begin{bmatrix} 1 & 0 & 0 & -50 \\ 0 & 0.707 & 0.707 & -100 \\ 0 & -0.707 & 0.707 & 50 \\ 0 & 0 & 0 & 1 \end{bmatrix} \tag{7.11}$$

And the position and orientation of the workpiece is given as

$$T_w^c = \begin{bmatrix} 1 & 0 & 0 & h/2 \\ 0 & 1 & 0 & 0 \\ 0 & 0 & 1 & 0 \\ 0 & 0 & 0 & 1 \end{bmatrix} \tag{7.12}$$

Then with two different values of h the triplet workspaces were obtained on the three cutting planes of XZ, YZ and XY planes of workpiece coordinate system. Figure 7.4.a shows the workspace of point C on XZ plane with h=1000 mm. In figure 7.4.b, the same workspace is shown when h=1500 mm. It can be observed that for the given grasp, h=1500 mm will produce a continuous and larger two dimensional contour for the triplet workspace as compare to the one obtained when h=1000 mm. Thus for the given grasp one may use the concept of triplet workspace in order to design the set-up of the workcell.

Figures 7.5.a, and b are the triplet workspaces on the YZ plane where h is 1000 and 1500 mm respectively. The same trend as was explained above can be observed here, that is increasing h to 1500 mm will produce a continuous and larger two-dimensional contour.

In figures 7.6.a and b the contours of the triplet workspace shown on plane XZ of the workpiece coordinate system with the two mentioned values of h, where again on this cutting plane the change in the shape of the triplet workspace is observed.

From the foregoing results, the importance of the set-up of the two-arm robot workcell can be concluded. In this regard, it was observed that by changing the distance h between the origins of the robots, the corresponding triplet workspaces can change significantly. Therefore a major question which may arise is that, what should be the best h, or how much apart should the bases of the robots be installed in order to produce an optimum workspace for a given task. In fact a more general question may arise in this regard, that

is what would be the best position and orientation of the base frames of the robots with respect to the world coordinate frame. In the following chapter the problem of synthesis of the workcell will be discussed where we propose a methodology in order to achieve an optimum workcell for a given task.

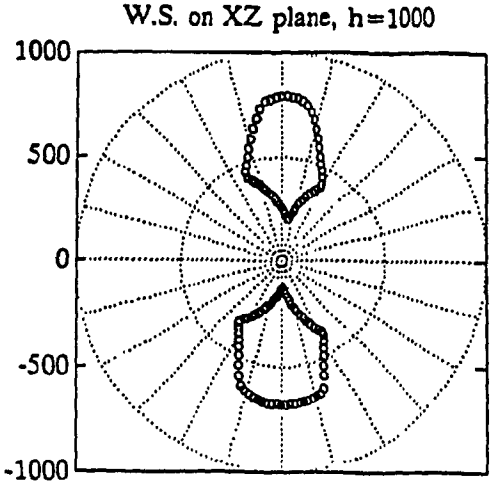

Figure 7.4.a

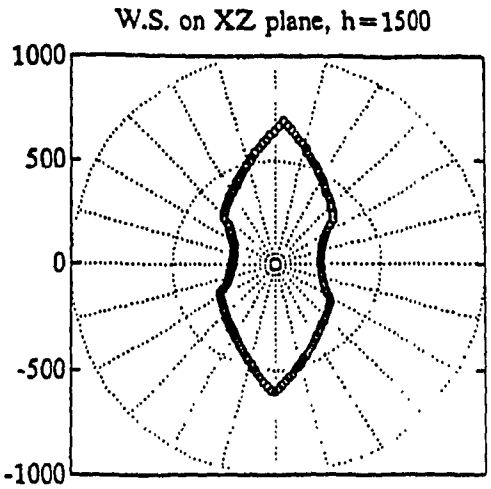

Figure 7.4.b

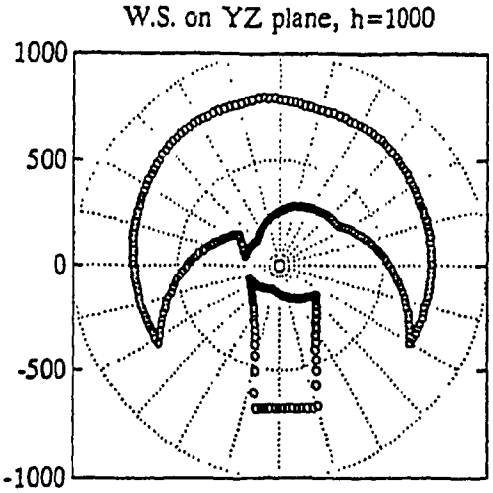

Figure 7.5.a

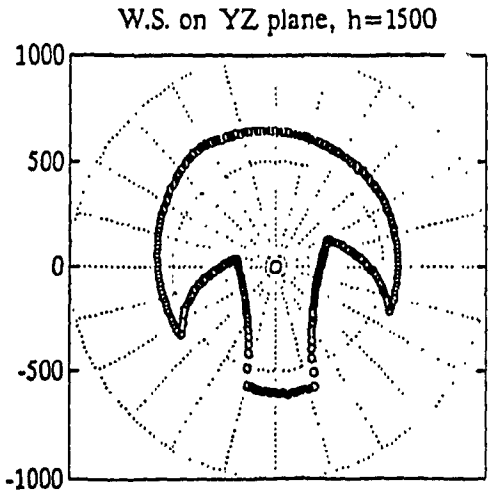

Figure 7.5.b

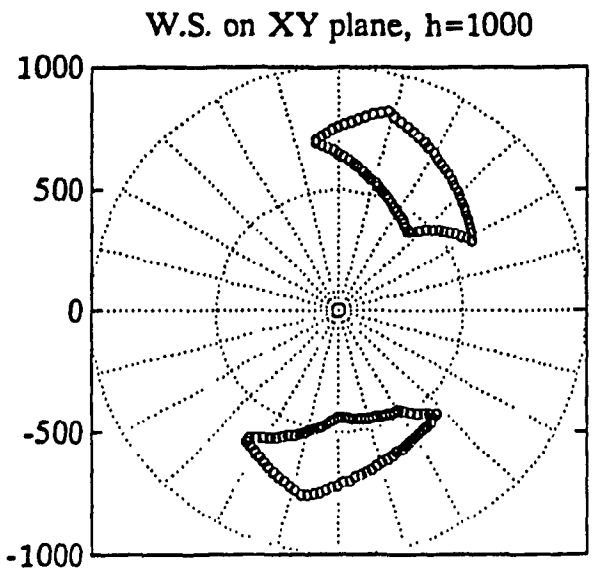

Figure 7.6.a

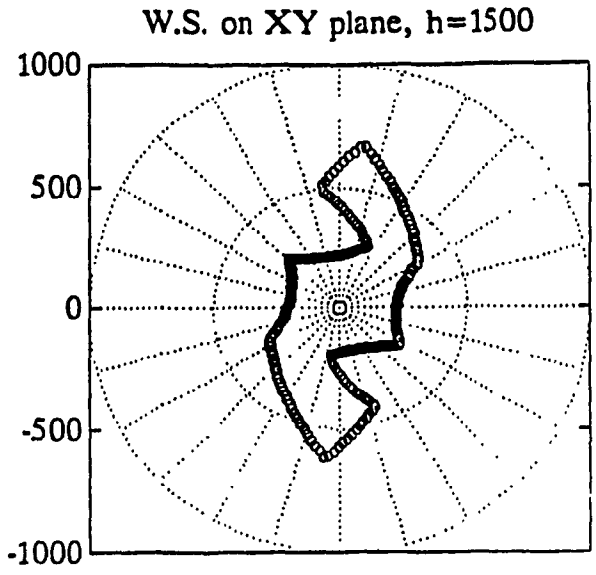

Figure 7.6.b

CHAPTER 8

WORKCELL LAY-OUT FOR COORDINATED TWO-ARM ROBOTS

8.1 INTRODUCTION

In this chapter the problem of the set-up of coordinated two-arm robotic systems will be addressed. In the previous chapters the workspaces associated with two coordinated robot arms were discussed and the concept of triplet workspace was introduced. So far, we have always assumed that the two robots are already placed in the workcell and their base coordinates are known with respect to the world coordinate frame. The analysis of the workcell have been made based on the given relative set-up of the workcell. By relative set-up of the workcell, it is meant, the relative position and orientation of the base frames of the main and the follower manipulators with respect to the world coordinate frame. In the following sections we will investigate the the set-up of a coordinated two-arm robotic workcell. In section 8.2 the general problem of the optimization of the workcell set-up will be defined and the corresponding formulations will be developed. Section 8.3 is devoted to expand on the optimization methods for solving the problem at hand. Exterior and Interior penalty function methods will be discussed for converting the constrained minimization problem to an unconstrained one. And also the conjugate gradient method will be discussed for solving the unconstrained problem.

It was shown in the previous chapters that how the distance between origins of the base frames of the coordinated robots (h) plays a significant role in the shape of the triplet workspace; thus, it is important to investigate the set-up of the workcell for tasks or family of similar tasks to be performed. As the first approach in synthesis of the workcell it is assumed that one has the flexibility to adjust the distance h between the origins of the two robots. In other words one may treat h as a design parameter for the synthesis of the workcell for certain operations. In fact this approach may well find applications in material handling or assembly operations, where the sizes of the objects may vary, and thus new adjustments for the workcell be in demand. This adjustment may be performed by placing one of the robots, the follower for instance, on a track which in turn will enable the distance between the bases to be adjustable. A case study in material handling operations of coordinated two-arm robots is given in chapter nine, in which we will investigate the set-up of the workcell in terms of h, (Hemami et al. 1991).

8.2 OPTIMIZATION OF THE SET-UP FOR COORDINATED TWO-ARM ROBOTS

We have demonstrated the effectiveness of the relative position of the base frames of the manipulators in the coordinated environments on the shape and size of the overall workspace of the system, and now we extend our investigation further more, taking into considerations both position and orientation of the base coordinate frames of the two robots with respect to the world coordinate frame. In fact in contrast to the case of finding an optimum value for the distance between the two robots' base frames (h), we

will attempt to optimize the position as well as the orientation of the robots with respect to the world frame. An optimization problem will thus be formulated to determine a relative set-up of the workcell in order to satisfy certain performance criteria. This will lead to a nonlinear programming problem which will be formulated and solved by using **Sequential Unconstrained Minimization Technique (SUMT).**

Although the method introduced here is for the synthesis of a two-arm robot, it can be used for single manipulator workcell or even coordinated multi-manipulators as well. As a general approach we will consider four design parameters for each manipulator, namely, three cartesian coordinates to define the position of the origin of the robot's base frame, and one rotation angle for its orientation. The performance criteria to be optimized in will be chosen as the **Joint Availability** of the manipulators throughout the execution of the task.

8.2.1 DEFINITION OF THE PROBLEM

In this section the definition of the problem for optimization of the set-up of a manipulator for a given task will be given. As a practical application, consider an object to be carried through m poses along a given trajectory (Figure 8.1). First we assign the object coordinate frame to the workpiece (frame C). Thus for every pose of the workpiece along the trajectory one can define a transformation matrix defining the position and orientation of the object with respect to the world coordinated frame as

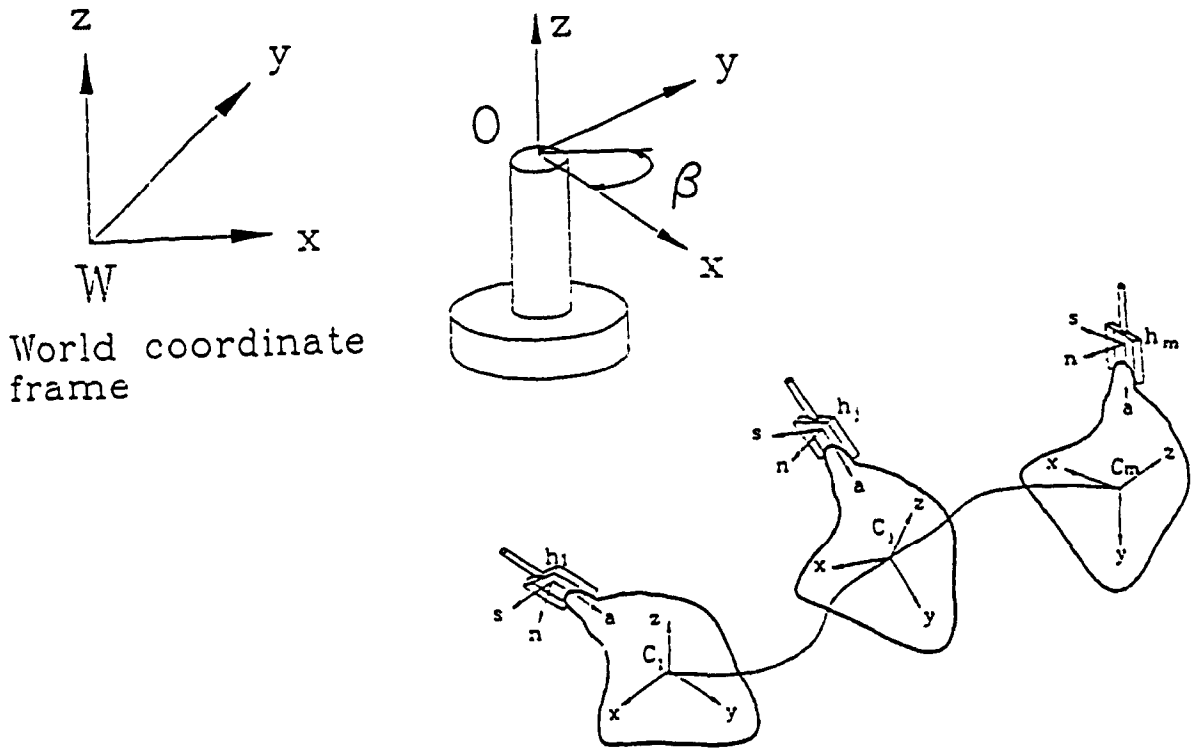

Figure 8.1 - A typical robotic task

$$(T_W^C)_j = \left[\begin{array}{c|c} (R_W^C)_j & (P_W^C)_j \\ \hline 0 & 1 \end{array}\right] \qquad j = 1,2,\ldots m. \tag{8.1}$$

The grasp configuration is defined in a similar fashion by a transformation matrix. If we denote the tool frame of the hand of a general manipulator by H, where for the case of the main and the follower manipulators H will be replaced by M and F respectively (chapter 6), then the position and orientation of the grasp will be defined by a transformation matrix T_C^H ,(for the case of material handling of a rigid object, this transformation will remain unchanged throughout the task). For each pose j of the object during motion, the transformation matrix of the end-effector with respect to the world reference frame is defined by

$$(T_W^H)_j = (T_W^C)_j \; T_C^H \tag{8.2}$$

Our main problem now, may be defined as follows: Having the transformation matrices of the end effectors for the m poses of the object, what would be the best position to fix the base of the robot(s) and with what orientation, in order that a performance index (PI) is optimized. An appropriate choice for this performance index will be the **Joint Availability** of each robot arm. Some other quantities that could be chosen for this purpose are the joint torque values, energy consumption, cycle time, etc. The reason for choosing joint availability as the performance index is the fact that our main concern is the workspace characteristics; also it was demonstrated, how important the physical limits of the joint variations are

on the workspaces (chapter 5). On the other hand, the joint availability, is a direct measure of the overall closeness of the joint values to their limits. Let q_i^u and q_i^L be the upper and the lower limits of the variations of joint i, respectively, and let

$$q_i^* = \frac{q_i^U + q_i^L}{2} \quad i = 1,2,...N. \tag{8.3}$$

where N is the number of joints in the arm and q_i^* is simply the midpoint of the range of operation for joint i. Moreover let

$$Q_j = \left[q_{1j}\ q_{2j}\ q_{3j}\ \cdots\ q_{Nj}\right]^T \tag{8.4}$$

and

$$Q^* = \left[q_1^*\ \ q_2^*\ \ q_3^*\ \ \cdots\ q_N^*\ \right]^T. \tag{8.5}$$

Where Q_j is the vector of joint variables for the robot, corresponding to pose j of the trajectory, and Q^* is the vector of joint midpoint values which is constant for all poses of the workpiece. Next the Euclidean norm of the difference between the current values of each joint Q and Q^* for a pose j of the trajectory will be defined as,

$$e_j = \|Q_j - Q^*\| = \sqrt{(q_{1j} - q_1^*)^2 + (q_{2j} - q_2^*)^2 + ...(q_{Nj} - q_N^*)^2} \tag{8.6}$$

Since the physical ranges of the joints for a manipulator are usually different in magnitude, it is preferable to introduce weighting factor w_i for

because of these differences. Thus equation 8.6 can be rewritten as,

$$e_j = \left(\sum_{i=1}^{N} w_i (q_{ij} - q_i^*)^2 \right)^{1/2} \qquad j = 1,2,\ldots m. \tag{8.7}$$

The weighting factors are selected as

$$w_i = \frac{\left[max(q_i^U - q_i^L) \right]^2}{(q_i^U - q_i^L)^2} \qquad i = 1,2,\ldots N, \tag{8.8}$$

Then, for a joint with a smaller range of motion, a larger weighting factor will be determined. And the factor for the joint with the largest range will be unity. In the light of equation 8.6, the sum of the square of the errors corresponding to all m poses can be expressed as

$$E = e_1^2 + e_2^2 + \ldots e_m^2. \tag{8.9}$$

Equations 8.9 and 8.7 can be combined and written in a compact form as follows,

$$E = \sum_{j=1}^{m} \sum_{j=1}^{N} w_i (q_{ij} - q_i^*)^2 \tag{8.10}$$

where E is the performance index to be minimized in order to maximize joint availability. In equation 8.10, E is defined in terms of the joint coordinates Q_j, however the vector $Q_j = [q_{1j}\ q_{2j} \ldots q_{Nj}]^T$ can be determined

from the inverse kinematics formulations of the manipulator only when the base frame of the robot is fixed with respect to the world coordinate frame. Therefore, we define a set-up vector Γ whose elements are yet to be found as,

$$\Gamma = [x,\ y,\ z,\ \beta]^T \tag{8.11}$$

where x, y and z are the cartesian coordinates of the origin of the robot's base frame, and β is the angle of rotation of the x-axes of the robot base frame and the world frame, assuming that their z-axes are parallel. This is in fact a rational assumption since usually the z-axis of the robot's base frame is vertical and thus rotations about the world's x and y axes which in turn make the z-axis of the base to be inclined, are not desirable. The objective is to find elements of the set-up vector (8.11) for a given task, while minimizing the performance criteria in equation 8.10.

8.2.2 FORMULATIONS OF THE PROBLEM

It is assumed that *m* desired poses of the object along the path are defined by equation 8.1, therefore by employing equation 8.2, one can determine *m* corresponding poses for the hand of the robot(s) involved. On the other hand in light of equation 8.11, we can express a homogeneous transformation matrix T_W^o , corresponding to the set-up vector Γ , which defines the position and orientation of the base frame of the robot with respect to the world coordinate frame as,

$$T_W^0 = \begin{bmatrix} \cos\beta & -\sin\beta & 0 & x \\ \sin\beta & \cos\beta & 0 & y \\ 0 & 0 & 1 & z \\ 0 & 0 & 0 & 1 \end{bmatrix} \tag{8.12}$$

it then follows from equations 8.1, 8.11 and 8.12 that at each of the given points on the trajectory

$$(T_0^H)_j = (T_W^0)^{-1} (T_W^C)_j T_C^H \qquad j=1,2,...m. \tag{8.13}$$

T_0^H is in fact the attitude matrix of the robot's hand, that can be used for determination of the joint angles for each point on the trajectory from the inverse kinematic solutions. Since T_0^H depends on the unknown elements of Γ in 8.13, for each point of the trajectory, we may write the vector of joint coordinates as a function ϕ of the elements of Γ and elements of the grasp matrix and the task matrix as

$$Q_j = \phi\left(x,\ y,\ z,\ \beta,\ T_W^C,\ T_C^H\right) \tag{8.14}$$

Now we are in the position to construct the objective function of the problem with x, y, z and β being the design parameters. Thus we rewrite the performance index given in 8.10, as a function of the design parameter as

$$E(x,y,z,\beta) = \sum_{j=1}^{m} \sum_{j=1}^{N} w_i (q_{ij}(x,y,z,\beta) - q_i^*)^2 \tag{8.15}$$

Equation 8.15, is the objective function or the performance index of the optimization problem, to be minimized, over the elements of the set-up vector

Γ. Having defined the objective function, next we have to take into account the constraints of nonlinear programming at hand. These constraints associated with the minimization problem are the limits on the joint motions, meaning that each joint's variation must fall within its physical range of operation, that is

$$q_i^L \leq q_{ij} \leq q_i^U \qquad \begin{cases} i = 1,2,...N \\ j = 1,2,...m \end{cases} \tag{8.16}$$

or

$$\begin{cases} (q_{ij} - {}^U q_i) \leq 0 & i = 1,2,...N \\ (q_i^L - q_{ij}) \leq 0 & j = 1,2,...m \end{cases} \tag{8.17}$$

This will introduce $2m$ x N inequality constraints to be satisfied in addition to the fact that the joint variables must be determined from the inverse kinematics solution, and singularities of the solutions will have to be avoided by constructing some additional constraints. In fact since a solution for the joint variables exist only when the end-effector moves within the Jacobian surfaces of its workspace (within the reachable area), then we resort to the reachability of the robot as a supplementary constraint. In order to consider the reachability of the end effector in terms of the singularities, we resort to the concept of maximum and minimum reaches of a manipulator which were discussed in chapter 5. Incidentally one may adequately substitute the conditions for an answer to exist, by stating that the end effector must remain within two concentric spheres denoting the maximum and minimum reaches of the robot. Let R_{max} and R_{min} be the radii of

the largest and the smallest spheres accessible by the end effector with their centers coincided at the origin of the robot's base (figure 8.2), and R_j represents the magnitude of the position vector (P_j^H) of the hand at each point j, that is,

$$R_j = \|P_j^H\| = \sqrt{p_{xj}^2 + p_{yj}^2 + p_{zj}^2} \; . \tag{8.18}$$

In equation 8.18, p_{xj}, p_{yj} and p_{zj} are the cartesian coordinates of the origin of the tool frame of the robot, thus it is essential that

$$R_{min} \leq R_j(x, y, z, \beta) \leq R_{max} \tag{8.19}$$

or

$$\begin{cases} R_j(x,y,z,\beta) - R_{max} \leq 0 \\ R_{min} - R_j(x,y,z,\beta) \leq 0 \end{cases} \qquad j=1,2,...m \tag{8.20}$$

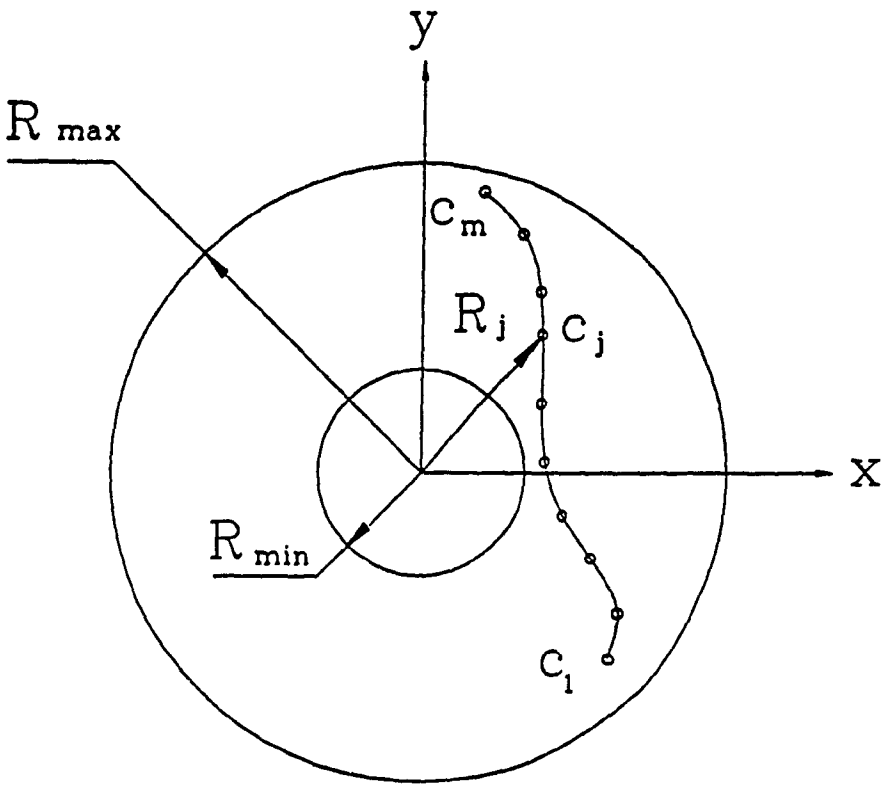

Figure 8.2 - Maximum and minimum reach of the robot

Thus the nonlinear minimization problem at hand can be formulated as follows,

Find x,y,z and β to minimize

$$E(x,y,z,\beta) = \sum_{j=1}^{m} \sum_{j=1}^{N} w_i (q_{ij}(x,y,z,\beta) - q_i^*)^2 \qquad (8.21)$$

subject to

f : The inverse kinematic relationships

$$\left.\begin{aligned} g_1&: (q_{ij} - q_i^U) \le 0 \\ g_2&: (q_i^L - q_{ij}) \le 0 \\ g_3&: (R_j - R_{max}) \le 0 \\ g_4&: (R_{min} - R_j) \le 0 \end{aligned}\right\} \quad \begin{matrix} i=1,2,\ldots N \\ j=1,2,\ldots m \end{matrix} \qquad (8.22)$$

8.3 OPTIMIZATION METHODS

In this section a brief review of some of the most popular nonlinear optimization methods will be made and one of them which best suits our problem will be chosen. In the most general case constrained nonlinear optimization problem can be stated as,

Minimize	F(x)	Objective function	(8.23)
Subject to;	$g_k(x) \le 0$	Inequality constraints	
	$h_j(x) = 0$	Equality constraints	
	$k = 1,2,\ldots m$		
	$j = 1,2,\ldots l$		

Where

$$x = \begin{Bmatrix} x_1 \\ x_2 \\ \vdots \\ x_n \end{Bmatrix}$$ Design variables

m and l are the number of inequality and equality constraints respectively.

The general approach to solve constrained nonlinear optimization problems is to convert the problem to an unconstrained optimization case, and solve it with one of the well-established unconstrained techniques. The motivation here is to minimize the objective function as an unconstrained problem but to provide some penalty in order to limit the constraint violations. Because the way in which this penalty is imposed, often leads to a numerically ill-conditioned problems, usually a method is devised whereby only a moderate penalty is provided in the initial optimization stage, and this penalty is increased as the optimization progresses. This requires the solution of several unconstrained minimization problems in obtaining the optimum constrained design, thus the term **Sequential Unconstrained Minimization Technique** or **SUMT** is used to indicate these methods.

The classical approach in using **SUMT** is to create a pseudo-objective function of the form

$$\Phi(x, r_p) = F(x) + r_p\, p(x) \qquad (8.24)$$

where $F(x)$ is the original objective function. $p(x)$ is an imposed penalty function the form of which depends on different methods of **SUMT** being used. The scalar r_p is a multiplier which determines the magnitude of the penalty and is held constant for a complete cycle of unconstrained

minimization. The subscript p is the unconstrained minimization index which corresponds to the sequences of the unconstrained minimization cycles. In what follows, two standard method of the penalization of the objective function are briefly reviewed (Fiacco and McCormick 1969),

8.3.1 Exterior Penalty Function Method

In this method the penalty function p(x) is typically given by

$$p(x) = \sum_{k=1}^{m} \left\{ max\left[0,\ g_k(x)\right] \right\}^2 + \sum_{j=1}^{l} \left[\ h_j(x)\right]^2 \qquad (8.25)$$

From 8.25, we see that no penalty is imposed if all constraints are satisfied (i.e. all $g_k(x) \leq 0$ and all $h_j(x) = 0$), but whenever one or more constraints are violated, the square of this constraint is included in the penalty function. The reason why the constraint violation is squared is that this provides a slope of zero for the penalty at the constraint boundary, thus ensuring a continuous slope of the pseudo-objective function $\Phi(x,\ r_p)$, however the second derivative is not continuous at the constraint boundary, and that is a possible source of numerical ill-conditioning if minimization methods which require second-order derivatives are used for the unconstrained minimization.

Consider now the multiplier r_p, if one chooses a small value for r_p, the resulting function $\Phi(x,\ r_p)$ is easily minimized but may result major constraint violation. On the other hand a large value of r_p will ensure near

satisfaction of all constraints but will create a very poorly conditioned optimization problem from a numerical standpoint. As a simple example figure 8.3.a shows a two dimensional constraint problem before penalizing the function and in figure 8.3.b and c, the penalized pseudo-objective functions are shown for two different values of r_p . From the foregoing discussion and figures 8.3.a and 8.3.b it can be seen that the best optimum solution of the exterior point method is always approached from outside of the feasible region, this characteristic is certainly undesirable for our minimization problem.

8.3.2 Interior Penalty Function Method

This method provides a sequence of improving feasible design but does so at the expense of creating a more complicated unconstrained problem. The difference here is in the form of the penalty function applied to inequality constraints and that the penalty parameter is decreased instead of increased during the optimization process. Probably the most common penalty function used in the interior method is (Fiacco and McCormick 1969),

$$p(x) = \sum_{j=1}^{m} \frac{-1}{g_j(x)} \tag{8.26}$$

Thus the pseudo-objective function will be given as,

$$\Phi(x, r_p') = F(x) - r_p' \sum_{j=1}^{m} \frac{1}{g_j(x)} \tag{8.27}$$

r_p' is the penalty parameter and is primed to distinguish from r_p. In fact r_p' starts as a relatively large positive number and decrease while r_p begins as a small positive number and increases. Here after each unconstrained minimization cycle r_p' is multiplied by γ', where γ' is a number less than 1.0, say 0.3. (Fox 1980). An alternative form of p(x) is

$$p(x) = \sum_{j=1}^{m} -log\left(-g_j(x)\right) \tag{8.28}$$

and this is often recommended as being slightly better numerically conditioned. The interior penalty function approach has the advantage that a sequence of feasible design is approached, but has the potential difficulty of having to deal with the discontinuity of $\Phi(x, r_p')$ at the constraint boundaries. Figure 8.4 shows the interiorly penalized constrained problem, note that the constraints are satisfied for all values of r_p' while $\Phi(x, r_p')$ is continuous.

In our optimization problem defined in 8.21, the satisfaction of the reachability constraints g_3 and g_4 are very crucial, since by violation of these constraints we are actually on the Jacobian surfaces of the workspace and the solution to the inverse kinematics on these surfaces will be singular. This will be a barrier for the continuation of the algorithm since in a singular cycle, one may not be able to calculate any values for the joint variables.

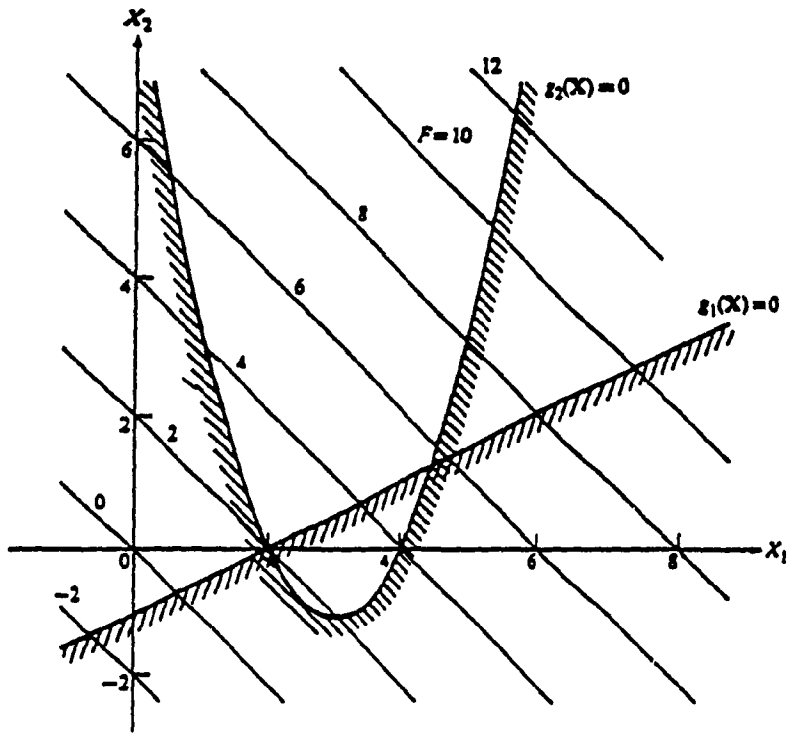

Figure 8.3.a - Objective function in Exterior penalty method

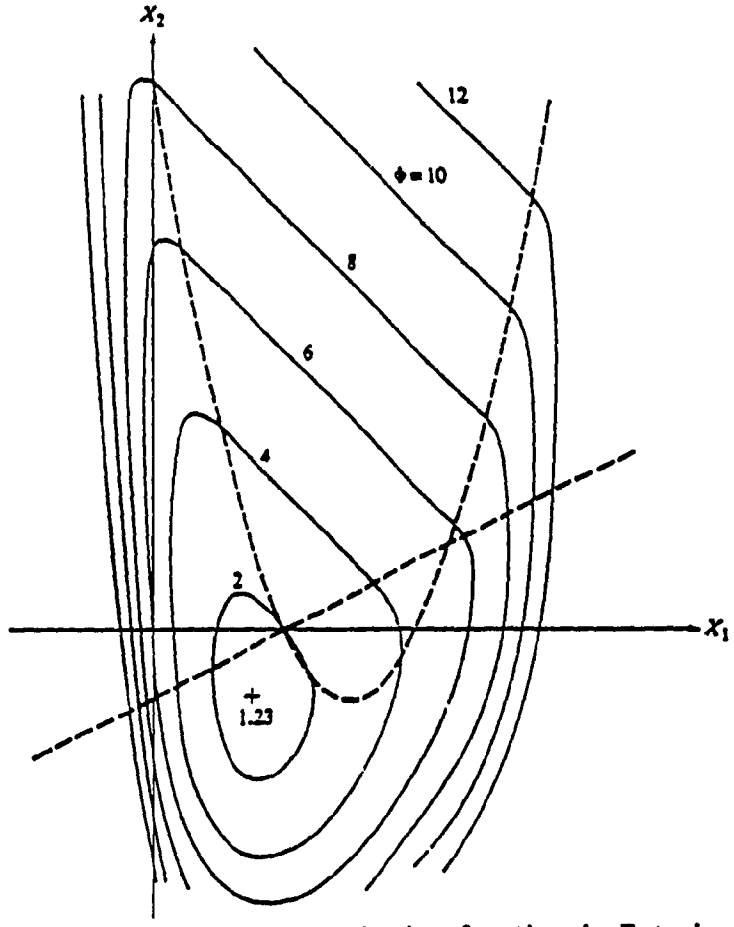

Figure 8.3.b - Pseudo-Objective function in Exterior penalty method

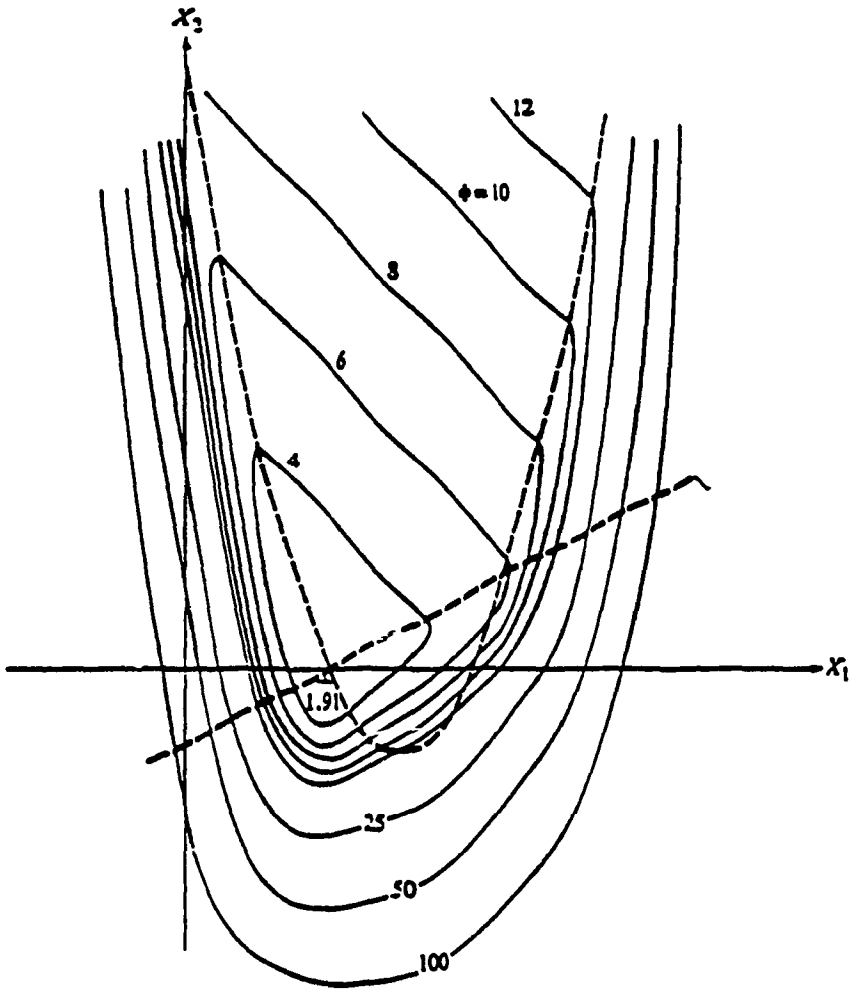

Figure 8.3.c - Pseudo-Objective function in Exterior penalty method

In the interior penalty function method the convergence is reached from within the feasible region (all constraints are satisfied) provided that $\Phi(x, r'_p)$ is continuous at the constraint boundaries, whereas in the exterior method even at the optimum solution, some of the constraints may be still unsatisfied. This feature is indeed undesirable for our minimization problem, and thus the method of interior penalty function was implemented to convert the constrained problem to an unconstrained one.

8.3.3 UNCONSTRAINED MINIMIZATION TECHNIQUE

For the minimization of the unconstrained problem the method of Conjugate Gradient was chosen, since only the first derivatives are necessary for this algorithm, and also it has been shown that this is a powerful technique and easy to incorporate in computer programs. The basic idea is minimization along conjugate directions. Two direction S^I and S^J are conjugate if

$$(S^I)\ H\ S^J = 0 \tag{8.29}$$

where **H** is the **Hessian Matrix** whose components are the second partial derivative matrix of the function Φ. Although we speak of the second derivatives here, however this is only to define conjugate directions and in the implemented algorithm the need for calculation of the Hessian matrix **H** will be bypassed. Conjugate directions are in fact the so called non-interfering directions. This means that the process of minimization along one variable is not spoiled by subsequent minimization along another variable (Press et. al., 1988). Next the conjugate directions will be chosen as the

one dimensional search directions along which every design variable x will be minimized. This is accomplished by specifying an initial search vector as the steepest descent direction defined by,

$$S^q = -\nabla\Phi(x^q) \tag{8.30}$$

On subsequent iterations the conjugate direction is defined as

$$S^q = -\nabla\Phi(x^q) + \lambda_q S^{q-1} \tag{8.31}$$

where the scalar λ_q is defined as,

$$\lambda_q = \frac{|\nabla\ \Phi(x^q)|^2}{|\nabla\ \Phi(x^{q-1})|^2} \tag{8.32}$$

One of the algorithms for the conjugate gradient method is called the Fletcher-Reeves approach, which was implemented for our minimization problem (Press et. al., 1988), a flow chart for this algorithm is given in figure 8.5.

A knowledge of the gradient vector of the objective function in the process of minimization is necessary, therefore we must obtain the elements of the gradient of the objective function with respect to the design variables x, or $\nabla\Phi(x)$; this requires a very lengthy process of differentiations. The final solutions for the elements of the gradient are given in the appendix, while the process of differentiations are skipped.

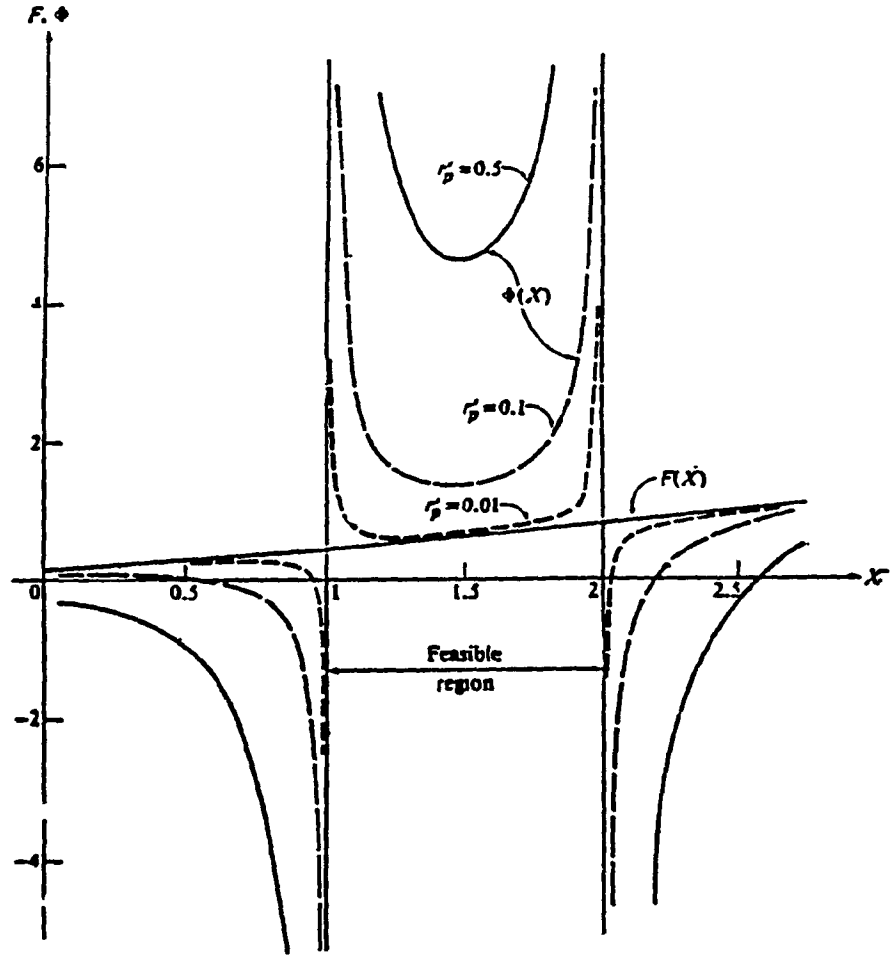

Figure 8.4 - Pseudo-Objective function in Interior penalty method

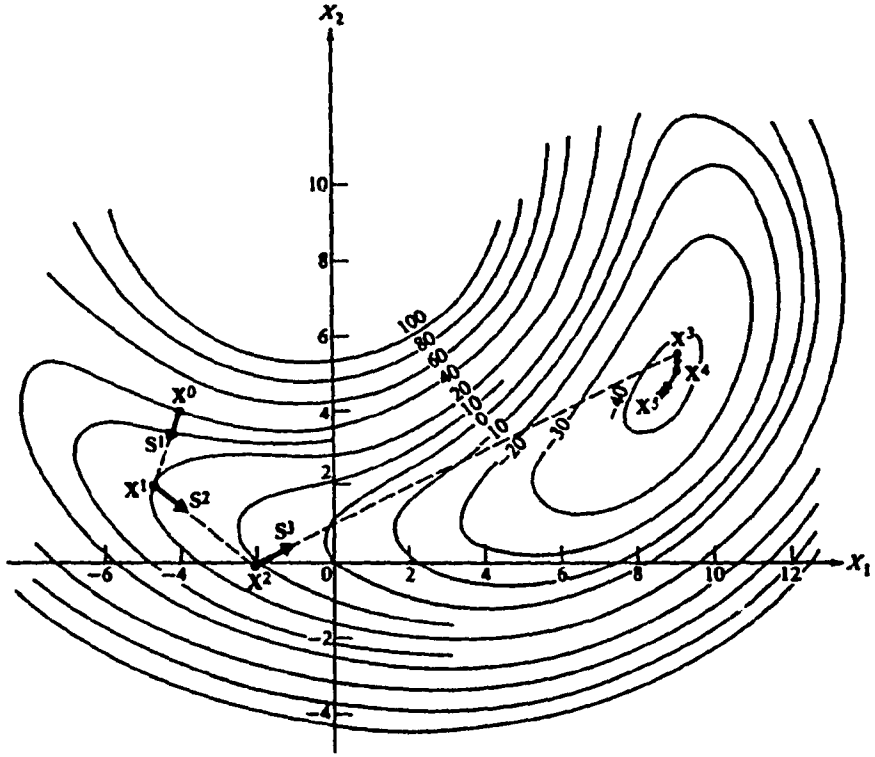

Figure 8.5 - Interpretation of the conjugate gradient method

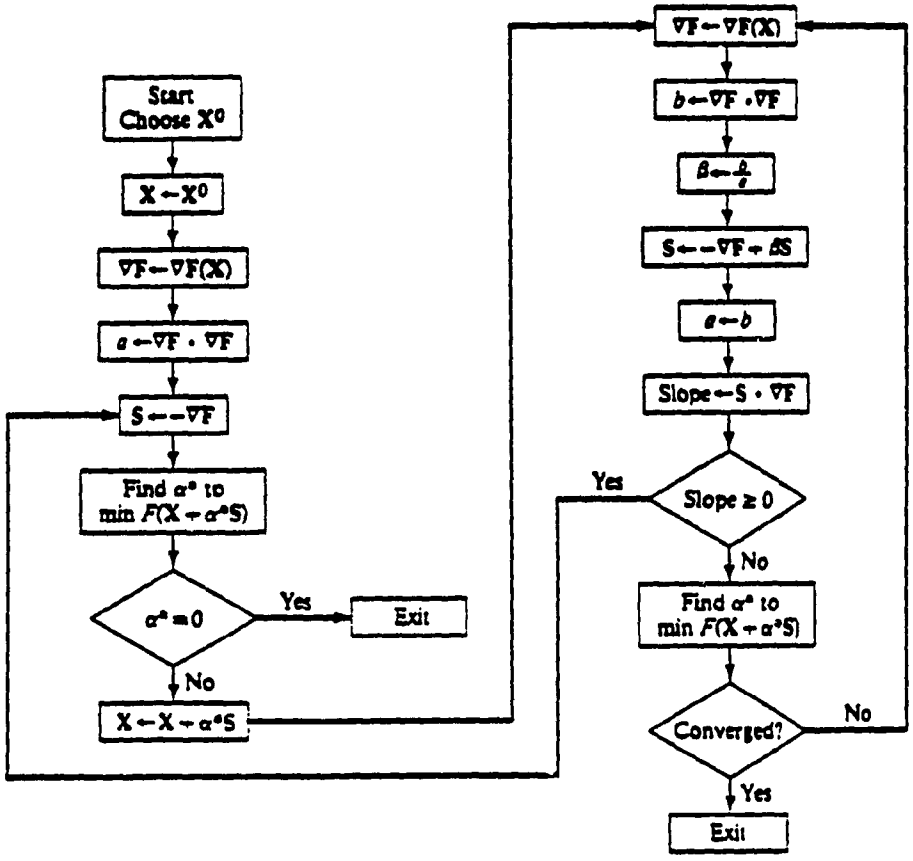

Figure 8.6 - Flowchart of the Fletcher-Reeves method

A major feature of the minimization problem at hand should be stated here, and that is, since the inverse kinematics are in the form of tangent inverse functions which are non-convex, therefore the objective function E will also be a non-convex function of x. Therefore we will not be able to determine any global minimum for the function, and thus depending on the choice of the starting point, we may locate different local minima on the boundary of the feasible region. Therefore a very important issue regarding this method is the choice of the starting points in minimization procedure. Because of the complexity of the kinematic formulations and task-dependent characteristics of the initial values, it is not possible to propose a generalized methodology for choosing the starting points for any given task. More elaboration on the initial values of x, y, z, and β is given in the following sections where numerical examples are presented.

A computer program called "SET_UP.C" was developed which implements the nonlinear constrained minimization problem, with Fletcher and Reeves method, while interior penalty function is used for the conversion of the constrained problem to an unconstrained problem. This program finds the optimum set-up of a robot manipulator with respect to the world coordinate frame, given an initial guess for the set-up vector of the arm. The flow chart corresponding to this program is given in the appendix c.

CHAPTER 9
APPLICATION CASE STUDIES

9.1 INTRODUCTION

In this chapter the methodology and formulations developed in the previous chapters will be applied to particular material handling operations. Primarily in section 2, we will illustrate two examples of the material handling with tightly coordinated two-arm robots, where the set-up of the workcell will be optimized by using the program SET_UP.C presented in chapter 8. In the first example the path to be followed is a straight line and in the second example a circular path will be used. Also in the second example effects of the weighting factors w_i of the joint variations which was defined in chapter 8, on the optimum solution will be observed. In section 8.3, we will present a case study in material handling operations in which only the distance between the two robots will be adjusted for handling of a family of beams whose lengths are variable.

9.2 OPTIMUM WORKCELL SET-UP

In what follows two examples regarding the set-up of a two-arm robotic workcell will be discussed. The program SET_UP.C discussed in chapter 8 is used for the optimization of the set-up of the workcell. The following notations will be used in these examples. Given m poses of the object (frame C_j) defined by $(T_W^C)_j$ the corresponding poses of the end effectors are denoted by $(T_W^M)_j$ and $(T_W^F)_j$. Grasp configurations of the end effector for the main and the follower arms are given by T_C^M and T_C^F respectively. Moreover, we

assign $\Gamma_m = [x_m \; y_m \; \beta]_m^T$ and $\Gamma_f = [x_f \; y_f \; \beta_f]^T$ to be the set-up vectors for the manipulators. It is assumed that the elevations of the two robots base frames are the same, thus z_m and z_f are not included in their corresponding vectors.

Furthermore Q^* defined in chapter eight is denoted by Θ_m^* for the main robot and by Θ_f^* for the follower arm. The numerical values of these two vectors are not necessarily equal. In fact these values will be used as means of controlling certain requirements for the workcell. For instance by a proper definition of these values, it will be shown that we can have control over the robots postures during the execution of the task (*e.g.* Shoulder/Elbow configurations). For the set-up of the workcell in the following examples specifications of two PUMA-560 manipulators will be employed.

9.2.1 EXAMPLE 1

It is required to set-up a coordinated two-arm robot with the following requirements.

The workpiece travels from an initial pose designated by C_1 on a straight line to the final pose of C_{10}, while keeping a constant orientation. Ten number of poses will be considered along the path and the C_1 and C_{10} are given as follows,

$$(T_w^c)_1 = \begin{bmatrix} 0.7071 & 0.0 & 0.7071 & 1050.0 \\ 0.0 & 1.0 & 0.0 & 650.0 \\ -0.7071 & 0.0 & 0.7071 & -100.0 \\ 0.0 & 0.0 & 0.0 & 1.0 \end{bmatrix} \quad (9.1)$$

$$(T_w^c)_{10} = \begin{bmatrix} 0.7071 & 0.0 & 0.7071 & 750.0 \\ 0.0 & 1.0 & 0.0 & 400.0 \\ -0.7071 & 0.0 & 0.7071 & -100.0 \\ 0.0 & 0.0 & 0.0 & 1.0 \end{bmatrix} \quad (9.2)$$

Moreover, the grasping configuration for the main and the follower are defined as

$$T_c^M = \begin{bmatrix} 0.0 & 0.0 & 1.0 & -60.0 \\ 1.0 & 0.0 & 0.0 & -15.0 \\ 0.0 & 1.0 & 0.0 & -20.0 \\ 0.0 & 0.0 & 0.0 & 1.0 \end{bmatrix} \quad (9.3)$$

and

$$T_c^F = \begin{bmatrix} 0.0 & 0.0 & 1.0 & 60.0 \\ 1.0 & 0.0 & 0.0 & 15.0 \\ 0.0 & -1.0 & 0.0 & 20.0 \\ 0.0 & 0.0 & 0.0 & 1.0 \end{bmatrix} \quad (9.4)$$

Also, it is required that both robots perform the task in Left-Shoulder Elbow-Up configurations, and in order to avoid collision between the robots it is important to install the robots on two opposite sides of the path. Thus to fulfill the foregoing requirements, the following values are chosen for Θ_m^* and Θ_f^*,

$$\Theta_m^* = \Theta_f^* = [10 \quad -22.5 \quad 155 \quad 30 \quad 10 \quad 10]^T \quad (9.5)$$

The starting values of the Γ_{om} and Γ_{of} are calculated in such a way that the base of the robots are located on the normal bisector of the line C_1C_{10} passing through C_5, with distance ρ_o on both sides, where the value of ρ_o is

defined as

$$\rho_o = \frac{R_{max} + R_{min}}{2} \tag{9.6}$$

and the calculated initial values of Γ_m and Γ_f are, $\Gamma_{om} = [481.1 \quad 978.6 \quad -45^\circ]^T$ and $\Gamma_{of} = [1347 \quad 71.3 \quad 135^\circ]^T$.

Results of this example are shown in figures 9.1 to 9.3, where the optimum set-up of the workcell shown in a top view is given in figure 9.1 and the joint variations throughout the trajectory are given in figures 9.2 and 9.3 for main and follower arms respectively. In these plots upper and lower limits of every joint as well as the guideline values of each joint θ_i^* are also given. The final optimum solution for the set-up vectors of the robots are

$$x_m = 355 \text{ mm}, \quad y_m = 360 \text{ mm} \quad \text{and} \quad \beta_m = -148^\circ \tag{9.7}$$

$$x_f = 1185 \text{ mm}, \quad y_f = -167 \text{ mm} \quad \text{and} \quad \beta_f = 100^\circ \tag{9.8}$$

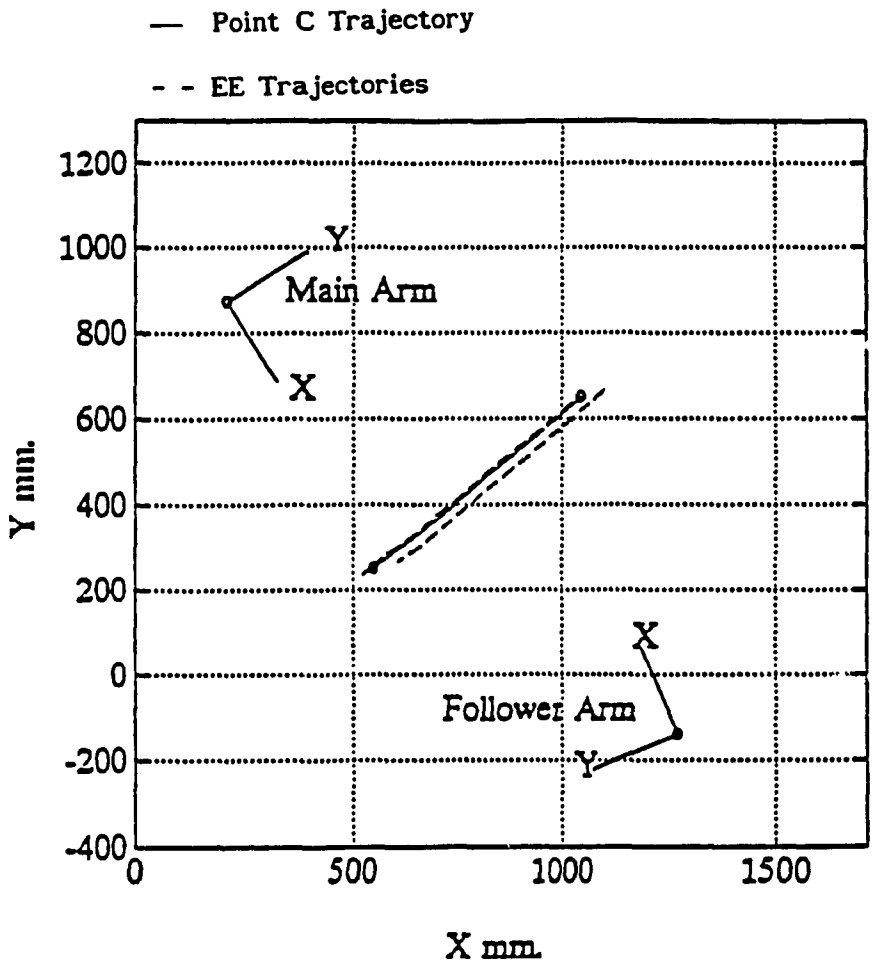

Figure 9.1 - Optimum set-up (Example 1)

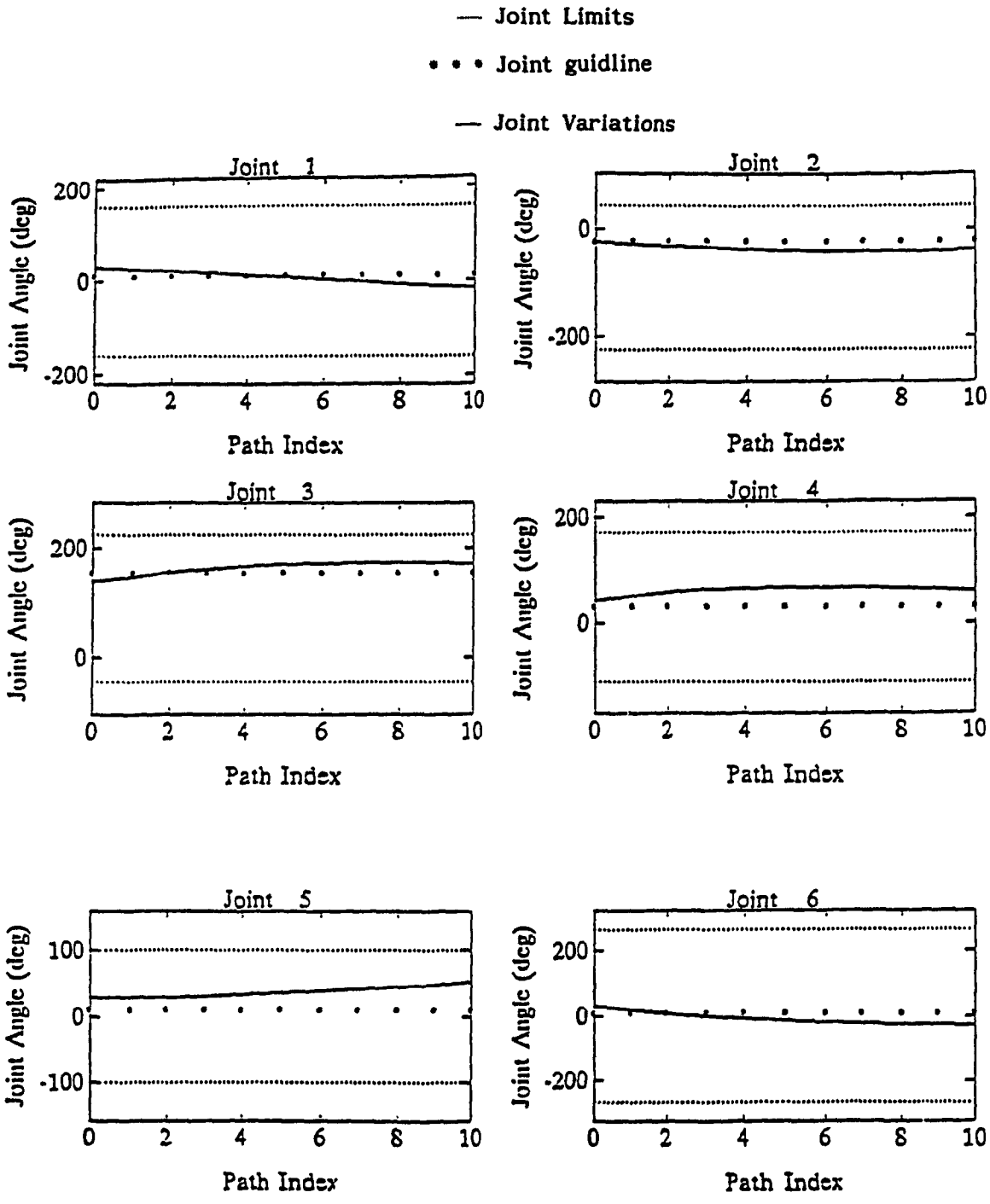

Figure 9.2 - Joint history for main arm (Example 1)

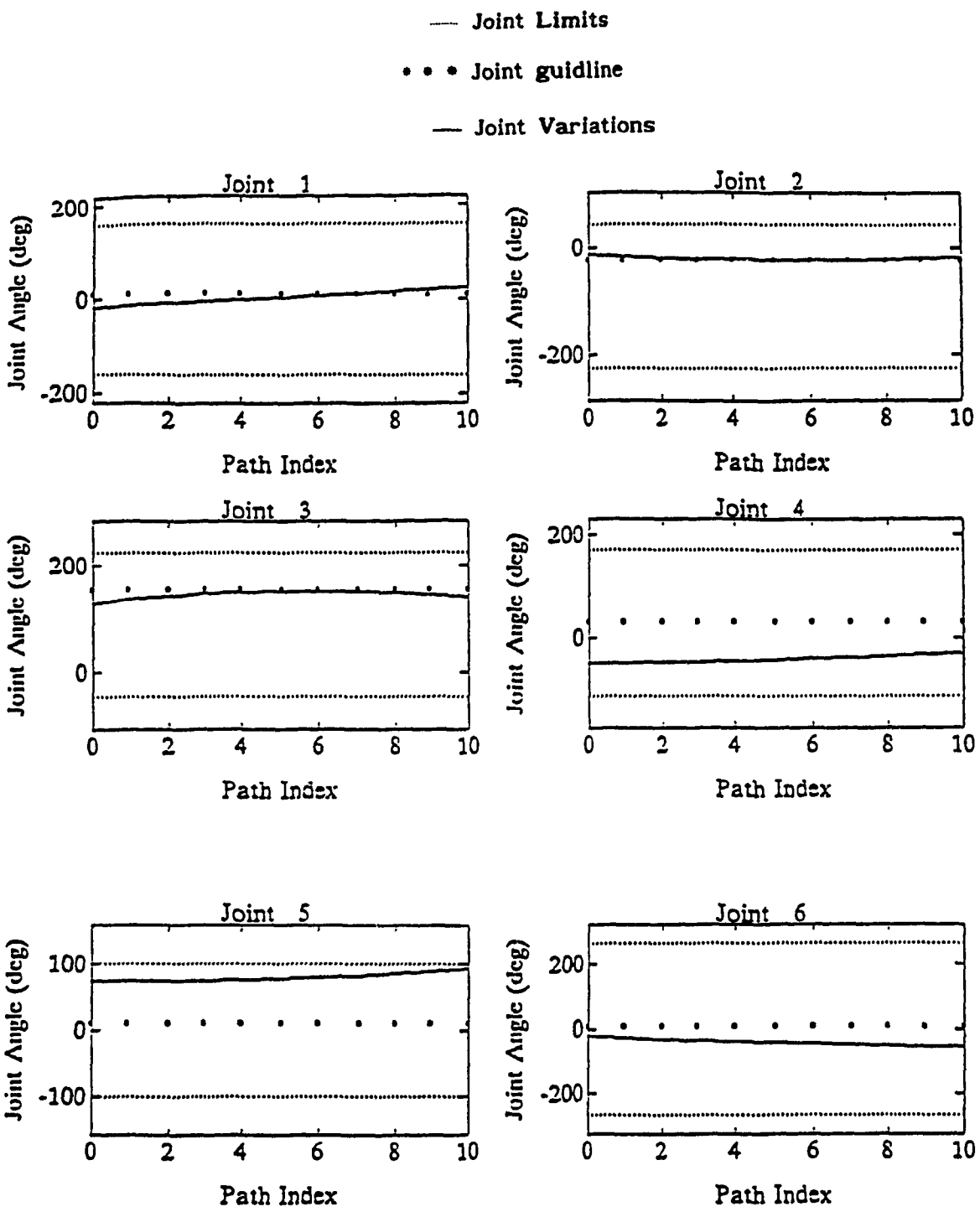

Figure 9.3 - Joint history for follower arm (Example 1)

9.2.2 EXAMPLE 2

In the second example, the path followed by C from C_1 to C_{10} is an arc of a circle with a radius of 900mm, while orientation of the object should change uniformly from the orientation of C_1 to that of C_{10}, where

$$(T_W^C)_1 = \begin{bmatrix} 1.0 & 0.0 & 0.0 & 500.0 \\ 0.0 & 1.0 & 0.0 & 500.0 \\ 0.0 & 0.0 & 1.0 & -100.0 \\ 0.0 & 0.0 & 0.0 & 1.0 \end{bmatrix} \tag{9.9}$$

$$(T_W^C)_{10} = \begin{bmatrix} 1.0 & 0.0 & 0.0 & 50.0 \\ 0.0 & 0.0 & 1.0 & 850.0 \\ 0.0 & -1.0 & 0.0 & -300.0 \\ 0.0 & 0.0 & 0.0 & 1.0 \end{bmatrix} \tag{9.10}$$

this is in fact a rotation of -90 degrees about the x axis of the C_1 frame.

We further assume that the grasp configurations are those given for example 1, but here we require that the main robot arm performs the task in a Left-Shoulder Elbow-Up configuration while the follower arm maintains a Right-Shoulder Elbow-Up arrangement. In order to satisfy these conditions, the following values of θ_m^* and θ_f^* are chosen,

$$\theta_m^* = [10 \quad -22.5 \quad 155 \quad 30 \quad 10 \quad 10]^T \tag{9.11}$$

$$\theta_f^* = [10 \quad -157 \quad 25 \quad 30 \quad 10 \quad 10]^T \tag{9.12}$$

and with the given information initial values of the set-up vectors for the main and the follower manipulators were determined as,

$\Gamma_{om} = [609.9 \quad 1143.8 \quad -45^\circ]^T$ and $\Gamma_{of} = [-41 \quad 213 \quad 135^\circ]^T$.

Primarily in this example, weighting factors of unity were assigned to each joint, and the following results were obtained,

$$x_m = 351 \text{ mm} \quad y_m = 1249 \text{ mm} \quad \beta_m = -116^0 \tag{9.13}$$

and

$$x_f = -334 \text{ mm} \quad y_f = 518 \text{ mm} \quad \beta_f = 210^0 \tag{9.14}$$

By using these results for this set-up of the robots, variation of the joint angles for the arms moving from initial to final positions were determined. from the inverse kinematics solutions It was observed that for this example the constraint on joint 5 of the main robot is being violated (Figure 9.4).

In order to overcome this problem a new set of weighting factors were assigned to the main robot as,

$$w_m = [1 \quad 1 \quad 1 \quad 1 \quad 1.5 \quad 1] \tag{9.15}$$

new results for Γ_m, using the aforementioned w_m are obtained as,

$$x_m = 89 \text{ mm} \quad y_m = 1264 \text{ mm} \quad \text{and } \beta_m = -103^0 \tag{9.16}$$

The final set-up of the system is shown in figure 9.5, and the simulation results for the joint variations of the main and the follower are given in figures 9.6 and 9.7, respectively.

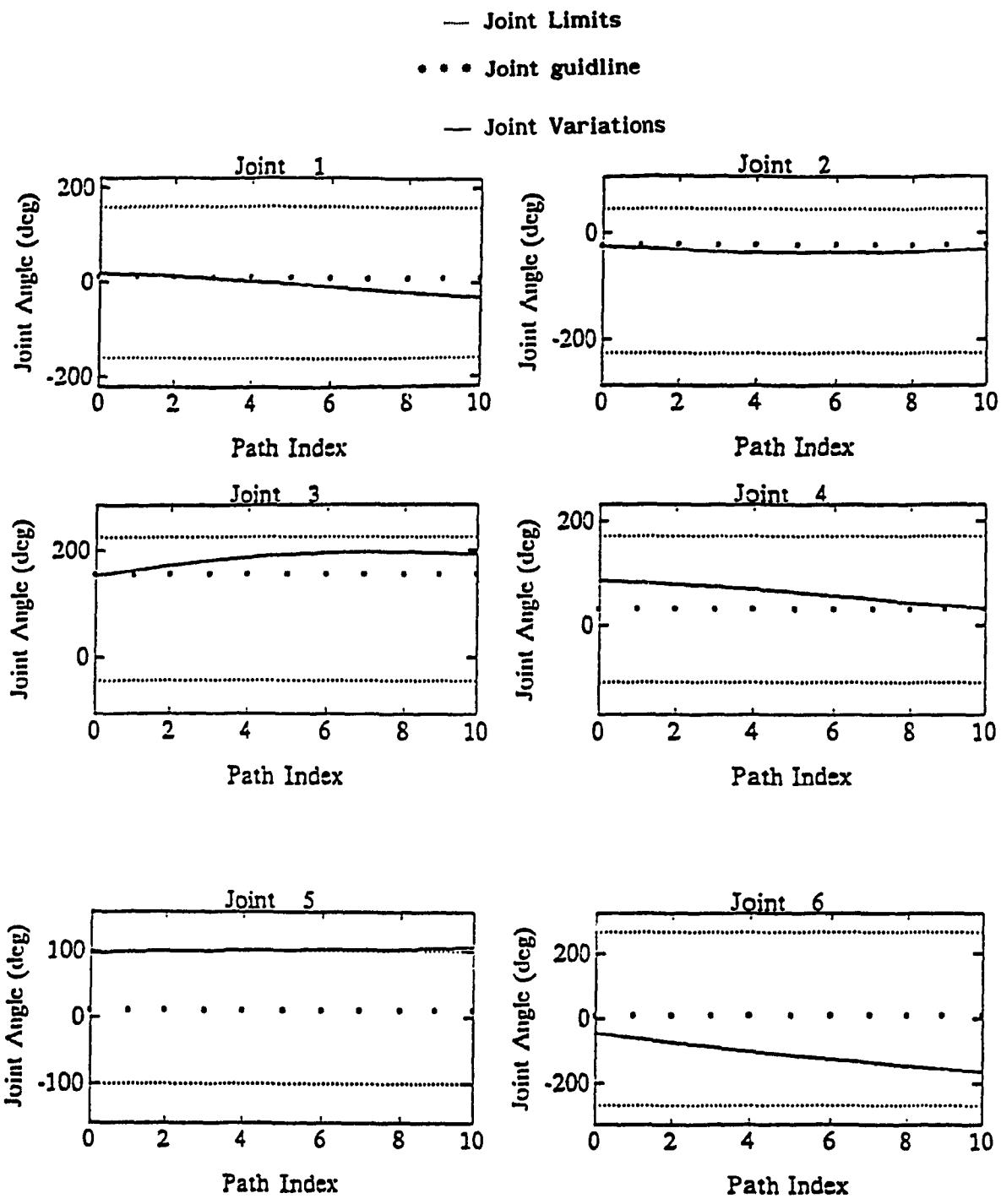

Figure 9.4 - Joint history for main arm (Equal Weighting Factors)

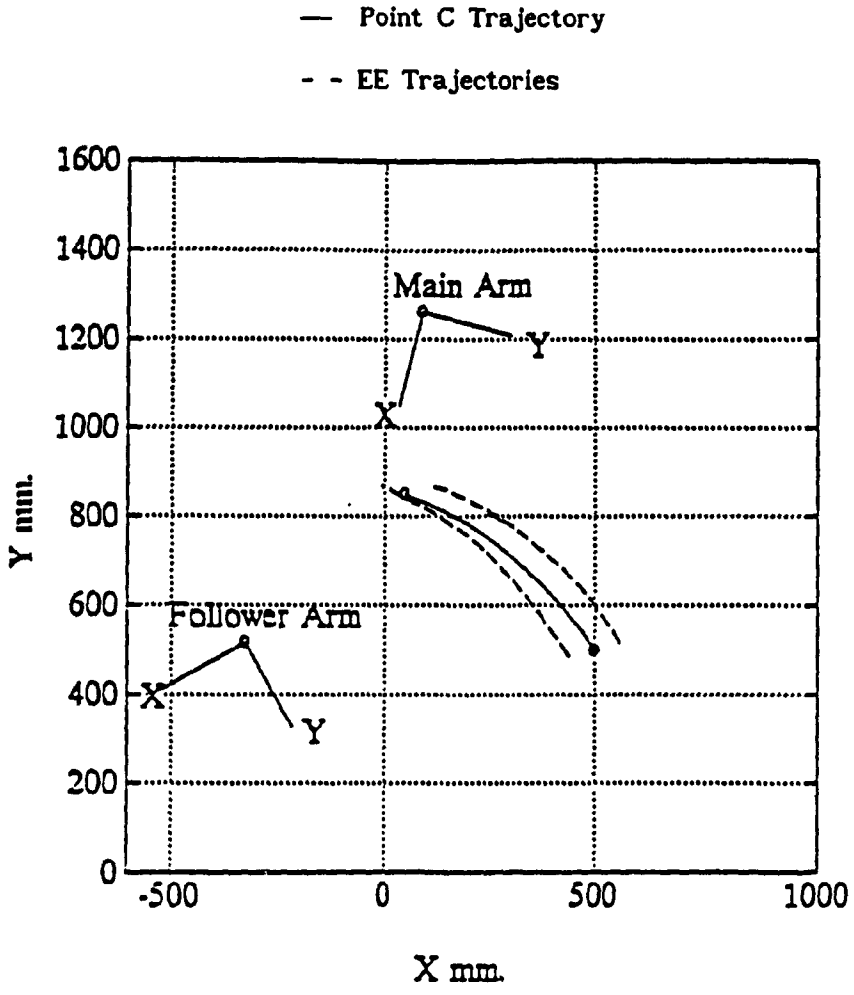

Figure 9.5 - Optimum set-up (Example 2)

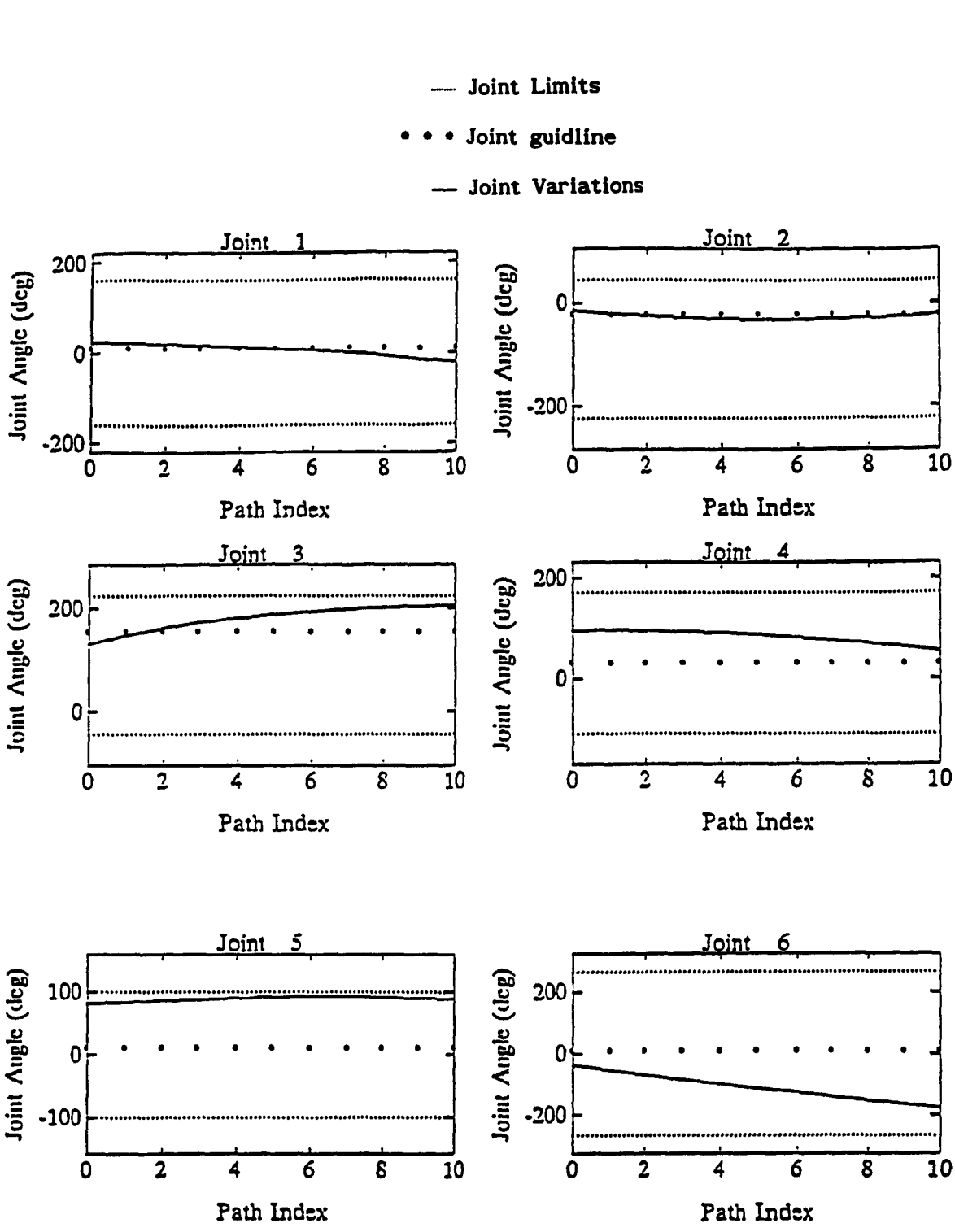

Figure 9.6 - Joint history for main arm (Unequal Weighting Factors)

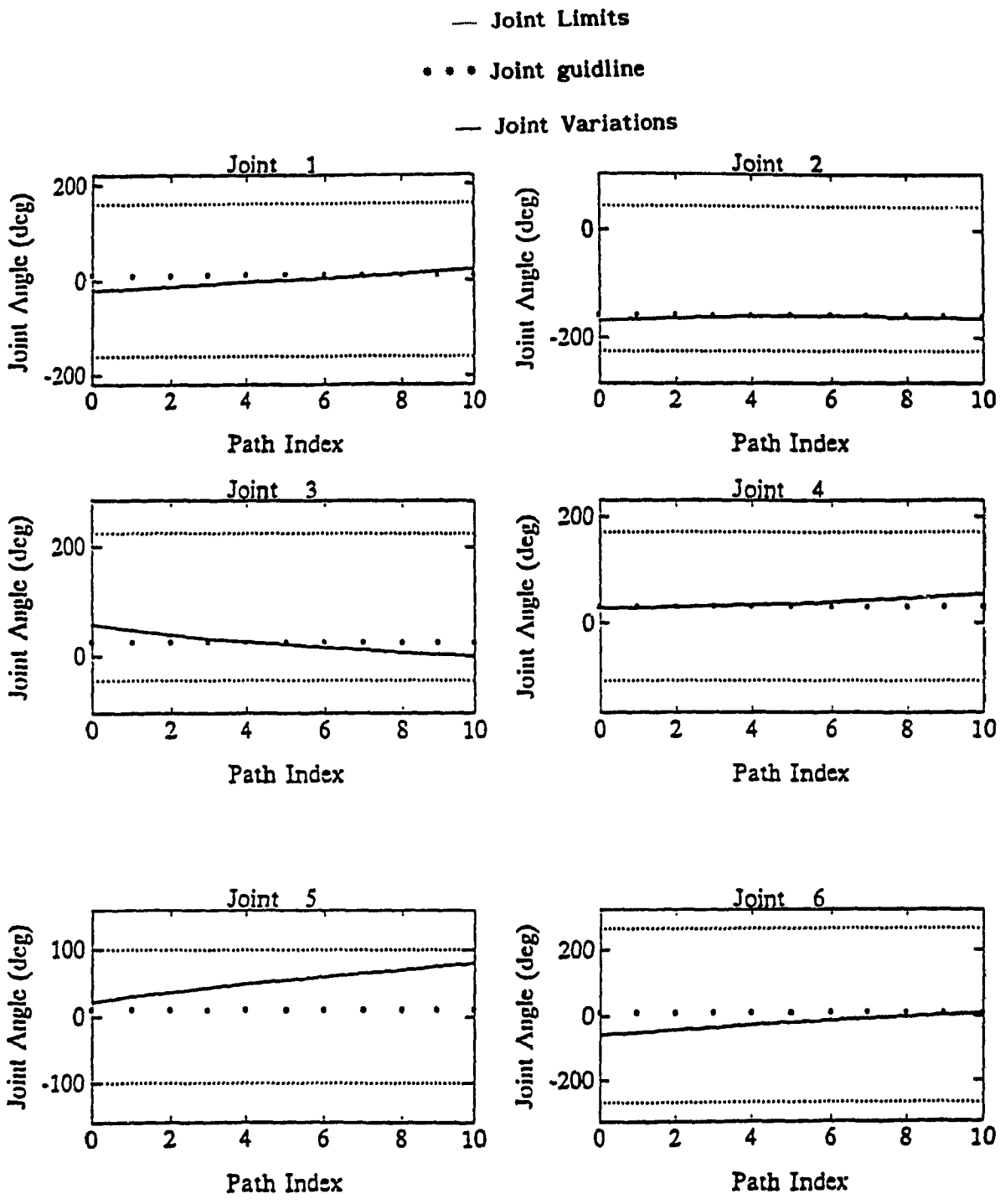

Figure 9.7 - Joint history for follower arm

9.3 A CASE STUDY OF TWO-ROBOT-ARM BEAM LOADING IIWORKCELL

A particular case of a material handling problem with two collaborating robot arms in loading/unloading of long objects from a conveyor is studied. In this case study the only design parameter is the distance between the bases of the two arms and arms are assumed to have their axes parallel to each other. The feasibility of the task from a kinematics point of view, and the necessary conditions and constraints for the relative set-up of the two manipulators are discussed. Also, it can be seen that changing the distance between the two arms may be considered as changing the length of the workpiece when handled with two fixed arms.

9.3.1 PROBLEM DEFINITION

The main purpose of this case study is to investigate the required set-up and the feasibility of a specific material handling task to be performed by a coordinated two-arm robot system. This particular task is a conveyor loading/unloading operation; two robot arms both mounted on one side of a conveyor pick up a long beam and carry it to the other side in a tightly coordinated fashion. Kinematics require that each of the two arms always remains in its working envelope. Furthermore, it is more economical if this operation can be carried out for beams with different lengths without readjusting the distance between the two arms. Two features, concerning the set-up and operation of this workcell will be investigated which are outlined as follows:

a) Given the maximum and minimum lengths of the beams , determine the

feasibility of the material handling task and (if feasible) the required distance between the two arms bases.

b) Having specified the distance between the bases of a pair of arms for a set of predefined initial and final positions/orientations of the workpiece for a given task, what will be the range of the beam lengths that meet the reachability requirements of both arms throughout the task.

The structure, notations and terminologies which will be utilized for this example as well as the formulations for solving the inverse kinematics of the tightly coordinated two-arm robots are those discussed in chapter 6. Moreover, for the workspace determination of the system algorithms presented in chapter 5, are used. Specifications of two PUMA-560 robot arms are used.

9.3.2 TWO-ARM CONVEYOR LOADING/UNLOADING PROBLEM

A common material handling problem in manufacturing is loading and unloading a conveyor (figure 9.8). The feasibility of this task as far as the kinematics of motion are concerned is studied in this section. This leads to the necessary conditions for the arrangement of the two arms. Both arms are on one side of the conveyor. Kinematically, it is necessary that the object be reachable by the two arms when on the conveyor, and remain reachable by them during the course of displacement.

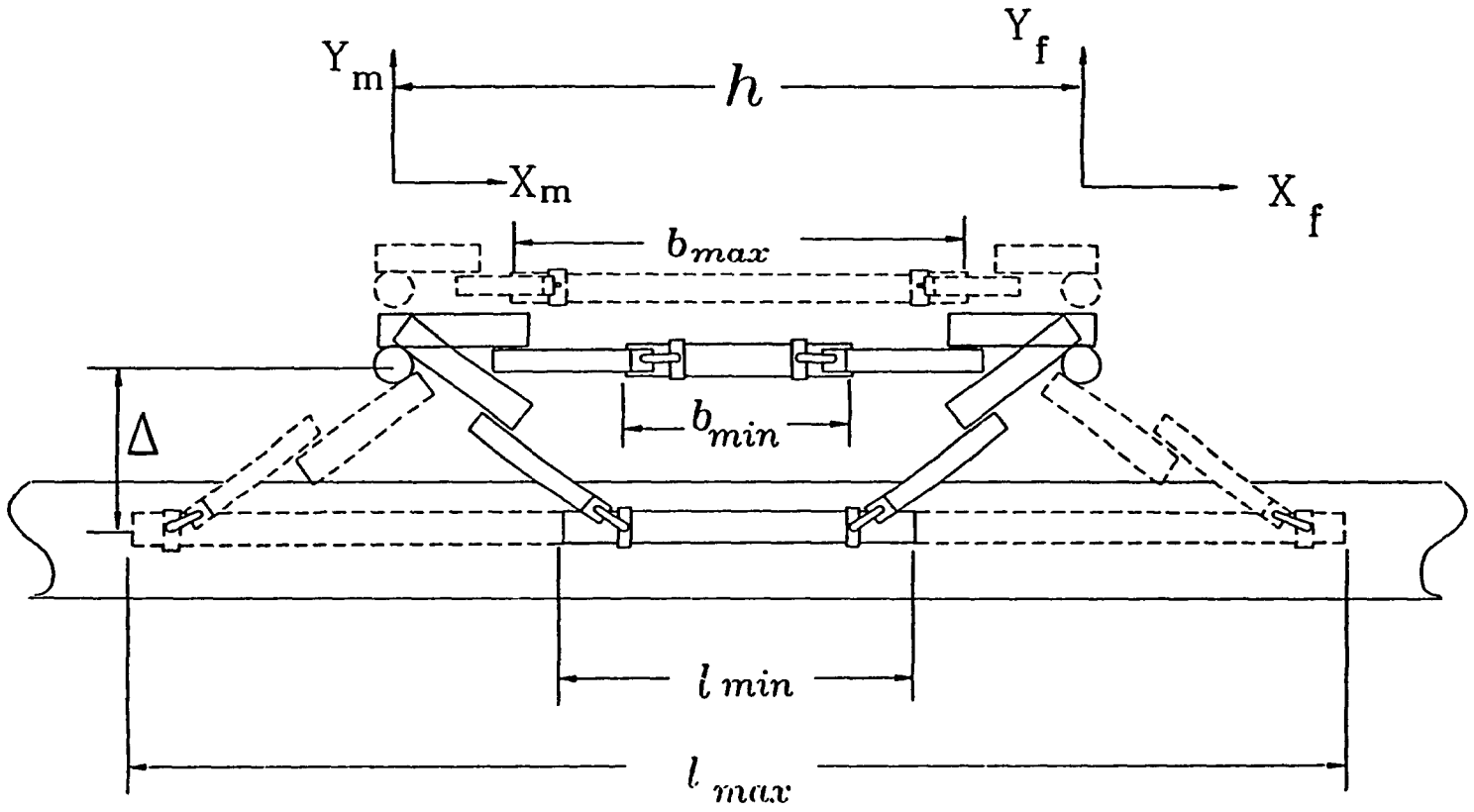

Figure 9.8 - Beam loading/unloading from a conveyor

The workpiece coordinate frame (frame C) origin is at its geometric center, or mass center. The base coordinate frame of the follower is at a distance h from that of the main arm (Fig.9.8). In this sense the transformation matrix of the follower base coordinate frame relative to the main arm base is given by

$$T_m^f = \begin{bmatrix} & & h \\ & I & 0 \\ & & 0 \\ 0 & 0 & 0 & 1 \end{bmatrix} \tag{9.17}$$

h can be considered as a parameter that may be adjusted for various tasks and for various objects. In other words, if the follower arm can travel along a rail, it can be fixed at a desirable distance h, depending on the geometry of the object to be handled.

For the case under study it is assumed that the conveyor is horizontal and parallel to the x-axes of the two arms ,and the object is symmetric about its mass centre and is parallel to the x-axes, when on the conveyor. It is also assumed that the object is lifted from above, that is, the approach vector of both end effectors are vertical. More specifically, the orientation matrix of the end-effectors are

$$R_m^M = R_f^F = \begin{bmatrix} 0 & 1 & 0 \\ 1 & 0 & 0 \\ 0 & 0 & -1 \end{bmatrix} \tag{9.18}$$

In what follows l is the effective length of the object, which is the distance between the tool points of the two end-effectors, since a long object is not necessarily held at both ends; instead it can be held at two other points.

With a constant h and a given orientation a number of parameters as discussed below can be defined for the material handing problem under study as illustrated in Figure 9.8:

1) l_{max} is the maximum length of an object reachable with the given orientation at a distance Δ from the xz-plane (representing the conveyor distance from the two arms) and at a level Γ (representing the height of the conveyor)
2) l_{min} is the minimum length reachable for the same orientation, Δ and Γ.
3) b_{max} is the maximum opening between the two arms end-effectors with a given orientation at $\Delta = 0$. This indicates the absolute maximum distance between the two end-effector tool points (b_{max} corresponds to completely folded configuration of the arms).
4) b_{min} is the minimum opening associated with b_{max} (b_{min} corresponds to fully extended configuration of arms which the desired orientation is achieved). b_{min} is of little practical interest, since the maneuverability of any object having a length b_{min} is almost zero, because the two arms are fully stretched towards each other.

If h changes to h + Δh then all the associated object length values change accordingly, that is

$$
\begin{aligned}
l_{min} &\longrightarrow l_{min} + \Delta h \\
b_{min} &\longrightarrow b_{min} + \Delta h \\
l_{max} &\longrightarrow l_{max} + \Delta h \\
b_{max} &\longrightarrow b_{max} + \Delta h
\end{aligned}
\tag{9.19}
$$

We note that the workpiece may be carried in any of the three following fashions, if possible:

a) The workpiece may be lifted from conveyor and without a change in orientation be translated in a symmetrical way to the other side of the arms where it is unloaded.

b) The workpiece may be rotated after being lifted so that it can pass through the arms by directing one end first and then reoriented before it is placed on the unloading platform.

c) The workpiece may be carried to the unloading platform overhead the two arms. In this way, during the transportation it will be rotated by 360 degrees about its longitudinal axis.

In (a) the length of the object cannot be more than b_{max}, thus, although a workpiece with length l_{max} can be reached by the two arms it cannot be transported in this fashion. (b) offers more flexibility as long as the length of the workpiece is concerned, in the sense that it allows objects longer than b_{max} to be carried. On the other hand it is more difficult to tackle because of the care for collision between the arm and the extension length from the grasp point at each end of the workpiece. Moreover, how much rotation is required and the whole maneuver must be studied for feasibility. For longer objects that we may not carry out the motion as in (a) and (b) we

may be able to use (c). Theoretically the length of the workpiece does not cause any restriction for this type of motion.

In this work only the (a)-type motion is studied; the other two require further research. For this type of motion as it is understood from the above discussion it is necessary that l_{min} < length < b_{max} . Moreover, it is assumed that a workpiece is held symmetrically, and it is moved in a symmetrical fashion with respect to the two arms. In this case the working envelope for the two end-effectors will be similar.

For a fixed h and known Δ, Γ and orientation of each end-effector, the working envelope of the two-arm workcell depends on the length of the workpiece. However, because of the assumption for symmetry, the effect of the length may be regarded as a change in the x-coordinate for the position of each end-effector. As a result, the problem of finding the working envelope for various lengths (of the workpiece) reduces to finding the two dimensional contours on some planes perpendicular to the x-axis and at different distances from the base of each robot arm.

Figure 9.9 indicates one of the contours (including two voids) for the main arm (PUMA 560). The corresponding relationship between l, the workpiece length, and x_0, for which the contour is determined, is

$$l = h - 2x_0 \tag{9.20}$$

From this contour it also may be found that for a conveyor at the same level as the arm bases, that is for $\Gamma = 0$, the maximum value for Δ is 0.8 m

(point C). Furthermore, supposing that the workpiece is picked up at point C_1, for which $\Delta = -0.75$ and $\Gamma = 0$, and it must be unloaded at a distance $\Delta' = 0.5^m$ on a platform which is 0.2^m lower than the conveyor (point C_2). This task is feasible, however, the paths for the two end-effectors (and, therefore, the workpiece centre) cannot be a straight line because of the void; a deviation from straight line becomes necessary to bypass the voids; preferably the workpiece must first be raised by, say, 0.1 *m* and then lowered after being taken to the other side.

Figure 9.10 shows a number of graphs which correspond to part of the workspace that is free of voids. These graphs represent the contours of the workspace of a PUMA 560 with the same orientation as in equation 9.18 when cut by various planes perpendicular to the x-axis. Equivalently it represents the relationship between maximum Δ and maximum Γ for objects of different lengths that can be handled with a pair of PUMA arms installed as in figure 9.8 with a constant h. Nevertheless, if h changes, that change will be reflected in each length according to relations 9.19. For the sake of clarity, a nominal value of 2.46^m is assigned to h and the associated length values are shown.

The two problems that have been addressed earlier in section 9.3.1 may now be investigated by using figure 9.10. Supposing that $h = 2.46\ ^m$, then b_{max} can be found to be $b_{max} = 2.06\ ^m$. Point A corresponds to a workpiece at a height $\Gamma = 0.2\ ^m$ and on the conveyor at $\Delta = -0.6\ ^m$. A is inside the working envelope for all the curves containing A (with the orientation in Eq. 9.18). Thus, according to the contours shown, the shortest workpiece capable of being handled is 1.22 meters long and the longest is $1.5\ ^m$ long. Since

$1.5 < b_{max}$, then $1.22 < l < 1.5$ represents the range of the beam lengths that may be carried by the two arms when installed 2.46 ^{m} from each other.

Moreover, if the distance must be set for carrying beams of length between 1.4 ^{m} and 1.8 ^{m} where they must be picked up at $\Gamma = 0$ and $\Delta = -0.5$ ^{m} corresponding to point B, and be unloaded at $\Gamma = -0.2$ ^{m} and $\Delta = 0.4$ ^{m} corresponding to point C, then it can be seen from figure 11 that the nearest contour containing both B and C corresponds to $l = 1.06$ ^{m}. If the difference $1.4 - 1.06 = 0.34$ ^{m} is taken as Δh and is added to the nominal distance of 2.46 ^{m}, then

$$h = 2.46 + 0.34 = 2.80 \text{ m}$$

For this h the longest beam is of length $1.5 + 0.34 = 1.84$ ^{m} (according to the given contours); since $1.84 > 1.8$, it is possible to carry beams between 1.4 ^{m} and 1.8 ^{m} with the associated Γ and Δ if the two arms are 2.8 ^{m} apart.

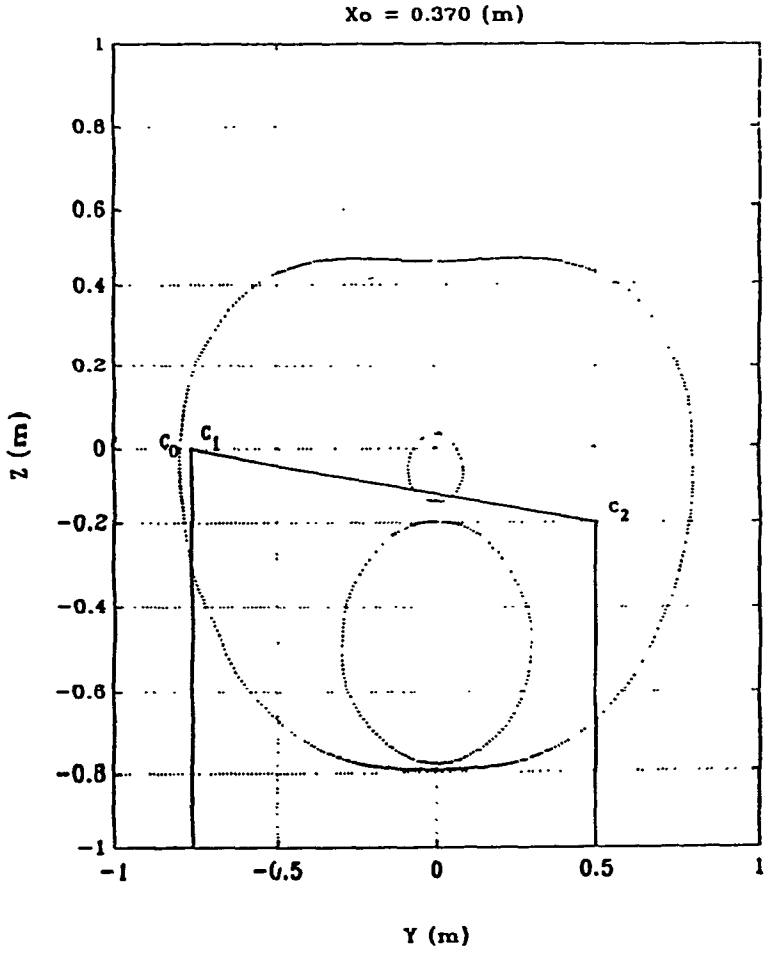

Figure 9.9 - Voids in Workspace on YZ plane

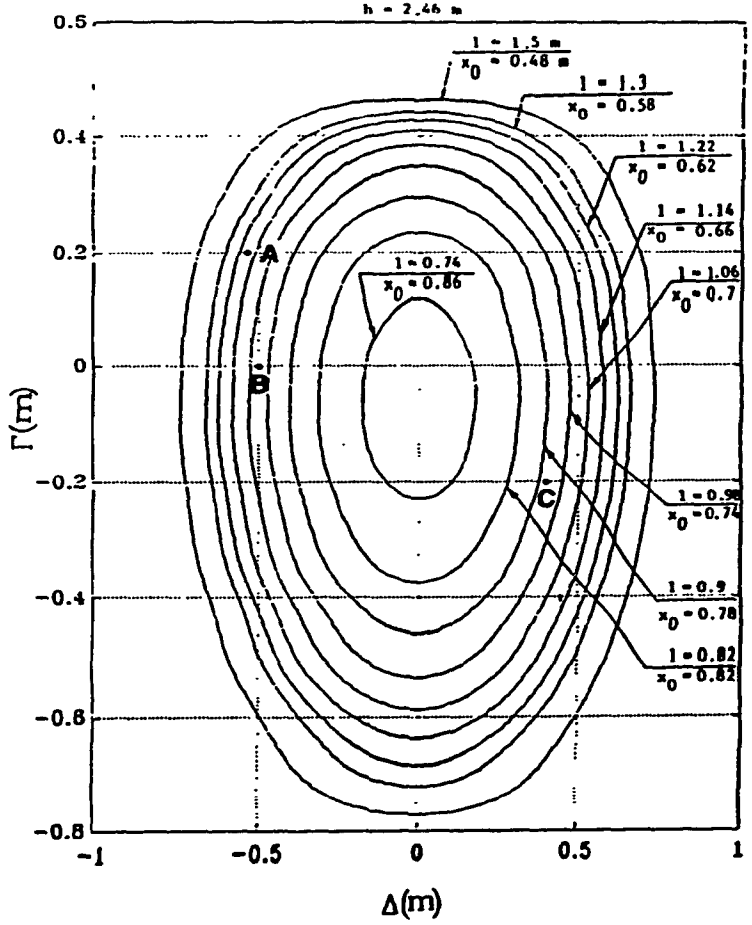

Figure 9.10 - Variation of Workspace in terms of spacing between EE

CHAPTER 10
CONCLUSION

10.1 SUMMARY

In this section a summary of the objectives and contributions of this thesis will be given. The main body of the thesis can be divided into three major parts with corresponding objectives and achievements as follows:

- In the first segment (Chapters 1 and 2), the following issues were discussed:

– A general introduction was provided with brief definitions of the concepts to appear in the remainder of the thesis. Moreover, the structure and objectives of this work were established (Chapter 1).

– A literature survey was conducted in chapter 2, to focus on the following issues:

1- General Robot kinematics, with emphasis on the homogeneous point coordinated transformation techniques, and the line coordinated transformations using screw coordinates.

2- The studies related to the working envelope or workspaces associated with robotic systems. This included a survey of the research papers dealing with definitions, formulations and discussions regarding the manipulator's workspaces and their characteristics in relation to the performance and feasibility of robotics operations.

3- Research work related to the problem of cooperative two or multi-manipulator systems. Dynamics and control of these systems were

the main focus of these research activities. However, for the scope of this thesis, only those papers which included an investigation of the general kinematics, and workspaces associated with two or multi-manipulator systems have been referred to.

- The second segment of the thesis (Chapters 3 and 4) was devoted to general kinematic concepts and relations for mechanical manipulators. One popular approach of the analysis, namely homogeneous point coordinate transformations and Denavit and Hartenberg notations, were investigated (Chapter 3). Chapter 4 develops the kinematic formulation for a specific industrial robot, namely PUMA-560. This was utilized for illustrative purposes through the remainder of the thesis.

- The third part of the thesis (Chapters 5 to 9) is the direct contribution of the research activities performed in this work as follows:

Chapter 5:

- Algorithms for contour detection of two-dimensional working envelopes in both Cartesian and Polar coordinates for single robot manipulators;
- A CAD-based methodology for the graphical three-dimensional representation of the workspaces of mechanical manipulators.
- Investigation of a measure of manipulability which were proposed in the literature.

Chapter 6:

- Examination of cooperative multi-manipulator systems with particular attention to coordinated two-arm robots, and the concept of tight and

loose coordinations.

- Analysis of kinematics and constraint relations as well as a general mobility criteria for tightly coordinated two-arm robotic systems.

Chapter 7:

- The concept of **Triplet Workspace** was proposed following a study of the workspace associated with tightly coordinated two-arm robots. Numerical examples were provided to show the usefulness of triplet workspace in the design of coordinated two-arm robots in material handling.
- Effects of the relative set-up of the two manipulators on the triplet workspace were also demonstrated.

Chapter 8:

- To meet a defined performance criteria (specifically maximum joint availability/better accessibility) for a given task, the problem of optimization of the workcell or the lay-out of the set-up for tightly coordinated two-arm robotics workcell was performed.

Chapter 9:

- the optimization method of Chapter 8 was used to obtain a solution for the workcell set-up in material handling, for two specific tasks; (a) the path is a straight line and the orientation of the object must remain unchanged. (b) the path is an arc of a circle and the orientation of the object changes.

- A case study was provided for loading/unloading of long beams of different lengths from a conveyor. The only design parameter was the distance between the two coordinated robots. Feasibility of the operation was discussed using the workspace knowledge gained in chapter 5, thus avoiding the nonlinear optimization method of chapter 8.

10.2 RECOMMENDATION FOR FURTHER RESEARCH

In this section further development of the main objectives of this work will be discussed. Recommendations will be given for enhancement of those aspects of the work which have not been fully explored. It was mentioned in the previous section that the first two segments of the thesis comprised an introduction and preparation of a general knowledge to be used in the last segment. Hence our recommendations regarding further research focus on the contents of the last segment (Chapters 6 to 9). These recommendations originate from certain restrictions imposed to simplify our approach. They are outlined as follows:

- In Chapter 6 the classification of the coordinated two-arm robotic tasks was discussed. Most of the time, the desired task will allow some flexibilities either on the position of the end effector or on its orientation. There are many practical examples where the orientation of the manipulated object is not restricted or only partially restricted. One example is the manipulation of a container filled with liquid where it may be

allowed to rotate in one way but prohibited from rotating in another. In the case of assembly operation, the position/orientation of the object for the via points of the trajectory are not rigidly specified. This flexibility may be used to improve other operational performance criteria. Therefore further research should be conducted to determine if an unaccessible point can be reached by changing the orientation of the workpiece, and if so, what axis and angle of rotation would be needed. On the other hand, when the position of the object defined on the trajectory is admissible and the orientation is not, it should be determined if by translating the object to any other neighboring point the desired orientation could be achieved.

- In Chapter 7, the concept of triplet workspace was proposed for tightly coordinated two-arm robots with constant orientation. The developed algorithms locate the contour of the triplet workspace on a cutting plane for a given and fixed orientation of the object. However, the boundary obtained will be a conservative estimate of all the accessible points on that plane. However by changing the orientation of the workpiece keeping one of its points (the reference point C) on the cutting plane, more distant points may be reached, thus expanding the workspace boundary. Therefore, further research may be conducted to investigate the effects of the object's orientation on the triplet workspace. This should result in a concept similar to that of dextrous workspace of single manipulators. For the cases where the orientation of the workpiece is partially restricted further development is also recommended to determine the workspace of the triplet for those orientations allowed.

- The triplet workspace of Chapter 7 was developed for two coordinated robot arms in material handling and their mutual impact on the shape of the workspace was shown. This concept should be further expanded to apply to coordinated multi-manipulator systems in material handling. Obviously the restrictions imposed on the workspace will be magnified by introducing each additional coordinated robot.

In conclusion, although some aspects of the workspace associated with coordinated two-arm robotic systems have been demonstrated in this thesis, much work remains to further develop and enhance the capabilities of the workspace analysis and synthesis of coordinated multi-manipulator systems.

REFERENCES

(1955) Denavit, J., and Hartenberg, R.S., "A Kinematic Notation For Lower-Pair Mechanisms Based on Matrices", ASME Journal of Applied Mechanics, June 1955, pp. 215-221.

(1964) Hartenberg, R.S., and Denavit, J., "Kinematic Synthesis of linkages", McGraw Hill, NY.

(1964) Yang, A.T., and Freudenstein, F., "Application of Dual-Number Quaternion Algebra to the Analysis of Spatial Mechanisms", ASME Journal of Applied Mechanics, June 1964, pp.300-308.

(1966) Guertz, R.C., Grimson, J., Potts, C., Minqesz, D., and Foster, G., "ANL Mark E4A Electric Master-Slave Manipulator", Proc. 14th Conference on Remote System Technology, 1966.

(1968) Fiacco, A.V., and McCormick, G.P., Nonlinear Programming: Sequential Unconstrained Minimization Techniques, John Wiley and Sons, Inc., pp. 39-59.

(1974) Gavrilovic M.M., Selic, B.V., "Synergistic Control of Bilateral Manipulator Systems", Proc. of The 14th International Symposium on Industrial Robots, pp. 239-250.

(1974) Nakano, E., Shotaro O., "Cooperational Control of the Anthropomorphous Manipulator -MELARM", Proc. of The 14th International Symposium on Industrial Robots, pp. 239-250.

(1975) Fichter, E.F., and Hunt, K.H., "The Fecund Torus, its Bitangent-Circles and Derived Linkages", Mechanisms and Machine Theory, vol. 10, pp.167-176.

(1976) Roth, B., "Performance Evaluation of Manipulators from a Kinematic Viewpoint", Report od a Workshop held at Annapolis, Maryland,

Edited by Sheridan, T.B., pp.39-61.

(1976) Veldkamp, G., R., "On the use of Dual Numbers, Vectors and Matrices in Instantaneous, Special Kinematics", Mechanisms and Machine theory ,vol. 11, pp.141-156.

(1977) Ishida, T., "Force Control in Coordination of two Arms", 5th International Joint Conference on Artificial Intelligence, MIT, Cambridge, Massachusetts, vol. 2, pp.717-722.

(1978) Hunt, K., H., Kinematic Geometry of Mechanisms, Clarendon Press, Oxford.

(1978) Suh, C.H., and Radcliff, C.W., Kinematics and Mechanisms Design, John Wiley & Son.

(1979) Bottema, O., and Roth, B., Theoretical Kinematics, North Holland Publ. Amsterdam.

(1980) Duffy, J., Analysis of Mechanisms and Robotic Manipulators", Mechanisms and Macnine Theory, vol.16, pp.255-261.

(1980) Konstantinov, M.S., Markov, M.D., "Two-Hand Robots for Sophisticated Manipulations in the Relative Space", Proc. of the 10th International Symposium on Industrial Robots, 5th Internationa Conference on Industrial Robot technology, Milan, Italy, pp. 475-480.

(1981) Derby, S., "The Maximum Reach of Revolute Jointed Manipulators", Mechanisms and Machine Theory, vol.16, pp.255-261.

(1981a) Kumar, A., Waldron K.J., "The Workspaces of a Mechanical Manipulator", ASME Journal of Mechanical Design, vol.103, pp.665-672.

(1981b) Kumar, A., Waldron K.J., "The Dextrous Workspaces ", ASME Publication, 80-DET-108.pp.665-672.

(1981) Orin, D.E., Oh, S.Y., "Control of Force Distribution in Robotic Mechanisms Containing Closed Kinematic Chains", ASME Journal of Dynamic Systems, Measurement, and Control, vol. 102, pp.134-141.

(1981) Paul, R.P., Robot Manipulators: Mathenmatics, Programming, and Control, MIT Press, Cambridge, MA.

(1981a) Sugimoto, K., Duffy, J., "Determination of Extreme Distances of a Robot Hand, Part 1, A General Theory", ASME Journal of Mechanical Design, vol.103, pp.631-636.

(1981b) Sugimoto, K., Duffy, J., "Determination of Extreme Distances of a Robot Hand, Part 2, Robot Arm with special Geometry", ASME Journal of Mechanical Design, vol.103, pp.776-783.

(1981) Tsai, Y.C., and Soni, A.H., "Accessible Region and Synthesis of Robot Arms", ASME Journal of Mechanical Design, vol.103, no.4, pp.803-811.

(1982) Angeles J., Spatial Kinematic Chains Analysis Synthesis Optimization, Springer-Verlag.

(1982) Gupta, K.C., and Roth, B., "Design Considerations for Manipulator Workspace", ASME Journal of Mechanical Design, vol.104, pp.704-711.

(1982) Lee, C.S.G., "Robot Arm Kinematics, Design, and Control", IEEE Transaction on Computers, vol.15, No.12, pp62-80.

(1983) Featherstone, R., "Calculation of Robot Joint rates and actuator torques from end effector velocities and apllied forces", Mecahnisms and Machine Theory, vol.18, No.3, pp.193-198.

(1983) Hansen, J.A., Gupta, K.C. and Kazerounian, S.M.K., "Generation and evaluation of the Workspace of a Manipulator", The International Journal of Robotics and Resaerch, vol.2, No.3, pp.22-31.

(1983) Jou, T.M., and Waldron, K.J. "Geometric Design of Manipulators

using interactive Computer Graphics", Proceedings of the sixth World congress on theory of Machines and Mechanisms, New Delhi, India, pp.949-954.

(1983) Konstantinov, M.S., Markov, M.D., Genova, P.I., Brankov, G.I., Anguelov, A.S., and Shivarov, N.S., "Performance and application of two-hand robots for assembly", Proc. of the Sixth World Congress of Machines and Mechanisms, pp. 1029-1031.

(1983) Lee T.W., and Yang, D.C.H., "On the evaluation of Manipulator Workspace", ASME Journal of Mechanisms, Transmission and Automation in Design, vol.105, pp.70-77.

(1983) Sefridge, R.g., "The Reachable Workspace of a Manipulator", Mechanisms and Machine Theory, vol.18, No.2, pp.131-137.

(1983) Tsai, Y.c. Soni, A.H., "An Algorithm for the Workspace of a general n-R Robot", ASME Journal of Mechanisms, Transmission and Automation in Design, vol.105, pp.52-57.

(1983) Yang, D.C.H., and Lee, T.W., "On the Workspace of Mechanical Manipulators", ASME Journal of Mechanisms Transmission ans Automation in Design, vol.105, pp.62-69.

(1984) Alford, C.O., and Belyeu, "Coordinated Control of Two Robot Arms", Proc. IEEE International Conference on Robotics, pp. 468-473.(1985) Pennock, G.R., "Application of Dual-Number Matrices to the Inverse Kinematics Problem of Robot Manipulators", ASME Journal of Mechanisms, Transmission, and Automation in Design, vol.107, pp.201-208.

(1984) Freund, E., "On the Design of Multi-Robot Systems", Proc. IEEE International Conference On Robotics, pp. 477-490.

(1984) Huang, Q., "Study of the Workspace of R-Robot", Robots 8, vol.4,

pp55-66.

(1984) Korein, J., U., A Geometric Investigation of Reach, An ACM Distinguished Dissertation, The MIT Press.

(1984) Yang D.C.H., Lee, T.W., "Heuristic Combinatorial Optimization in the Design of Manipualtor workspace", IEEE Transaction on Systems, Man and Cybernetics, vol. SMC-14, No.4, pp.571-580.

(1985) Acker, F.E., Ince, I.A. and Ottinger, B.D., "TROIKABOT- A Multi-Armed Assembly Robot", Robots 9, Conference Proc. vol. 2, Detroit, Michigan, pp. (15-1)-(15-19).

(1985) Algazar, S., "Efficient Kinematic Transformations for the PUMA-560 Robot", IEEE Journal of Robotics and Automations. vol. RA-1, No.3.

(1985) Angeles, J., "On the Numerical Solution of the Inverse Kinematic Problem", The International Joournal of Robotics Research, vol.4, No.2.

(1985) Cwiakala, M., and Lee, T.W., "Generation and evaluation of a Manipulator Workspace based on Optimum Path search", ASME Journal Mechanisms Transmission and Automation in Design, vol. 107, pp. 245-255.

(1985) Goldenberg, A.A., Benhabib, B., and Fenton, R.G., "A complete Generalized solution to the Inverse Kinematics of Robots", IEEE Journal of Robotics and Automation, vol., RA-1, No.1.

(1985) Kohli, D., and Spanos, J., "Workspace Analysis of Mechanical Manipulators Using Polynomial Discriminants", ASMS Journal of Mechanisms, Tranmissions, and Automation in Design, vol.107, pp. 209-215.

(1985) Liegeois, A., Borrel, P., and Tanner, P., "Automatic Modeling of the Workspace for Robots", Robotics Research, The Third

International Symposium, pp. 205-212.

(1985) Luh, J.Y.S., and Zheng, Y.F., "Computation of Input Generalized Forces for Robots with Closed Kinematic Chain Mechanisms", IEEE Journal of Robotics and Automation, vol. RA-1, No. 2, pp. 95-103.

(1985) Schmidtt, D., Soni, A.H., Srinivasan, v., and Naganthan, G., "Optimal Motion Programming of Robot Manipulators", ASME Journal of Mechanisms, Transmissions, and Automation in Design, vol. 107, pp.239-244.

(1985) Spanos, J., and Kohli, D., "Workspace Analysis of Regional Structures of Manipulators", ASMS Journal of Mechanisms, Tranmissions, and Automation in Design, vol.107, pp. 216-222.

(1985) Yang, D.C.H., and Lai, Z.C., "On the Dexterity of Robotic Manipulators-Service angle", ASME Journal of Mechanisms Transmission and Automation in Design, vol. 107, pp. 262-270.

(1985a) Zheng Y.F., and Luh, J.Y.S., "Constrained Relations Between two Coordinated Industrial Robots", Proc. od 1985, Conference of Intelligence Systems and Machines, Rochester Michigan, pp. 1761-1766.

(1985b) Zheng Y.F., and Luh, J.Y.S., "Control of Two Coordinated Robots In Motion", Proc. of 24th Conference on Decision and Control, Fort Lauderdale, Fl., pp. 1761-1766.

(1986) Bajbai, A., and Roth, B., "Workspace and Mobility of a Closed-Loop Manipulator", The International Journal of Robotics Research, vol. 5, No. 2, pp.131-142.

(1986) Borrel, P., Liegeois, A., "A study of multiple manipulator Inverse Kinematic solutions with applications to Trajectory Planning and Workspace determination", Proceedings, IEEE International

Conference on Robotics and Automation, San Fransisco, vol. 2, pp.1180-1185.

(1986) Craig, J., Introduction to Robotics: Mechanics and Control, Addison Wesley, Reading MA.

(1986) Fortune, S., Wifong, G., and Yap, C., "Coordinated Motion of Two Robot Arms", IEEE International Conference on Robotics and Automation, vol. 2, pp.1216-1223.

(1986) Hayati, S., "Hybrid Position/Force Control of Multi-Arm Cooperating Robots", Proc. of IEEE International conference on Robotics and Automation, San Francisco, vol. 1, pp. 82-89.

(1986a) Hemami, A., "Collision-Free Operation of two-arm Robots,", Proc. Robots 10 Conference, pp. 3.41-3.50.

(1986b) Hemami, A., "Kinematics of Two-ARm Robots", IEEE Journal of Robotics and Automation, vol. RA-2, No. 4, pp. 225-228.

(1986) Kumar, A., Patel, M.S., "Mapping the Manipulator Workspace Using Interactive Computer Graphics", The International Journal of Robotics Research, vol. 5, No., 2, pp. 122-130.

(1986) Paul, B., and Rosa, J., "Kinematics Simulation of Serial Manipulators", The International Journal of Robotics Research, vol. 5, No. 2.

(1986) Shaik, M.A., and Datseris, P., "A Workspace Optimization Approach to Manipulator Linkage Design", Proceedings, IEEE International Conference on Robotics and Automation, San Fransisco, vol. 1, pp.75-181.

(1986) Tarn, T.J., Bejczy, A.K., and Yun, X., "Coordinated Control of Two Arms", Proc. of IEEE International conference on Robotics and Automation, San Francisco, vol. 2, pp. 1193-1202.

(1986) Zheng, Y.F., and Sias, F.R. Jr., "Two Robot Arms in Assembly", Proc. of IEEE International conference on Robotics and Automation, San Francisco, vol. 2, pp. 1230-1235.

(1987) Chen, C.H., "Applications of Algebra of Rotations in Robot Kinematics", Mechanisms and Machine Theory, vol.22, No.1, pp.77-83.

(1987) Hunt, K.H., "Robot Kinematics - A Compact Analytic inverse solution for velocities", ASME Journal of Mechanisms, Transmission and Automation in Design, vol. 109, pp. 42-49.

(1987) Lim, J., Chyung, D.H., "Resolved Position Control for Two Cooperating Arms", Robotica, vol. 5, pp. 9-15.

(1987) Longman, R.W., Linberg, R.E., and Zedd, M.F., "Satellite-Mounted Robot Manipulators- New Kinematics and Reaction Moment Compensation", The International Journal of Robotics Research, vol. 6, No. 3, pp. 87-103.

(1987) Nakamura Y., Nagi, K. Yoshikawa, T., "Mechanics of Coordinative Manipulation by Multiple Robotic Mechanisms", Proc. of IEEE International Conference on Robotics and Automation, Raleigh, North Carolina, vol. 2, pp. 991-998.

(1987) Nelson, B., Pedersen, K. and Donath, M., "Locating Assembly Tasks in a Manipulator's workspace", Proceedings, IEEE International Conference on Robotics and Automation, Raleigh, North Carolina, vol. 3, pp.1367-1372.

(1987) Roach, J.W., and Boaz, M.N., "Coordinating the motions of Robot Arms in a Common Workspace", IEEE Journal of Robotics and Automation, vol. RA-3, No. 5, pp. 437-443.

(1987) Shahinpoor, M., A Robot Engineering Textbook, Harper & Row, NY.

(1987) Shirkhodaie, A.H., "AI Assisted Multi-Arm Robotics", Proc. of IEEE

International Conference on Robotics and Automation, Raleigh, North Carolina, vol. 3, pp. 1672-1676.

(1987) Tarn, T.J., Bejczy, A.K., Yun, X., "Design of Dynamic Control of Two Cooperating Robot Arms: Closed Chain Formulation", Proc. of IEEE International Conference on Robotics and Automation, Raleigh, North Carolina, vol. 1, pp. 7-13.

(1987) Wolovich, W.A., Robotics: Basic Anlysis and Design, HRW, NY.

(1988) Freund, E. and Hoyer, H., "Real-Time Pathfinding in Multirobot Systems Including Obstacle Avoidance", The International Journal of Robotics Research, vol. 7, No. 1, pp. 42-70.

(1988) Fu, K.S., Gonzales, R.C., and Lee, C.S.G., Robotics, Control, Sensing, Vision and Intelligence, McGraw Hill.

(1988a) Hemami, A. "A more general closed-form solution to the Inverse Kinematics of Mechanical Arms", Advanced Robotics, vol. 2, No. 4, pp.315-328.

(1988b) Hemami, A., "Kinematic equations and solutions of a Human-Arm-Like Robot Manipulator", Robotics 4, pp. 65-72.

(1988) Kazerooni, H., "Compliance Control and Stability analysis of Cooperating Robot Manipulators", Robotica, vol. 7, pp.191-198.

(1988) Koivo, A.J., and Bekey, G.A. , "Report of Workshop on Coordinated Multiple Robot Manipulators: Planning, Contro, and Applications", IEEE Journal of Robotics and Automation, vol. 4, No. 1, pp. 91-93.

(1988) Lim, J., and Chyung, D.H., "Admissible Trajectory determination for two Cooperating Robot Arms", Robotica, vol. 6, pp. 107-113.

(1988) Oblak, D., and Kohli, D., "Boundary Surface, Limit Surfaces, Crossable Surfaces in Workspace of Mechanical Manipulators", ASME Journal of Mechanisms, Transmissions, and Automation in Design,

vol. 110, pp. 389-396.

(1988) Press, W.H., Flannery, B.P., Teukolsky, S.A., and Vetterling, W.T., Numerical Recipes in C, Cambridge University Press, Cambridge, pp.309-324.

(1988) Swern, L., and Tricamo, S.J., "An approach to controlling Multi-Arm Robotic Manipulation of a single Body", Proc. of IEEE International conference on Robotics and Automation, pp. 516-521.

(1988) Zheng Y.F., Luh, J.Y.S., "Optimal Load Distribution for Two Industrial Robots Handling a Single Object", Proc. IEEE International Conference on Robotics and Automation, pp.344-349.

(1989) Autodesk, Inc., AutoCad Reeference Manual.

(1989) Carignan, C.R., and Akin, D.L., "Optimal Force Distribution for Payload Positioning using a Planar Dual-Arm Robot", ASME Journal of Dynamic Systems, Measurement, and Control, vol. 111, pp. 205-210.

(1989) Gardner, J.F., Kumar, V., and Ho, J.H., "Kinematics and Control of Redundantly Actuated Closed Chains", Proc. IEEE International Conference on Robotics and Automation, vol 1, pp. 418-424.

(1989) Hemami, A., Class Notes of Introduction to Robotics I.

(1989) Hu, Y.R., and Goldenberg, A.A., "An Adaptive Approach to Motion and Force Control of Multiple Coordinated Robot", Proc. IEEE International Conference on Robotics and Automation, vol 2, pp. 1091-1096.

(1989) Khatib, O., Craig, J.J., and Lozano-Perez, T., The Robotics Review 1, The MIT Press Cambridge, Massachusetts.

(1989) Nahon, M.A., Angeles, J., "Force Optimization in Redundantly-Actuated Closed Kinematic Chains", Proc. IEEE International Conference on Robotics and Automation, vol 2, pp.

951-956.

(1989) O'Donnell, P.A., and Lozano-Perea, T., "Deadlock-Free and Collision-Free Coordination of Two Robot Manipulators", Proc. IEEE International Conference on Robotics and Automation, vol 1, pp. 489-484.

(1989) Shin, Y., Bien, Z.,"Collision-Free Trajectory planning for two Robot Arms", Robotica, vol. 7, pp. 205-212.

(1989) Tao, J.M., and Luh, J.Y.S, "Coordination of Two Redundant Robots", Proc. IEEE International Conference on Robotics and Automation, vol 1, pp. 425-430.

(1989) Walker, I.D., Freeman, R.A., and Marcus,S.I.,"Internal Object Loading for Multiple Cooperating Robot Manipulators", Proc. IEEE International Conference on Robotics and Automation, vol 1, pp. 606-611.

(1989) Walker, M.W., Kim, D., Dionise J., "Adaptive Coordinated Motion Control of Two-Manipulator Arms", Proc. IEEE International Conference on Robotics and Automation, vol 2, pp. 1084-1090.

(1989) Zheng, Y.F., "Kinematics and Dynamics of Two Industrial Robots in Assembly", Proc. IEEE International Conference on Robotics and Automation, vol 3, pp. 1360-1365.

(1990) Djurovic, M.D., and Vukobratovic, M.K., "A Contribution to Dynamic Modeling of Cooperative Manipulation", Mechanism and Machine Theory, vol. 25, No. 4, pp. 407-415.

(1990) Hemami, A., Cheng, R.M.H., and Ranjbaran, F., "Path Verification for Coordinated Motion of Two Arms", Accepted for Publication in the International Journal of Robotics and Autonomous Systems, (1991).

(1990) Hemami, A., Ranjbaran, F., and Cheng, R.M.H., "A Case Study Of

Two-Robot-Arm Workcell In Material Handling", Accepted for publication in the Journal of Robotics Systems (Feb. 1991.).

(1990) Koivo, A.J., and Unseren, M.A., "Modeling Closed Chain Motion of Two Manipulators holding A Rogid object", Mechanism and Machine Theory, vol. 25, No. 4, pp. 427-438.

(1990) Murphy, S. H., Wen, J.T., and Saridis, G.N., "Simulation of Cooperating Robot Manipulators on a Moboile Platform", Proc. IEEE International Conference on Robotics and Automation, vol 2, pp. 1190-1195.

(1990) Ranjbaran, F., Cheng., R.M.H. and Hemami, A., "On the Optimum Set-Up of a Robotic Work-station", submitted for Publication in the Journal of Robotics Systems.

(1990) Tsai, M.J., and Chiou, Y.H., "Manipulability of Mnipulators", Mechanisms and Machine Theory, vol. 25, No. 5, pp. 575-585.

(1990) Yoshikawa, T., and Zheng, X., "Coordinated Dynamic Hybrid Position/Force Control for Multiple Robot Manipulators Handling One Constrained Object", Proc. IEEE International Conference on Robotics and Automation, vol 2, pp. 1178-1183.

APPENDIX A

CALCULATIONS OF THE ELEMENTS OF THE GRADIENT VECTOR

The elements of the gradient vector of the objective function for a PUMA-560 are given in the following. The lengthy process of evaluation of these elements is not outlined here and only the final expressions for the derivatives are presented.

The objective function is rewritten as:

$$E(\Gamma) = \sum_{j=1}^{m} \sum_{i=1}^{6} \left[\theta_{ij}(\Gamma) - \theta^{*}_{ij}\right]^2 - r\sum_{k=1}^{p} \frac{1}{g_k(\Gamma)} \qquad \text{(A.1)}$$

Differentiating Eq. (A.1) with respect to Γ will result in

$$\frac{\partial E(\Gamma)}{\partial \Gamma} = \sum_{j=m}^{m} \sum_{i=1}^{6} 2\left[\theta_{ij}(\Gamma) - \theta^{*}_{ij}\right] \frac{\partial}{\partial \Gamma} (\theta_{ij}) -$$

$$r\sum_{k=1}^{p} \frac{-1}{(g_k(\Gamma))^2} \frac{\partial}{\partial \Gamma} (g_k(\Gamma)) \qquad \text{(A.2)}$$

Thus primarily we need to determine the following derivatives

$$\partial\theta_{ij}/\partial\Gamma = \left[\partial\theta_{ij}/\partial x \quad \partial\theta_{ij}/\partial y \quad \partial\theta_{ij}/\partial\beta\right]^T \qquad \text{(A.3)}$$

$$\text{and} \quad \partial g_k/\partial\Gamma = \left[\partial g_k/\partial x \quad \partial g_k/\partial y \quad \partial g_k/\partial\beta\right]^T \qquad \text{(A.4)}$$

For the sake of simplicity, the subscript j is omitted in what follows, and also some abreviations are used in the expressions which are defined next:

$$\xi \equiv p_x - d_6 a_x - x \qquad \text{and} \qquad \eta \equiv p_y - d_6 a_y - y \tag{A.5}$$

Where p_x, p_y, a_x and a_y are given in the transformation matrix T_w^h.

Moreover:
$$S_1 \equiv \sin(\theta_1), \quad C_1 \equiv \cos(\theta_1), \quad T_1 \equiv \tan(\theta_1) \tag{A.6}$$

$$S_{1k} \equiv \sin(\theta_1 + \theta_k), \quad C_{1k} \equiv \cos(\theta_1 + \theta_k) \tag{A.7}$$

$$S_{1\beta} \equiv \sin(\theta_1 + \beta), \quad C_{1\beta} \equiv \cos(\theta_1 + \beta) \tag{A.8}$$

And a_1, a_2, a_3, d_2, d_4 and d_6 are the D.H. parameters.

Thus the final expressions for the derivatives can be written as:

$$\partial\theta_1/\partial x = \frac{S_{1\beta}}{a_2 C_2 + d_4 S_{23}}, \qquad \partial\theta_1/\partial y = \frac{C_{1\beta}}{a_2 C_2 + d_4 S_{23}},$$
$$\partial\theta_1/\partial\beta = -\frac{\eta S_{1\beta} + \xi C_{1\beta}}{a_2 C_2 + d_4 S_{23}} \tag{A.9}$$

$$\partial\theta_2/\partial x = \frac{S_{23}\left[C_{1\beta}(a_2 C_2 + d_4 S_{23}) - d_2 S_{1\beta}\right]}{a_2 C_3 (a_2 C_2 + d_4 S_{23})} \tag{A.10}$$

$$\partial\theta_2/\partial y = \frac{S_{23}\left[S_{1\beta}(a_2 C_2 + d_4 S_{23}) + d_2 C_{1\beta}\right]}{a_2 C_3 (a_2 C_2 + d_4 S_{23})}$$

$$\partial\theta_2/\partial\beta = -\frac{S_{23}\left[\eta(a_2 C_2 C_{1\beta} + d_4 S_{23} C_{1\beta} + d_2 S_{1\beta}) - \xi(a_2 C_2 S_{1\beta} + d_4 S_{23} S_{1\beta} + d_2 C_{1\beta})\right]}{a_2 C_3 (a_2 C_2 + d_4 S_{23})}$$

$$\partial\theta_3/\partial x = -\frac{C_{1\beta}(a_2C_2 + d_4S_{23}) - d_2S_{1\beta}}{d_4a_2C_3}, \quad \partial\theta_3/\partial y = \frac{S_{1\beta}(a_2C_2 + d_4S_{23}) + d_2C_{1\beta}}{d_4a_2C_3}$$

$$\partial\theta_3/\partial\beta = \frac{\eta(a_2C_2C_{1\beta} + d_4S_{23}C_{1\beta} + d_2S_{1\beta}) - \xi(a_2C_2S_{1\beta} + d_4S_{23}S_{1\beta} + d_2C_{1\beta})}{a_2C_3(a_2C_2 + d_4S_{23})}$$

(A.11)

$$\partial\theta_5/\partial x = \frac{\frac{\partial\theta_1}{\partial x}(C_{23}^2S_4S_5 + C_{23}S_{23}C_5T_4 - S_4S_5) + (\frac{\partial\theta_2}{\partial x} + \frac{\partial\theta_3}{\partial x})(C_{23}C_5 - S_{23}C_4S_5)}{S_{23}S_5 - C_{23}C_4C_5 - S_4C_{23}C_5}$$

$$\partial\theta_5/\partial y = \frac{\frac{\partial\theta_1}{\partial y}(C_{23}^2S_4S_5 + C_{23}S_{23}C_5T_4 - S_4S_5) + (\frac{\partial\theta_2}{\partial y} + \frac{\partial\theta_3}{\partial y})(C_{23}C_5 - S_{23}C_4S_5)}{S_{23}S_5 - C_{23}C_4C_5 - S_4C_{23}C_5}$$

$$\partial\theta_5/\partial\beta = \frac{\zeta + \frac{\partial\theta_1}{\partial\beta}(C_{23}^2S_4S_5 + C_{23}S_{23}C_5T_4 - S_4S_5) + (\frac{\partial\theta_2}{\partial\beta} + \frac{\partial\theta_3}{\partial\beta})(C_{23}C_5 - S_{23}C_4S_5)}{S_{23}S_5 - C_{23}C_4C_5 - S_4C_{23}C_5}$$

Where : $\zeta = a_yS_{1\beta}C_{23}T_4 + a_xC_{1\beta}C_{23}T_4 - a_yC_{1\beta} + a_xS_{1\beta}$

(A.12)

$$\partial\theta_4/\partial x = \frac{\frac{\partial\theta_1}{\partial x}(C_{23}C_4S_5 + S_{23}C_5) - \frac{\partial\theta_5}{\partial x}S_4C_5}{C_4S_5}$$

$$\partial\theta_4/\partial y = \frac{\frac{\partial\theta_1}{\partial y}(C_{23}C_4S_5 + S_{23}C_5) - \frac{\partial\theta_5}{\partial y}S_4C_5}{C_4S_5} \qquad \text{(A.13)}$$

$$\partial\theta_4/\partial\beta = \frac{\frac{\partial\theta_1}{\partial\beta}(C_{23}C_4S_5 + S_{23}C_5) - \frac{\partial\theta_5}{\partial\beta}S_4C_5 - (a_yS_{1\beta} + a_xC_{1\beta})}{C_4S_5}$$

$$\partial\theta_6/\partial x = \frac{\mu\left(\frac{\partial\theta_2}{\partial x} + \frac{\partial\theta_3}{\partial x}\right) + \nu\frac{\partial\theta_4}{\partial x} + \lambda\frac{\partial\theta_5}{\partial x}}{\delta}$$

$$\partial\theta_6/\partial y = \frac{\mu\left(\frac{\partial\theta_2}{\partial y} + \frac{\partial\theta_3}{\partial y}\right) + \nu\frac{\partial\theta_4}{\partial y} + \lambda\frac{\partial\theta_5}{\partial y}}{\delta} \qquad \text{(A.14)}$$

$$\partial\theta_6/\partial\beta = \frac{\mu\left(\frac{\partial\theta_2}{\partial\beta} + \frac{\partial\theta_3}{\partial\beta}\right) + \nu\frac{\partial\theta_4}{\partial\beta} + \lambda\frac{\partial\theta_5}{\partial\beta}}{\delta}$$

Where: $\mu = C_{23}S_4S_6 + S_{23}S_5C_6 - C_{23}C_4C_5C_6$

$\nu = S_{23}S_4C_5C_6 + S_{23}C_4S_6$

$\lambda = S_{23}C_4S_5C_6 - C_{23}C_5C_6$

and, $\delta = S_{23}C_4C_5S_6 + C_{23}S_5S_6 + S_{23}S_4C_6$

In what follows the derivatives of the constraints with respect to the elements of Γ are derived:

$$\frac{\partial g_k}{\partial\Gamma} = \begin{cases} -\frac{\partial\theta_k}{\partial\Gamma} & k = \text{odd} \\ \frac{\partial\theta_k}{\partial\Gamma} & k = \text{even} \end{cases} \qquad k = 1,2,\ldots,12m \qquad \text{(A.15)}$$

$$\frac{\partial g_k}{\partial x} = 2(p_y^* S_\beta - p_x^* C_\beta)$$

$$\frac{\partial g_k}{\partial y} = 2(p_y^* C_\beta - p_x^* S_\beta) \qquad k = 12m+1,\ 12m+2,\ldots,\ 13m \qquad \text{(A.16)}$$

$$\frac{\partial g_k}{\partial\beta} = 2\eta(p_y^* S_\beta - p_x^* C_\beta) + 2\xi(p_x^* S_\beta + p_y^* C_\beta)$$

$$\frac{\partial g_k}{\partial x} = -2(p_y^* S_\beta - p_x^* C_\beta) \qquad (A.17)$$

$$\frac{\partial g_k}{\partial y} = -2(p_y^* C_\beta - p_x^* S_\beta) \qquad k = 13m+1,\ 12m+2, \ldots,\ 14m$$

$$\frac{\partial g_k}{\partial \beta} = -[2\eta(p_y^* S_\beta - p_x^* C_\beta) + 2\xi(p_x^* S_\beta + p_y^* C_\beta)]$$

Where p_x^* and p_y^* are cartesian coordinates of the wrist point of the PUMA robot with respect to it's base coordinate frame.

APPENDIX B

MOBILITY ANALYSIS OF COORDINATED TWO-ARM ROBOTS

Sometimes it is required for the two robots to handle an object a device, or a tool which cannot be considered as rigid and in fact posses internal mobilities. This can produce relative freedom between the grasping points or in turn between the end effectors. As an example consider manipulation of a pair of pliers by two robot (Fig B.1) or turning a nut held by one robot over a screw secured by the second robot (Fig. B.2). Moreover the grasp itself can be designed in a way which produces freedom(s) between the hands and the manipulated object. For instance consider using hinged end effectors to carry a rigid object (Fig. B.3) or as handling the pair of pliers with hinged end effectors (Fig. B.4).

Next we will develop a general mobility criterion for coordinated two-arm robots in handling and manipulations of general objects with known degrees of freedom while the grasps also possess non-zero mobilities. We define the **internal joint mobility** of the manipulated object f_{IM} to be the relative degree of freedom between the internal links, comprising the manipulated object, and let n_I be the number of such internal links, and finally g_I be the number of joints embedded in the object. Also we denote the **grasp mobility** or relative degree of freedom between the object and the main and follower end effectors respectively as f_{MG} and f_{FG}. Therefore by using equation **6.5** we can write

$$m = 6(n - 1 + n_I - g - g_I - 1) + \sum_{1=1}^{g} f_1 + \sum_{1=1}^{g_I} (f_{IM})_1 + f_{MG} + f_{FG} \qquad \text{(B.1)}$$

Note that in the foregoing equation we substituted $n - 1 + n_I$ for n and the appearance of this minus one is because we are in fact taking one link out of the original chain and replacing it with n_I links, then we have

$$m = 6(12 + n_I - 12 - g_I - 2) + 12 + \sum_{1=1}^{g_I} (f_{IM})_1 + f_{MG} + f_{FG}$$

$$\text{or} \quad m = 6(n_I - g_I) + \sum_{1=1}^{g_I} (f_{IM})_1 + f_{MG} + f_{FG} \qquad \text{(B.2)}$$

One can use equation B.2 to obtain the overall mobility of a coordinated two-arm robot. In what follows we evaluate the mobility of the four examples stated above and shown in figures B.1 to B.4.

For both figures B.1 and B.2 we have,

$n_I = 2$, $g_I = 1$ and $f_{IM} = 1$

$f_{MG} = 0$, $f_{FG} = 0$

Thus the overall degrees of freedom of a coordinated two-arm robots in handling the pair of pliers will be calculated by equation B.2 as,

$$m = 7$$

In this case the extra degree of freedom of the system shown in figure B.1 is due to the jaw angle β_j at each instant j. For the case of the screw and nut (Fig. B.2) the extra degree of freedom can be considered as the distance d_j for each instant designated by j. This distance can be related to

the rotation angle of the nut given h the lead of the threads as

$$\beta_j = d_j / h$$

Therefore in addition to $(T_w^C)_j$, T_C^M and T_C^F for each point j of the trajectory, the angle β_j also has to be defined by the application.

For figure B.3,

$n_I = 1$, $g_I = 0$ and $f_{IM} = 0$

$f_{MG} = 1$ and $f_{FG} = 1$

and $\therefore$ $m = 8$

The two extra degrees of freedom in this case are due to the rotation of the end effectors about their normal vector n. Therefore two rotation angles need to be defined for a unique definition of the motion. These two degree of freedom can be utilized for more dexterity or reachability along the path or to accommodate any other criteria such as the load balance requirement.

For figure B.4 we can write,

$n_I = 2$, $g_I = 1$ and $f_{IM} = 1$

$f_{MG} = 1$ and $f_{FG} = 1$

$m = 9$

This case is a combination of B.1 and B.3. Thus three extra degrees of freedom are introduced in the system.

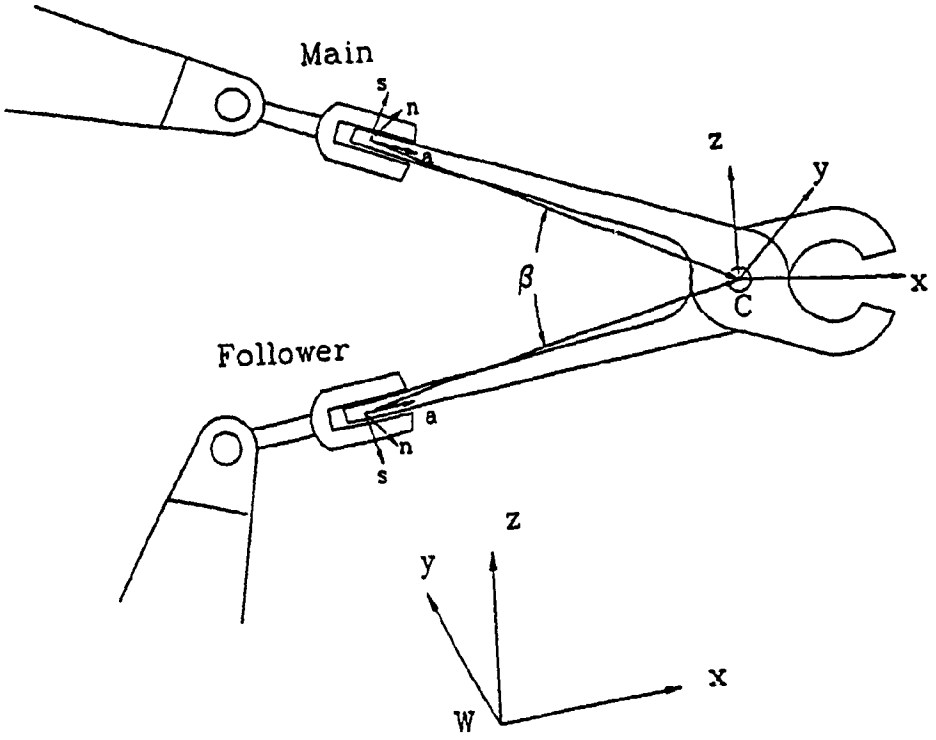

Figure B.1 - Handling pliers with two arms

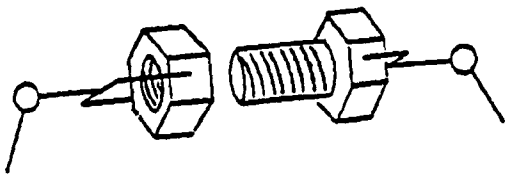

Figure B.2 - Turning nut with two arms

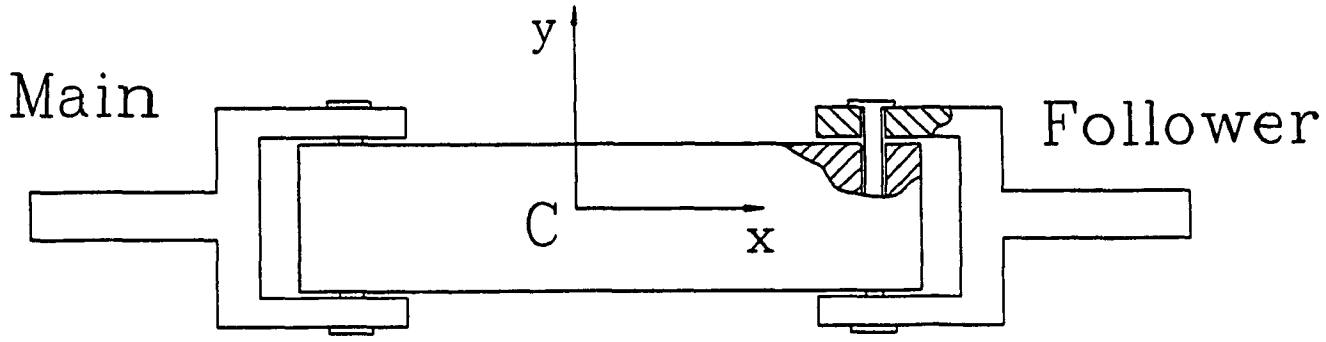

Figure B.3 - Handling rigid object with hinged EE's

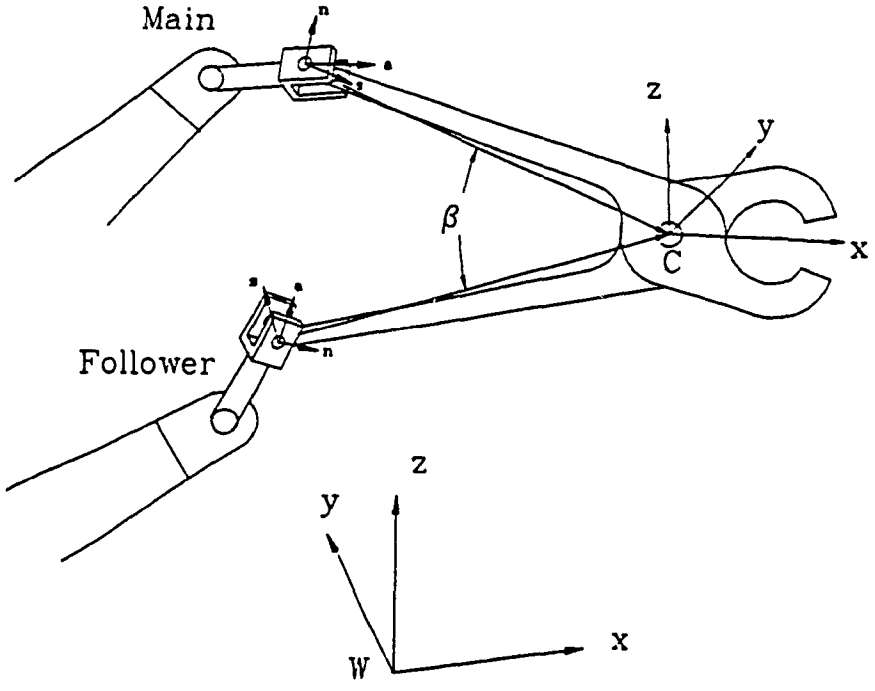

Figure B.4 - Handling pliers with hinged EE's

APPENDIX C

FLOW CHARTS OF THE COMPUTER PROGRAMS

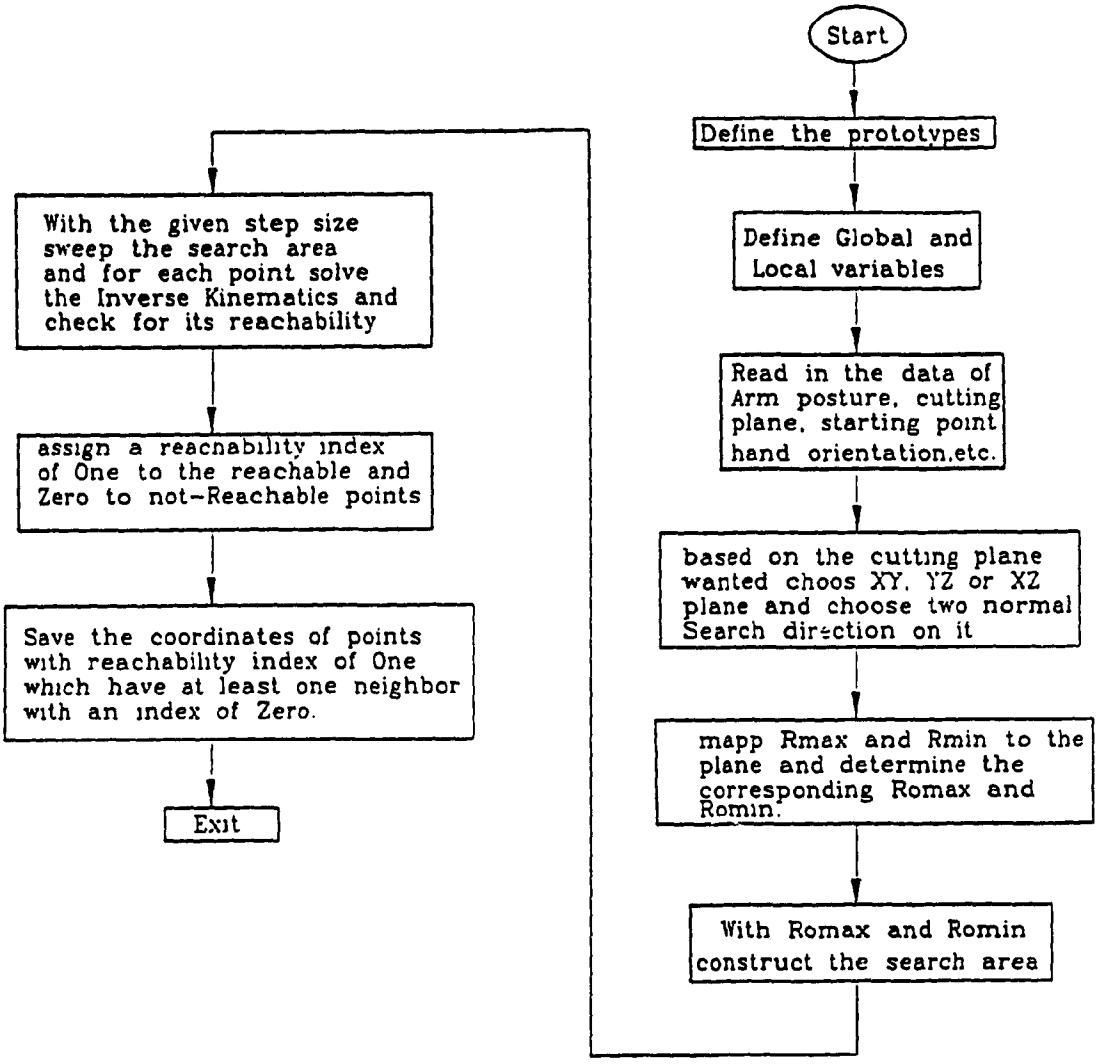

Figure C.1 - Flowchart of Direct Search Algorithm (CONTOUR1.C)

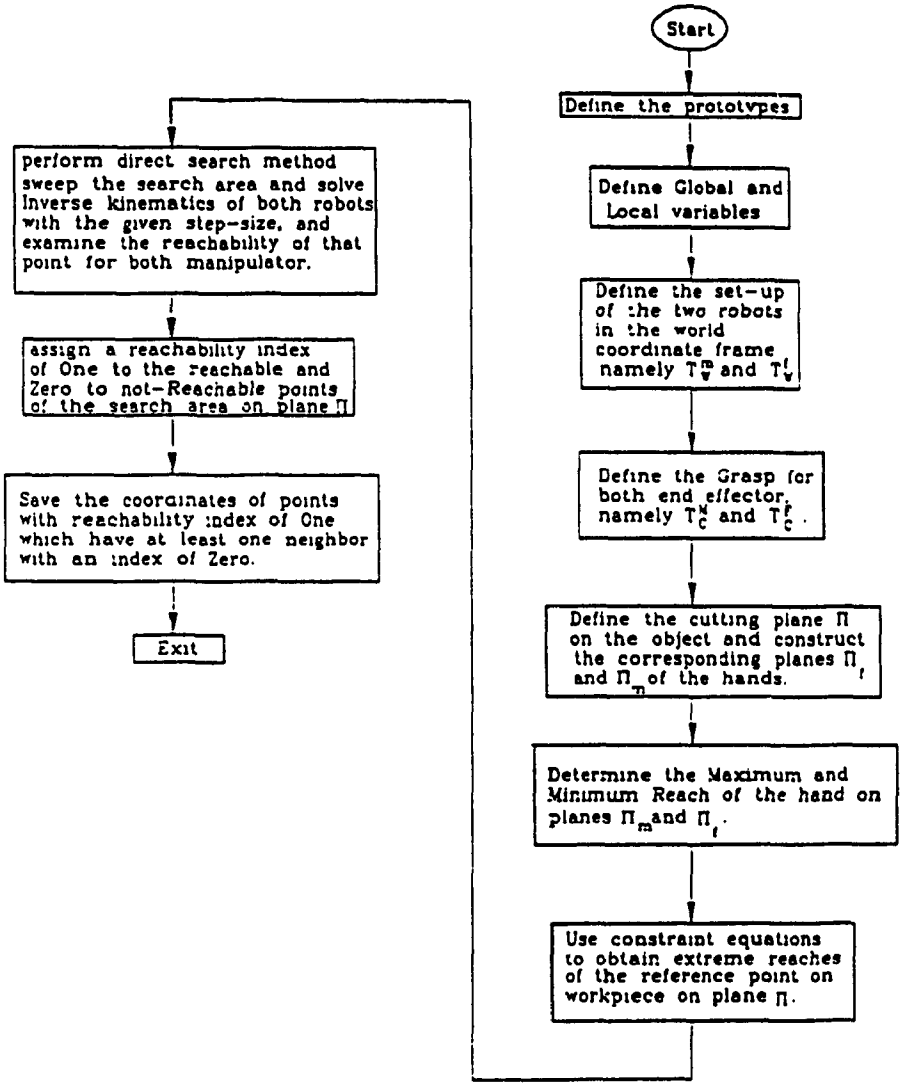

Figure C.2 - Flowchart of Triplet Workspace Algorithm (TRIPWC.C)

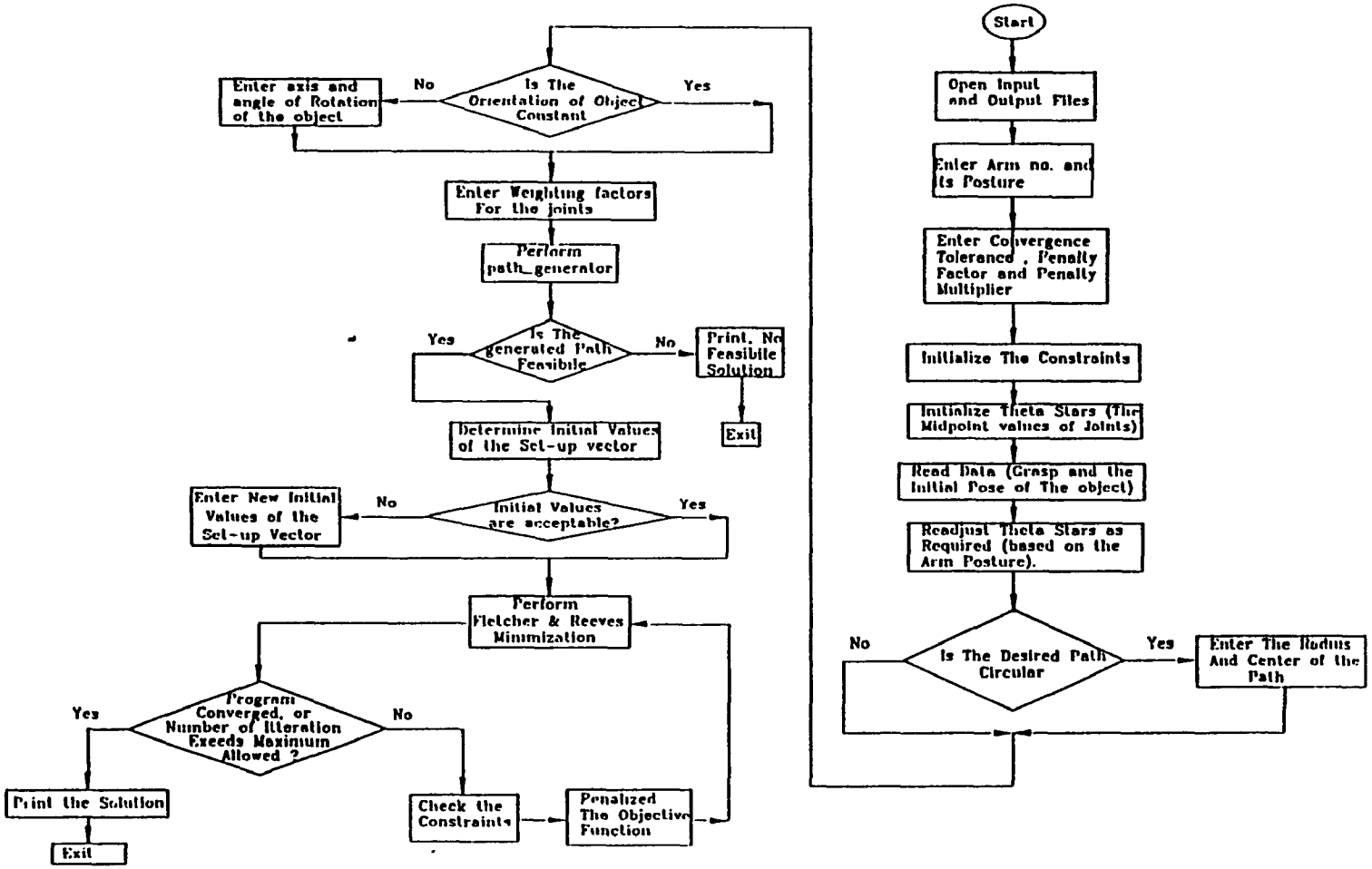

Figure C.3 - Flowchart of Optimum Setup of Workcell (SET_UP.C)